Elucidating the mechanisms of HIF1A mediated age-related retinal degeneration

---

Dissertation

Zur Erlangung der naturwissenschaflichen Doktorwürde
(Dr. sc. Nat.)

vorgelegt der
Mathematisch-naturwissenschaftlichen Fakultät der

Universität Zürich

von
Divya Ail
aus Indien

Promotionskomitee

Prof. Dr. Christian Grimm (Vorsitz und Leitung)
Dr. Corinne Kostic
Prof. Dr. Ian Frew

Zürich, 2015

SUMMARY

Visual impairment adversely affects the quality of life of the sufferer and is a major economic burden. Retinal degenerative diseases are one of the leading causes of visual impairment. Photoreceptor loss is a hallmark of many retinal degenerative diseases such as age-related macular degeneration (AMD). There are many genetic and environmental factors resulting in this photoreceptor loss. One such factor is hypoxia, as age-related changes in the retina may result in a hypoxic microenvironment. At the cellular level the hypoxic response is mainly executed by transcription factors called – hypoxia inducible factors (HIFs), which are heterodimers composed of a hypoxia-responsive - α subunit (HIFA) and a constitutively expressed β subunit (HIFB). HIFA is degraded under normoxic conditions by a Von hippel lindau (VHL) - mediated mechanism and stabilized under hypoxic conditions in an oxygen dependent manner. Earlier research in our lab showed that conditional knockdown of *Vhl* by the Cre-Lox system in the rod-photoreceptors (using an Opsin promoter to drive CRE expression) resulted in stabilization of HIF1A and HIF2A, and most importantly this resulted in cell death and loss of retinal function at older age.

Here, I show that this degeneration is due to HIF1A as in the mice with the double knockdown of *Vhl* and *Hif1a* in the rods, this phenotype was completely rescued. Further characterization revealed that other features such as the blood vessels, retinal pigment epithelium and bruch's membrane were not severely affected. To analyze molecular and cellular changes I compared the transcriptomes of retinas when HIF1A is stabilized or deleted in the rods, which revealed the differential regulation of several genes. On stabilization of HIF1A there is a potential metabolic shift in energy production to glycolysis from oxidative phosphorylation. According to the transcriptome data, one of the major groups of genes upregulated in the HIF1A stabilized mice included complement factors and hence these were further characterized. But our studies revealed that complement factors are not direct targets of HIF1A and are most likely upregulated as part of the ongoing degeneration mechanisms in these mice. Lastly, the knockdown of *Hif1a* in the hypoxic retina, by subretinal injections of Adeno-associated viruses packaging shRNA against *Hif1a* was envisioned as a gene therapy for combating degeneration. Towards this goal I performed in vitro analysis of different siRNAs against *Hif1a* that could be further used for injections.

One of the candidates from the transcriptome data - Stanniocalcin 2 (*Stc2*) was selected for further analysis. I was able to show that both *Stc2* and its paralog *Stc1* are expressed in the retina, but only *Stc2* is hypoxia responsive and regulated in a HIF1A-dependent manner. Further I showed that the normal expression of *Stc2* is in the inner nuclear layer (INL) and the ganglion cell layer (GCL), and the protein localizes to the neurofilaments. The retinal morphologies of both the *Stc1* and *Stc2* knockout mice were

normal, indicating that *Stc2* may not be essential for the normal development of the retina, but may be involved in hypoxic stress mechanisms.

In addition to hypoxic stress, the retina is also susceptible to pH changes and the ensuing acidosis during degeneration. Hence, we analysed a class of proton sensing G-protein coupled receptors (GPRs) – *Gpr4, Gpr65* and *Gpr68* in the retina. Our studies revealed that all the three Gprs are expressed in the retina, but only *Gpr65* is upregulated during induced (light damage model) and inherited (*rd10* mice) degeneration. Knockout mice lacking GPR65 had normal retinal structure and function, but the additional loss of *Gpr65* in *rd10* mice accelerated degeneration.

Understanding the complex cellular responses to stress is important for recognising therapeutic targets and development of an effective therapy. In this context, my work sheds light on stress related mechanisms in retinal degeneration with specific focus on the role of the key transcription factor HIF1A in photoreceptor death and survival.

ZUSAMMENFASSUNG

Sehbehinderungen und Blindheit beeinträchtigen nicht nur die Lebensqualität der Patienten, sondern stellen auch eine erhebliche ökonomische Belastung für Betroffene und die Gesellschaft dar. Eine der häufigsten Ursachen für Sehbehinderungen sind degenerative Erkrankungen der Netzhaut, zu denen zum Beispiel die altersabhängige Makuladegeneration (AMD) zählt. Ein Kennzeichen von AMD und vielen anderen Netzhautdegenerationen ist der irreversible Verlust von Sehzellen.

Zahlreiche genetische oder umweltbedingte Faktoren können zum Verlust der Sehzellen führen. Einer dieser Faktoren ist Sauerstoffarmut (Hypoxie), die auch durch normale altersbedingte Veränderungen in der Netzhaut entstehen kann. Dies führt zu einer hypoxischen Reaktion der Zellen, welche hauptsächlich durch die Aktivierung von 'hypoxia inducible factors' (HIFs) charakterisiert ist. HIFs sind heterodimere Transkriptionsfaktoren, die aus einer Sauerstoff-sensitiven alpha (HIFA) und einer konstitutiv exprimierten beta Untereinheit (HIFB) aufgebaut sind. HIFA wird bei normaler Sauerstoffkonzentration hydroxyliert und durch einen proteolytischen Mechanismus rasch abgebaut, der durch das Van Hippel Lindau (VHL) Protein kontrolliert wird. Unter hypoxischen Bedingungen greift dieser Mechanismus nicht und HIFA wird in Abhängigkeit der Sauerstoffkonzentration stabilisiert. Frühere Untersuchungen in unserem Labor haben gezeigt, dass die konditionelle Inaktivierung von *Vhl* in den Stäbchen die Stabilisierung beider isoformen, HIF1A und HIF2A in Normoxie bewirkt, und vor allem, dass dies zu einem altersabhängigen Verlust der Netzhautfunktion durch das Absterben der Sehzellen führt.

In meiner Dissertation gelang es mir zu zeigen, dass der Grund für diese langsam fortschreitende Erblindung die chronische Stabilisierung des HIF1A Proteins ist, denn der Phänotyp wurde durch die Zusätzliche Inaktivierung von HIF1A (nicht aber von HIF2A) vollständig unterdrückt. Ich zeigte weiter, dass die durch HIF1 hervorgerufene Degeneration weder die Blutgefässe, noch das retinale Pigmentepithel oder die Bruch'sche Membran stark beeinträchtigte, sondern spezifisch die Sehzellen betraf. Um die molekularen und zellulären Veränderungen beim Degenerationsprozess zu analysieren verglich ich die Transkriptome von Netzhäuten mit stabilisiertem oder inaktiviertem HIF1A in den Stäbchen. Dies führte zur Identifizierung von einer grossen Anzahl von Genen die durch die chronische Stabilisierung von HIF1A ein verändertes Expressionsmuster aufwiesen. Durch die Stabilisierung von HIF1A wurden zum Beispiel mehrere Gene verstärkt exprimiert, die eine Verlagerung der Energieproduktion von der oxidativen Phosphorylierung zur Glykolyse bewirken können. Dies könnte zu einer verminderten Energieproduktion führen und somit ein Hauptgrund für den Zelltod der Photorezeptoren sein. Eine andere identifizierte Gruppe von differenziell regulierten Genen kodierte für verschiedene Faktoren des Komplementsystems. Da diese

Faktoren wesentlich an der Entwicklung von AMD beim Menschen beteiligt sind, habe ich diese Gruppe im Hinblick auf die Degeneration weiter charakterisiert. Die Daten deuten darauf hin, dass die Aktivierung der Komplementgene nicht direkt durch Stabilisierung von HIF1A, sondern durch die Degeneration, also sekundär, ausgelöst wurde. Um die durch HIF1A ausgelöste Netzhautdegeneration therapeutisch angehen zu können, habe ich begonnen siRNA Sequenzen gegen *Hif1a* in der Zellkultur zu testen, um die Sequenz mit der höchsten Effizienz zu definieren. Diese Sequenz soll als shRNA in adeno-assoziierte Viren verpackt und durch subretinale Injektionen der viralen Partikel in die Sehzellen eingeschleust werden. Das mittelfristige Ziel ist, mit dieser gentherapeutischen Massnahme die Degeneration zu stoppen oder zumindest zu verlangsamen.

Aus den Transkriptom-Daten wählte ich das stark regulierte *Stanniocalcin 2* (*Stc2*) für weitere Untersuchungen aus. Ich konnte zeigen, dass sowohl *Stc2* als auch sein Paralog *Stc1* in der Netzhaut exprimiert werden, aber nur *Stc2* auf Hypoxie reagiert. Weiter gelang es mir zu zeigen, dass *Stc2* vornehmlich in der inneren Körnerschicht und der Ganglienzellschicht exprimiert wird und dass das STC2 Protein hauptsächlich in den Neurofilamenten der Ganglienzellen lokalisiert ist. Da die Netzhautmorphologien von *Stc1* und *Stc2* knockout Mäusen normal war, scheint *Stc2* für die normale Entwicklung der Netzhaut nicht essentiell zu sein, könnte aber an der Antwort auf einen hypoxischen Stress beteiligt sein.

Die Netzhaut ist nicht nur anfällig auf hypoxischen Stress, sondern auch auf die Veränderung des pH-Wertes und der daraus folgenden Azidose während einer Degeneration. Deshalb analysierten wir auch die Expression einer Klasse von G-Protein-gekoppelten Rezeptoren (GPRs) – *Gpr4*, *Gpr65* und *Gpr68* in der Netzhaut. Unsere Untersuchungen zeigten, dass die Netzhaut alle drei *Gprs* exprimiert, dass aber nur *Gpr65* auf eine Degeneration reagiert. Die Expression von *Gpr65* war sowohl in einem induzierten (Lichtschaden) als auch einem vererbten (rd10) Degenerationsmodell stark erhöht. Mäuse ohne GPR65 entwickelten eine normale Netzhautstruktur und –funktion, zeigten aber in rd10-Mäusen einen leicht beschleunigten Verlust der Sehzellen.

Für die Entwicklung einer effektiven Therapie für Erblindungserkrankungen ist es wichtig, die komplexen molekularen Reaktionen der Netzhautzellen auf Stress zu verstehen. Meine Arbeit gibt in diesem Zusammenhang Aufschluss über die stressbedingten Mechanismen in der degenerativen Netzhaut unter besonderer Beachtung der Rolle des zentralen Transkriptionsfaktors HIF1A beim Tod von Photorezeptoren.

TABLE OF CONTENTS

1. INTRODUCTION

1.1 The Retina

1.1.1 Vision and the eye

Vision is one of the most important sensory systems by which humans perceive their surroundings. The visual system aids in discerning the location, shape, size, colour, texture as well as movement of objects. The human visual system has the ability of processing information over a broad range of stimulus intensities – from faint starlight to bright sunlight.

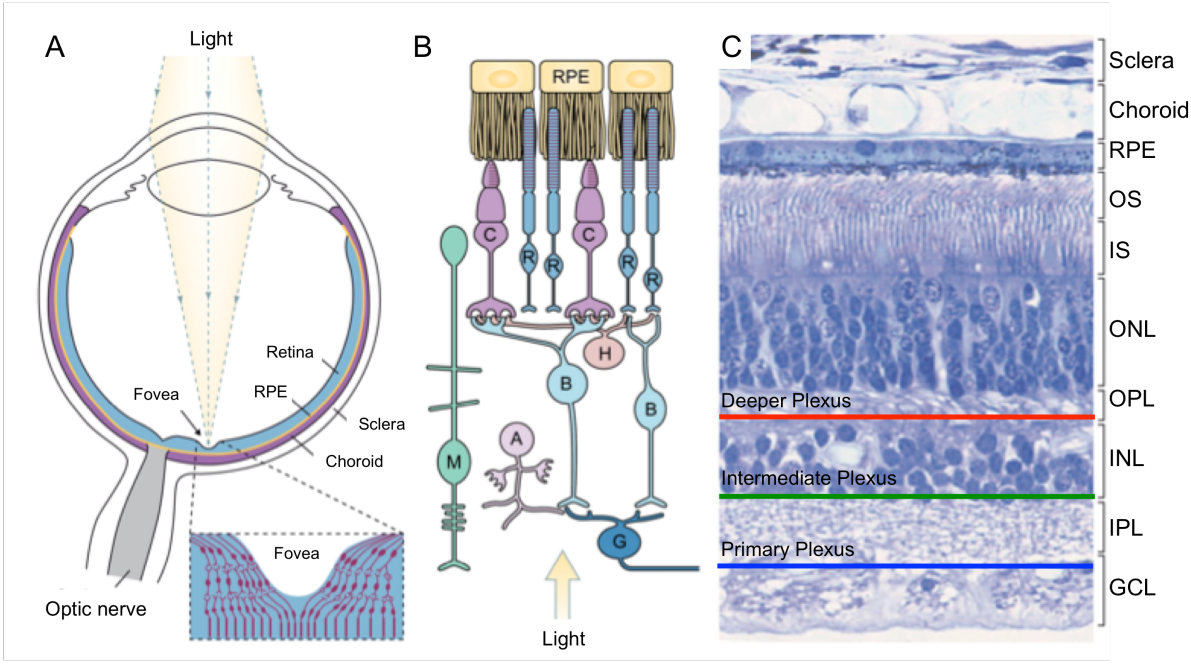

***Figure 1**. Structure of the eye and organization of the retina. (A) Eyes are the optical part of the visual system that send transmitted light for synaptic processing to the retina. (B) The retina is composed of different cell types with specialized functions – RPE: Retinal Pigment Epithelium, C: Cone photoreceptors, R: Rod photoreceptors, H: Horizontal cells, B: Bipolar cells, A: Amacrine cells, M: Muller cells, G: Ganglion cells. (C) The different cells are organized in stratified layers – RPE: Retinal Pigment Epithelium, OS: Outer Segments (of photoreceptors), IS: Inner Segments, ONL: Outer Nuclear Layer, OPL: Outer Plexiform Layer, INL: Inner Nuclear Layer, IPL: Inner Plexiform Layer, GCL: Ganglion Cell Layer. A schematic representation of the different layers of retinal vasculature is shown – Deeper plexus (red line), Intermediate plexus (green line) and the Primary plexus (Blue line). (Figure adapted from Sung CH et al, 2010)*

Eyes are the organs of vision, which send signals via the optic nerve to the brain. At the front of the eye is the cornea - a specialized transparent tissue that allows light to enter the eye. The coloured part of the eye is the iris and the opening in its centre is the pupil. Behind this is the lens, whose refractive ability is controlled by ciliary muscle. The ciliary muscle is

connected to the lens by zonular fibers, made predominantly of the connective tissue protein fibrillin and when the ciliary muscle relaxes, the zonular fibers apply tension on the lens, in order to focus light onto the retina. This plays an important role in accommodation to light. The innermost layer of the eye is the retina, which processes and sends signals to the visual cortex in the brain (Purves et al., 2008) (Figure 1A).

1.1.2 Structure of the retina

During development, the retina forms from the optic vesicle of the diencephalon, and hence is part of the central nervous system. The retina is a complex tissue composed of stratified layers of different cell types interspersed by the retinal vasculature (Figure 1B and 1C).

1.1.2.1 Retinal pigment epithelium (RPE)

The RPE is a single-cell layer of melanin-containing cells. It reduces the back scattering of light entering the eye. The RPE cells have microvilli that extend into the photoreceptor layer and surround the outer segments (Figure 1B). The RPE cells have many functions, including the 2 critical roles – first they help in clearing the disks that are shed by the outer segments of the photoreceptors and most importantly they help in the regenerating and recycling of the photopigment molecules that have been exposed to light (Strauss, 2005). In addition to these functions, the RPE forms a barrier between the choroid and the inner retina (blood-retina barrier), and hence protects the retina from the harmful particles being circulated in the blood, as well as from triggering an immune response. But, while protecting the inner retina, it also provides the oxygen and essential nutrients, which are selectively transported across the membrane.

1.1.2.2 Retinal Neurons

There are five different types of neurons – photoreceptors, bipolar cells, horizontal cells, amacrine cells and ganglion cells. The cell bodies are stacked together in layers named nuclear layers – the cell bodies of photoreceptors form the outer nuclear layer (ONL), the cell bodies of bipolar cells, horizontal cells and amacrine cells form the inner nuclear layer (INL) and the ganglion cell bodies form the ganglion cell layer (GCL). The processes and synaptic connections of these cells form two distinct layers called the outer plexiform layer (OPL) and the inner plexiform layer (IPL) (Sung and Chuang, 2010). There are two types of photoreceptors – rods and cones. These are the light sensitive cells of the retina involved in phototransduction. The bipolar cells are so named because they have two processes extending on either sides of the cell body. A bipolar cell accepts signals from the photoreceptors (either rods or cones, not both) as well as horizontal cells and then relays this

to ganglion cells either directly or via the amacrine cells. Horizontal cells are laterally interconnecting neurons that integrate and regulate the signals from the photoreceptors. Their cell bodies are in the INL and their processes are in the OPL. They are mainly responsible for maintaining the visual system's sensitivity to contrast over a broad range of light intensities. The amacrine cells are postsynaptic to bipolar cells and presynaptic to the ganglion cells with their processes in the IPL. There are more than 20 different sub-types of amacrine cells that are thought to contribute to retinal function in distinct ways although relatively little is known about them. There are several different sub-types of ganglion cells that receive and integrate signals from amacrine and bipolar cells. The axons of the ganglion cells and some displaced amacrine cells are packed into a nerve fibre layer (NFL), and the axons of the ganglion cells converge to form the optic nerve (Masland, 2001).

1.1.2.3 Retinal glial cells

In addition to the neurons there are three types of glial cells in the retina. The Muller cells are the principle glial cells in the retina. They span almost the entire width of the retina. They are involved in supplying metabolic products to the neurons, protecting neurons from stress, and phagocytosis of neuronal debris (Bringmann et al., 2006). Astrocytes are the second type of glial cells. They do not develop from the retinal progenitors, but enter the retina from the brain during development. Their main known function is the involvement in the development of the primary plexus of vasculature (Schnitzer, 1988). The third type of retinal glial cells is the microglia, which are often described as the immune cells of the retina. They are constantly surveying the surroundings, can get activated on receiving stress signals, and migrate to the region of insult in case of neuronal stress (Chen et al., 2002).

1.1.2.4 Retinal Vasculature

The retina is a tissue with a high metabolic demand for oxygen and to supply this it has an extensive vascular system. This demand for oxygen and nutrients is fulfilled by the vascular system which has two parts – the choroidal vasculature and the retinal vasculature (Figure 1C). In vascularized retinas (rodents, primates, cats etc), the choroid mainly supplies to the outer retina (the photoreceptors), and the retinal vasculature provides for the inner layers (especially the plexiform layers depend on this system). Certain species with avascular retinas depend solely on the choroidal system. Avascular retinas are generally thinner than the vascular ones, as they are limited by the ability of the choroidal system to provide oxygen by diffusion across all retinal layers. The disadvantage of vascularized retinas is that the blood vessels scatter light that reduce the light reaching the photoreceptors and also affects visual acuity as vessels take up space of the other cell types. But over time the retinas of most species have evolved towards a vascular system providing a compromise between

efficient supply of oxygen and visual sensitivity. The retinal vasculature has three distinct layers or plexi. The primary plexus forms a network in the inner retina at the nerve fibre layer. It consists of arteries and veins that both emerge and exit via the optic nerve. This layer then forms two parallel inter-connected layers at the plexiform layers – the intermediate plexus and the deeper plexus (Figure 1C). However, the metabolic demands of photoreceptors are mainly fulfilled by choroidal vasculature (Fruttiger, 2007).

1.1.3 Structure and function of photoreceptors

The outer nuclear layer is composed of 2 types of photoreceptors – rods and cones. The rods and cones differ in several properties like shape, distribution across the retina, photopigment, as well as the synaptic connections they form, and these differences contribute to their specialized functions in different aspects of vision (Purves et al.,2008).

Structurally the photoreceptor consists of a cell body that contains the cell organelles. On one side of the cell body are the axons that end at the synaptic terminal, which forms synapses with the neurons from the inner nuclear layer. On the other side of the cell body is the photoreceptor segment. The segments are divided into two parts – the inner and the outer segments. The inner segments are rich in mitochondria and meet the high metabolic demand of the photoreceptors. The outer segments are specialized structures that contain stacked membranous disks (Figure 2A and 2B), which form a rod-like structure and cone-like structure in rods and cones respectively. The disk membranes have trans-membrane proteins called opsins (Figure 2C and 2D), which are G-protein coupled receptors of the retinylidene family, and the associated chromophore – retinal (Blaurock and Wilkins, 1969; Blaurock, 1972). Outer segments of the rods are cylindrical in shape and those of cones have a conical shape. The opsin in rods is called rhodopsin. In cones there are 3 types of opsins, which respond to different regions of the visible spectrum – OPN1LW (long wavelength), OPN1ML (middle wavelength) and OPN1SL (short wavelength) (Marc and Sperling, 1977).

The photoreceptors are involved in the process of phototransduction, wherein a photon absorbed by the retinal triggers a series of molecular responses and biochemical reactions that convert the absorbed light into an electrical stimulus that can be sent to the brain for processing. The molecular events in phototransduction can be broadly divided into 5 steps. The first step involves the absorption of light by rhodopsin, which photo-isomerizes 11-*cis*-retinal to the all-*trans*-retinal conformation. The second step involves rhodopsin to undergo several conformational changes, generating metarhodopsin I and metarhodopsin II (MII). MII is the active form of rhodopsin and is crucial for the catalytic activation of the G protein transducin. Transducin is a trimeric protein composed of α, β and γ subunits, which in the

inactive state is bound to guanosine diphosphate (GDP). In the third step, MII rhodopsin interacts with transducin, which leads to the exchange of GDP for GTP and the separation of the α subunit (Gα) from the trimeric complex. The Gα is the active portion of transducin, which interacts with phosphodiesterase (PDE) to propagate the signal to the next step. Phosphodiesterase is a heterotetrameric protein composed of one α and one β subunit, which form the catalytic core to hydrolyze cyclic guanosine monophosphate (cGMP) to GMP. Two γ subunits bind the α and β heterodimer and inhibit their hydrolytic activity. In the fourth step, active Gα interacts with PDE, the γ subunits inhibition on the enzymatic activity of PDE is released. Finally in the fifth and last step, PDE hydrolyses cGMP to GMP closing cGMP nucleotide-gated ion channels and hyperpolarizing the cells.

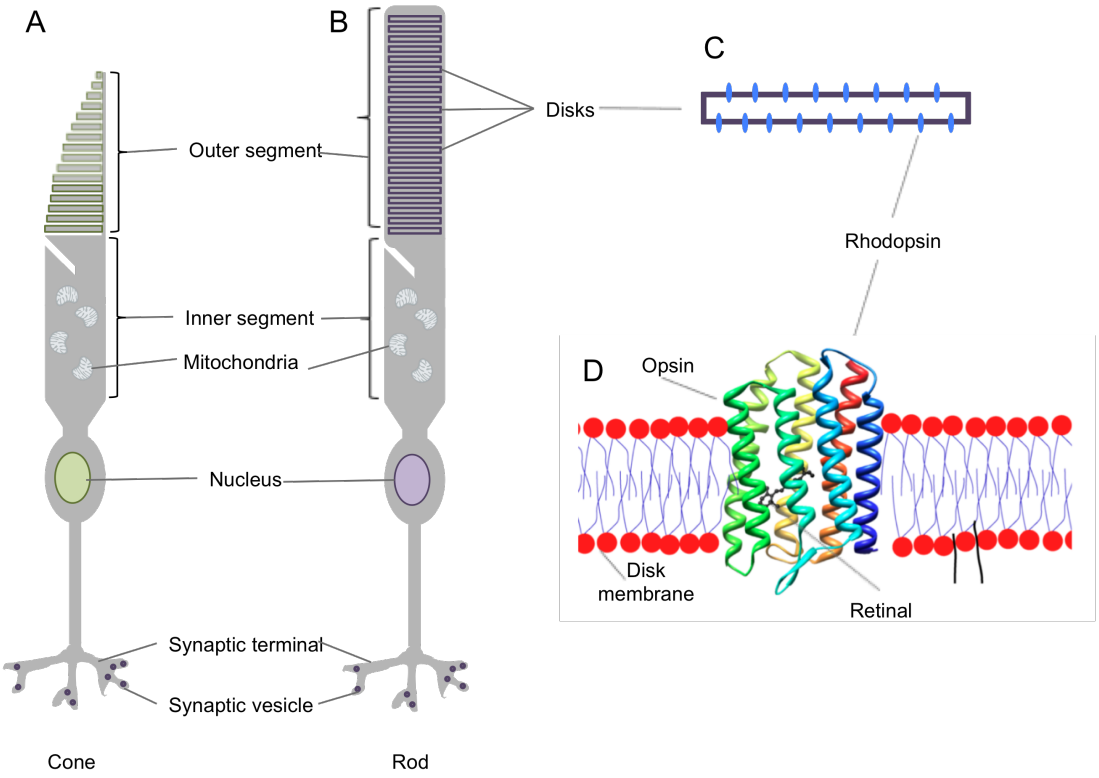

Figure 2 *Structure of the photoreceptors* ***(A)*** *A cone photoreceptor with distinctively cone-shaped outer segment in contrast to the* ***(B)*** *rod photoreceptor.* ***(C)*** *The outer segments are composed of membranous disks containing transmembrane proteins called rhodopsin.* ***(D)*** *The rhodopsin molecule is composed of the protein opsin and the chromophore – retinal. (Figure 2D adapted from www.wordpress.mrreid.org)*

Cyclic nucleotide gated channels in outer segments control the influx of calcium ions (Ca^{2+}) thereby keeping the photoreceptor cells constantly depolarized in darkness. Intracellular cGMP levels determine whether these channels are open or closed thereby controlling the influx of Ca^{2+} ions. In the depolarized state, photoreceptors continually release glutamate neurotransmitter at the photoreceptor synaptic cleft. In contrast, in the presence of light, as cGMP is hydrolyzed to GMP by PDE, the intracellular levels of cGMP decrease. As a result

cyclic nucleotide gated channels close, Ca^{2+} influx ceases and the cell hyperpolarizes. In the hyperpolarized state the release of glutamate is reduced proportionally to the intensity of the light stimulus. This adaptive response of glutamate release to light signal, is carried to second order neurons such as the bipolar cells (Arshavsky et al., 2002).

The rod system is extremely sensitive to light but has low spatial resolution, whereas the cone system has high spatial resolution (in the macula where the cones are concentrated) but low light sensitivity. The rod system aids in vision at lowest levels of illumination (scotopic vision) and the cone system becomes active at higher illuminations such as indoor light (photopic vision). The human eye is capable of detecting luminance from 10^{-6} cd/m^2 to 10^8 cd/m^2. A single photon can elicit a response from a rod photoreceptor, whereas more than 100 photons would be required to elicit a similar response from a cone photoreceptor (Fein and Szuts, 1982).

In the human retina, the number of rods (about 90 million), exceeds the number of cones (about 4.5 million) hence the density of rods is higher than cones in most part of the retina. But the central region of the retina called the macula has a cone rich region called the fovea (Figure 1A), which is responsible for high visual acuity (Provis et al., 1998). In fact loss of photoreceptors in the macula (macular degeneration) is one of the leading causes of blindness.

1.2 Retinal Degeneration

Damage and death of photoreceptors cause degeneration of the retina, which might eventually lead to vision impairment and blindness. Genetic mutations responsible for inherited retinal degenerations have been identified, but the exact molecular mechanisms causing photoreceptor death is not well understood, especially in complex, multi-factorial diseases such as Age-related Macular Degeneration (AMD).

1.2.1 Age-related Macular Degeneration (AMD)

Age-related Macular Degeneration (AMD) is a leading cause of blindness among the elderly. The prevalence of AMD increases with age, affecting about 2% of the population at the age of 40, and one in four people by age of 80 (Group, 2004). Several population-based epidemiological studies have provided estimates of prevalence of the disease among various racial/ethnic groups worldwide. These observations consistently conclude that the incidence of both - geographic atrophy (dry AMD) and the neovascular form (wet AMD) is rare before 55 years of age, and becomes common in people above the age of 75, and the occurrence is more common among the white population than the blacks (Klein et al., 2004).

1.2.1.1 Types and Symptoms

AMD is typically defined by the death of RPE cells and photoreceptors in the macular region of the retina, which leads to loss of central vision. Hence AMD patients have a blurry spot in their field of vision, and the size of this spot depends on the extent of degeneration. There are two forms of AMD – dry form (geographic atrophy) and the wet form (neovascular AMD). Dry AMD is the chronic form of the disease that occurs progressively, and leads to visual impairment of varying degree in different patients. On the other hand, wet AMD can occur abruptly and rapidly leads to blindness if left untreated. Wet AMD occurs only in 10-15% of the AMD patients, and typically the patients first develop the dry form before progressing into the wet form of the disease (Ferris III et al., 2013).

With increasing age the efficiency of RPE cells in clearing the degradation products of the photoreceptor outer segments is reduced (Boulton, 1991). This results in lipofuscin accumulation in the lysosomes of RPE cells. Lipofuscin consists of several molecules, dominantly the fluorophore A2E – a by-product of the visual cycle (Suter et al., 2000). Another early indication of AMD is accumulation of drusen in the macular region. Drusen are tiny soft extracellular material, which accumulate between the RPE and Bruch's Membrane (BM). In the aging retina the RPE cells become less efficient with the clearance of extracellular debris, and the accumulation of few small drusen is a normal age-related event. However, the accumulation of excessive amounts of large drusen indicates the onset of dry AMD. Clinically AMD is defined based on number and type of drusen (large and soft), pigmentary changes in the macula and the extent of geographic atrophy. The drusen accumulation is often accompanied by hyper/hypo pigmentation of the RPE. Slight thickening of the Bruch's membrane (BM) occurs as a normal aging process, but in AMD patients irregular thickening of the BM is observed. In early/ intermediate stages the visual acuity is often affected (Rickman et al., 2013; Holz et al., 2014).

The late stage is distinguished by scotomas in the macular region that lead to progressive loss of central vision. The patients also have decreased night vision. In some patients there is abrupt invasion of blood vessels into the RPE and retina – choroidal neovascularization (CNV). The ingrowing blood vessels develop poorly, and result in blood leakage in the retina, causing discomfort and a rapid progression of vision loss (Rickman et al., 2013).

1.2.1.2 Risk Factors

AMD is a multi-factorial disease hence there is no single cause for the disease. However there are several environmental and genetic risk factors that increase the propensity towards developing AMD.

Environmental factors – Studies have shown a strong correlation of AMD with smoking, with more than a 2 fold increased incidence of AMD in smokers compared to non-smokers. Obesity and higher BMI also increased the risk of AMD (Seddon and Chen, 2004). Increased plasma levels of C-reactive protein (due to inflammation) (Seddon et al., 2006), or complement activation fragments Bb and C5a have been independently implicated as risk factors (Reynolds et al., 2009). On the other hand dietary intake of lutein and zeaxanthin showed a protective effect, and reduced the risk (Seddon et al., 1994). Exposure to bright sunlight is also a risk factor.

Genetic factors – Several genes have been identified to be associated with AMD. These genes have been shown to be associated with high-density lipoprotein collagen, cholesterol, collagen, extracellular matrix and mechanisms such as angiogenesis (Consortium, 2013). Many of these genes are involved in the complement pathway. CFH R1210C was the first rare penetrant mutant to be reported for AMD (Raychaudhuri et al., 2011). Rare variants in *C3, Cfi* and *C9* have also been shown to confer a high risk (Seddon et al., 2013).

1.2.1.3 Available treatments

Currently there is no cure available for AMD. Most of the therapies/ treatments provided are either aimed at delaying the onset of the disease or at controlling the progress into severe late stage symptoms and vision loss.

Preventive/ delaying measures - Several studies have shown benefits of dietary intake of macular carotenoids – lutein and zeaxanthin and food rich in these nutrients (Seddon et al., 1994). It has also been shown that dietary supplements containing high doses of antioxidants and minerals (vitamin C and E, beta-carotene, and zinc) delayed the progression from intermediate to advanced stage of the disease (Group, 2001). Another potentially beneficial supplement is Omega-3 fatty acid, which is present in enriched amounts in fish (SanGiovanni et al., 2008). Lifestyle factors that can be modified are – avoidance of smoking (Seddon et al., 1996), controlling obesity, increasing physical exercise (Seddon et al., 2003) and reducing exposure to bright sunlight (Mitchell et al., 1998).

Wet AMD treatments – Laser photocoagulation is a method by which newly formed vessels are destroyed using a laser. It was shown effective in a study in the 1980s but is much less used now due to a risk of immediate moderate visual loss after treatment (Group, 1986).

Photodynamic therapy was used in the 1990s. It is a two-stage process wherein verteporfin (a photosensitising dye that accumulates in the neovascular membranes) is injected and then activated by infrared light. This generates oxygen-free radicals that damage the endothelium resulting in the closure of newly formed vessels (Bressler, 2001).

Anti-VEGF (Vascular Endothelial Growth Factor) is currently the most widely used therapy to control CNV. VEGF plays a key role in the development of new vessels, this led to the development and testing of several VEGF inhibitors that can be provided to patients as intravitreal injections at regular intervals (Dixon et al., 2009; Mitchell, 2011).

As mentioned earlier only 10-15% of the patients develop wet AMD and the remaining suffer from the dry form. But there is no treatment available and the development of therapies for dry AMD remains an unmet medical need.

1.2.2 The Complement System and AMD

1.2.2.1 The complement pathways

The immune system has two parts – the innate immune system, which provides the first line of defence against pathogens and does not change over the course of a person's lifetime and the adaptive immune system, which adapts and develops when exposed to pathogens. The complement pathway is part of the innate immune system. The main functions of the complement system are - cell lysis of microorganisms, removal of foreign particles and dead cell debris, recruitment and activation of inflammatory cells, regulation of antibody production, and elimination of immune complexes.

The complement system has 3 pathways – classical, lectin and alternative pathway. These three differ in their mode of activation and the components/factors that are involved in the cascade (Figure 3). Binding of circulating C1q to antigen-antibody complexes activates the classical pathway. The C1 complex consists of C1q and two molecules each of C1r and C1s. The binding of the recognition subcomponent C1q to the Fc portion of immunoglobulins results in autoactivation of the serine protease C1r. C1r then cleaves and activates C1s, which translates the activation of the C1 complex into complement activation through the cleavage of C4 and C2 to form a C4bC2a enzyme complex. C4bC2a acts as a C3 convertase and cleaves C3, which results in products that bind to and cause the destruction of invading pathogen. The Lectin Pathway is initiated by the binding of either mannose-binding lectin (MBL) or ficolin — associated with MBL-associated serine protease 1 (MASP1), MASP2, MASP3 and small MBL-associated protein (sMAP) — to an array of carbohydrate groups on the surface of a bacterial cell. Similar to C1s, MASP2 is responsible for the activation of C4 and C2, which leads to the generation of the same C3 convertase (C4bC2a) as in the classical pathway. MASP1 is able to cleave C3 directly. The alternative pathway is initiated by the low-grade activation of C3 by hydrolyzed C3 ($C3(H_2O)$) and activated factor B (Bb). The activated C3b binds factor B (B), which is then cleaved into Bb by factor D (D) to form the alternative pathway C3 convertase, C3bBb. Once C3b is attached

to the cell surface, the amplification loop consisting of the alternative-pathway components is activated, and the C3-convertase enzymes cleave many molecules of C3 to C3b, which bind covalently around the site of complement activation. After activation the three pathway recruit different factors, but all pathways merge at the C3 hydrolysis step, and then further culminate in the formation of a cytolytic membrane attack complex (MAC) (Fujita, 2002; Purves et al.).

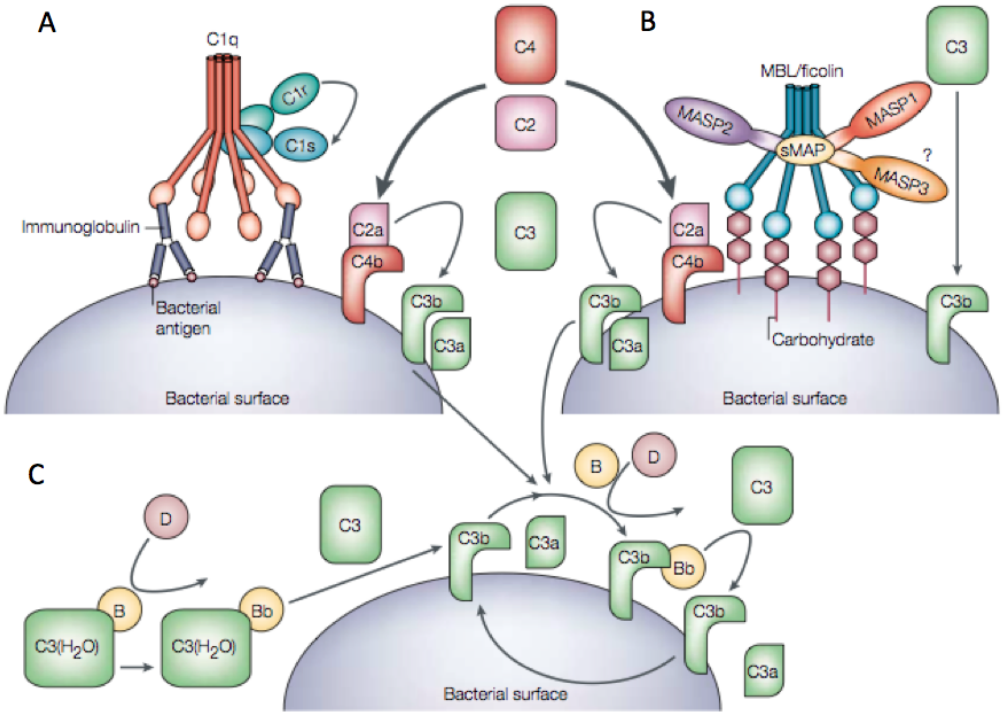

Figure 3 *Activation mechanisms of complement pathways and the complement factors involved* ***(A)*** *The Classical Pathway is initiated by the binding of the C1 complex to antibodies that are bound to antigens on the surface of the pathogen.* ***(B)*** *The lectin pathway is activated when mannose-binding lectin recognises and binds to specific carbohydrates on the pathogen surface.* ***(C)*** *The alternative pathway is in a continuous low-level activation state, and is characterized by spontaneous hydrolysis of C3 to C3a and C3b. (Figure adapted from Fujita T, 2002)*

1.2.2.2 Implications in AMD

As mentioned earlier, AMD is a multi-factorial disease and several genetic polymorphisms have been associated with the disease. Many of these high-risk associated genes are part of the complement system, such as – Complement Factor H (CFH) (Edwards et al., 2005; Hageman and Anderson, 2005; Haines et al., 2005; Klein et al., 2005), Complement component 3 (C3) (Despriet et al., 2009; Maller et al., 2007; Park et al., 2009; Yates et al., 2007), Complement Factor B (CFB) and Complement component 2 (C2) (Gold et al., 2006; Jakobsdottir et al., 2008). In European and North American population it was shown that

CFH and CFB/C2 variants accounted for 75% of all AMD cases (Gold et al., 2006). The total population risk attributable to the variants of the C3 gene was estimated to be 14.5% (Despriet et al., 2009). There is evidence for some protective haplotypes of CFH. This is due to the deletion of two members of the CFH family – CFHR1 and CFHR3, which act downstream and modulate the function of C5 convertase (Hageman et al., 2006). Hence, several studies have shown and new studies continue to show that mutations in genes of the complement pathway increase the risk/ provide protection from developing AMD (Anderson et al., 2010).

In addition to genetic linkage studies, biochemical examination of the drusen composition revealed the presence of complement factor fragments/ components. Immunochemical and proteomic analysis of drusen showed the presence of immunoglobulins, activated complement components (C3a, C3b, Cfb, C5 and C5a), complement regulators (vitronectin, clusterin, and cfh, acute phase proteins and the Alzheimer's disease amyloid-beta peptide). Other oxidative stress and inflammation related components were also present – oxidized lipids, microglia and macrophage cells (Anderson et al., 2010). These genetic-association and drusen composition studies suggest that the disease has a chronic inflammatory component and have led to the 'inflammation model' of AMD pathogenesis.

1.2.3 Animal models to study AMD

AMD is a complex disease with multiple factors - age, genetics, diet and lifestyle, that contribute to the onset. In addition the time and extent of manifestation of the symptoms vary among individual patients (Evans, 2001). This makes it very difficult to emulate all the features of the disease in a single AMD animal model. Therefore, there are several different animal models that are used to study and test therapies for various aspects of the disease (Ramkumar et al., 2010).

Anatomically and physiologically the primate retina would be the most suitable model for AMD study because they possess a macula, but factors like limited supply, ethical concerns, financial constraints and the challenge of genetic modifications restrict their utilization. Instead, several mouse models have been and continue to be developed for AMD research despite the significant differences between human and mouse retina. The most important difference being the lack of a macula – the region where the cone photoreceptors are concentrated in the human retina. Mice are nocturnal animals, yet the photoreceptor ratios are comparable with the mouse retina composed of 97% rods and 3% cones, and human retina with 95% rods and 5% cones (Carter-Dawson and Lavail, 1979). But, mice have only two cone types – S-cones (blue light) and M-cones (green light), while the human retina has in addition a third type – L-cones (red light) (Szel et al., 1992). It has been hypothesized that

RPE phagosomes cause drusen accumulation via the basal pathway into the bruch's membrane (Mishima and Hasebe, 1978). However, in mice lysosomal bodies accumulate in the RPE cytoplasm and are extruded into the sub-retinal space, hence drusen accumulation is difficult to detect in aged mice (Mishima and Kondo, 1981).

Mouse models with mutations in several genes such as *ABCR* and *ELOVL4,* known to cause the juvenile macular dystropy – Stargardt disease, are often used for study as these display the phenotype of RPE and photoreceptor atrophy, and also show elevated levels of lipofuscin and its by-product A2E (Mata et al., 2001; Vasireddy et al., 2006; Vasireddy et al., 2009).

An important aspect of AMD pathology is inflammation – microglia activation and accumulation and macrophage infiltration (Karlstetter and Langmann, 2012; Perez and Caspi, 2015). As outlined above, mutations in several complement factor genes are highly correlated with the disease and biochemical analysis of drusen revealed the presence of complement factor fragments, pro-inflammatory cytokines and chemokines. Genetic mutations in the *Cfh* gene are highly correlated with the disease (Raychaudhuri et al., 2011). CFH is a negative regulator of the alternative complement pathway and inhibits C3. Hence in *Cfh-/-* mice an accumulation and activation of C3 is observed. In addition these mice had reduced visual function at old age and significant thinning of the bruch's membrane (Coffey et al., 2007). CCL2 and its receptor CCR2 are responsible for recruiting and modulating the function of macropahges. Both *Ccl2-/-* and *Ccr2-/-* mice developed several features of AMD including sub-retinal deposits similar to drusen, late degeneration and choroidal neovascularization (CNV) at 24 months of age (Ambati et al., 2003). Retinal microglia cells express the CX3 chemokine receptor 1 (CX3CR1) affecting microglia migration and activation. *Cx3cr1-*/- mice showed significant thinning of the outer retina at 18 months of age (Combadière et al., 2007). The *Ccl2-/-;Cx3cr1-/-* showed more severe and an early onset of the phenotype (Tuo et al., 2007).

Apart from the genetic models for inflammation related genes, an induced model was developed by immunizing mice with carboxyethylpyrrole (CEP)-modified serum albumin. CEP is formed as an oxidation product of docosahexaenoic acid (DHA), which then interacts with and modifies tissue proteins. The levels of CEP-modified proteins is elevated in AMD patients compared to age-matched controls. The CEP-immunized mice showed RPE atrophy and loss, accumulation of BlamD (basal laminar deposits), accumulation of complement factors and thickening of BM (Hollyfield et al., 2008).

Inefficient metabolism results in accumulation of lipids and proteins in the sub-RPE and BM region, resulting in impaired transport of nutrients to the photoreceptors. Neprilysin is a peptidase that is required for the break-down of Aβ peptides. Neprilysin-/- mice showed RPE

abnormalities at old age, though this did not affect the photorecptors or result in CNV induction (Iwata et al., 2001 ; Yoshida et al., 2005).

Apolipoprotein E (apoE) is important for lipid and cholesterol metabolism and genetic association studies have shown many *APOE* polymorphisms to be risk factors for AMD. ApoE-/- mice had an early onset (starting at 2 months of age) of RPE abnormalities that worsened with age (Dithmar et al., 2000). Transgenic mice expressing one of three APOE isoforms – apoE2, apoE3 or apoE4 were raised on a low/high fat diet. The mice on a high-fat diet showed certain AMD features with varying severity (Malek et al., 2005).

The retina consumes high levels of oxygen (Sickel, 1972), hence being suseptible to oxidative stress resulting from molecular changes and cellular damage caused by reactive oxygen species (ROS). One of the important anti-oxidants responsible for clearing ROS is superoxide dismutase (SOD). There are three isoenzymes – SOD1 (cytosolic), SOD2 (mitochondrial) and SOD3 (extracellular), with SOD1 being most abundant in the retina. *Sod1-/-* mice show drusen-like deposits, thickening of BM and CNV at 10 months of age (Imamura et al., 2006). *Sod2* mutants do not survive till adulthood (Sandbach et al., 2001). But AAV mediated knock-down of *Sod2* in the RPE of WT mice showed several features in an age-dependent manner including thinning of the ONL (Justilien et al., 2007).

About 10-15% of the patients develop wet AMD (Ferris III et al., 2013). Most sucessfully used CNV model uses lasers to mechanically induce lesions resulting in CNV. *Vegf* is the main factor involved in angiogenesis, but *Vegf* overexpression alone does not suffice, as a compromise to the BM is essential for CNV induction. Several models have shown that a combination of laser induction, VEGF and inflammatory cytokines' expression has been most successful in inducing CNV. (Grossniklaus et al., 2010).

Several age-related changes such as thickening of BM, lipofuscin accumulation, choriocapillary changes, reduced clearance ability of RPE cells may contribute to restricted oxygen supply from the choroid to the outer retina. And as these features are further enhanced in AMD patients, it has been postulated that the AMD retinas are hypoxic. Also hypoxic related genes are involved in mechanisms implicated in AMD - such as oxidative stress, angiogenesis and inflammation (Arjamaa et al., 2009a). But, so far a specific model to study hypoxic aspects of the disease in the retina has not been available.

1.3 Hypoxia and Retinal Degeneration

1.3.1 Hypoxia in health and disease

Hypoxia is defined as a condition of low/ inadequate levels of oxygen. Healthy people may experience systemic hypoxia while climbing mountains resulting in altitude sickness. In fact, populations of people living at high altitudes, such as Tibetan tribes are often studied to analyse genetic and metabolic adaptations that allow them to survive the hypoxic conditions (Beall, 2006; Simonson et al., 2010).

Prematurely born infants may experience systemic hypoxia, as the lungs may not be completely developed and fully functional. Hence they are placed in an incubator with continuous positive airway pressure (Baraldi and Filippone, 2007). But on the other hand, these infants are at a risk of developing retinopathy of prematurity (ROP) as the oxygen provided causes the retinal vessels to develop in an arbitrary manner resulting in poorly developed vessels, retinal detachment and severe vision problems in some cases (Gilbert, 2008).

Local hypoxia occurs when oxygen supply gets restricted in specific tissues such as during ischemic insults. Ischemia is the restriction of blood supply to the tissue. When the blood is unable to carry oxygen and nutrients to specific tissues, hypoxia ensues and when this condition is prolonged, cell death and tissue damage occurs. In case of patients who experienced a stroke, parts of the brain tissue may get hypoxic and be irreversibly damaged (Dirnagl et al., 1999).

Cellular hypoxia is a hallmark of cancers, as the tumor microenvironment is usually hypoxic (Vaupel and Mayer, 2007). Cancer cells' survival and proliferation depends on several genetic and metabolic adaptations to overcome limitations in oxygen and nutrient supply. One such well-studied mechanism is angiogenesis (sprouting of new blood vessels), which occurs when hypoxic tumor cells send signals to the surrounding vessels to fulfil their energy demands (Carmeliet and Jain, 2000; Vaupel and Mayer, 2007). Also tumor cells often have mutations in mitochondrial genes that impair oxidative phosphorylation, hence there is a metabolic switch to aerobic glycolysis to produce energy (Warburg effect) (Semenza, 2007; Vander Heiden et al., 2009).

1.3.2 Hypoxia Inducible Factors

At the cellular level, the hypoxic response is mediated by transcription factors called Hypoxia Inducible Factors (HIFs). The target genes that are transcribed by HIFs are involved in diverse mechanisms such as – angiogenesis, cellular metabolism, apoptosis, ROS formation

and oxidative stress, extracellular matrix regulation, immune response and inflammation (Majmundar et al., 2010; Semenza, 2012).

1.3.2.1 HIFs – types and structure

HIF is a heterodimer composed of an α and a β subunit (Wang et al., 1995). The HIFβ subunit also known as aryl hydrocarbon receptor nuclear translocator (Arnt) is constitutively expressed and has a nuclear localization. On the other hand the HIFα subunit is also constitutively expressed but immediately degraded in the presence of oxygen (normoxic conditions) with a half-life of 5 minutes (Aimee et al., 1998).

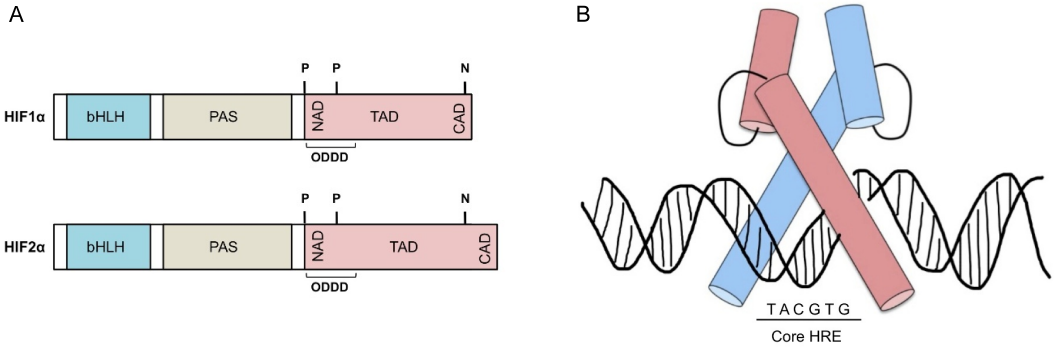

Figure 4. Structure and DNA-binding of HIF. **(A)** Schematic representation of HIF1a and HIF2a. The α subunit of HIF consists of the bHLH and PAS domains, as well as the transactivation domain (TAD). The NAD region overlaps with the oxygen-dependent degradation domain (ODDD) and consists of the conserved proline residues (marked as P) that are hydroxylated by PHDs. The conserved arginine (marked as N) that is hydroxylated by FIH is present at the CAD. **(B)** On translocation to the nucleus the α subunit forms a heterodimer with the β subunit to form the functional HIF that binds the target genes' HRE element to regulate transcription.

There are three HIFα paralogs– HIF1α, HIF2α and HIF3α as well as 3 paralogs of HIFβ – HIF1β, HIF2β and HIF3β (Lisy and Peet, 2008). The oxygen dependent regulation and transcription activity of both HIF1α and HIF2α are well characterized, whereas the regulation and activity of HIF3α is not well understood. The *Hif3α* gene has several splice variants and some studies have also postulated a negative regulation by HIF3α. A splice variant of HIF3α has been shown to form a dimer with HIF1β, and prevent its dimerization with HIF1α, thereby inhibiting transcription of target genes (Gu et al., 1997; Makino et al., 2001).

Both the α and β subunits are members of the basic helix-loop-helix/Per-Arnt-Sim (bHLH/PAS) family of transcription factors, and they both contain transactivation domains. The bHLH and PAS domains are present in both the subunits and are required for the recognition and binding of the hypoxia-responsive elements (HRE) in the promoter region of

the target genes (Figure 4B). The HRE is composed of the core-HRE or the HIF-binding site (HBS) containing the sequence – T(A/G)CGTG and the HIF ancillary sequence (HAS), which is an imperfect inverted repeat of this sequence. In addition the α subunit has an oxygen-dependent degradation domain (ODDD) (Kimura et al., 2001). This domain contains two proline residues that are critical for its oxygen dependent regulation – P402 and P564 in HIF1α and P405 and P531 in HIF2α. The transactivation domain (TAD) is composed of two main regions – N-terminal transactivation domain (NAD) and C-terminal transactivation domain (CAD) (Figure 4A). The two domains do not have much amino acid similarity implying distinct and divergent functions. A study comparing the two domains revealed that CAD is the most important domain controlling the regulation of most HIF target genes. The CAD has an asparagine residue that is critical for the oxygen dependent binding of transcriptional co-activators (Dayan et al., 2006; Jiang et al., 1997).

1.3.2.2 Molecular Mechanism of HIF1α stabilization

In normoxic conditions, prolyl hydroxylases (PHDs) hydroxylate the HIF1α subunit at the specific proline residues (P402 and P564) (Jaakkola et al., 2001). Three PHDs capable of performing this hydroxylation have been recognised – PHD1, PHD2 and PHD3 (Bruick and McKnight, 2001). Hydroxylated HIFA is recognized by the Von-Hippel-Lindau (VHL) which recruits elongin-C/ elongin-B/ cullin-2 E3-ubiquitin-ligase protein complex (Cockman et al., 2000; Maxwell et al., 1999). The E3 ubiquitin ligase in this protein complex poly-ubiquitinates HIF1A targeting the protein for proteosomal degradation (Ohh et al., 2000). Hence, under normoxic conditions the α subunit is degraded rapidly. Furthermore, Factor inhibiting HIF (FIH) (Mahon et al., 2001) hydroxylates HIF1α at an aspargine residue present in the CAD preventing recruitment of p300 (a transcriptional co-activator) and thus transcription of HIF target genes (Mahon et al., 2001).

These hydroxylation events are O_2 dependent and hence under hypoxic conditions PHD and FIH do not hydroxylate HIFα. As a result HIFα cannot be targeted by VHL- E3-ubiquitin-ligase complex for degradation and HIF1α gets stabilized, translocates to the nucleus, associates with HIF1β and the p300 co-activator (Gu et al., 2001) and regulates transcription of target genes. The FIH has been shown to be more tolerant to hypoxia than the PHDs, hence as the O_2 levels reach a particular threshold the PHDs lose their activity first, resulting in the expression of NAD-dependent target genes, and at more severe hypoxia, when FIH loses its activity, CAD-dependent targets are also expressed (Koivunen et al., 2004). This oxygen-dependent VHL mediated mechanism of regulation of the α subunit is one of the main mechanisms controlling cellular HIF activity (Figure 5). HIF2α has also been shown to be regulated in a similar manner (Loboda et al., 2010).

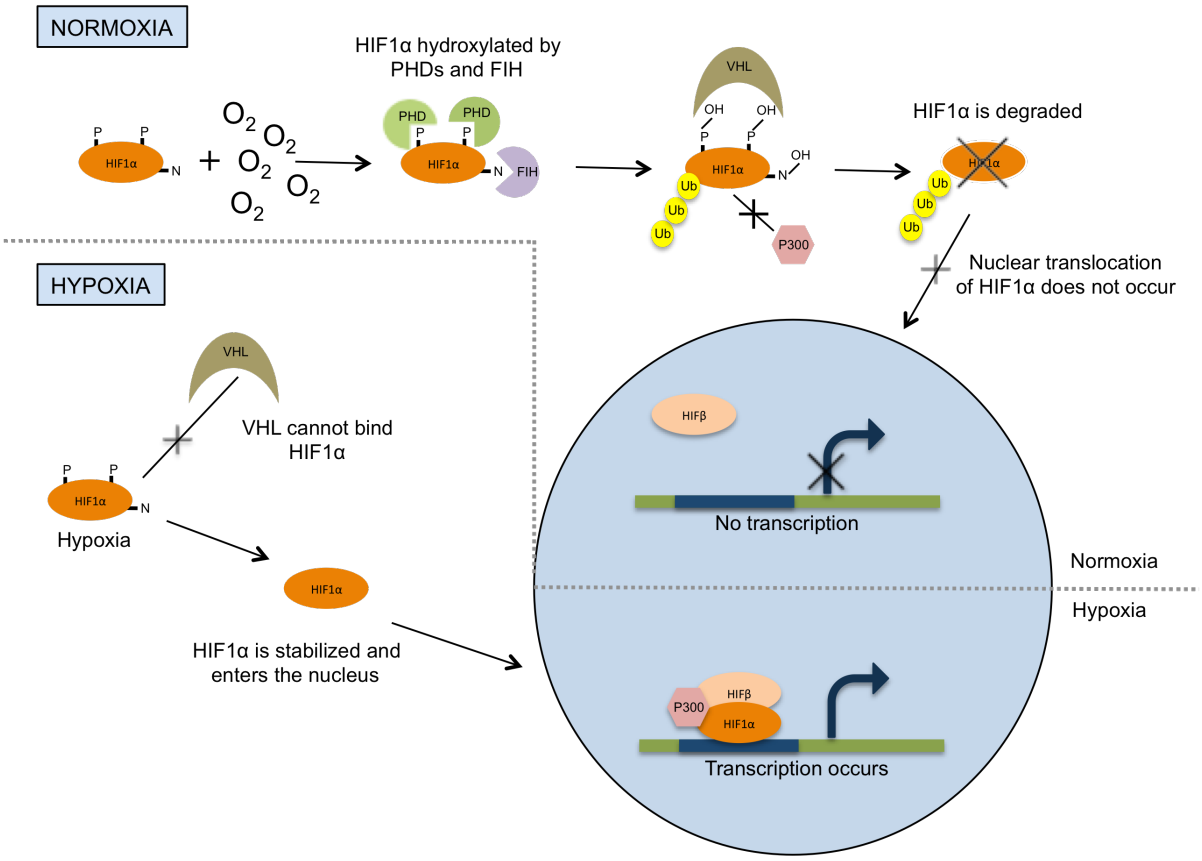

Figure 5. *Schematic representation of the molecular mechanism of oxygen-dependent stabilization and degradation of HIF1α. Under normoxic conditions, HIF1α is hydroxylated by PHDs and FIH. The hydroxylation event allows the recognition and binding by VHL, which is part of a protein complex. The ubiquitin-ligase in the complex ubiquitinates HIF1α, thereby resulting in its proteosomal degradation. On the other hand, under hypoxic conditions PHDs do not hydroxylate HIF1α which evades the VHL-mediated degradation, gets stabilized, translocates to the nucleus and causes transcription of the target genes.*

1.3.2.3 HIF1 target genes and responses

Hypoxia and stabilization of HIF results in the transcription of several genes that may be involved in pro-survival mechanisms such as angiogenesis, warburg effect and cell migration that allow tumor growth. On the other hand long term effects may be detrimental to the cells as in regulation of ECM, apoptosis and ROS accumulation.

Angiogenesis is the mechanism of sprouting of blood vessels from pre-existing ones and is required when a tumor grows beyond the size that can be supported by diffusion from existing vasculature. The HIF1 and HIF2 target gene *Vegf* (Vascular endothelial growth factor) is one of the best analysed HIF targets involved in angiogenesis (Ema et al., 1997). Anti-VEGF therapy is often used to control tumor growth and is presently also the only known

effective therapy to control wet AMD (Mitchell, 2011). Other HIF1 targets involved in angiogenesis are *Tgf-β3* (transforming growth factor), leptin and endoglin. And other targets such as nitric oxide synthase 2, heme-oxygense-1 and endothelin-1 can increase the permeability of vessels and cause vasodilation (Maynard and Ohh, 2007).

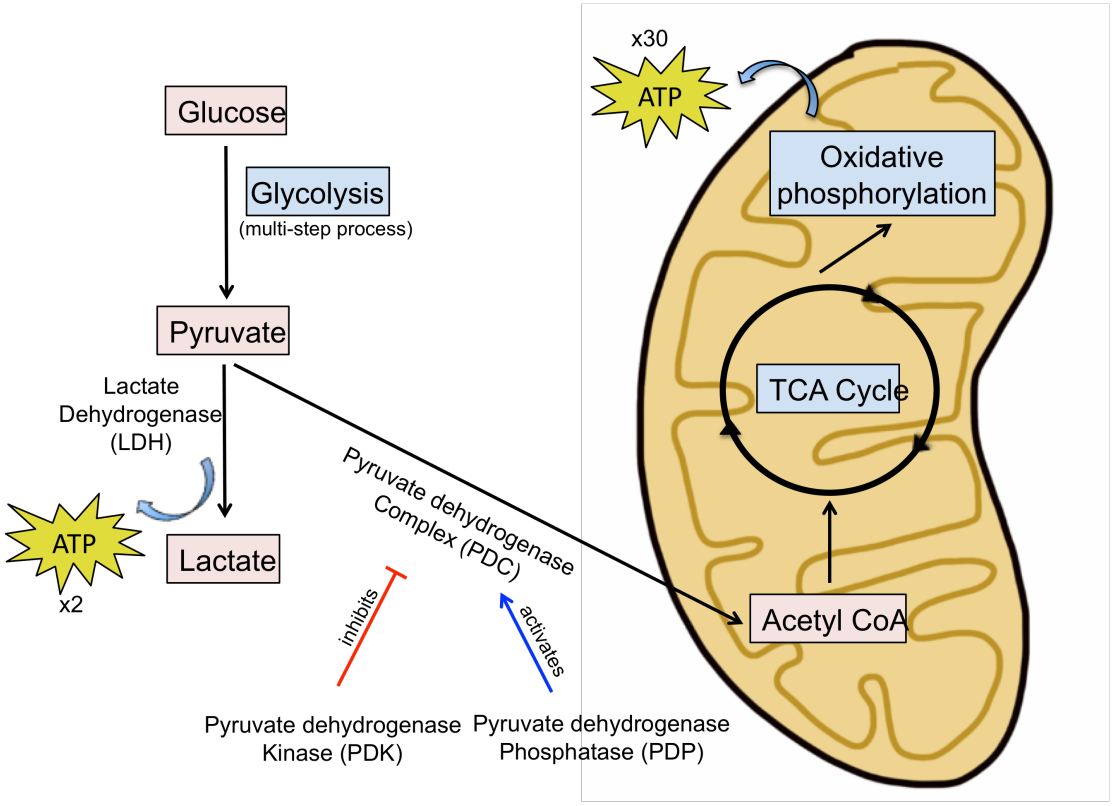

Figure 6. *Schematic representation of major energy producing cellular mechanisms. Glucose is converted to pyruvate by the multi-step process of glycolysis. Under aerobic conditions this is further converted to Acetyl-CoA by the pyruvate dehydrogenase complex (PDC). Components of the PDC are tighly regulated by the opposing effects of pyruvate dehydrogenase kinase (PDK), which inhibits the complex and Pyruvate dehydrogenase phosphatase (PDP), which activates the complex. Acetyl-CoA in the mitocondria enters the TCA cycle as well as undergoes oxidative phosphorylation to produce energy. Under anaerobic conditions Lactate dehydrogenase (LDH) acts on the pyruvate converting it to lactate and producing lower amounts of energy than produced by oxidative phosphorylation (For each glucose molecule 2 ATPs are produced by glycolysis, whereas 30 ATPs are gained from each glucose molecule by oxidative phosphorylation).*

Cells normally produce energy by both glycolysis and oxidative phosphorylation, wherein pyruvate produced during the last step of glycolysis gets converted to acetyl-CoA under aerobic conditions, and undergoes multiple steps of oxidative phosphorylation in the mitochondria to produce energy. Under anaerobic conditions the pyruvate is converted to lactate instead of acetyl-CoA producing lower amounts of energy (Figure 6). It has been

observed that cancer cells have a much higher glycolytic rate even under aerobic conditions, indicating that cancer cells produce most of their energy by aerobic glycolysis. This metabolic switch from oxidative phosphorylation to glycolysis is known as the 'Warburg effect'. HIF1 is involved in enhancing this effect by upregulating the enzymes involved in glycolysis such as hexokinase-2, glucose-6-phosphate isomerase and pyruvate kinase M2 (PKM2), Pyruvate dehydrogenase kinase (Pdk) as well as glucose transporters such as GLUT1 and GLUT3 (Stubbs and Griffiths, 2010).

HIF1 targets that are involved in cell migration are AMF (autocrine motility factor), urokinase-type plasminogen activator receptor (uPAR), E-cadherin and chemokine receptor 4. Growth and survival factors that are HIF1 mediated include TGF-α (transforming growth factor), survivin, COX-2 (cyclooxygenase), PDGF (platelet-derived growth factor), IGF-2 (insulin-like growth factor) and insulin-like growth factor binding proteins (IGFBPs) (Erler et al., 2006; Esteban et al., 2006; Graham et al., 1999; Liu et al., 2006). EPO (erythropoietin) is another HIF-mediated protective factor. It is a secreted glycoprotein that prevents apoptosis of early erythroid progenitor cells and allows their differentiation. *Epo* has been shown to have a HIF-dependent transcriptional regulation under hypoxic conditions, that results in an EPO upregulation followed by an increase in erythrocyte population and thus in the oxygen transport capacity of the blood (Jelkmann, 2004). In the retina, it has been shown that hypoxic preconditioning protects the tissue from subsequent toxic insult (degeneration by light exposure) and locally produced EPO among other factors has been suggested to be responsible for this protective effect (Grimm et al., 2002; Caprara and Grimm, 2012; Grimm and Willmann, 2012).

Short-term hypoxia may induce protective or pro-survival factors, but long-term hypoxia may be detrimental to tissue health as HIF1 also has the potential to induce several pro-apoptotic genes including Bnip3 (BCL2/ adenovirus E1B 19 kDa interacting-protein 3) and DDIT4 (DNA damage inducible transcript 4) (Bruick, 2000; Shoshani et al., 2002; Sowter et al., 2001). *Vhl* is one of the main regulators of HIF1α and in the retina, it has been shown that photoreceptor specific knock-down of *Vhl* resulted in stabilization of HIF1α, and these mice had photoreceptor loss and severe retinal degeneration after 1 year of age (Lange et al., 2011).

1.3.3 Hypoxia in the retina

The retina is known to consume more oxygen than most other tissues and hence is highly sensitive to alterations in oxygen levels, and hypoxia has a diverse range of effects on retinal function.

1.3.3.1 Hypoxia in retinal development

In the retina hypoxia plays an important role during early developmental stages, wherein it aids in the proper development of the retinal vasculature. Vascular endothelial growth factor (VEGF), involved in the process of vasculogenesis and angiogenesis is a target of the HIF transcription factors, which are the main regulators of the hypoxic response. So local hypoxia at the NFL and GCL result in the increased production of VEGF by astrocytes and ganglion cells that results in the formation of the primary plexi of the vasculature. Furthermore VEGF poduction by Muller cells is crucial for angiogenic sprouting of the deeper plexi. It was shown that mice lacking HIF1A failed to develop the intermediate plexi, whereas the primary and deeper plexi seemed less affected (Caprara et al., 2011). On the other hand mice with over-stimulated HIF1A also failed to develop the correct vessel architecture, as the vessels penetrated all cell layers- including the ONL (Kurihara et al., 2010; Lange et al., 2011).

During early development many retinal neurons undergo apoptosis, before the retina achieves the correct neuronal cell number and tissue architecture. Spatially and temporally controlled occurrence of hypoxia aids in this process of developmental apoptosis (Stone et al., 1995; Yancopoulos et al., 2000).

1.3.3.2 Hypoxia in retinal protection

Prolonged hypoxia is detrimental to the tissue, but several studies have shown that short term or acute hypoxia might have protective effects. It was shown that mice that were preconditioned with hypoxia were protected against damage by bright light that results in photoreceptor degeneration in non-preconditioned wild type mice. Such hypoxic preconditioning also protected against ischemia-reperfusion injury (Ara et al., 2011; Chouker et al., 2012; Zhan et al., 2011). This is most likely because acute hypoxia activates protective mechanisms by causing cells to secrete factors that might help the tissue cope with a subsequent toxic insult. One such hypoxia-induced factor is erythropoietin (EPO) that was shown to partially protect the photoreceptors in some situations (Grimm et al., 2002). Identification of such factors could be one approach towards developing therapies for preventing retinal degeneration (Grimm et al., 2002; Grimm et al., 2007).

1.3.3.3 Hypoxia in retinal degeneration and disease

Hypoxia during the early stages of development aids in the development of the retinal vasculature, but in the developed retina hypoxia may result in pathological choroidal neovascularization. These newly formed vessels penetrate the RPE and grow into the neuronal retina, but develop inadequately eventually leaking blood into the retina. This occurs in patients with wet AMD. Many age-related changes such as thickening of the Bruch's membrane, reduced ability of choriocapillaries to supply nutients and oxygen, drusen accumulation, reduced clearance capability of RPE cells and accumulation of products of oxidative stress are responsible for a reduced blood oxygen supply to the inner retina leading to mild but chronic hypoxia in dry AMD patients (Arjamaa et al., 2009b).

Glaucoma is the second leading cause of blindness worldwide. An increased intraocular pressure (IOP) and damage to ganglion cells are distinct features of the disease. But clinical features also include vascular abnormalities and impaired blood flow, that may cause hypoxia. Post mortem donor eyes showed higher staining for HIF1α in the retina and optic nerve head of glaucoma patients (Tezel and Wax, 2004).

Retinopathy of Prematurity (ROP) is a condition occuring in infants born prematurely. In utero the oxygen tension averages around 32 mmHg, while in normal room air the oxygen tension is between 60-100 mmHg. At full-term the retinal vasculature is completely developed, but in case of infants born pre-term the development is incomplete and the relative hyperoxic experience may prevent complete development of vessels due to the lack of hypoxia-induced angiogenic factors such as VEGF. It has been shown that administration of VEGF or EPO during the vaso-obliterative phase can preserve the retinal vasculature from hyperoxia-induced drop-out (Chen and Smith, 2007).

1.3.4. HIF1α in the retina

In new-born mice the total HIF1α level is high and decreases as the retina gets vascularized (Grimm et al., 2005). In the adult retina *Hif1α* has been detected in all the retinal layers although the spatio-temporal distribution varies during development. A systemic knock-out of *Hif1α* is mostly lethal, hence conditional knock-outs are used to elucidate it's function/ effect. Knockdown of *Hif1α* in adult rod photoreceptors (Thiersch et al., 2009) and Muller cells (Lin et al., 2011) did not result in morphological or functional abnormalities. But when *Hif1α* was knocked down in most cells of the developing retina, the intermediary plexus of vasculature failed to develop (Caprara et al., 2011). On the other hand, stabilization of HIF1α by knocking down the *Vhl* gene resulted in severe degeneration, gliosis and reduction in retinal function in older mice (Lange et al., 2011). In addition, stabilization of HIF1α in the retina was shown to

affect retinal vasculature resulting in reduced density and defects in the vasculature. These vascular defects in the *Vhl* knock-down mice could be rescued by injecting VEGF inhibitor, or by genetic inactivation of *Hif1α*, but not *Hif2α* (Kurihara et al., 2010).

Exposure to light causes retinal degeneration and in mice, is used as an experimental model for induced degeneration (Grimm and Remé, 2013). It was shown that when mice were treated with hypoxia (6 hrs at 6% O_2)(hypoxic preconditioning), they were protected from light-induced retinal degneration. These hypoxic pre-conditioned mice showed HIF1α stabilization and the extent of protection varied with the extent of hypoxia – 6-10% O_2 showed highest HIF1α stabilization and protection, 14% O_2 showed intermediate protection which was further reduced at 18% O_2 (Grimm et al., 2002; Grimm et al., 2007). The rod photoreceptor specific deletion of *Hif1a* did not affect the structure and function of the retina, and these mice also displayed protection to light damage conferred by hypoxic preconditioning (Thiersch et al., 2009). Taken together, these studies reveal that acute or short term hypoxia may upregulate some pro-survival genes that activate protective mechanisms, whereas long-term hypoxic effects might tend more towards cell death and degeneration (Grimm and Willmann, 2012).

AIM OF THE THESIS

The retina is a metabolically active tissue with high oxygen consumption hence is sensitive to hypoxia. The transcription factor HIF1 is a master regulator of the hypoxic response. In our lab it was shown that long-term inactivation of *Vhl* in the rod photoreceptors results in retinal degeneration. The main focus of my thesis was to study HIF1A, which is involved in hypoxic stress, but as a side project I also studied a receptor – GPR65, which is involved in pH stress.

The specific aims of my thesis are as follows –

1. HIF1A in the rod photoreceptors

- Characterization of the rod-specific single (*Vhl*) and double (*Vhl* and *Hif1a*) knockdown mice.
- In vitro studies for testing siRNAs against *Hif1a* that could be used for therapy.

2. HIF1A target genes in the retina

- Comparison of the transcriptomes of the rod-specific single (*Vhl*) and double (*Vhl* and *Hif1a*) knockdown mice.
- Analysis of complement factors.
- Role of a HIF1A target gene - Stanniocalcin2 in the retina.

3. pH stress in the retina

- Role of proton sensing G-protein coupled receptors in the retina.

3. RESULTS

3.1. Hypoxic stress and HIF1A in the retina

3.1.1 Rod-specific knockdown of *Vhl* and *Hif1a*

Hif1a knockdown rescues retinal degeneration caused by _Vhl_ deletion.

Divya Ail (DA)[1,2], Christian Caprara (CC)[1,4], Jadwiga Oczos (JO)[1], and Christian Grimm (CG)[1,2,3]

[1] Lab for Retinal Cell Biology, Department of Ophthalmology, University of Zürich, Zürich, Switzerland.

[2] Neuroscience Center(ZNZ), University of Zürich, Zürich 8057, Switzerland.

[3] Center for integrative human physiology (ZIHP), University of Zürich, Zürich, Switzerland.

[4] Present address: Swiss Stem Cell Foundation, Gentilino, Switzerland.

Author contributions:

Design: CG, DA

Experiment: DA (Maintenance of mice and genotyping, transcriptome data analysis, RT-PCR, Western blots, Immunohistochemistry, Imaging of morphologies, Fundus imaging, Fluorescein angiography), CC (lactate assay, Vessel flatmounts), JO (RPE flatmounts).

Interpretation: DA, CG

Manuscript: DA, CG

ABSTRACT

Several age-related changes affect the oxygen and nutrient supply to the retina and might cause a mild but chronic state of hypoxia. The retina is a metabolically active tissue with high oxygen consumption and is hence sensitive to hypoxia. The cellular hypoxic response is mainly executed by transcription factors called hypoxia inducible factors (HIFs). Earlier, it was shown that rod-specific deletion of Von Hippel-Lindau (*Vhl)* results in stabilization of HIF1A and HIF2A, which causes retinal degeneration at older age. Here we show that HIF1A is responsible for this degeneration, as the additional deletion of *Hif1a* rescues this phenotype. Furthermore, the stress related mechanisms activated in the mice with stabilization of HIF1A and HIF2A are not observed on *Hif1a* deletion. A comparison of retinal transcriptomes on rod photoreceptor specific stabilization and deletion of HIF1A revealed several differentially regulated genes. Analysis of some enzymes suggested a potential metabolic shift in cellular energy production from oxidative phosphorylation to glycolysis.

Keywords: *Vhl, Hif1a*, hypoxia, retinal degeneration, metabolism

INTRODUCTION

Age-related macular Degeneration (AMD) is the leading cause of blindness among the elderly – a survey estimates 50 million people to be affected by AMD worldwide. The cause of AMD is multifactorial including ageing (Evans, 2001), smoking (Thornton et al., 2005) and genetic predisposition (Evans, 2001). AMD can be categorized into two types – dry AMD and wet (exudative) AMD. The dry form of AMD is characterized by the formation and accumulation of drusen (extracellular deposits between the RPE and Bruch's membrane), and occurrence of geographic atrophy. AMD is a multi-factorial disease; hence several animal models are used to emulate the different features and study the mechanisms involved. Several age-related changes such as reduced density of choriocapillaries, thickening of the bruch's membrane, drusen accumulation, inability of the RPE to clear lipofuscin and by-products of oxidation, as well as a genetic predisposition and lifestyle contribute to a mild but chronic hypoxia in the aged and diseased retinas. Hypoxia and oxidative stress have been implicated in the pathogenesis of AMD (Beatty et al., 2000). Thus, a hypoxia model for degeneration would shed light on the molecular mechanisms involved in photoreceptor loss and retinal degeneration.

Transcription factors called hypoxia inducible factors (HIFs) are known to be involved in the regulation of gene expression in response to reduced oxygen levels (Webb et al., 2009). HIF is a heterodimer composed of an α and a β subunit (HIFA and HIFB) (Wang et al., 1995). The HIFB subunit also known as aryl hydrocarbon receptor nuclear translocator (Arnt) is constitutively expressed and has a nuclear localization. On the other hand the HIFA subunit is also constitutively expressed but immediately degraded in the presence of oxygen (normoxic conditions) with a half-life of 5 minutes (Aimee et al., 1998). There are three HIFA paralogs– HIF1A, HIF2A and HIF3A as well as 3 paralogs of HIFB – HIF1B, HIF2B and HIF3B (Lisy and Peet, 2008). In normoxic conditions, prolyl hydroxylases (PHDs) hydroxylate the HIF1A subunit at specific proline residues (Jaakkola et al., 2001). Hydroxylated HIFA is recognized by Von-Hippel-Lindau (VHL) which recruits elongin-C/ elongin-B/ cullin-2 E3-ubiquitin-ligase protein complex (Cockman et al., 2000; Maxwell et al., 1999). The E3 ubiquitin ligase in this protein complex poly-ubiquitinates HIF1A targeting the protein for proteosomal degradation (Ohh et al., 2000). Hence, under normoxic conditions the A subunit is degraded rapidly. Furthermore, Factor inhibiting HIF (FIH) (Mahon et al., 2001) hydroxylates HIF1A at an aspargine residue preventing recruitment of p300 (a transcriptional co-activator) and thus transcription of HIF target genes (Mahon et al., 2001). These hydroxylation events are O_2 dependent and hence under hypoxic conditions PHD and FIH do not hydroxylate HIF1A. As a result HIFA cannot be targeted by VHL- E3-ubiquitin-ligase complex for degradation and HIF1A gets stabilized, translocates to the nucleus, associates

with HIF1B and the p300 co-activator (Gu et al., 2001) and regulates transcription of target genes. HIF2A has also been shown to be regulated in a similar manner (Loboda et al., 2010).

On deletion of *Hif1a* in the developing retina using the Pax6 promoter, the intermediary plexus of vasculature failed to develop (Caprara et al., 2011). Furthermore pan-retina deletion of *Vhl* results in reduced vascular density, degeneration and loss of function (Kurihara et al., 2010; Lange et al., 2011b). It was shown that the rod photoreceptor-specific deletion of *Hif1a* did not affect the morphology and function of the retina (Thiersch et al., 2009), but the deletion of *Vhl* (causing stabilization of HIF1A and HIF2A in the rods) resulted in an age-related slowly progressing retinal degeneration and loss of function (Lange et al., 2011a). HIF1A and HIF2A have distinct target genes hence potentially activate different molecular pathways. To assess if the degeneration is caused by HIF1A, we generated double knock-down mice with rod photoreceptor-specific deletion of *Vhl* and *Hif1a*. In addition comparison of the retinal transcriptomes of Opsin-Cre;Vhl^{flox} and Opsin-Cre;Vhl^{flox};$Hif1a^{flox}$ mice revealed differential regulation of several potential HIF1A target genes.

EXPERIMENTAL PROCEDURES

Animals, Genotyping and verification of CRE-mediated sequence deletion - Animals were treated in accordance with the regulations of the veterinary authority of Zurich and the statement of the Association for Research in Vision and Ophthalmology (ARVO) for the use of animals in vision research. All mice were kept at the animal facility of the University Hospital Zurich in a light-dark (12h:12h) cycle with food and water ad libitum. Light was maintained at 60 lux at cage level during the light period. Mice were euthanized by CO_2 inhalation followed by cervical dislocation.

The 129S-$Vhlh^{tm1jae}$/J-mice, which have *lox*P sites flanking exon1 and part of the promoter of the Vhl gene (both the alleles are floxed and hereafter these mice are referred to as Vhl^{flox}), were purchased from Jackson laboratory (Bar Harbour, USA), the Opsin-Cre mice were acquired from Yun-Zheng Le (Oklahoma, USA) and the Opsin-Cre;Vhl^{flox} mice were generated as described earlier (Lange et al., 2011a). The $Hif1\alpha^{flox/flox}$ mice (hereafter referred to as $Hif1\alpha^{flox}$) were kindly provided by R.Johnson (UCSD, USA) and M.Gassmann (UZH, Switzerland). The Vhl^{flox} mice were crossed with $Hif1\alpha^{flox}$ mice to generate Vhl^{flox};$Hif1\alpha^{flox}$ and further with Opsin-Cre mice to generate Opsin-Cre;Vhl^{flox};$Hif1\alpha^{flox}$.

The presence or absence of the Cre transgene was detected by PCR using the following primer pair: forward – 5'-AGG TGT AGA GAA GGC ACT TAG C-3' and reverse – 5'-CTA

ATC GCC ATC TTC CAG CAG G-3'. In the presence of the transgene the amplification resulted in a 411 bp fragment. DNA was isolated from retinal tissue and the excision of the *Vhl* gene was tested by PCR using the following primers - forward-excised – 5'-CTG GTA CCC ACG AAA CTG TC-3', forward-unexcised- 5'-CTA GGC ACC GAG CTT AGA GGT TTG CG-3' and reverse-both- 5'CTG ACT TCC ACT GAT GCT TGT CAC AG-3'. The excised allele was identified as a 260 bp fragment and the unexcised allele as a 460 bp fragment. Similarly the excision of *Hif* was tested by PCR using the following 3 primers – forward-unexcised – 5'-GCA GTT AAG AGC ACT AGT TG-3', forward-excised-5'-TTG GGG ATG AAA ACA TCT GC-3' and reverse-both-5'-GGA GCT ATC TCT CTA GAC C-3'. The wt allele is amplified as a 240 bp fragment; floxed allele as a 260 bp fragment and the excised allele is a 270 bp fragment.

Transcriptome analysis – Retinas were isolated from 10-12 week old animals (N = 3) of the following genotypes - $Vhl^{flox};Hif1\alpha^{flox}$ (control), Opsin-Cre;Vhl^{flox} (single knock-down) and Opsin-Cre;$Vhl^{flox};Hif1\alpha^{flox}$ (double knock-down). RNA was isolated using the QIAGEN RNeasy isolation kit (Qiagen, Hilden, Germany), including a DNase treatment step to digest residual genomic DNA. The samples were further processed at the Functional Genomics Centre Zurich (FGCZ, Zurich, Switzerland). The RNA was processed using standard procedures and hybridized to Agilent Mouse 44K Microarray (Agilent Technologies, Santa Clara, USA). The lists of upregulated and downregulated genes were provided by the FGCZ and were subsequently filtered to generate lists of genes with fold change ≥ 2 and pValue < 0.05. To group differentially regulated genes according to their biological function; the Agilent IDs were imported into Database for Annotation, Visualization and Integrated Discovery (DAVID Bioinformatics Resources, National Institute of Allergy and Infectious Diseases, NIH, USA) (Huang et al., 2008).

Hypoxic treatment of animals – WT mice were exposed to reduced oxygen levels (7% O_2) in a chamber with food and water ad libitum. By altering the O_2:N_2 ratio, O_2 was reduced to the desired level in steps of 2% over a time period of 1 hr. Mice were kept at 7% O_2 for 6 hrs, and then retinas were immediately isolated for western blot analysis (as controls).

Light exposure – WT mice were dark-adapted overnight (16 h). Pupils were dilated with 1% cyclogyl (Alcon, Risch, Switzerland) and 5% neosynephrine (UrsaPharm, Saarbrücken, Germany) 30 minutes before exposure to 15'000 lux of white light for 2 hours. After exposure retinas were isolated from these mice for western blot analysis (as controls).

Morphology and light microscopy – To analyze retinal morphology by light microscopy, eyes were enucleated and fixed in 2.5% glutaraldehyde in 0.1 M cacodylate buffer (pH 7.3) at 4°C overnight. After fixation, cornea and lens were removed, and the eyecup was

separated into a superior and an inferior half by cutting through the optic nerve head. The trimmed tissue was washed in cacodylate buffer, contrasted with osmium tetroxide (1%, 1 h, room temperature), dehydrated by incubations in increasing ethanol concentrations, and embedded in Epon 812. Semi-thin sections (0.5 µm) were prepared and counterstained with toluidine blue. An Axioplan digitalized microscope (Zeiss Meditec, Jena, Germany) was used to examine the slides.

RNA isolation, cDNA synthesis and semiquantitative real-time PCR – Retinas were isolated through a corneal incision and immediately snap frozen in liquid nitrogen. Total RNA was isolated using RNeasy isolation kit (catalogue number: 74104, Qiagen, Hilden, Germany) or the High Pure RNA isolation kit (catalogue number: 11828665001, Roche Diagonistics, Basel, Switzerland). Residual genomic DNA was removed by a DNase I incubation step. RNA (650-1000 ng) was reverse transcribed using oligo(dT) and M-MLV reverse transcriptase (catalogue number: M1701, Promega, Madison, WI, USA). 10 ng of cDNA was used for gene expression analysis by semiquantitative real-time PCR using a LightCycler 480 instrument (Roche Diagnostics), the LightCycler 480 SYBR Green I Master mix (catalogue number: 04887352001, Roche Diagonistics), and specific primer pairs (Table 1). The primer pairs were designed to span large intronic sequences or to cover exon-intron boundaries. Gene expression was normalized to actin beta (*Actb*), and relative quantification was calculated using the comparative threshold method ($\Delta\Delta C_T$).

Western Blotting – Retinas were homogenized in 0.1 M Tris-HCL (pH 8) at 4°C and the protein content was determined using Bradford assay. Proteins (30 µg each) were separated by SDS- polyacrylamide gel electrophoresis using a 10% gel, and then blotted onto a nitrocellulose membrane by semi-dry transfer. After blocking the membrane for 1 hr with 5% non-fat dry milk (Bio-Rad, Munich, Germany) in TBST (10 mM Tris/HCl[pH8], 150 mM NaCl, and 0.05% Tween-20) membranes were incubated overnight with the primary antibodies (dilution 1:500) (Table 2). This was followed by incubation with HRP-conjugated secondary antibodies for 1 hr at room temperature. The protein bands were then visualized using the Renaissance Western Blot Detection Kit (PerkinElmer Life Sciences, Boston, MA, USA).

Immunofluorescence on retinal cryosections – Eyes were enucleated and fixed in 4% paraformaldehyde (PFA) overnight. The cornea and lens were removed and the eye-cups were transferred into a tube containing 30% sucrose in phosphate buffered saline (PBS). Eye-cups were then embedded in tissue cryoprotective medium (Leica Microsystems Nussloch GmbH, Nussloch, Germany) and snap – frozen in a 2-methylbutane bath cooled in liquid nitrogen. 12 µM thick sections were cut through the optic nerve head on a cryostat (Leica), air-dried, and stored at -80°C till further use. The retinal sections were incubated with

blocking solution (3% goat serum + 0.3% Triton-X in PBS) for 1 hr at room temperature. Then the primary antibody was applied and left at 4°C overnight (Table 2). Slides were washed 3 times with PBS followed by incubation with Cy2 or Cy3 conjugated secondary antibodies (Jackson Immunoresearch, Soham, UK) in blocking solution (dilution = 1:500) for 1 hr at room temperature. After 3 PBS washes the sections were nuclei-stained with DAPI, and the slides were mounted with the anti-fade medium Mowiol (Calbiochem, San Diego, CA, USA). Immunofluorescently labeled proteins were visualized using an Axioplan fluorescence microscope (Carl Zeiss AG).

RPE flatmount preparation and analysis - Eyes were enucleated and incubated in 2% paraformaldehyde (PFA) in 0.1 M phosphate buffer pH 7.4 (PB, 0.081 M Na_2HPO_4, 0.019 M $NaH_2PO_4.3H_2O$) for 5 minutes. Cornea and lens were removed and the remaining tissue was left in PB-salt (PB containing 140 mM NaCl and 2.7 mM KCl) for 20 minutes to allow the retina to separate from the eyecup. The retina was removed gently and the eyecup containing the RPE cut into a ‘‘clover-leaf’’ shape and post-fixed in 4% PFA in PB for 1 hr. Flat mounts were blocked with blocking solution (3% normal goat serum, 0.3% Triton X-100 in PBS) for 1 hr and incubated with the primary antibody anti-β-catenin (1:300 in blocking solution) overnight at 4°C. After washing 3x for 10 mins in PBS, Cy3- conjugated anti-mouse secondary antibody (1:200 in blocking solution; Jackson ImmunoResearch, Soham, UK) was applied for 2 hrs. Flat mounts were washed with PBS and mounted with anti-fade medium (10% Mowiol 4–88 (wt/vol); Calbiochem, San Diego, CA, USA; 25% glycerol (wt/vol); 0.1% 1,4-diazabicyclo [2.2.2] octane in 100 mM Tris, pH 8.5). The RPE sheets were examined using a digitalized fluorescence microscope (Axioplan 2; Carl Zeiss AG).

Four images were acquired from different quadrants of each retinal flatmount from 3 animals (A total of 12 images were analyzed for each genotype/condition). Quantification was done by manually counting the number of RPE cells.

Lactate assay – Both retinas were isolated in a single tube and homogenized in water, centrifuged and the supernatant was collected for lactate determination. Reactions were prepared with the Lactate Rapid Test kit (Catalogue number: LAC342, Diaglobal GmBH; Berlin, Germany) and measured using the Lactate Photometer Plus DP 110 (Diaglobal GmBH; Berlin, Germany).

Statistical analysis – Statistical analysis was performed using Prism 4.0 software (GraphPad, San Diego, CA, USA). All data are presented as mean ± standard deviation (SD). The number of samples (N) used for individual experiments is given in the figure legends. Student’s t-tests were used to measure the statistical differences of means and differences between two groups. A *P* value below 0.05 was considered significant.

RESULTS

Successful knockdown of *Vhl* and *Hif1a* in rod photoreceptors

The genomic DNA extracted from the retinas of 11 week old Opsin-Cre;*Vhl*^{flox} and Opsin-Cre;*Vhl*^{flox};*Hif1a*^{flox} mice and their corresponding controls (lacking Cre) were analyzed for the excision of the floxed sequence in *Vhl* and *Hif1a*. In the presence of Cre, *Vhl* was successfully excised from both Cre expressing mice (260 bp band). All mice show the unexcised allele (460 bp band), as the retinal genomic DNA consists of DNA from all cell types, whereas the excision is only in a specific cell type (rod photoreceptors). PCR for *Hif1a* resulted in the amplification of the WT allele (240 bp band) in case of the single knockdown mice, the floxed allele in case of the *Vhl*^{flox};*Hif1a*^{flox} control mice (260 bp band) and the floxed and excised allele (270 bp band) in case of the Opsin-Cre;*Vhl*^{flox};*Hif1a*^{flox} mice. Hence, these mice showed successful knockdown of the *Vhl* and the *Hif1a* gene (Figure 1A).

Then we analyzed whether the knockdown of Vhl resulted in stabilization of the HIF1A protein. Retinal protein extracts from 11 week old mice revealed increased levels of HIF1A and HIF2A under normoxic conditions in the Opsin-Cre;*Vhl*^{flox} mice, whereas the Opsin-Cre;*Vhl*^{flox};*Hif1a*^{flox} mice had HIF2A stabilized but not HIF1A. As expected both HIF1A and HIF2A were also detected in animals treated with hypoxia (7% O_2 for 6 hrs), but not in the normoxic controls. (Figure 1B).

Furthermore, to test if the stabilized HIF1A is transcriptionally active, we checked the expression of some known target genes. We observed a significant upregulation of Adrenomedullin (*Adm),* Vascular endothelial growth factor *(Vegf)* as well as Signal transducer and activator of transcription (*Stat3)* in the Opsin-Cre;*Vhl*^{flox} mice. Moreover, the gene expression of *Vhl* and *Hif2a* did not vary, but *Hif1a* was downregulated as expected in the Opsin-Cre;*Vhl*^{flox};*Hif1a*^{flox} mice (Figure 1C). Thus, our mice showed the inactivation of *Vhl* and *Hif1a*, resulting in the stabilization or absence of functionally active HIF1A under normoxia.

Deletion of *Hif1a* rescues HIF1A-mediated degeneration phenotype

Earlier work in our lab showed that long-term inactivation of *Vhl* under normoxic conditions in the rods caused photoreceptor death resulting in retinal degeneration and functional loss (Lange et al., 2011a). This was again confirmed by morphological analysis of the Opsin-Cre;*Vhl*^{flox} mice which, had normal retinal structure at 11 weeks but severe degeneration at 6 months of age. On the other hand the additional deletion of *Hif1a* in the Opsin-Cre;*Vhl*^{flox};*Hif1a*^{flox} mice rescued this degeneration phenotype and the retinas of these mice were comparable to controls at 11 weeks and 6 months of age (Figure 2A).

Quantification of the retinal thickness revealed a 30% loss in the ONL from 11 weeks to 6 months of age, which further deteriorated by 1 year of age (data not shown). There was not much difference at 11 weeks, but at 6 months of age, thickness of the photoreceptor layer (PR), ONL and outer segments was significantly reduced in the Opsin-Cre;*Vhl*^{flox} mice, while the double knockdown mice appeared similar to controls (Figure 2B).

Rod-specific stabilization and inactivation of HIF1A does not have a significant effect on the other retinal cell types

The RPE cells are important for the general health maintenance of the photoreceptors (Fuhrmann et al., 2014) and have a crucial role in the visual cycle (Bok, 1993). Hence, it is not a surprise that they are affected during disease processes. In AMD patients there is geographic atrophy caused by loss of RPE cells and photoreceptors (Holz et al., 2014), thus we prepared retinal flatmounts stained with beta-catenin to analyze the state of the RPE in our mice at 11 weeks and 6 months of age. The shape and the size of RPE cells did not vary between the different genotypes. In some regions of the Opsin-Cre;*Vhl*^{flox} RPE the beta-catenin appeared to have a more cytoplasmic localization, but this observation was not consistent (Figure 3A). Also the RPE of these mice at 6 month of age had vacant regions with no cells, but this is most likely an artifact from mechanical damage during tissue preparation. This is also supported by the evidence from immunostaining of retinal cryosections of 6 month-old mice with RPE65, which show that the RPE is structurally intact at 11 weeks and 6 months of age (Figure 3B).

Immunostaining on retinal cryosections at 11 weeks showed normal structure of the RPE, rods and cones, though in the Opsin-Cre;*Vhl*^{flox} mice the structure of the retina is slightly disorganized especially at the outer segments and the ONL, indicating an onset of degeneration. There appear to be fewer SWL cones, but the levels were comparable when tested by qPCR (data not shown). At 6 months of age the RPE appears intact, but about 30% of the photoreceptors are lost and the ONL is thinner as seen by the nuclear staining (Figure 3B).

One of the most important mechanisms triggered by hypoxia is angiogenesis, and 10-15% of all AMD patients' progress into the wet form of the disease characterized by aberrant vessel formation and leakage (Holz et al., 2014). Thus, we analyzed the blood vessels in these mice, which is elaborated in Section 3.1.2.

Rod-specific HIF1A stabilization activates stress-pathways in the retina

Degeneration is preceded by stress signaling pathways (Beatty et al., 2000; Samardzija et al., 2012) and hence, we tested some genes that are activated in stress related mechanisms.

We observed a significant upregulation of Caspase 1 (*Casp1),* CCAAT/ enhancer binding protein (C/EBP), delta *(Cepbd),* Endothelin 2 *(Edn2),* Fibroblast growth factor 2 *(Fgf2)* and *Stat3* in the Opsin-Cre;*Vhl*^{flox} mice at 11 weeks of age. This upregulation was not observed at 6 months of age, most likely because the cells that have the HIF1A stabilized are lost by this age (Figure 4A).

When the levels of protein was tested in these mice, we observed a stabilization of HIF1A at 11 weeks of age in the Opsin-Cre;*Vhl*^{flox} mice, with protein levels much higher than the controls or the Opsin-Cre;*Vhl*^{flox}*; Hif1a*^{flox} mice. At 6 months of age, HIF1A was still detected but the levels appeared comparable to the Opsin-Cre;*Vhl*^{flox}*; Hif1a*^{flox}. STAT3 levels were higher in the Opsin-Cre;*Vhl*^{flox} mice and interestingly remained high at 6 months of age. HIF2A was detected in the Opsin-Cre;*Vhl*^{flox}, Opsin-Cre;*Vhl*^{flox}*; Hif1a*^{flox} and hypoxic control mice as expected, but the levels of HIF2A was much higher in the Opsin-Cre;*Vhl*^{flox}*;Hif1a*^{flox} mice at 6 months of age, suggesting that the long-term presence of HIF2A is not detrimental to the photoreceptors. The phosphorylated and active form of STAT3 – pSTAT was detected only in the Opsin-Cre;*Vhl*^{flox} mice and hypoxic controls, reiterating the relation between HIF1A and STAT3 (Kim et al., 2008; Pawlus et al., 2014) (Figure 4B).

Retinal gliosis is an early sign of stress experienced by the retina. This is observed as activated Muller cells and astrocytes (Pekny et al., 2014; Wang and Wong, 2014). We observed higher levels of GFAP proteins (marker for gliosis) in the retinal sections of Opsin-Cre; *Vhl*^{flox} mice, which further increased at 6 months of age (Figure 4C). Taken together the gene expression and protein levels emphasized and supported the evidence that the stabilization of HIF1A in photoreceptors activates stress related pathways that eventually result in death and degeneration.

For a clearer understanding of the different mechanisms involved, it is important to systematically analyze specific components of the stress pathways with regard to hypoxia and retinal degeneration. As a first step towards this goal, we compared the transcriptomes of the mice with *Vhl* inactivated in the rods to the mice lacking both *Vhl* and *Hif1a* in the rods. The results from this analysis are elaborated in Section 3.1.3.

A potential shift in metabolism occurs in the Opsin-Cre; *Vhl*^{flox} mice

Normal cells produce energy by the efficient process of oxidative phosphorylation, whereas cancer cells produce energy by glycolysis. This metabolic shift in energy production is termed Warburg effect (Vander Heiden et al., 2009a). Since cancer cells thrive in a hypoxic microenvironment, hypoxia is implicated and HIF1A is associated with this phenomenon. We wanted to test if such a metabolic shift occurs in a hypoxia-like situation as

seen in the Opsin-Cre;*Vhl*^{flox} mice. We observed an upregulation of lactate dehydrogensae a - *Ldha* (Figure 5B) and pyruvate dehydrogenase kinase 1 - *Pdk1* (Figure 5A). LDHA is the enzyme that catalyzes the interconversion of pyruvate and lactate in the terminal step of glycolysis. Under aerobic conditions pyruvate enters the mitochondria to undergo oxidative phosphorylation, but oxygen deficiency drives lactate production (Gatenby and Gillies, 2004). However, when we tested the levels of lactate, the difference observed was not significant (Figure 5D). It is known that there are several monocarboxylate transporters (MCTs) that aid in the immediate and efficient efflux of the lactate produced (Bergersen and Eid, 2014), and a study reported that in rats the transporters – MCT1, MCT2, MCT3 and MCT 4 are distributed throughout the retina (Chidlow et al., 2005). A quick search through the transcriptome data for monocarboxylate transporters revealed that *Mct4* had a 4-fold upregulation on stabilization of HIF1A. We could confirm this upregulation by qPCR although the variation within the sample group was high. (Figure 5C). In most healthy normal cells, the pyruvate from glycolysis is converted to Actely-CoA by the enzyme complex - pyruvate dehydrogensae complex (PDC). This step is regulated by the action of pyruvate dehydrogenase phosphatase (PDP), which activates it and PDK that inhibits it (Holness and Sugden, 2003). We observed a 5-fold upregulation in *Pdk1* expression on stabilization of HIF1A (Figure 5A). In addition the catalytic and regulatory components of *Pdp1* showed a downregulation in the transcriptome data, but we were not able to confirm this by real-time PCR. Nonetheless, together these observations hint towards a potential metabolic shift in the energy production in a HIF1A-dependent manner.

DISCUSSION

The Opsin-Cre;*Vhl*^{flox} mice showed stabilization of HIF1A and in the Opsin-Cre;*Vhl*^{flox};*Hif1a*^{flox} mice both *Vhl* and *Hif1a* were inactivated in the rod photoreceptors (Figure 1A and 1B). On deletion of *Vhl*, HIF1A protein was stabilized and functional as observed by the upregulation of some target genes – *Adm, Vegf* and *Stat3* (Figure 1C). *Adm* encodes for a small signal peptide shown to be hypoxia regulated and a HIF1A target (Sena et al., 2014). VEGF is involved in angiogenesis and implicated in wet AMD (Mitchell, 2011). STAT3 is transcription factor involved in stress signaling. Some studies have suggested that HIF1A and STAT3 together modulate the expression of *Vegf* (Jung et al., 2005).

The inactivation of *Vhl* results in the accumulation of stable HIF1A and HIF2A proteins, and this results in severe degeneration and loss of function (Lange et al., 2011a). We observed that this degeneration is due to HIF1A and not HIF2A, as the additional deletion of *Hif1a* with *Vhl,* resulted in the rescue of phenotype. The Opsin-Cre;*Vhl*^{flox};*Hif1a*^{flox} mice had a retinal morphology comparable to controls at 6 months of age (Figure 2A). In

addition the stable HIF1A protein was detected in the Opsin-Cre;*Vhl*^{flox} at 11 weeks of age, but not at 6 months of age, most likely because the cells accumulating HIF1A were lost by this age. HIF1A protein was not detected in the double knockdown mice. HIF2A protein was detected in both genotypes at 11 weeks of age, and the levels were even higher in the double knockdown mice at 6 months of age (Figure 4B), further confirming that the accumulation of HIF1A and not HIF2A results in photoreceptor death and degeneration. Degeneration was also observed by immunohistochemistry, where there was a clear reduction in rhodopsin staining and thinning of the ONL at 6 months of age (Figure 3B). Also the rod specific transducin – *Gnat1* gene expression levels were significantly reduced at 6 months of age (Figure 4A).

RPE atrophy is one of the main clinical features of AMD (Holz et al., 2014); therefore we proceeded to test the effect of HIF1A stabilization and inactivation in the rods on the RPE structure and function. The RPE flatmounts stained with beta-catenin at 11 weeks and 6 months of age did not show any major differences in structure and number (Figure 3A). However, in several areas of the 6-month-old Opsin-Cre;*Vhl*^{flox} retinal flatmounts, beta-catenin did not have a clear localization at the cell membranes, but was present in the cytoplasm as well as the nucleus (Figure 3A). Beta-catenin has dual and distinct functions in the cell - it maintains cellular structural integrity as part of the adherens junction and also acts as a transcription factor (Ben-Ze'ev, 1999). A study on RPE cells in vitro showed that oxidative stress affected the integrity of the cells and caused cytoplasmic localization of beta-catenin (Bailey et al., 2004). Hence, the nuclear and cytoplasmic localization may hint towards secondary effects of the hypoxia-like situation and death of photoreceptors on the RPE. At 11 weeks and 6 months of age the RPE is intact as also evidenced by the immunohistochemical analysis (Figure 3B). It would be important to investigate the RPE changes at older age when most photoreceptors are lost.

STAT3 signaling is activated on phosphorylation (Imada and Leonard, 2000), and the phosphorylated STAT3 (pSTAT3) was observed only in the Opsin-Cre;*Vhl*^{flox} mice, suggesting the activation of JAK-STAT pathway on stabilization of HF1A. But interestingly, the levels of *Stat3* gene (Figure 4A) and of pSTAT3 protein remained high even at 6 months of age (Figure 4B), when most of the HIF1A-stabilized cells are probably lost suggesting that *Vhl* deletion may cause HIF1A stabilzation by a STAT3 mediated mechanism. But this might not be the case, as the pSTAT3 is not detected in the Opsin-Cre;*Vhl*^{flox}*; Hif1a*^{flox} mice, indicating the requirement of HIF1A for STAT3 activation. Hence, it is likely that HIF1A activates mechanisms that result in STAT3 activation in adjacent cells types, and these mechanisms persist even after HIF1A-stabilzed cells are lost, and may be responsible for the near complete degeneration observed at older age. Additional investigations to test STAT3-

mediated mechanisms in different retinal cell types will be essential to establish and understand this connection.

Cells produce energy in the cytoplasm by glycolysis and further by a more efficient mitochondrial mechanism of oxidative phosphorylation. In cancer cells mutations in mitochondrial genes (Gasparre et al., 2013), hypoxia (Weljie and Jirik, 2011), and lower ATP content (Vander Heiden et al., 2009b) are all reasons for tumor cells to switch from oxidative phosphorylation to glycolysis (Warburg effect) (Stubbs and Griffiths, 2010; Vander Heiden et al., 2009a). Relying on glycolysis for extended periods of time may result in energy deprivation as lesser energy is produced from this process compared to oxidative phosphorylation (Stubbs and Griffiths, 2010). The gene expressions for all three subunits of *Ldh* were tested in the normal WT retinas. *Ldha* had a very high expression in the retina, and very low levels of *Ldhb* and *Ldhc* were detected (data not shown). *Ldha* levels were higher in Opsin-Cre;Vhl^{flox} mice, but this did not result in a significant accumulation of lactate (Figure 5B and D). There could be two reasons - LDH can drive the pyruvate to lactate conversion and vice versa, depending on the availability of NADH and NAD+, so lactate can be converted back to pyruvate. This could be tested by measuring the levels of pyruvate in these mice. Another more likely possibility is that the lactate produced is immediately shuttled away from the cells into the blood stream for clearance (Bergersen and Eid, 2014) or for usage as a metabolite by other cell types (Brooks, 2009). This is supported by the higher levels of the transporter *Mct4* that we observed in the mice with *Ldha* upregulation. *Mct4* was tested because it was the only transporter that showed a 4-fold upregulation in the transcriptome analysis. It would be crucial to observe the localization of the MCT4 protein in the retina for a better understanding of mechanisms involved. Apart from the occurrence of aerobic glycolysis an important aspect of this effect is the reduction of oxidative phosphorylation. We observed a 5-fold upregulation of *Pdk1* (Figure 5A), which inhibits the PDC complex hence preventing the entry into the mitochondrial energy processes. This has been shown in several studies to be one of the crucial indicators of Warburg effect (McFate et al., 2008). Taken together, these observations strongly hint towards a potential metabolic shift in the retinas with HIF1A stabilized and further testing of specific metabolites and proteins in the different mice will be required to confirm this hypothesis.

In conclusion the stabilization of HIF1A in the rod photoreceptors results in activation of stress related pathways and a potential metabolic shift in energy production mechanisms that may eventually result in retinal degeneration. These changes observed are essentially due to HIF1A and not HIF2A; hence targeting *Hif1a* could be potentially used as a therapy to rescue hypoxia-mediated degeneration in the aged retinas.

ACKNOWLEDGEMENTS

The authors would like to thank members of the Swiss Stem Cell Foundation for assistance with lactate assays, Cornelia Imsand, Andrea Gubler and Christel Beck for their skillful assistance in experimental procedures and Dr. Thorsten Hornemann for helpful discussions. The Swiss National Science Foundation supported this work.

REFERENCES

Aimee, Y Yu, et al. (1998), 'Temporal, spatial, and oxygen-regulated expression of hypoxia-inducible factor-1 in the lung', *American Journal of Physiology-Lung Cellular and Molecular Physiology*, 275 (4), L818-L826.

Bailey, TA, et al. (2004), 'Oxidative stress affects the junctional integrity of retinal pigment epithelial cells.', *Invest Ophthalmol Vis Sci*, 45 (2), 675-84.

Beatty, S, et al. (2000), 'The role of oxidative stress in the pathogenesis of age-related macular degeneration.', *Surv Ophthalmol*, 45 (2), 115-34.

Ben-Ze'ev, A (1999), 'The dual role of cytoskeletal anchor proteins in cell adhesion and signal transduction.', *Ann N Y Acad Sci*, 886 37-47.

Bergersen, LH and T Eid (2014), 'Monocarboxylate transport matters.', *N Engl J Med*, 371 (20), 1931-32.

Bok, D (1993), 'The retinal pigment epithelium: a versatile partner in vision.', *J Cell Sci Suppl*, 17 189-95.

Brooks, GA (2009), 'Cell-cell and intracellular lactate shuttles.', *J Physiol*, 587 (Pt 23), 5591-600.

Caprara, Christian, et al. (2011), 'HIF1A is essential for the development of the intermediate plexus of the retinal vasculature', *Investigative ophthalmology & visual science*, 52 (5), 2109-17.

Chidlow, Glyn, et al. (2005), 'Expression of monocarboxylate transporters in rat ocular tissues', *American Journal of Physiology-Cell Physiology*, 288 (2), C416-C428.

Cockman, Matthew E, et al. (2000), 'Hypoxia inducible factor-α binding and ubiquitylation by the von Hippel-Lindau tumor suppressor protein', *Journal of Biological Chemistry*, 275 (33), 25733-41.

Evans, JR (2001), 'Risk factors for age-related macular degeneration.', *Prog Retin Eye Res*, 20 (2), 227-53.

Fuhrmann, S, C Zou, and EM Levine (2014), 'Retinal pigment epithelium development, plasticity, and tissue homeostasis.', *Exp Eye Res*, 123 141-50.

Gasparre, G, et al. (2013), 'Relevance of mitochondrial genetics and metabolism in cancer development.', *Cold Spring Harb Perspect Biol*, 5 (2),

Gatenby, Robert A and Robert J Gillies (2004), 'Why do cancers have high aerobic glycolysis?', *Nature Reviews Cancer*, 4 (11), 891-99.

Gu, Jie, Justine Milligan, and L Eric Huang (2001), 'Molecular mechanism of hypoxia-inducible factor 1α-p300 interaction A leucine-rich interface regulated by a single cysteine', *Journal of Biological Chemistry*, 276 (5), 3550-54.

Holness, MJ and MC Sugden (2003), 'Regulation of pyruvate dehydrogenase complex activity by reversible phosphorylation.', *Biochem Soc Trans*, 31 (Pt 6), 1143-51.

Holz, Frank G, et al. (2014), 'Geographic Atrophy: Clinical Features and Potential Therapeutic Approaches', *Ophthalmology*, 121 (5), 1079-91.

Huang, Da Wei, Brad T Sherman, and Richard A Lempicki (2008), 'Systematic and integrative analysis of large gene lists using DAVID bioinformatics resources', *Nature protocols*, 4 (1), 44-57.

Imada, K and WJ Leonard (2000), 'The Jak-STAT pathway.', *Mol Immunol*, 37 (1-2), 1-11.

Jaakkola, P, et al. (2001), 'Targeting of HIF-alpha to the von Hippel-Lindau ubiquitylation complex by O2-regulated prolyl hydroxylation.', *Science*, 292 (5516), 468-72.

Jung, JE, et al. (2005), 'STAT3 is a potential modulator of HIF-1-mediated VEGF expression in human renal carcinoma cells.', *FASEB J*, 19 (10), 1296-98.

Kim, HL, et al. (2008), 'HIF-1alpha and STAT3 client proteins interacting with the cancer chaperone Hsp90: therapeutic considerations.', *Cancer Biol Ther*, 7 (1), 10-14.

Kurihara, Toshihide, et al. (2010), 'von Hippel-Lindau protein regulates transition from the fetal to the adult circulatory system in retina', *Development*, 137 (9), 1563-71.

Lange, C, et al. (2011a), 'Normoxic activation of hypoxia-inducible factors in photoreceptors provides transient protection against light-induced retinal degeneration.', *Invest Ophthalmol Vis Sci*, 52 (8), 5872-80.

Lange, Christina, et al. (2011b), 'Retina-specific activation of a sustained hypoxia-like response leads to severe retinal degeneration and loss of vision', *Neurobiology of disease*, 41 (1), 119-30.

Lisy, K and DJ Peet (2008), 'Turn me on: regulating HIF transcriptional activity', *Cell Death & Differentiation*, 15 (4), 642-49.

Loboda, Agnieszka, Alicja Jozkowicz, and Jozef Dulak (2010), 'HIF-1 and HIF-2 transcription factors—similar but not identical', *Molecules and cells*, 29 (5), 435-42.

Mahon, PC, K Hirota, and GL Semenza (2001), 'FIH-1: a novel protein that interacts with HIF-1alpha and VHL to mediate repression of HIF-1 transcriptional activity.', *Genes Dev*, 15 (20), 2675-86.

Maxwell, Patrick H, et al. (1999), 'The tumour suppressor protein VHL targets hypoxia-inducible factors for oxygen-dependent proteolysis', *Nature*, 399 (6733), 271-75.

McFate, T, et al. (2008), 'Pyruvate dehydrogenase complex activity controls metabolic and malignant phenotype in cancer cells.', *J Biol Chem*, 283 (33), 22700-08.

Mitchell, Paul (2011), 'A systematic review of the efficacy and safety outcomes of anti-VEGF agents used for treating neovascular age-related macular degeneration: comparison of ranibizumab and bevacizumab', *Current Medical Research & Opinion*, 27 (7), 1465-75.

Ohh, M, et al. (2000), 'Ubiquitination of hypoxia-inducible factor requires direct binding to the beta-domain of the von Hippel-Lindau protein.', *Nat Cell Biol*, 2 (7), 423-27.

Pawlus, MR, L Wang, and CJ Hu (2014), 'STAT3 and HIF1alpha cooperatively activate HIF1 target genes in MDA-MB-231 and RCC4 cells.', *Oncogene*, 33 (13), 1670-79.

Pekny, M, U Wilhelmsson, and M Pekna (2014), 'The dual role of astrocyte activation and reactive gliosis.', *Neurosci Lett*, 565 30-38.

Samardzija, Marijana, et al. (2012), 'Activation of survival pathways in the degenerating retina of rd10 mice', *Experimental eye research*, 99 17-26.

Sena, JA, et al. (2014), 'HIFs enhance the transcriptional activation and splicing of adrenomedullin.', *Mol Cancer Res*, 12 (5), 728-41.

Stubbs, Marion and John R Griffiths (2010), 'The altered metabolism of tumors: HIF-1 and its role in the Warburg effect', *Advances in enzyme regulation*, 50 (1), 44-55.

Thiersch, Markus, et al. (2009), 'Retinal neuroprotection by hypoxic preconditioning is independent of hypoxia-inducible factor-1α expression in photoreceptors', *European Journal of Neuroscience*, 29 (12), 2291-302.

Thornton, J, et al. (2005), 'Smoking and age-related macular degeneration: a review of association.', *Eye (Lond)*, 19 (9), 935-44.

Vander Heiden, Matthew G, Lewis C Cantley, and Craig B Thompson (2009a), 'Understanding the Warburg effect: the metabolic requirements of cell proliferation', *science*, 324 (5930), 1029-33.

Vander Heiden, MG, LC Cantley, and CB Thompson (2009b), 'Understanding the Warburg effect: the metabolic requirements of cell proliferation.', *Science*, 324 (5930), 1029-33.

Wang, Guang L, et al. (1995), 'Hypoxia-inducible factor 1 is a basic-helix-loop-helix-PAS heterodimer regulated by cellular O2 tension', *Proceedings of the national academy of sciences*, 92 (12), 5510-14.

Wang, M and WT Wong (2014), 'Microglia-Muller cell interactions in the retina.', *Adv Exp Med Biol*, 801 333-38.

Webb, JD, ML Coleman, and CW Pugh (2009), 'Hypoxia, hypoxia-inducible factors (HIF), HIF hydroxylases and oxygen sensing.', *Cell Mol Life Sci*, 66 (22), 3539-54.

Weljie, AM and FR Jirik (2011), 'Hypoxia-induced metabolic shifts in cancer cells: moving beyond the Warburg effect.', *Int J Biochem Cell Biol*, 43 (7), 981-89.

FIGURE LEGENDS

Figure 1. Successful knockdown of *Vhl* and *Hif1a* in the rod photoreceptors. (A) PCR amplification of the floxed and excised fragments of the *Vhl* and *Hif1a* gene from the genomic DNA isolated from total retinal tissue of 11 week old mice. The floxed and excised fragments of the *Vhl* allele have lengths of 460 bp and 260 bp respectively, and the amplified fragments of the *Hif1a* excised, floxed and wt allele have lengths of 270 bp, 260 bp and 240 bp respectively. (B) Western blot analysis of HIF1A and HIF2A protein levels in (CRE-) and (CRE+) Vhl^{flox} and Vhl^{flox};$Hif1a^{flox}$ mice at 11 weeks of age, and control mice [N-Normoxia, H-Hypoxia (6 hr at 6% O_2), LD-Light damage (2 hr at 13000 lux)]. ACTB served as the loading control. (C) Relative gene expression of *Adm, Vegf, Stat3, Vhl, Hif1a* and *Hif2a* in (CRE-) controls (black bars), Opsin-Cre; Vhl^{flox} (red bars) and Opsin-Cre;Vhl^{flox};$Hif1a^{flox}$ mice (blue bars) at 11 weeks of age. . Expression was determined by semi-quantitative real-time PCR, normalized to *Actb* and expressed relative to the levels in Vhl^{flox} (set to 1). Shown are mean values ± SD of N = 3. Significance was tested using the Student's t-test (* $P < 0.05$, ** $P < 0.01$, ns-not significant).

Figure 2. Deletion of *Hif1a* rescues HIF1A-mediated degeneration phenotype. (A) Retinal morphology of Vhl^{flox};$Hif1a^{flox}$, Opsin-Cre;Vhl^{flox} and Opsin-Cre;Vhl^{flox};$Hif1a^{flox}$ mice at 11 weeks and 6 months of age. Shown are representative images of N = 3 retinas per genotype and time point. Scale bar: 50 µM. (B) Retinal thickness measured across the retina and averaged for four different regions in 3 sections per retina (total of 12 images measured for each genotype). Shown are measurements of the photoreceptor layer (PR), outer nuclear layer (ONL), inner segments (IS) and outer segments (OS) at 11 weeks and 6 months for the Vhl^{flox};$Hif1a^{flox}$ (black bars), Opsin-Cre;Vhl^{flox} (red bars) and Opsin-Cre;Vhl^{flox};$Hif1a^{flox}$ (blue bars). Measurements in each group are normalized to the control - Vhl^{flox};$Hif1a^{flox}$ (100%).

Shown are mean values ± SD for N = 3. Significance was tested using Student's t-test (* P < 0.05, ** P < 0.01, *** P < 0.001, ns- not significant).

Figure 3. Rod-specific stabilization and inactivation of *Hif1a* does not have a significant effect on the other retinal cell types. (A) RPE flatmounts of the different genotypes at 11 weeks and 6 months of age, immunostained for β-catenin. Shown are representative images of N = 3 mice per genotype. The number of RPE cells was counted from 12 images per genotype (4 images of N = 3 mice). (B) Retinal cryosections of the different genotypes immunostained for RPE65 (RPE), rhodopsin (Rod photoreceptors), cone-SWL (Short wavelength cone photoreceptors) and co-stained with DAPI (nucleus) at 11 weeks and 6 months of age. Scale bar: 50 µM

Figure 4. HIF1A stabilization results in activation of stress related mechanisms. (A) Relative gene expression of *Casp1, Cepbd, Edn2, Fgf2, Gnat1* and *Stat3* in (CRE-) controls (black bars), Opsin-Cre;*Vhl*^{flox} (red bars) and Opsin-Cre;*Vhl*^{flox};*Hif1a*^{flox} mice (blue bars) at 11 weeks and 6 months of age. Expression was determined by semi-quantitative real-time PCR, normalized to *Actb* and expressed relative to the levels in *Vhl*^{flox} (set to 1). Shown are mean values ± SD of N = 3. Significance was tested using Student's t-test (* *P* < 0.05, ** *P* < 0.01, *** *P* < 0.001). (B) Western blot analysis of HIF1A, STAT3 and pSTAT3 protein levels in (CRE-) and (CRE+) *Vhl*^{flox} and *Vhl*^{flox};*Hif1a*^{flox} mice at 11 weeks and 6 months of age, and control mice [N-normoxia, H-hypoxia (6 hr at 6% O_2), LD-light damage (2 hr at 13000 lux)]. ACTB served as the loading control. (C) Retinal flatmounts immunostained for GFAP and co-stained with DAPI (nucleus) at 11 weeks and 6 months of age. Scale bar: 50 µM.

Figure 5. Potential metabolic shift occurs on stabilization of HIF1A. Relative gene expression of (A) *Pdk1, (B) Ldha* and *(C) Mct4* in (CRE-) controls (black bars), Opsin-Cre;*Vhl*^{flox} (red bars) and Opsin-Cre;*Vhl*^{flox};*Hif1a*^{flox} mice (blue bars) at 11 weeks and 6 months of age. Expression was determined by semi-quantitative real-time PCR, normalized to *Actb* and expressed relative to the levels in *Vhl*^{flox} (set to 1). (D) Lactate levels in (CRE-) controls (black bars), Opsin-Cre; *Vhl*^{flox} (red bars) and Opsin-Cre; *Vhl*^{flox}; *Hif1a*^{flox} mice (blue bars) at 11 weeks of age, represented relative to the levels in *Vhl*^{flox} (set to 1). Shown are mean values ± SD of *N* = 3. Significance was tested using the Student's t-test (* *P* < 0.05, ** *P* < 0.01, *** *P* < 0.001).

Figure 1

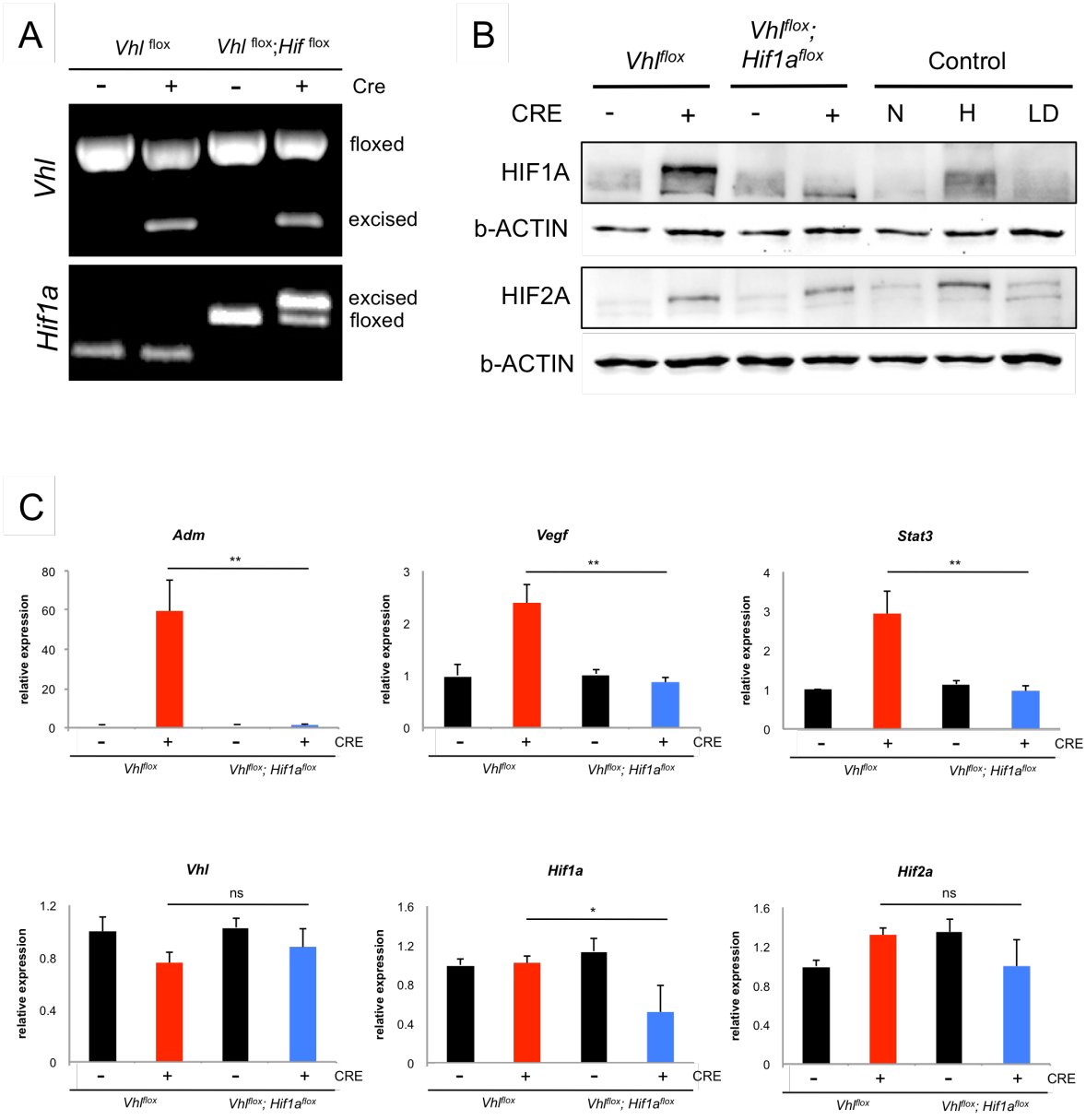
A
Vhl flox
Vhl flox;Hif flox
- + - + Cre
Vhl
floxed
excised
Hif1a
excised
floxed
B
Vhlflox
Vhlflox; Hif1aflox
Control
CRE - + - + N H LD
HIF1A
b-ACTIN
HIF2A
b-ACTIN
C
Adm
Vegf
Stat3
Vhl
Hif1a
Hif2a
relative expression
CRE
Vhlflox
Vhlflox; Hif1aflox
**
*
ns

Figure 2

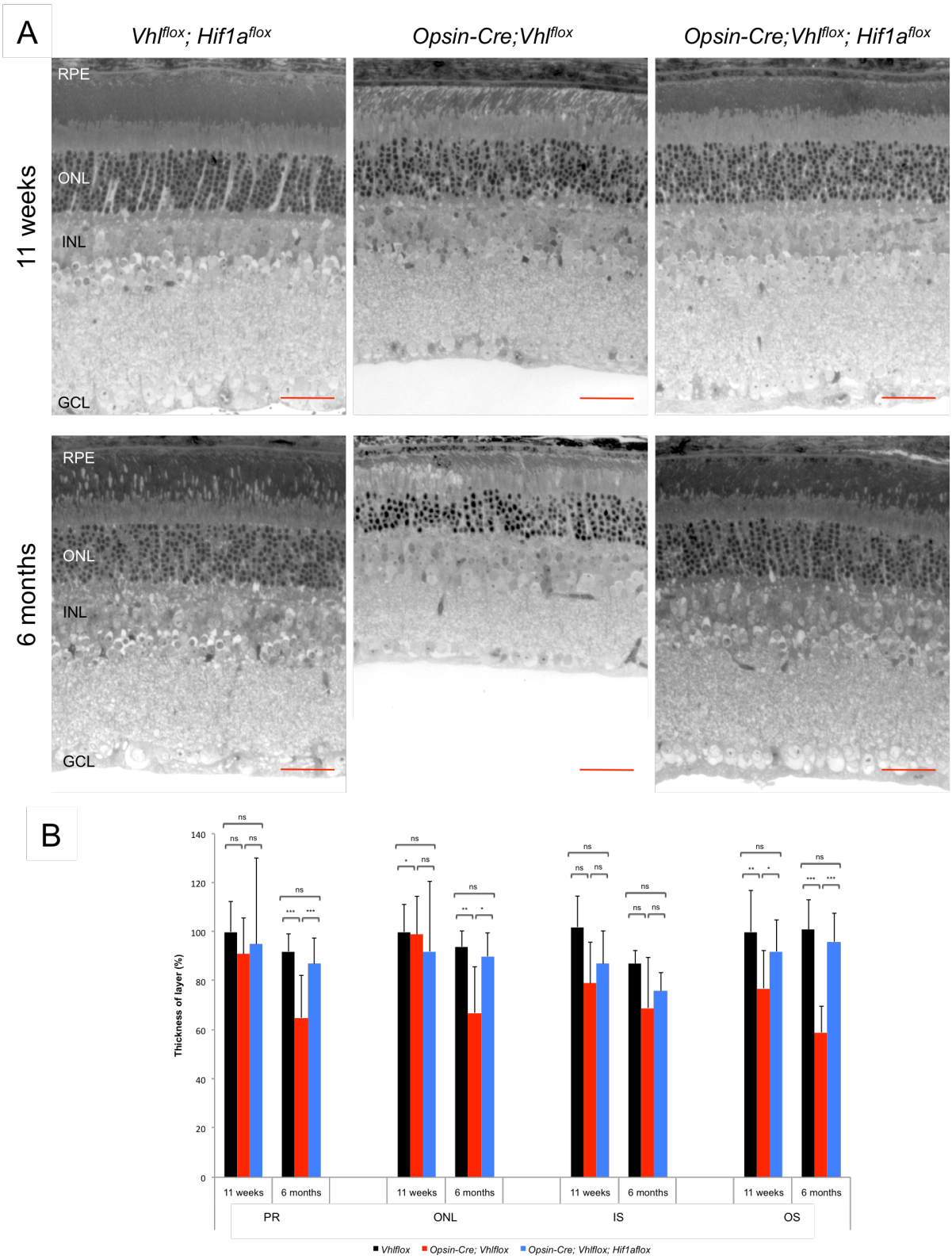
A
Vhlflox; Hif1aflox
Opsin-Cre;Vhlflox
Opsin-Cre;Vhlflox; Hif1aflox
11 weeks
6 months
RPE
ONL
INL
GCL
B
Thickness of layer (%)
0
20
40
60
80
100
120
140
ns
*
**
***
11 weeks
6 months
PR
ONL
IS
OS
Vhlflox
Opsin-Cre; Vhlflox
Opsin-Cre; Vhlflox; Hif1aflox

Figure 3

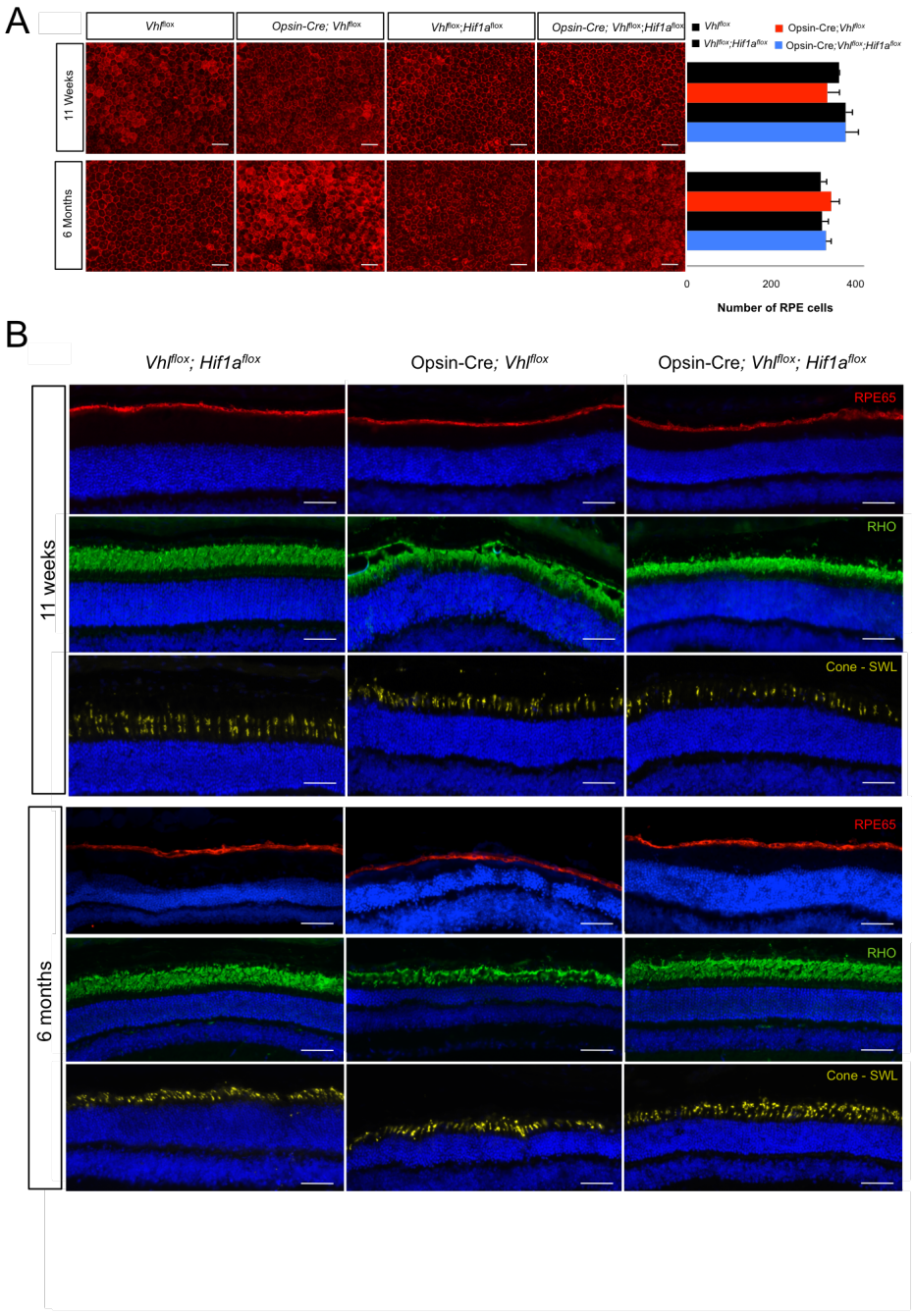
A
Vhlflox
Opsin-Cre; Vhlflox
Vhlflox;Hif1aflox
Opsin-Cre; Vhlflox;Hif1aflox
11 Weeks
6 Months
Vhlflox
Opsin-Cre;Vhlflox
Vhlflox;Hif1aflox
Opsin-Cre;Vhlflox;Hif1aflox
0
200
400
Number of RPE cells
B
Vhlflox; Hif1aflox
Opsin-Cre; Vhlflox
Opsin-Cre; Vhlflox; Hif1aflox
11 weeks
6 months
RPE65
RHO
Cone - SWL

Figure 4

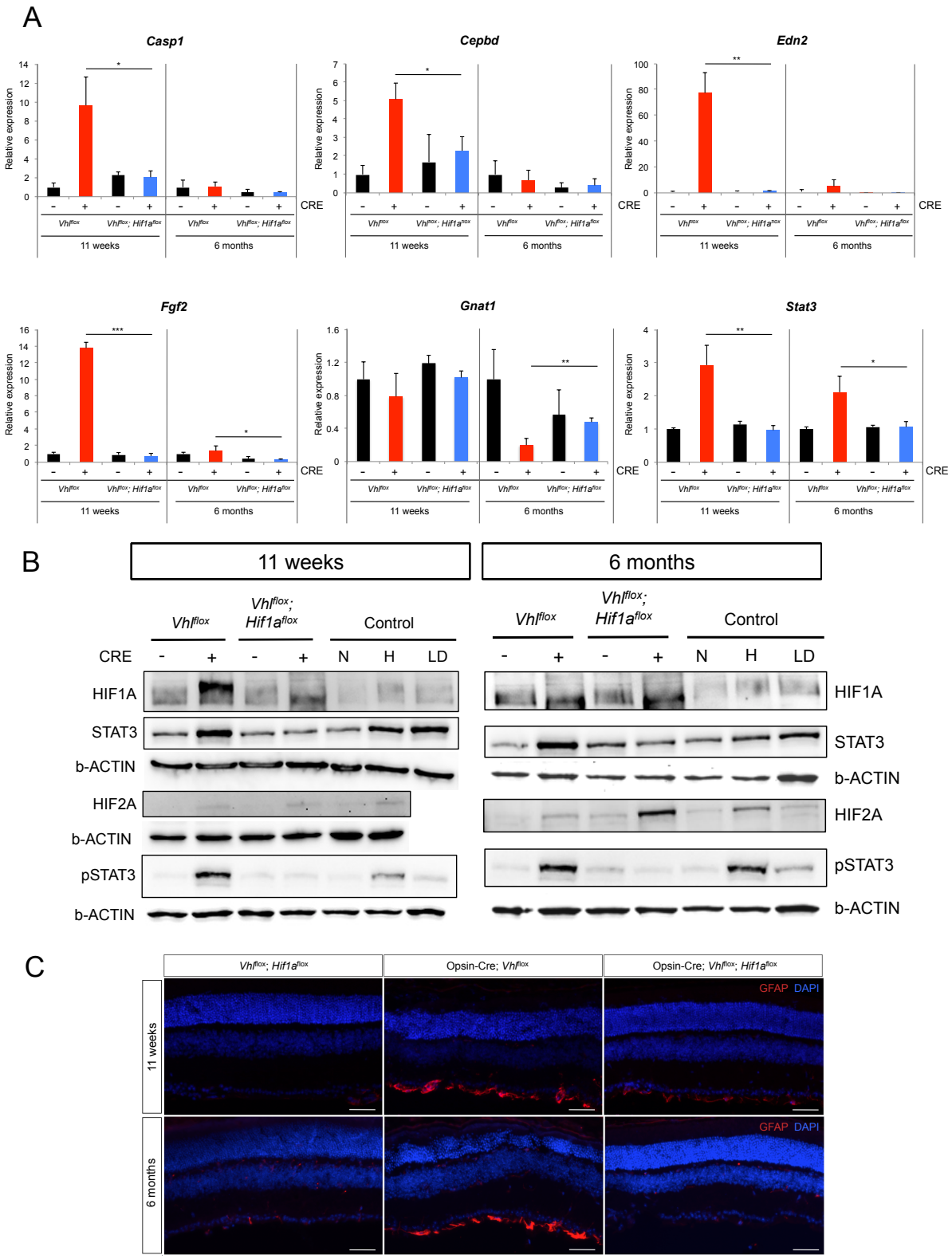
A
Casp1
Cepbd
Edn2
Fgf2
Gnat1
Stat3
Relative expression
CRE
Vhlflox
Vhlflox; Hif1aflox
11 weeks
6 months
B
11 weeks
6 months
Vhlflox
Vhlflox; Hif1aflox
Control
CRE
N
H
LD
HIF1A
STAT3
b-ACTIN
HIF2A
pSTAT3
C
Vhlflox; Hif1aflox
Opsin-Cre; Vhlflox
Opsin-Cre; Vhlflox; Hif1aflox
11 weeks
6 months
GFAP DAPI

Figure 5

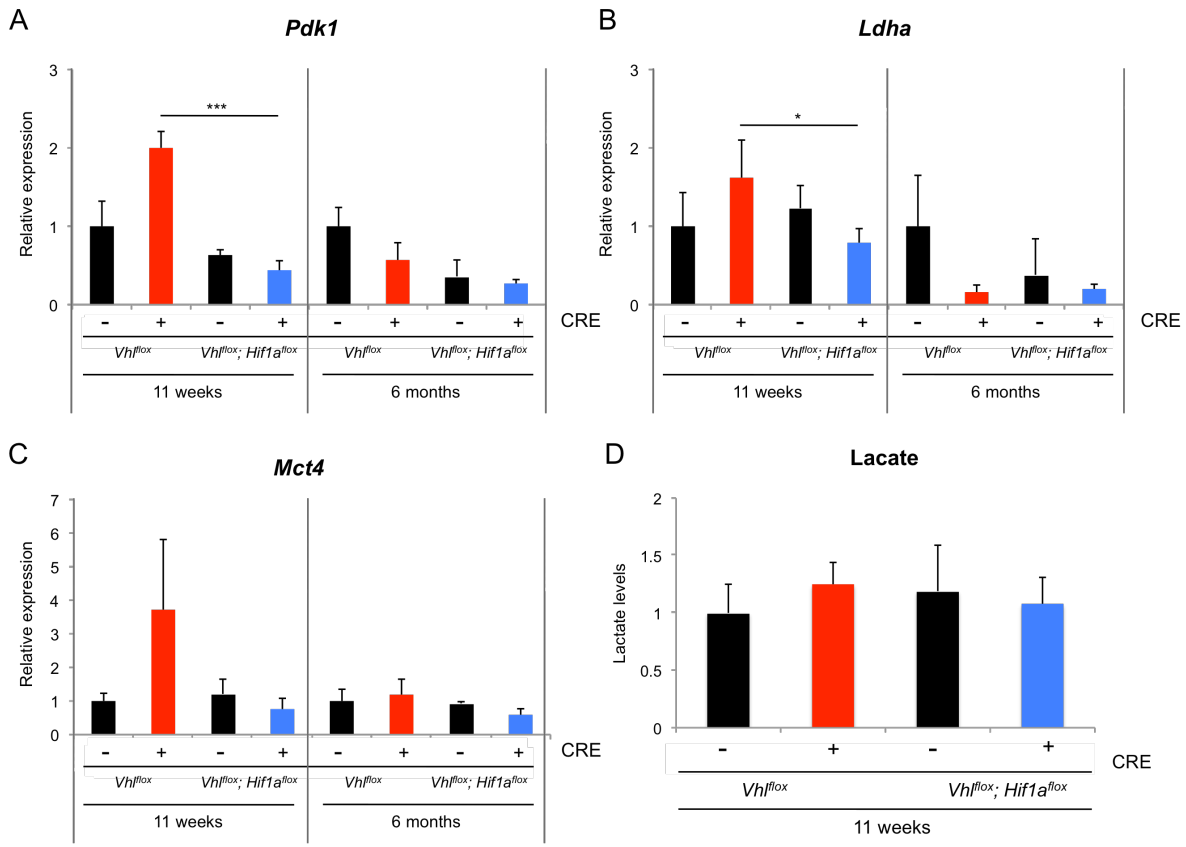
A
Pdk1
Relative expression
***
CRE
Vhlflox
Vhlflox; Hif1aflox
11 weeks
6 months
B
Ldha
*
C
Mct4
D
Lacate
Lactate levels

Table 1. Primers used for semiquantitative real-time PCR

Gene	Forward primer	Reverse primer	Annealing temp (°C)	Amplicon (bp)
Actb	CAACGGCTCCGGCATGTGC	CTCTTGCTCTGGGCCTCG	62	153
Adm	TTCGCAGTTCCGAAAGAAGT	GGTAGCTGCTGGATGCTTGTA	62	77
Casp1	GGCAGGAATTCTGGAGCTTCAA	GTCAGTCCTGGAAATGTGCC	60	138
Cebpd	CTTTTAGGTGGTTGCCGAAG	GCAACGAGGAATCAAGTTTCA	60	70
Edn2	AGACCTCCTCCGAAAGCTG	CTGGCTGTAGCTGGCAAAG	60	64
Fgf2	TGTGTCTATCAAGGGAGTGTGTGC	ACCAACTGGAGTATTTCCGTGACCG	62	158
Gnat1	GAGGATGCTGAGAAGGATGC	TGAATGTTGAGCGTGGTCAT	58	209
Hif1a	TCATCAGTTGCCACTTCCCCA	CCGTCATCTGTTAGCACCATC	60	198
Hif2a	GGAGCTCAAAAGGTGTCAGG	CAGGTAAGGCTCGAACGATG	60	61
Ldha	GGCACTGACGCAGACAAG	CTCATTGATTCCATAGAGAC	62	201
Mct4	CCGCTCTGCAGTGTGTGTGT	GCCAGACCCAAGCCAGTGAT	62	155
Pdk1	GTTGAAACGTCCCGTGCT	AGTCTCCTCGACGGATTCTGT	62	170
Stat3	CAAAACCCTCAAGAGCCAAGG	TCACTCACAATGCTTCTCCGC	62	133
Vegf	ACTTGTGTTGGGAGGAGGATGTC	AATGGGTTTGTCGTGTTTCTGG	60	171
Vhl	GAGGGACCCGTTCCAATAAT	TTGGCAAAAATAGGCTGTCC	60	364

Table 2. Antibodies used for immunofluorescence on retinal sections/ flatmounts

Protein	Host	Supplier	Catalogue number	Dilution
RPE65	rabbit	Pineda antibodies, Berlin, Germany	Pin-5	1:500
RHO	mouse	Sigma, st. Loiuis, MO, USA	O4886	1:1000
Cone-SWL	goat	Santa Cruz, Dallas, TX, USA	Sc-14363	1:500
Beta - catenin	rabbit	BD Biosciences, Allschwill, Switzerland	610153	1:300
GFAP	mouse	Sigma, st. Loiuis, MO, USA	G3893	1:500

3.1.2. Analysis of retinal vessels

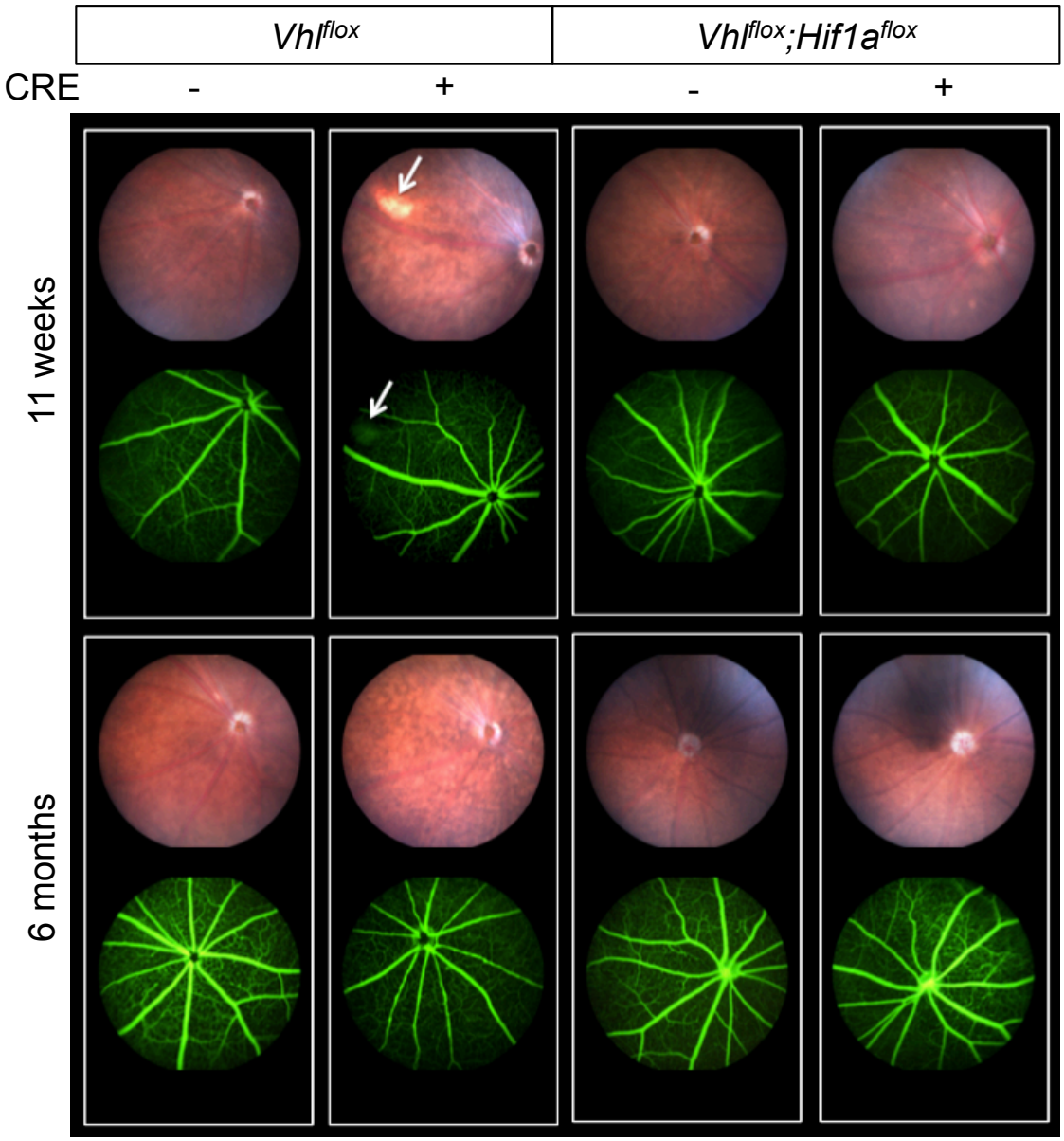

Figure 7. *Analysis of the fundus and the leakage of blood vessels. Images of the fundus (top) and the retinal blood vessels - fluorescein angiography (bottom) of the Opsin-Cre;Vhl^{flox} and Opsin-Cre;Vhl^{flox};Hif1a^{flox} and their corresponding controls - Vhl^{flox} and Vhl^{flox};Hif1a^{flox} (lacking the CRE) mice at 11 weeks and 6 months of age. Shown are representative images from N= 3 for each genotype at each time point.*

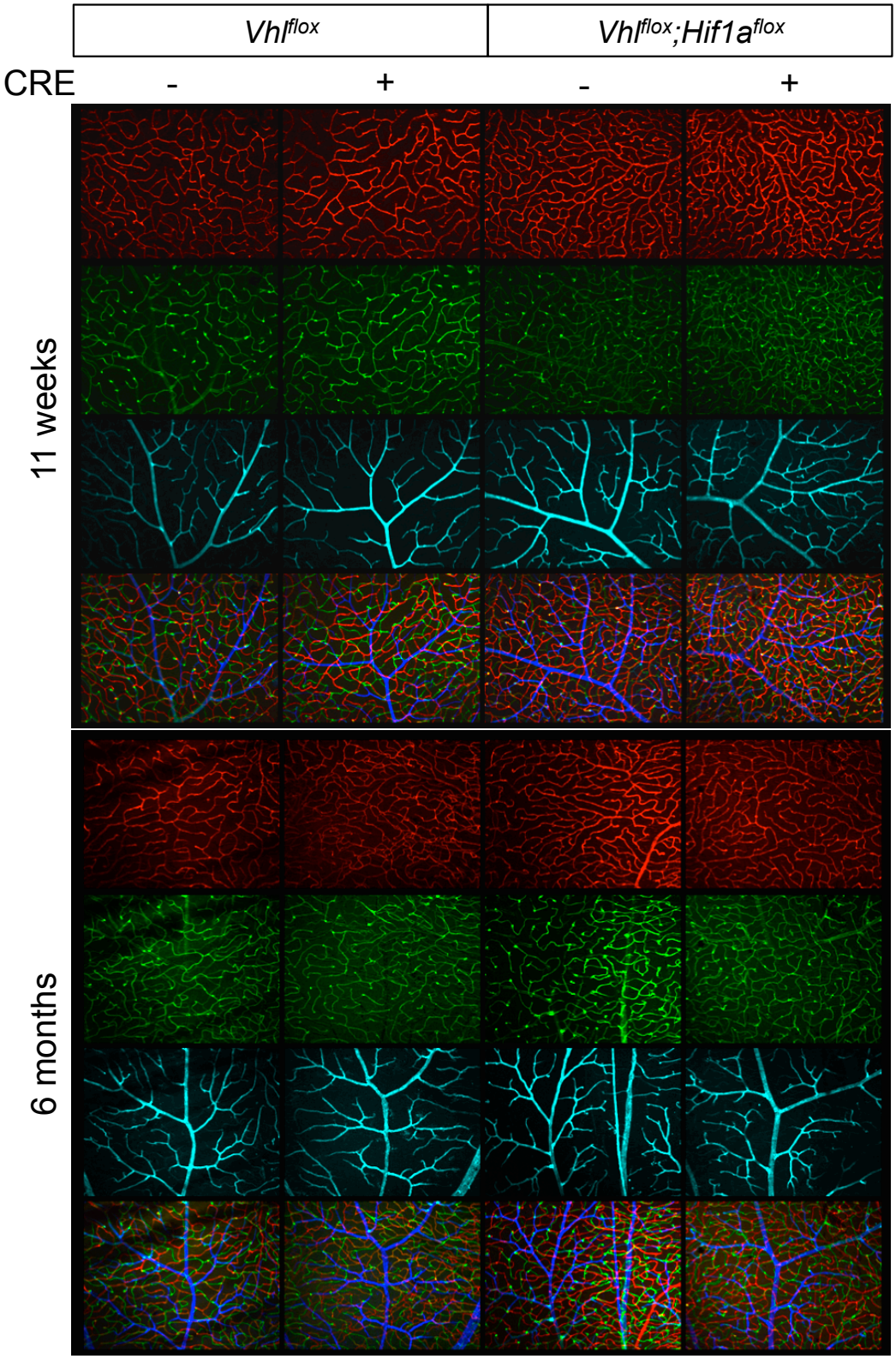

Figure 8. *Analysis of the primary, intermediate and deep plexus of retinal blood vessel layers. Retinal flatmounts of the Opsin-Cre;Vhl^{flox} and Opsin-Cre;Vhl^{flox};Hif1a^{flox} and the corresponding controls - Vhl^{flox} and Vhl^{flox};Hif1a^{flox} (lacking the CRE), immunostained for blood vessels (with Isolectin) at 11 weeks and 6 months of age. Images for each layer are acquired separately and digitally post-processed in different colors – red (deeper plexus), green (intermediate plexus) and blue (primary*

plexus). The bottom panel shows a merged image of all three layers. Shown are representative images from N= 3 for each genotype at each time point.

Analysis of retinal vessels

The retina relies on the choroid and the retinal vasculature for supply of oxygen and nutrients, hence vessel dystrophy is often observed as a cause or consequence during retinal degeneration. We analyzed the vessels by fluorescein angiography, but did not observe any particular anomalies. In some mice a scar was seen in the fundus images with corresponding vessel leakage (arrow in Figure 7), but these were observed only in a few mice (also in the controls). We repeated the analyses for these mice at later time points (4, 6, 9 and 12 months) to monitor the development or changes. But in most cases the scars and the corresponding leakage remained the same (data not shown). In the fundus images of the Opsin-Cre;*Vhl*^{flox} mice dark spots were observed due to the degeneration process, already at 11 weeks of age and these were particularly distinct at 6 months of age.

Retinal flatmounts were prepared and immunostained for the blood vessels. Then each of the layers – superficial, intermediate and deep plexus, was imaged separately. At 11 weeks of age, the deep plexus of the Opsin-Cre;*Vhl*^{flox} mice seem less dense. There were some differences in the intermediate layer too, but these were more difficult to discern, as the layers could not be distinguished well, so the images of deep and intermediate layers appear merged. This distinction becomes even more difficult at 6 months of age as due to the degeneration and thinning of the retina, the layers seem to be overlapping. Nonetheless, there were no major differences in the vessel structure as seen in the flatmounts, and no vessel leakage, as seen by fluorescein angiography.

3.1.3. Testing siRNAs against *Hif1a*

Long-term stabilization of HIF1A in the rods results in degeneration whereas in mice lacking HIF1A the retina is intact. Hence as a future therapeutic approach, we wanted to test the rescue of phenotype in Opsin-Cre;*Vhl*^{flox} mice by knock-down of *Hif1a* by RNA interference using small-interfering RNAs (siRNAs). The siRNA sequences could be used to design small hairpin RNAs (shRNAs), as they are more stable upon transfection and less likely to be degraded by cellular RNAses. The shRNA would be then packaged into adeno-associated vector – AAV2/8, which has been shown to successfully target the photoreceptors (Koch et al., 2012). The Hif1a-shRNA packaged into AAVs can then be injected sub-retinally into the Opsin-Cre;*Vhl*^{flox} mice to test for the rescue of the degeneration phenotype (Figure 9A). For this 4 different pre-designed sequences were ordered from a company (Dharmacon, Wohlen, Switzerland) and tested in NIH3t3 cells after 6 hours hypoxia. Seq1 was not efficient, Seq2, Seq3 and Seq4 were able to knock-down *Hif1a*, with Seq2 being the most efficient (Figure9B). From Seq2 we would need to design the shRNA and testing the shRNA requires an expression vector.

We received a plasmid expressing shRNA against Hif1a (*Hif1a*-shRNA-IF) (kindly provided by Prof.Ian Frew) and decided to test the efficiency of this sequence compared to Seq2. The functional part of this shRNA (named siRNA-IF) was ordered for testing. Both the Seq2 and siRNA-IF were equally efficient in the knock-down of Hif1a (Figure 9A)

Sequencing of the Opsin-Cre;*Vhl*^{flox} mice revealed some differences in binding regions of the siRNAs in the mouse and human *Hif1a* sequence – 2 bp difference for Seq2 and 1 bp difference for siRNA-IF (Figure 9D). Hence, we ordered human and mouse specific sequences of both Seq2 and siRNA-IF. These were then tested in mouse cells (NIH3t3) and human cells (HEK). And we observed that the mouse specific sequence was efficient in mouse cells while the human sequence was not efficient and vice versa, even though the difference is in just 1-2 bp. The *Hif1a*-shRNA-IF received is mouse specific, but in the future if this is translated for gene therapy experiments in mice or human clinical trials then care has to be taken to design very specific sequences. The *Hif1a*-shRNA-IF plasmid was sent to our collaborators (Prof. Martin Biel's lab in LMU, Munich, Germany) for cloning and packaging into the AAVs.

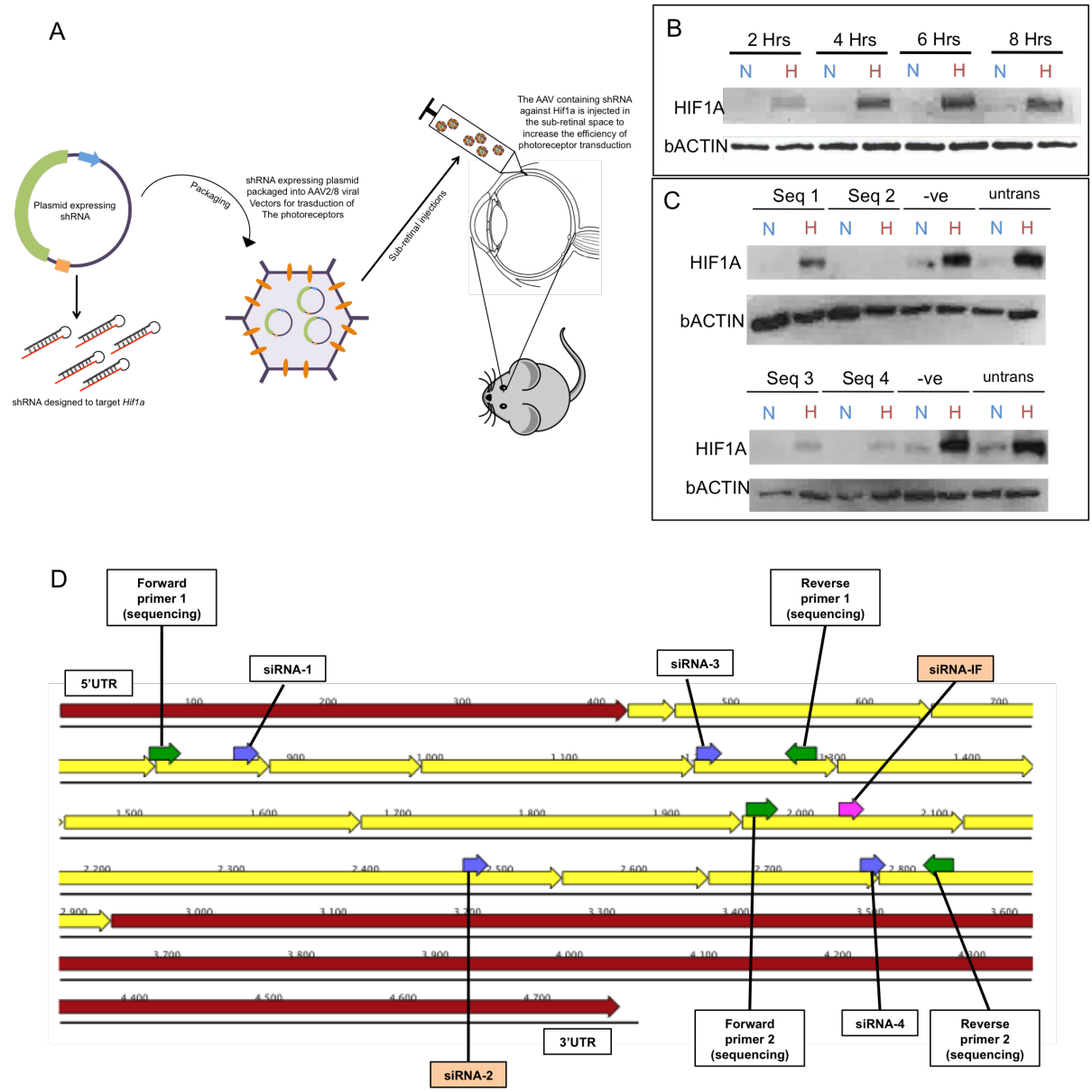

Figure 9. *In vitro testing of siRNAs against Hif1a. (A) Schematic representation of the intended use of the siRNAs for silencing the Hif1a gene in the Opsin-Cre;Vhl^{flox} mice to rescue the degeneration phenotype. (B) Western blot analysis of HIF1A in NIH3t3 cells kept at hypoxia (H) - 0.2% O_2 or normoxia (N) for 2, 4, 6 and 8 hours. bACTIN was used as the loading control. (C) Western blot analysis for HIF1A after treatment with 4 different siRNAs against Hif1a – Seq1, Seq2, Seq3 and Seq4, scrambled siRNA (-ve control) and untransfected control (untrans). (D) Specific binding regions of the Hif1a siRNAs. The UTR is in red, exons in yellow, Seq1, Seq2, Seq3 and Seq4 are shown as purple arrows, and the sequencing primers are shown as green arrows. The short interfering portion of the Hif1a-shRNA-IF is shown as a pink arrow.*

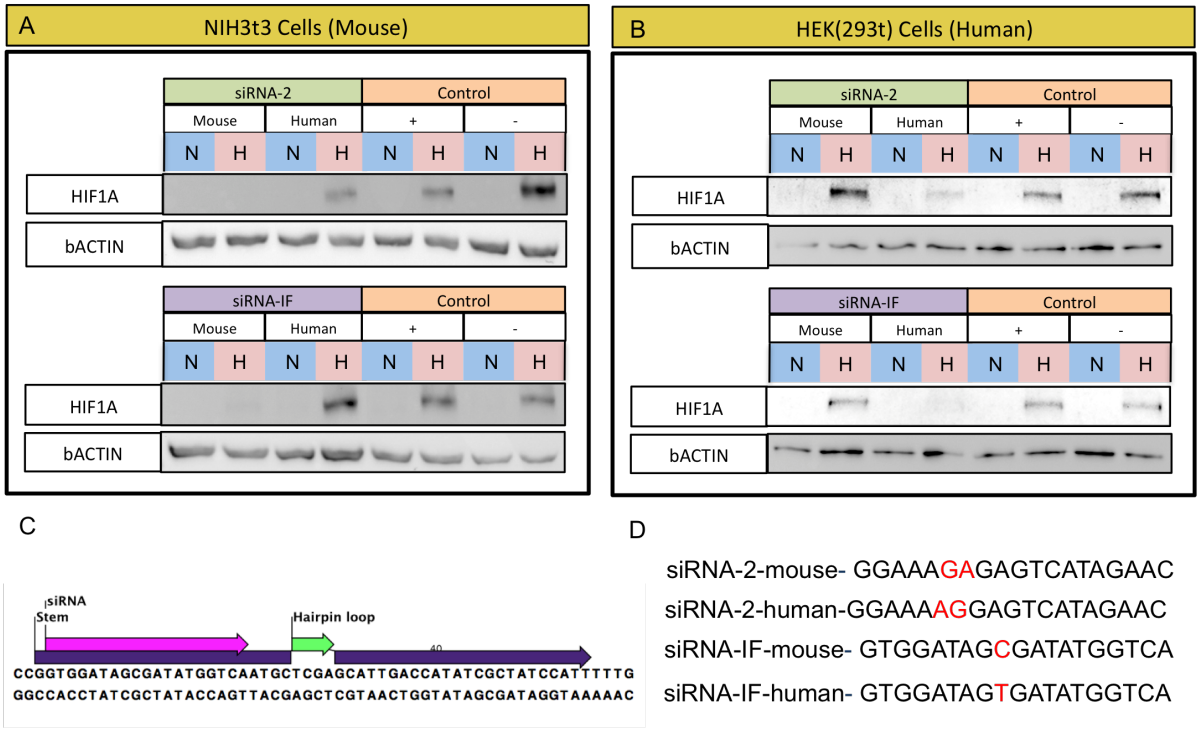

Figure 10. *Testing of human and mouse specific Hif1a siRNAs. (A-B) Western blot analysis of HIF1A in NIH3t3 cells (A) and HEK cells (B) treated with mouse and human Hif1a-specific sequences for siRNA-2 and siRNA-IF. Treated cells were kept at hypoxia (H) – 0.2% O_2 for 6h or normoxia (N). Controls were treated with scrambled siRNA (+) or left untransfected (-). bACTIN was used as the loading control. (C) The sequence of Hif1a-shRNA-IF showing the functional short interfering portion (siRNA-IF) as a pink arrow, the hairpin loop as a green arrow and the stem forming the sequence as purple arrows. (D) The mouse and human specific sequences of siRNA-2 and siRNA-IF with the differences highlighted in red.*

3.2. HIF1A target genes in the retina

3.2.1 Transcriptome analysis

The Opsin-Cre;*Vhl*^{flox} mice have HIF1A and HIF2A stabilized while the Opsin-Cre;*Vhl*^{flox};*Hif1α*^{flox} mice lack HIF1A in the rod photoreceptors. Since HIF1 is a major transcription factor involved in regulation of many genes, these mice can be used to identify the HIF1 target genes in the rods. Retinas were isolated from 10-12 week old animals (N = 3) of the following genotypes - *Vhl*^{flox};*Hif1α*^{flox} (control), Opsin-Cre;*Vhl*^{flox} (single knock-down) and Opsin-Cre;*Vhl*^{flox};*Hif1α*^{flox} (double knock-down) and the transcriptomes were acquired as described earlier (Methods – 3.1.1).

Generation of lists – A list of genes was generated by comparing the transcriptomes of the Opsin-Cre;*Vhl*^{flox} samples to Opsin-Cre;*Vhl*^{flox};*Hif1α*^{flox} samples. This list should contain all the HIF1 target genes in the rods. The list was filtered to get results with pValue < 0.05 for the upregulated genes and pValue < 0.5 for the downregulated genes. Similarly filtered lists were generated by comparing the control with the single knock-down. This list should comprise of all the genes regulated by HIF1 as well as HIF2 (HIF2A is VHL-regulated by mechanisms similar to HIF1A). Further a third list was acquired by comparing the control to the double knock-down wherein only HIF2 is present and hence the list must essentially comprise of HIF2A target genes. These were then sorted starting from the maximum fold change and the top 50 genes in each category are listed in Table 1.

Functional groups – All the upregulated genes from the first list (double vs single) were entered into the online analysis software – DAVID. This resulted in Table 2, which is a list of all the functional groups [enrichment scores between 17.02 (group1) to 0.07 (group9)]. The group 1 comprises of crystallins, which are major proteins in the lens – this could indicate a contamination from the lens in the retinal tissues. But there have been some recent studies showing enzymatic activities of certain crystallins as well as their expression in the retina (Jones et al., 1999; Magabo et al., 2000). Hence, it would be worthwhile to test the role of crystallins in the healthy and degenerating retina, especially in connection with hypoxia. The group 2 consisted of several secreted proteins, some (*Angptl7, Rspon1, Bpil3, Stc2*) of which have been implicated in hypoxic mechanisms. The group 4 consists of complement factors, which are implicated in AMD and hence were analyzed further (3.2.2).

Validation of selected candidates – Some of the HIF1A regulated candidates from the list were selected to verify the transcriptome data - Alpha 2 macroglobulin (A2M) is a large plasma protein that acts as an anti-protease and inactivates various proteinases. It is

implicated in Alzheimer's disease, which is an age-related progressive degenerative disease (Blacker et al., 1998; Rudrasingham et al., 1999). A disintegrin and metalloproteinase with thrombospondin motifs 4 (ADAMTS4) is an enzyme responsible for the degradation of aggrecan (a proteoglycan of the cartilage) and brevican (a brain specific extra-cellular matrix protein) (Nakamura et al., 2000; Song et al., 2007). Adrenomedullin (ADM) is a peptide hormone that has been shown to be hypoxia regulated and may function as a vasodilator (Deville et al., 2010). Caspase 1 (CASP1) is an enzyme with proteolytic functions that is involved in developmental apoptosis, and has been shown to be hypoxia-mediated (Kim et al., 2003). Chemokine (C-C motif) ligand 2 (CCL2) is chemokine that recruits immune cells and is involved in inflammation and has been shown to be HIF1-regulated (Mojsilovic-Petrovic et al., 2007). CCAAT/enhancer-binding protein delta (CEBPD) is a transcription factor that is involved in the regulation of apoptosis and cell proliferation (Balamurugan and Sterneck, 2013). Cleavage and polyadenylation specific factor 3-like (CPSF3L) is a protein involved in RNA processing as part of an integrator protein which is composed of 12 subunits (CPSF3L is subunit 11 of the integrator) (Baillat et al., 2005). Endothelin 2 (EDN2) is a protein shown to be hypoxia induced in many systems, has vasocontrictive functions (Ling et al., 2013), and is involved in angiogenesis in the retina (Rattner et al., 2013). Basic fibroblast growth factor (FGF2) is a protein present in the basement membrane, is involved in angiogenesis and shown to reduce retinal degeneration in rats (Lau et al., 2000). Glial fibrillary acidic protein (GFAP) is present in the activated retinal astrocytes and glia cells and indicates stress and gliosis (Erickson et al., 1987; Grosche et al., 1995). Glycosylation-dependent cell adhesion molecule-1 (GLYCAM1) is a proteoglycan ligand expressed in endothelial cells in lymph nodes. It is able to bind to the receptor L-selectin and attracts leukocytes to site of inflammation (Suguri et al., 1996). Ladinin-1 (LAD1) is a protein component of the basement membrane and is responsible for maintaining stability of the ECM (Motoki et al., 1997). Leukemia inhibitory factor (LIF) is an interleukin 6 class cytokine that affects cell growth by inhibiting differentiation. The cytokine binds to the LIF receptor and activates the JAK/STAT and the MAPK pathways (Kunisada et al., 1996). In the retina *Lif* is expressed in Muller cells and has been shown to have protective and prosurvival properties (Joly et al., 2008). Lysyl oxidase like 4 (LOXL4) is elevated in Head and neck carcinoma and may be involved in oxidative stress (Molnar et al., 2003). Myosin VII A (MYO7A) is a mechanochemical protein and part of the myosin family. It is implicated in Usher syndrome (a rare genetic disorder resulting in deafness and visual impairment) (Williams and Lopes, 2011). Neuregulin 4 (NRG4) belongs to a family of proteins that bind to the EGF receptors and may mediate prosurvival mechanisms (Falls, 2003). Oocyte specific homeobox 6 (OBOX6) is a protein involved in development although the *Obox6* null mice developed normally and were fertile (Cheng et al., 2007). Peroxisome proliferator activated receptor

alpha (PPARA) is a nuclear receptor and a transcription factor that is activated during energy deprivation (Kliewer et al., 1994). Pituitary tumor-transforming gene 1 (PTTG1) is involved in cell-cycle regulation and the *Pttg1* nulll mice have normal retinal morphology and function (Yetemian and Craft, 2011). Smoothelin like-2 (SMTNL2) is not well characterized but a study showed it to be part of the MAPK pathway (Gordon et al., 2013). Signal transducer and activator of transcription 3 (STAT3) is a transcription factor that is activated by various cytokines and acts via the JAK/STAT pathway. In the retina *Stat3* was shown to promote survival of photoreceptors in inherited degeneration models (Jiang et al., 2014). Stanniocalcin 2 (STC2) is a secreted glycoprotein upregulated in several cancers and shown to be involved in store operated calcium entry (Zeiger et al., 2011). Transglutaminase 3 (TGM3) is an enzyme that catalyzes cross-linking of peptides in a calcium dependent manner and implicated in dermatitis (Taylor et al., 2015). Vascular endothelial growth factor (VEGF) is a secreted protein, which is hypoxia-regulated and involved in angiogenesis (Ferrara et al., 2003). Anti-VEGF is provided as a therapy for wet AMD (Mitchell, 2011). Most of the genes tested showed the expected trend – *A2M, Adm, Casp1, Cebpd, Edn2, Fgf2, Gfap, Lad1, Lif, Loxl4, Obox6, Smntl2, Stat3, Stc2* and *Vegf* were upregulated significantly in the Opsin-Cre;*Vhl*^{flox} mice compared to the Opsin-Cre;*Vhl*^{flox};*Hif1a*^{flox} mice. *Myo7a* and *Pttg1* were downregulated, but there was variation in the expressions of these genes in the controls as well. Some of the genes – *Adamts4, Ccl2, Cpsf3l, Glycam1, Nrg4, Tgm3* and *Ppara* did not show differential regulation, although these genes were shown as highly upregulated in the gene chip analysis (Figure 11).

HIF1 is a major transcription factor, and hence the genes regulated by HIF1 may be involved in many signaling pathways. The activation of these pathways could then further cause upregulation of other genes, which may not be direct targets of HIF1. Hence, many of the upregulated genes in the transcriptome data could be due to a secondary effect of HIF1A stabilization. Additionally the VHL complex could be involved in the other cellular mechanisms, and thus effects of mechanisms unrelated to HIF1A cannot be excluded.

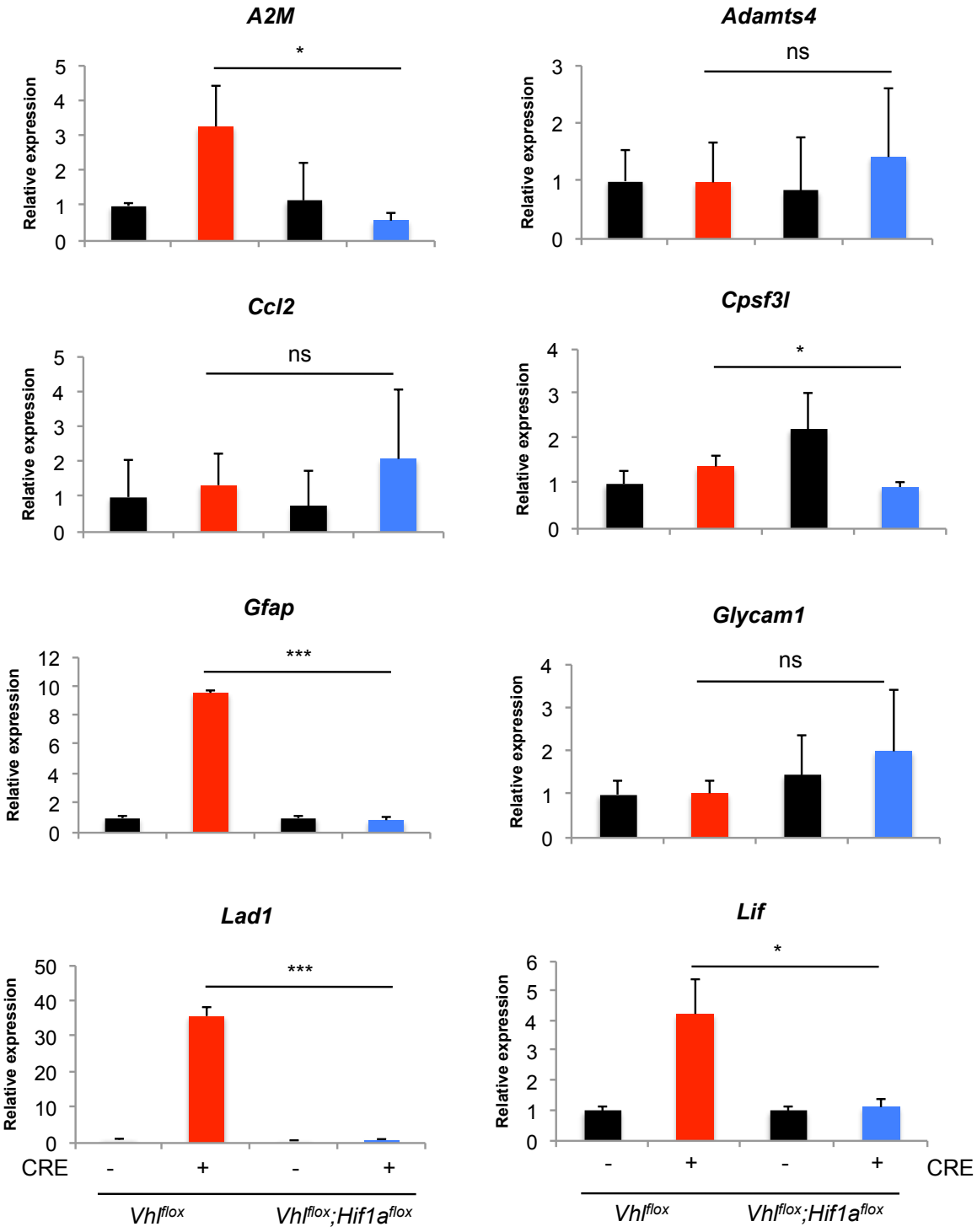
A2M
*
Relative expression
0
1
2
3
4
5
Adamts4
ns
Relative expression
0
1
2
3
Ccl2
ns
Relative expression
0
1
2
3
4
5
Cpsf3l
*
Relative expression
0
1
2
3
4
Gfap
***
Relative expression
0
2
4
6
8
10
12
Glycam1
ns
Relative expression
0
1
2
3
4
Lad1
***
Relative expression
0
10
20
30
40
50
CRE
-
+
-
+
Vhlflox
Vhlflox;Hif1aflox
Lif
*
Relative expression
0
1
2
3
4
5
6
-
+
-
+
CRE
Vhlflox
Vhlflox;Hif1aflox

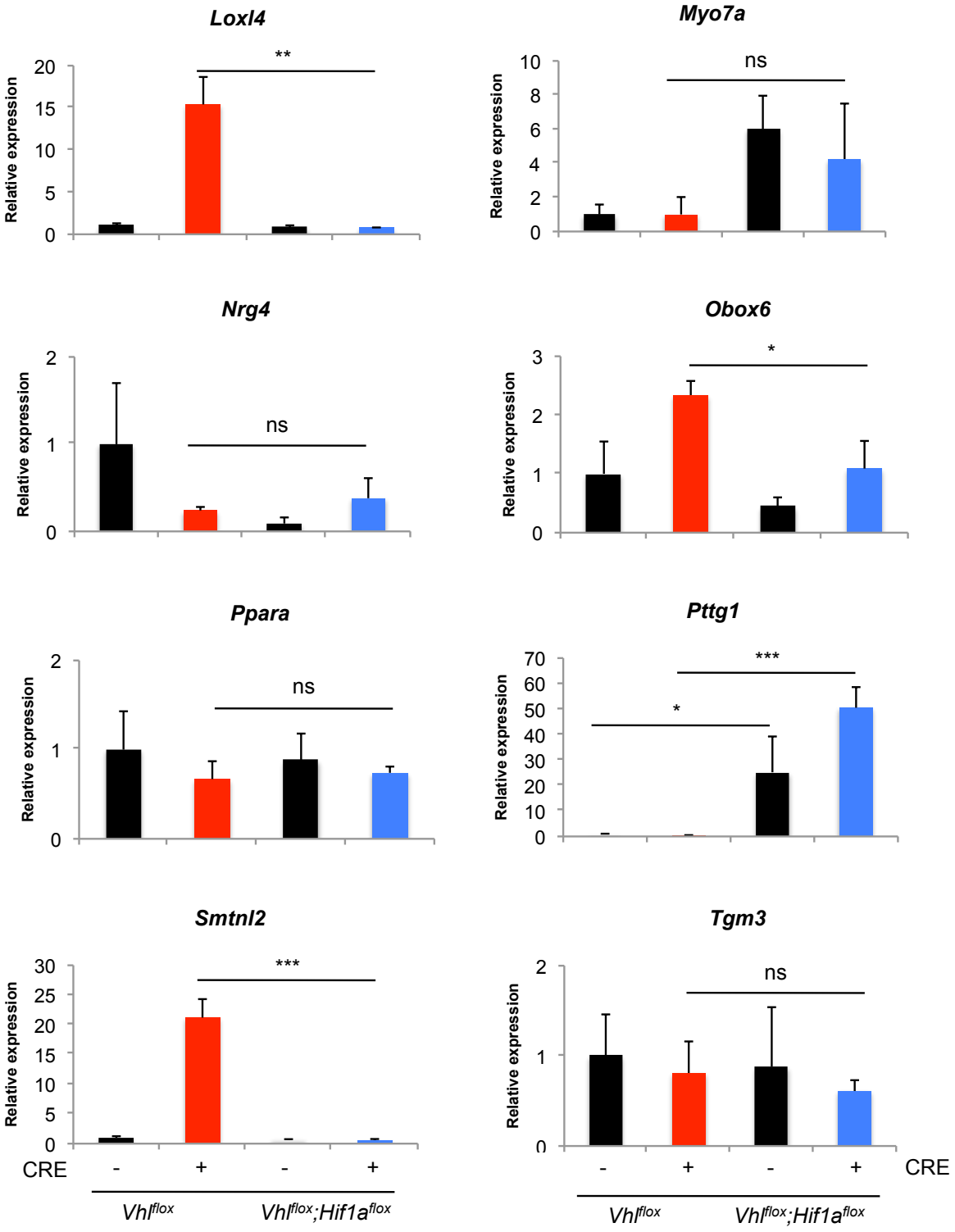

Figure 11. *Validation of selected genes from the transcriptome data. Relative expression of the selected genes in Vhl^{flox} (black bars), Opsin-Cre;Vhl^{flox} (red bars), Vhl^{flox};Hif1a^{flox} (black bars) and Opsin-Cre Vhl^{flox};Hif1a^{flox} (blue bars) mice at the age of 11 weeks. Expression was determined by semi-quantitative real-time PCR, normalized to Actb and shown relative to the levels in Vhl^{flox} (set to 1). Shown are mean values ± SD of N = 3. Significance was tested using Student's t-test (* P < 0.05, ** P < 0.01, *** P < 0.001).*

3.2.2 Complement hypothesis and analysis

AMD is a multi-factorial disease and there are several features of the disease that manifest to varying degrees in different patients. Some age-related changes such as drusen accumulation, inability of the RPE cells to clear oxidation products and lipofuscin, choriocapillary changes affecting the oxygen supply to the outer retina and thickening of the bruch's membrane result in the photoreceptors experiencing mild but chronic hypoxia. This led to the hypothesis that the aged retina is hypoxic. In addition genetic factors might contribute to aggravating these features resulting in the diseased situation (AMD). Hypoxic response is carried out by the transcription factors HIF1 and HIF2, although their levels have never been directly tested in diseased patients. Furthermore, biochemical analysis of drusen, which is one of the disctinctive features of AMD revealed that it is composed of fragments of complement factors (C3a, C3b, CFB, C5 and C5a) and other proteins. Linkage studies have shown mutations in complement factors (*C3, Cfh, C2, Cfb*) are highly correlated with AMD (Anderson et al., 2010).

Complement hypothesis

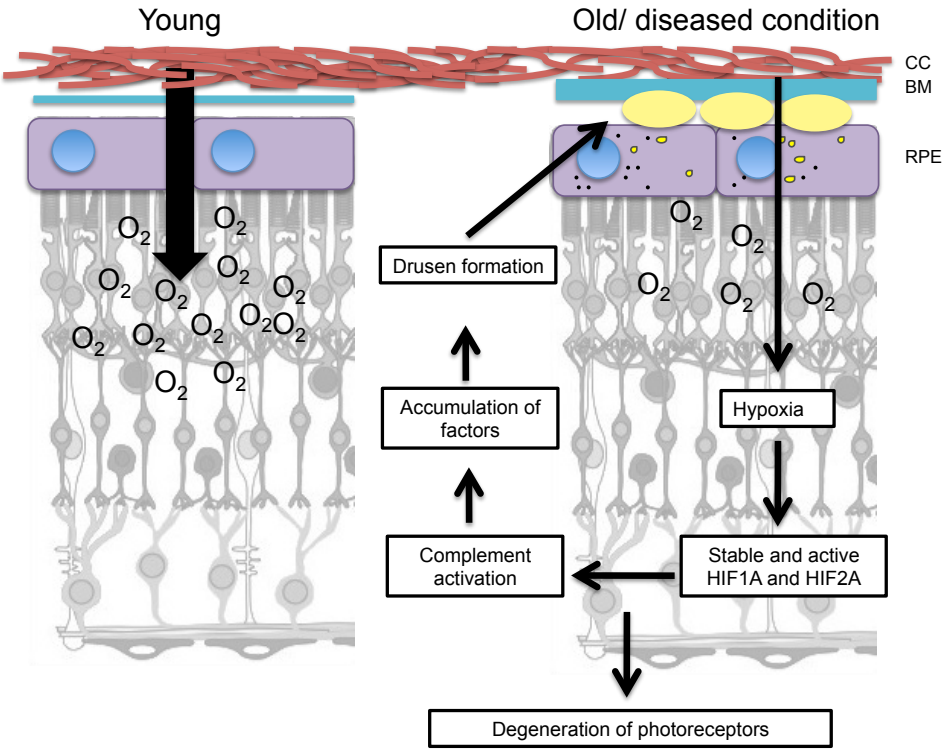

Figure 12. *Hypoxia and complement hypothesis for AMD. Age-related changes in the bruch's membrane (BM), choriocapillaries (CC) and retinal pigment epithelium (RPE) restrict the oxygen and nutrient supply to the outer retina causing hypoxia. This leads to the stabilization of HIF1A and*

HIF2A, which may result in an upregulation of complement factors. Chronic hypoxia will result in accumulation of these factors, which may accumulate as drusen and aggravate the symptoms.

Our transcriptome data revealed that HIF1A stabilization in the rod photoreceptors resulted in the upregulation of several complement factor genes (Table 2- Group4). Also these mice showed an age-related degeneration (3.1.1). Hence, we hypothesized that maybe hypoxia in the outer retina results in stabilization of HIF1A and this leads to an upregulation of complement factors. These factors are not completely cleared away, accumulate over time near the bruch's membrane and form a diffusion barrier, The resulting nutrient and oxygen deprivation aggravates the symptoms, eventually leading to death of photoreceptors and degeneration. (Figure 12)

Complement factors are upregulated on HIF1A stabilization

The expression of complement factor genes were tested in the Opsin-Cre;*Vhl*^{flox} and the Opsin-Cre;*Vhl*^{flox};*Hif1a*^{flox} mice from 11 weeks to 1 year of age. There were huge variations in the *C3* expression and the levels were much reduced in all the older mice (including controls). *C4b* expression was generally higher on HIF1A stabilization (in Opsin-Cre;*Vhl*^{flox} mice). *Cfb* and *Cfh* did not appear to be affected much. *Cfi* and *Serping1* were slightly upregulated in the younger mice and the effect was lost at older age. Though the standard deviations were high due to variation among animals in the same genotype group, we observed a general trend in the upregulation of complement factors in the Opsin-Cre;*Vhl*^{flox} mice. (Figure 13)

We also looked at the C3 and CFH protein levels on retinal cryosections of these mice. But the immunohistochemical analysis did not produce relaiable results, most likely because even the upregulated levels are very low and may be below the detection limit. The C3 protein appeared as puncta-like structures near the RPE in some sections. But this localization was not consistently observed (data not shown). We analyzed the promoter region of *C3* and *Cfb* genes for HRE elements but did not find any canonical HIF binding regions. Also a literature search did not show any work suggesting complement factors to be targets of HIF1A. Hence, it is likely that complement factors are upregulated indirectly or by other mechanisms that are hypoxia and HIF1A regulated.

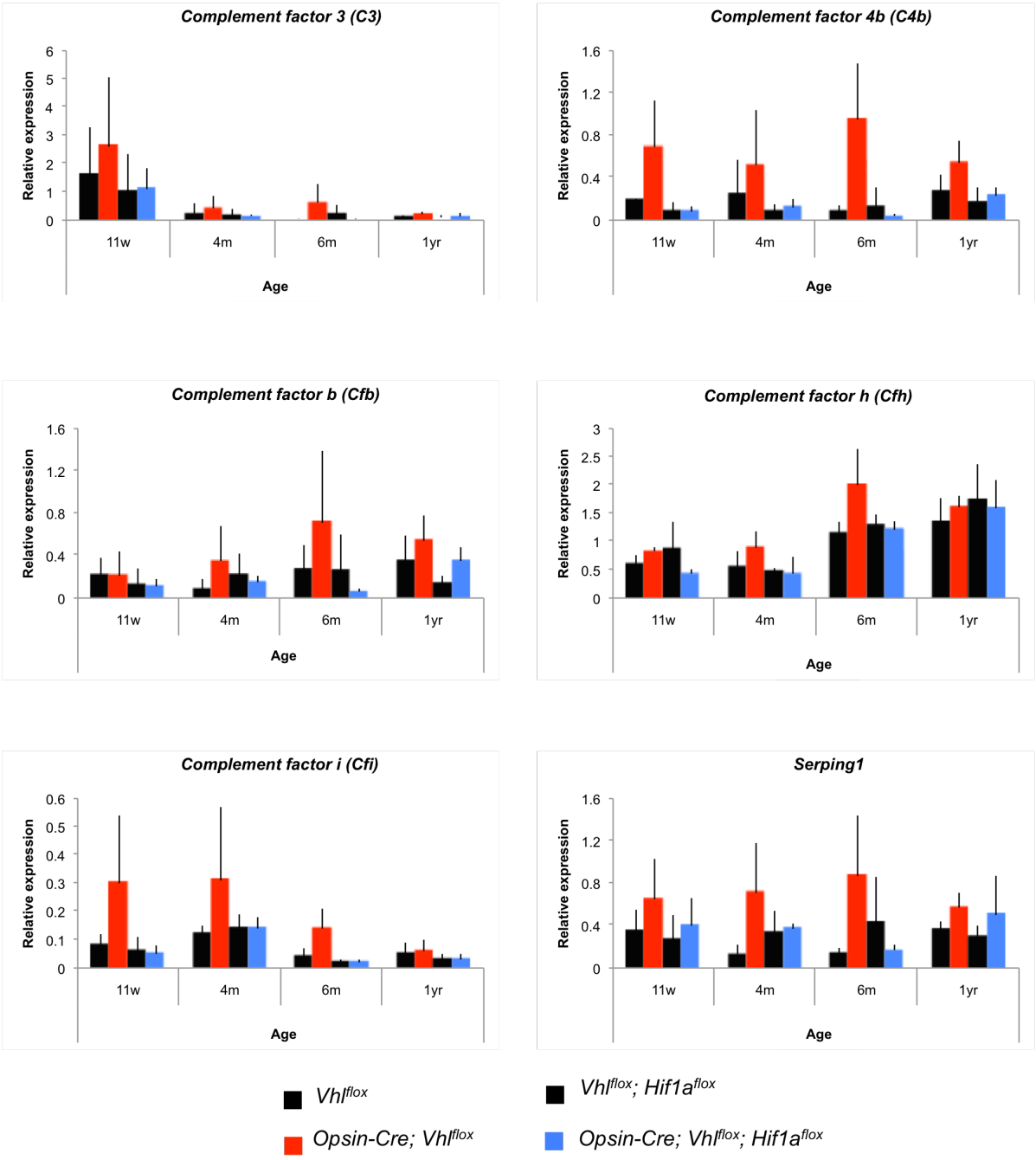

Figure 13. *Upregulation of complement factor genes on HIF1A stabilization. Relative expression of C3, C4b, Cfb, Cfh, Cfi and Serping1 in Vhl^{flox} (black bars), Opsin-Cre; Vhl^{flox} (red bars), Vhl^{flox}; Hif1a^{flox} (black bars) and Opsin-Cre; Vhl^{flox}; Hif1a^{flox} (blue bars) mice at the age of 11 weeks, 4 months, 6 months and 1 year. Expression was determined by semi-quantitative real-time PCR and normalized to Actb. Shown are mean values ± SD of N = 3.*

Complement factors are upregulated during degeneration

Since complement factors did not seem to be direct targets of HIF1 we wanted to test if these factors are upregulated during the degeneration process. Thus, we analyzed the expression of these genes in WT mice (C57BL/6) and a model for inherited degeneration (*rd10*) mice. We observed a significant upregulation of these factors after PND21 in the *rd10* mice. The degenerative processes already begin by PND21 and by PND56 most photoreceptors are lost in the *rd10* mice (Samardzija et al., 2012). Most of these factors seem to peak between PND42 and PND56 after the peak of degeneration (between PND18-PND21) and then eventually the levels lower, although they are still higher than the controls at PND180. Taken together with the previous data, we could conclude that maybe in the Opsin-Cre;*Vhl*^{flox} mice the stabilization of HIF1A might activate mechanisms resulting in degeneration. During these processes complement factors are upregulated not directly by HIF1A. Additionally HIF1A is stabilized in the rods of these mice, but in the *rd10* mice the complement factor genes are upregulated even after loss of all rods, suggesting that other cell types might be expressing the complement factors.

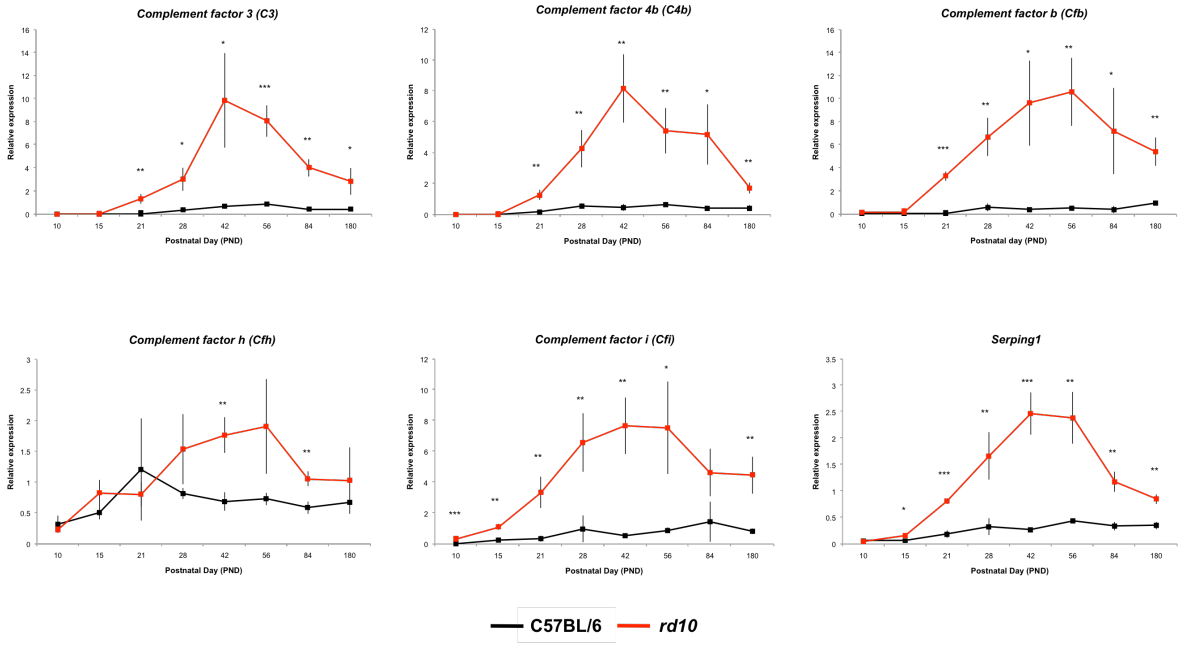

Figure 14. *Upregulation of complement factor genes during degeneration. Relative expression of C3, C4b, Cfb, Cfh, Cfi and Serping1 in WT- C57BL/6 (black line) and rd10 (red line) mice from PND10 to PND180 (X-axis). Expression was determined by semi-quantitative real-time PCR and normalized to Actb. Shown are mean values ± SD of N = 3. Significance was tested using Student's t-test (* P < 0.05, ** P < 0.01, *** P < 0.001).*

3.2.3 Study of a HIF1A target gene - Stanniocalcin 2

The comparison of transcriptomes of the Opsin-Cre;*Vhl*^{flox} and Opsin-Cre;*Vhl*^{flox};*Hif1a*^{flox} mice revealed the differential regulation of several genes. One of these – Stanniocalcin 2 (*Stc2*), had a 14-fold upregulation in the Opsin-Cre;*Vhl*^{flox} mice (HIF1A is stabilized in rod photoreceptors). A literature search showed several studies in cancer cells wherein *Stc2* and its paralog *Stc1* were upregulated. Since the tumor microenvironment is hypoxic and HIF1A is implicated in cancer, Stanniocalcins may indeed play an important role in hypoxic mechanisms. The gene chip results were validated by semi-quantitative RT-PCR and the *Stc2* upregulation was confirmed. As hitherto there has been no study of stanniocalcins in the retina, we aimed to characterize this further. Our data suggest that in the retina only *Stc2* and not *Stc1* is hypoxia responsive and is a target of HIF1A. Intriguingly the protein localized at the neurofilaments although in Opsin-Cre;*Vhl*^{flox} mice used for the initial transcriptome analysis, the stabilization of HIF1A was in rod photoreceptors. Furthermore, by extracting RNA from the separate layers by laser capture microdissection (LCM) we were able to show that the normal expression of *Stc2* is in the INL and GCL of WT mice, whereas there was a strong upregulation in the ONL of the Opsin-Cre;*Vhl*^{flox} mice. Retinal morphologies of the *Stc2-/-* and *Stc1-/-* mice were comparable to WT controls. This study serves as a first report of expression and hypoxic regulation of stanniocalcins in the retina. To understand exact molecular/ cellular mechanisms and function of STC2 in the neurofilaments further investigation would be required.

In the retina, *Stc2* and not *Stc1*, responds to hypoxia in a HIF1A-dependent manner.

Divya Ail[1,2] (DA), Andy Chang (AC), Roger Reddel (RR)[3] and Christian Grimm[1,2,4] (CG)

[1] Lab for Retinal Cell Biology, Department of Ophthalmology, University of Zürich, Zürich, Switzerland.

[2] Neuroscience Center (ZNZ), University of Zürich, Zürich 8057, Switzerland.

[3] Cancer Research Unit, Children's Medical Research Institute, Westmead, NSW, Australia.

[4] Center for integrative human physiology (ZIHP), University of Zürich, Zürich, Switzerland.

Author contributions:

Design: DA, CG

Experiment: DA (RT-PCR, Immunohistochemistry, Imaging of morphologies, laser capture microdissection, hypoxia), AC/RR (*Stc1-/-* and *Stc2-/-* mice samples)

Interpretation: DA, CG

Manuscript: DA, CG

ABSTRACT

Stanniocalcins (STC1 and STC2) are secreted glycoproteins that are implicated in different cancers and have been shown to be hypoxia regulated in various cell culture studies. The retina is sensitive to hypoxia and several retinal disorders have a hypoxic aspect to them. Hence we investigated the expression of stanniocalcins in the normal, degenerating and hypoxic retina. We show that *Stc1* and *Stc2* were similarly expressed in the normal and degenerating retina. Under hypoxic conditions, however *Stc2* showed a strong upregulation whereas *Stc1* did not. Further we report that hypoxic upregulation of *Stc2* expression is HIF1A dependent. Although, the lack of *Stc1* and *Stc2* does not seem to affect the structure of the retina, the normal expression is restricted to specific cell types (in the INL and GCL). Taken together our data provide evidence for the differential regulation of STC1 and STC2 in the retina.

Keywords: *Stc1*, *Stc2*, hypoxia, HIF1A, retina.

INTRODUCTION

Stanniocalcin (STC) is a secreted glycoprotein, which was first identified in a gland called corpuscle of stannius in fish (Stannius, 1939). It was shown to have an anti-hypercalcemic effect by preventing Ca^{2+} influx and hence aiding the fish to survive in high-calcium surroundings (Lafeber et al., 1988). The human STC1 was first identified in a screen for genes attributing the immortalization phenotype to cancer cells (Chang et al., 1995; Olsen et al., 1996). Human STC1 is almost 60% identical to fish STC. Later, another paralog called STC2 was identified (Chang and Reddel, 1998; DiMattia et al., 1998; Ishibashi et al., 1998), which shares only 30% identity with STC1 but the exon-intron boundaries, glycosylation site and cystine residues are conserved between the two suggesting a common ancestor (Wagner and Dimattia, 2006). STC1 forms homodimers, most likely through the interaction of 11 cycteine residues in the protein (Hulova and Kawauchi, 1999). STC2 has in addition 15 conserved histidine residues clustered at the C-terminal region. Both STC1 and STC2 are secreted proteins with short signal peptides of about 24 amino acids (Moore et al., 1999). The mammalian STC1 gene is expressed as a 4 kb transcript that has a wide distribution in kidney, heart, lung, prostrate, thyroid and the highest levels in the ovary. STC2 is also widely expressed in tissues including kidney, spleen and pancreas predominantly as a 2 kb transcript as well as a 4.4kb transcript in certain tissues (Chang and Reddel, 1998; DiMattia et al., 1998).

Both stanniocalcins have been implicated in the pathophysiology of several cancers. The expression of STC1 was elevated in human colorectal cancer, lung cancer, ovarian cancer, breast cancer and leukemia. And STC2 was elevated in human gastric cancers, neuroblastomas, prostrate cancer, colorectal cancer and renal cell carcinoma, (Yeung et al., 2012) and suggested as a marker for gastric cancer (Yokobori et al., 2010). The tumor microenvironment is hypoxic (Vaupel et al., 1989), so not surprisingly several studies have shown *Stc1* and *Stc2* to be regulated by hypoxia. Elevated levels of *Stc1* were reported in mice treated with hypoxic preconditioning that resulted in ischemic tolerance in the heart (Westberg et al., 2007a) and brain (Westberg et al., 2007b). It was also shown that hypoxic treatment of various cancer cell lines derived from colon carcinomas, nasopharangeal cancer and ovarian cancer resulted in an upregulation of STC1 (Yeung et al., 2005). STC2 was induced by hypoxia in proximal tubular epithelial cells (Leonard et al., 2003), breast cancer, ovarian cancer cells (Law and Wong, 2010b). Both the STC1 and STC2 promoter analysis revealed putative hypoxia responsive elements (HRE) and in-vitro studies analyzing mutated HREs, suggested that both STC1 and STC2 are HIF1A target genes, though the association for STC1 was not consistent (Law and Wong, 2010b; Law et al., 2010).

The master regulator of hypoxic response is a transcription factor called - Hypoxia-inducible factor (HIF1) belonging to a family of proteins that also includes HIF2 and HIF3 (Semenza, 2012). HIF1 is a dimmer composed of a nuclear-localized beta subunit and an alpha subunit (Wang et al., 1995) that is constitutively produced but undergoes immediate degradation via oxygen-dependent (Maxwell et al., 1999), VHL-mediated proteosomal degradation (Jaakkola et al., 2001). Under hypoxic conditions, *Vhl* cannot bind to the HIF1A, which stabilizes by evading degradation, translocates to the nucleus, dimerizes and causes transcription of HIF1 responsive gene (Cockman et al., 2000; Ohh et al., 2000). As photoreceptors are the major cell-type in the retina and the loss of these is an important cause of several vision impairments, we generated mice with rod photoreceptor-specific deletion of *Vhl*. This resulted in a hypoxia-like response by stabilization of HIF1A and HIF2A and these mice showed progressive retinal degeneration (Lange et al., 2011).

There have been few studies aiming at understanding the molecular mechanisms and subcellular functions of the stanniocalcins, several of which aimed at elucidating their role in calcium homeostasis (Yeung et al., 2012). Other studies reported STC1 binding sites on the mitochondrial membrane (McCudden et al., 2002), as well as the uncoupling effect of STC1 on oxidative phosphorylation, suggesting a role in cellular metabolism (Ellard et al., 2007). Using fibroblasts from STC2 knockout mice, it was shown that STC2 is a negative regulator of store operated calcium entry (Zeiger et al., 2011).

In a presumptive retinal ganglion cell line - RGC-5, it was shown that transduction with STC1 resulted in a dose-dependent increase in cell viability (Kim et al., 2013). Furthermore, intravitreal injection of STC1 rescued retinal degeneration in two inherited rat models (RCS and S334ter-3), wherein they also showed an upregulation of mitochondrial uncoupling protein - UPC2 involved in oxidative phosphoryplation (Roddy et al., 2012). But so far there has been no study of STC2 in the retina. As the retina is a tissue with a high oxygen demand, it is very sensitive to variations in oxygen levels and hypoxia is implicated in degenerative diseases of the retina (Arjamaa and Nikinmaa, 2006; Grimm and Willmann, 2012; Lange and Bainbridge, 2011). Here we report for the first time, the differences in hypoxic regulation of both *Stc1* and *Stc2* in the mouse retina.

EXPERIMENTAL PROCEDURES

Animals and Genotyping - Animals were treated in accordance with the regulations of the veterinary authority of Zurich and the statement of the Association for Research in Vision and Ophthalmology (ARVO) for the use of animals in vision research. All mice were kept at the animal facility of the University Hospital Zurich in a light-dark (12h:12h) cycle with food and water ad libitum. Light was maintained at 60 lux at cage level during the light period. Mice were euthanized by CO_2 inhalation followed by cervical dislocation.

The C57BL/6 mice were purchased from Charles River (Chatillon-sur-Chalaronne, France) and the *rd10* (C57BL/6 background) mice from Jackson laboratories (Bar Harbor, ME, USA). The 129S-Vhlh^{tm1jae}/J-mice, which have *lox*P sites flanking exon1 and part of the promoter of the Vhl gene (both the alleles are floxed and hereafter these mice are referred to as *Vhl^{flox}),* were purchased from Jackson laboratory (Bar Harbour, USA), the Opsin-Cre mice were acquired from Yun-Zheng Le (Oklahoma, USA) and the Opsin-Cre;*Vhl^{flox}* mice were generated as described earlier (Lange et al., 2011). The *Hif1α$^{flox/flox}$* mice (hereafter referred to as *Hif1α^{flox})* were kindly provided by R.Johnson (UCSD, USA) and M.Gassmann (UZH, Switzerland). The *Vhl^{flox}* mice were crossed with *Hif1α^{flox}* mice to generate *Vhl^{flox};Hif1α^{flox}* and further with Opsin-Cre mice to generate Opsin-Cre;*Vhl^{flox};Hif1α^{flox}*.These mice were genotyped as described before (Section 3.1.1). The hypoxia and reoxygenation treatment was performed on 6-week old WT (129S6) mice as described earlier (Grimm et al., 2002). The *Stc1-/-* and *Stc2-/-* mice were generated by the R. Reddel lab as described (Chang et al., 2005; Chang et al., 2008).

Morphology and light microscopy – To analyze retinal morphology by light microscopy, eyes were enucleated and fixed in 2.5% glutaraldehyde in 0.1 M cacodylate buffer (pH 7.3) at 4°C overnight. After fixation, cornea and lens were removed, and the eyecup was separated into a superior and an inferior half by cutting through the optic nerve head. The trimmed tissue was washed in cacodylate buffer, contrasted with osmium tetroxide (1%, 1 h, room temperature), dehydrated by incubations in increasing ethanol concentrations, and embedded in Epon 812. Semi-thin sections (0.5 µm) were prepared and counterstained with toluidine blue. An Axioplan digitalized microscope (Zeiss Meditec, Jena, Germany) was used to examine the slides.

Western Blotting – Retinas were homogenized in 0.1 M Tris-HCl (pH 8) at 4°C and the protein content was determined using Bradford assay. Proteins (30 µg each) were separated by SDS- polyacrylamide gel electrophoresis using a 10% gel, and then blotted onto a nitrocellulose membrane by semi-dry transfer. After blocking the membrane for 1 hr with 5% non-fat dry milk (Bio-Rad, Munich, Germany) in TBST (10 mM Tris/HCl [pH8], 150 mM NaCl,

and 0.05% Tween-20) membranes were incubated overnight with the primary antibodies (dilution 1:500) (Table 2). This was followed by incubation with HRP-conjugated secondary antibodies for 1 hr at room temperature. The protein bands were then visualized using the Renaissance Western Blot Detection Kit (PerkinElmer Life Sciences, Boston, MA, USA).

RNA isolation, cDNA synthesis and semiquantitative real-time PCR – Retinas were isolated through a corneal incision and immediately snap frozen in liquid nitrogen. Total RNA was isolated using RNeasy isolation kit (catalogue number: 74104, Qiagen, Hilden, Germany) or the High Pure RNA isolation kit (catalogue number: 11828665001, Roche Diagonistics, Basel, Switzerland). Residual genomic DNA was removed by a DNase I incubation step. RNA (650-1000 ng) was reverse transcribed using oligo(dT) and M-MLV reverse transcriptase (catalogue number: M1701, Promega, Madison, WI, USA). 10 ng of cDNA was used for gene expression analysis by semiquantitative real-time PCR using a LightCycler 480 instrument (Roche Diagnostics), the LightCycler 480 SYBR Green I Master mix (catalogue number: 04887352001, Roche Diagonistics), and specific primer pairs (Table 1). The primer pairs were designed to span large intronic sequences or to cover exon-intron boundaries. Gene expression was normalized to actin beta (*Actb*), and relative quantification was calculated using the comparative threshold method ($\Delta\Delta C_T$).

Laser capture microdissection (LCM) - Eyes from 8-week old WT (129S6) and 11-week old Opsin-Cre;*Vhl*^{flox} mice were enucleated and immediately embedded in tissue freezing medium (Leica Microsystems Nussloch GmbH, Nussloch, Germany), and frozen in a 2-methylbutane bath cooled in liquid nitrogen. 20 µm thick retinal sections were collected on Arcturus PEN Membrane Glass Slides (Applied Biosystems, Foster City, CA, USA). The slides were then fixed for 5 min in acetone, followed by 5 min of air drying and two dehydration steps (30 s with 100% ethanol and 5 min with xylol). Retinal layers were isolated using an Arcturus XT Laser Capture Microdissection system (Bucher Biotec AG, Basel, Switzerland) and Arcturus CapSure Macro LCM Caps (Applied Biosystems). Extraction of RNA was done using the Arcturus PicoPure RNA Isolation Kit (Applied Biosystems) according to the manufacturer's instructions, including a DNase treatment to remove residual genomic DNA. cDNA was synthesized using random hexamer primers (High-Capacity cDNA Reverse Transcription Kit; Applied Biosystems), and further analyzed by semi-quantitative real-time PCR.

Immunofluorescence on retinal cryosections – Eyes were enucleated and fixed in 4% paraformaldehyde (PFA) overnight. Cornea and lens were removed and the eye-cups were transferred into 30% sucrose in phosphate buffered saline (PBS). Eye-cups were then embedded in tissue cryoprotective medium (Leica Microsystems Nussloch GmbH, Nussloch,

Germany) and snap – frozen in a 2-methylbutane bath cooled in liquid nitrogen. 12 µM thick sections were cut through the optic nerve head on a cryostat (Leica), air-dried, and stored at -80°C until further use. The retinal sections were incubated with blocking solution (3% goat serum + 0.3% Triton-X in PBS) for 1 hr at room temperature. Then the primary antibody was applied (Table 2) and left at 4°C overnight. The slides were then washed 3 times with PBS followed by incubation with Cy2 or Cy3 conjugated secondary antibodies (Jackson Immunoresearch, Soham, UK) in blocking solution (dilution = 1:500) for 1 hr at room temperature. After 3 PBS washes, nuclei were stained with DAPI, and the slides were mounted with the anti-fade medium Mowiol (Calbiochem, San Diego, CA, USA). Immunofluorescently labeled proteins were visualized using an Axioplan fluorescence microscope (Carl Zeiss AG).

Statistical analysis – Statistical analysis was performed using Prism 4.0 software (GraphPad, San Diego, CA, USA). All data are presented as mean ± standard deviation (SD). The number of samples (N) used for individual experiments is given in the figure legends. Student's t-tests were used to measure the statistical differences of means between two groups. A *P* value below 0.05 was considered significant.

RESULTS

Expression of *Stc1* and *Stc2* in the retina

Stanniocalcins have been implicated in several cancers (Chang et al., 2003), and their expression patterns have been shown in diverse tissues (Chang and Reddel, 1998; Chang et al., 1995; Olsen et al., 1996; Varghese et al., 1998), but their expression and potential role in the retina has not been studied. Hence first we analyzed the expression of *Stc1* and *Stc2* in the mouse retina as well as in brain, heart, kidney, liver, lung and spleen for positive controls. Both *Stc1* and *Stc2* were highly expressed in the retina and the expression of *Stc1* is highest in the retina compared to all the other tissues tested (Figure1A).

We also analyzed the expression of the stanniocalcins during postnatal development from PND10 to PND180. In wild type (WT) mice both genes had steady gene expression levels that did not vary during ageing. Furthermore, to investigate whether expression of these genes is affected by retinal degeneration we analyzed their expression in the *rd10* mice from PND10 to PND180. The *rd10* mouse is a model for inherited retinal degeneration. It has a spontaneous mutation in the beta subunit of the rod phosphodiesterase (*Pde6b*) resulting in an autosomal recessive and progressive form of retinal degeneration which starts around PND18, peaks at PND21 and at PND56 most photoreceptors are lost (Chang et al.,

2002; Samardzija et al., 2012). The expressions of *Stc1* and *Stc2* did not show much variation in the retinas of *rd10* mice during the course of degeneration, suggesting that these genes may not have direct or important role in the degenerating retina (Figure1B and 1C).

In the retina, *Stc2* but not *Stc1* is responsive to hypoxia

Previous studies have shown both STC1 (Lal et al., 2001) and STC2 (Law and Wong, 2010a) to be responsive to hypoxia. The retina is a metabolically active tissue and has a high oxygen consumption rate (Yu and Cringle, 2001a). Hence we tested the expression of these genes in response to hypoxia in the retina. Surprisingly, *Stc1* expression remained unaffected by hypoxia, whereas there was a 9-fold upregulation of *Stc2* immediately after hypoxia. This reduced to 4-fold, when the mice were reoxygenated for 2 hours after hypoxia and retuned to basal levels after 4 hours of reoxygenation (Figure 2A). To test if the hypoxic-response might be affected by age, 7-week old and 7-months old mice were kept at hypoxia. Again, *Stc1* did not respond to the hypoxic treatment whereas *Stc2* showed an upregulation, although the response did not vary in older mice. The known hypoxia-regulated genes *Adm* and *Epo* were used as controls and showed the expected upregulation (Figure 2B).

Hypoxic regulation of *Stc2* requires HIF1A

Stc2 expression was strongly induced in the Opsin-Cre;Vhl^{flox} mice at 11-weeks of age and gradually reduced to basal levels in 1-year old mice. This can be attributed to the loss of Cre expressing cells and retinal degeneration. Furthermore the Opsin-Cre;Vhl^{flox};$Hif1a^{flox}$ mice with a double deletion of *Vhl* and *Hif1a* were generated. *Stc2* levels were not altered in these mice whereas, comparatively the Opsin-Cre;Vhl^{flox} mice showed a 48-fold, 19-fold and 7-fold upregulation at 11-weeks, 4-months and 6-months respectively (Figure 3). *Stc1* expression was tested in these mice at 11 weeks of age, but as expected there was no alteration in expression (data not shown).

Stc2 is expressed in the INL and GCL, and the protein localizes to the neurofilaments

Immunostaining on retinal flatmounts and sections of WT retina revealed that the STC2 protein localizes to the neurofilaments (Figure 4A and B). These sections were then co-stained with STC2 and markers for common retinal cell types such as GFAP for activated muller cells and astrocytes, GS for muller cells, isolectin for blood vessels, synaptophysin for marking the synapses at the plexiform layers and BRN3A for retinal ganglion cells. STC2 did not co-localize with any other cell type and the localization was distinctly observed only in the neurofilaments (Figure 4C-H). But in the Opsin-Cre;Vhl^{flox} and Opsin-Cre;Vhl^{flox};$Hif1a^{flox}$ mice STC2 protein was observed in the neurofilaments as well as Muller cells (Figure 6D and 6E).

Expression of *Stc2* in the inner retina was confirmed by LCM, as the expression was analyzed in the retinal pigment epithelium (RPE), outer nuclear layer (ONL), inner nuclear layer (INL) and the ganglion cell layer (GCL). We observed that in 8-week old WT mice *Stc2* is normally expressed in the INL and GCL, and is not detectable in the RPE and ONL (Figure 5A). The amplified PCR product from 3 mice was then run on a gel, which confirmed that *Stc2* was indeed detected only in the INL and GCL (Figure 5B). Layer specific markers such as *Mct3* for RPE, *Gnat1* for ONL, *Vsx2* for INL and *Opn4* for GCL showed that the layers were separated efficiently with insignificant amounts of cross-contamination (Figure 5C).

Stc2 is expressed in the ONL when HIF1A is stabilized in the rod photoreceptors

There is a 48-fold upregulation of *Stc2* in the retinas of Opsin-Cre;Vhl^{flox} mice compared to the Opsin-Cre;Vhl^{flox};$Hif1a^{flox}$ mice on stabilization of HIF1A in the photoreceptors. We wanted to test if this increase is in the INL and GCL where the *Stc2* is normally expressed. The ONL, INL and GCL of Opsin-Cre; Vhl^{flox} retina was separated by LCM, and the expression revealed an increase in the ONL where HIF1A is stabilized while the levels in INL and GCL remained the same (Figure 6A). But the STC2 protein localization did not seem to alter much. The signal was stronger in Opsin-Cre; Vhl^{flox} mice, compared to the control – Vhl^{flox}; $Hif1a^{flox}$ and Opsin-Cre; Vhl^{flox}; $Hif1a^{flox}$ mice (Figure 6C-E). Also the localization seems to have a more striated pattern (characteristic of Muller cells) compared to the WT control (Figure 6B).

Both *Stc1-/-* and *Stc2-/-* mice have normal retinal morphology

The two transgenic mouse lines overexpressing STC1 displayed a dwarf phenotype suggesting a role for stanniocalcins in muscle and bone development (Filvaroff et al., 2002; Varghese et al., 2002), and the transgenic mice overexpressing human-STC2 were shown to be about 45% smaller than their littermates, and their growth was affected already by embryonic day 12.5 (Gagliardi et al., 2005). On the other hand, Chang et al. generated the *Stc1*-/- mice, which did not show a significant phenotype (Chang et al., 2005). Hence to check if the loss of *Stc1* is compensated by *Stc2* they further generated the *Stc2*-/- mice and the double knockout *Stc1-/-, Stc2-/-* mice. They showed that the *Stc2-/-* mice had a growth-related phenotype - these mice were 10-15% larger and grew at a faster rate from 4-week onwards (Chang et al., 2008). We acquired the eyes of *Stc1-/-* and *Stc2-/-* mice and prepared sections for morphology and immunohistochemistry. The retinal morphology of 9-month old *Stc1-/-* and *Stc2-/-* mice was normal and comparable to the WT controls (Figure 7A-C). Interestingly, the STC2 protein was not only absent in the *Stc2-/-* mice, but was also not detectable in the *Stc1-/-* mice, whereas in the WT mice STC2 localized to the neurofilaments (Figure 7D-F). The control immunostainings with other proteins - BRN3A,

Synaptophysin and GFAP appeared normal in the *Stc2-/-* mice (Figure 7G-I), and *Stc1-/-* mice (not shown) and comparable to the WT mice.

DISCUSSION

The retina is a metabolically active tissue and has high oxygen consumption (Yu and Cringle, 2001b). Several age-related changes and disease conditions could affect the oxygen supply to the retina and cause hypoxia. This local hypoxia is an important aspect of retinal degeneration and disease (Lange and Bainbridge, 2011). Secreted proteins are often involved in cellular signaling, as well as in the activation of different pro-survival or apoptotic mechanisms under stress conditions like hypoxia. Hence study of such proteins might lead to a better understanding of disease mechanisms. We show here that the genes for the secreted glycoproteins called stanniocalcins – *Stc1* and *Stc2* are highly expressed in the retina of WT mice and does not vary significantly during retinal degeneration as seen in the *rd10* mice. In a recent study it was shown that intravitreal injection of STC1 rescued degeneration in two rat models – S334ter-3 (fast degeneration model) and RCS (a slow degeneration model). The rescue was more efficient in the S334ter-3 rats (Roddy et al., 2012). In the *rd10* mice we observe a slight upregulation of *Stc1* at PND15 but after the onset of degeneration at PND21 there is not much difference compared to the controls. It would be interesting to test if maintaining high levels of STC1 prevents degeneration (STC1 could be injected between PND10-15 to test rescue of degeneration after PND21).

Since a majority of studies have shown stanniocalcins in cancers and hypoxia (Chang et al., 2003), we looked at the hypoxic regulation of these two genes, and surprisingly found only *Stc2* to be responsive to hypoxia in the retina. Although *Stc1* is often implicated in cancer and hypoxia we do not observe a change in its expression after hypoxic treatment in the retina. However, in NIH3t3 cells treated with hypoxia, both *Stc1* and *Stc2* were upregulated (not shown). It has also been shown that STC1 receptors are at the mitochondrial membrane (McCudden et al., 2002), and may be directly involved in the uncoupling process of oxidative phosphorylation (Ellard et al., 2007). In the retina study on rats, the uncoupling protein-2 was shown to be slightly upregulated and there was a reduction in ROS products after treatment with STC1 (Roddy et al., 2012), suggesting the involvement of STC1 in mitochondrial or metabolic processes. Furthermore, the activation of the transcription factor HIF1A was sufficient to cause an upregulation in *Stc2* expression even under normoxic conditions. In previous in-vitro studies HIF1A binding sites were recognized and characterized in the promoter region of the *Stc2* gene (Law and Wong, 2010b). Though a similar study was done for *Stc1*, the results were not conclusive, as the

luciferase assays could not be repeated for *Stc1* gene expression (Law et al., 2010). Taking this into account with our present data, we conclude that in the retina *Stc2* and not *Stc1* is regulated by HIF1A under hypoxia.

Intriguingly, we observed the localization of the STC2 protein at the neurofilaments although in Opsin-Cre;*Vhl*^{flox} mice, HIF1A stabilization was in the rod photoreceptors. Hence this raised questions about the exact cell types in the retina that express *Stc2*. In the WT retina we were able to show that the normal expression of *Stc2* is in the INL and GCL, and this would be consistent with the protein localization at the vicinity of these layers in the neurofilaments. However, in the mice with HIF1A stabilized in the photoreceptors, the level of *Stc2* expression remained the same in the INL and GCL whereas there was strong upregulation in the ONL, although the protein did not appear to be accumulating at the photoreceptors. This raises questions about if and how the protein is transported to the NFL (addressing this is beyond the scope of the present study). In the Opsin-cre;*Vhl*^{flox} mice HIF1A stabilization in the rods results in an age-related degeneration and loss of retinal function (Lange et al., 2011), which is rescued in the Opsin-cre;*Vhl*^{flox}*;Hif1a*^{flox} mice (Section 3.1.1). These mice show a strong upregulation of *Stc2* in the ONL although the protein is still predominantly detected in the NFL hinting towards potential signaling between dying photoreceptors and other cell types.

In the retinas of *Stc2-/-* mice the protein could not be detected. But surprisingly, STC2 could not be detected in the retinas of *Stc1-/-* either, hinting at a potential cross-talk in the regulation of the two stanniocalcins. In this respect it would be essential to test the gene expression of *Stc2* in the *Stc1-/-* mice and vice versa. The retinal morphology of *Stc1-/-* and *Stc2-/-* mice appears normal, which is not surprising as these mice generally have mild phenotypes. The *Stc2-/-* mice are 15% larger compared to WT controls, a phenotype that is seen in the double *Stc1-/-;Stc2-/-* knockouts as well (Chang et al., 2008), while the *Stc1-/-* mice do not have an obvious growth phenotype (Chang et al., 2005). Both mice do not have any variations in serum calcium or phosphate levels, indicating normal mineral homeostasis. STC2 or the lack of it, may not affect the retina under normal physiological conditions, but only under stress conditions. Hence, it would be further essential to investigate how *Stc2-/-* and *Stc1-/-;Stc2-/-* mice respond to hypoxia. Taken together our study shows for the first time the expression of stanniocalcins in the normal, degenerating and hypoxic retina, as well as the regulation of *Stc2* by HIF1A. The differential regulation of *Stc1* and *Stc2* under hypoxic conditions hints towards the possibility of distinct and non-redundant functions for the two proteins in the retina, which would require further investigation.

ACKNOWLEDGEMENTS

We thank Cornelia Imsand, Andrea Gubler and Christel Beck for their skillfull assistance in experimental procedures. This work was supported by the Swiss National Science Foundation.

REFERENCES

Olsen, Henrik S, et al. (1996), 'Human stanniocalcin: a possible hormonal regulator of mineral metabolism', *Proceedings of the National Academy of Sciences*, 93 (5), 1792-96.

Arjamaa, Olli and Mikko Nikinmaa (2006), 'Oxygen-dependent diseases in the retina: role of hypoxia-inducible factors', *Experimental eye research*, 83 (3), 473-83.

Chang, A CM, DA Jellinek, and RR Reddel (2003), 'Mammalian stanniocalcins and cancer.', *Endocrine-related cancer*, 10 (3), 359-73.

Chang, AC-M and Roger R Reddel (1998), 'Identification of a second stanniocalcin cDNA in mouse and human: stanniocalcin 2', *Molecular and cellular endocrinology*, 141 (1), 95-99.

Chang, Andy C-M, et al. (1995), 'A novel human cDNA highly homologous to the fish hormone stanniocalcin', *Molecular and cellular endocrinology*, 112 (2), 241-47.

Chang, Andy C-M, et al. (2005), 'The murine stanniocalcin 1 gene is not essential for growth and development', *Molecular and cellular biology*, 25 (23), 10604-10.

Chang, Andy C-M, et al. (2008), 'The murine stanniocalcin 2 gene is a negative regulator of postnatal growth', *Endocrinology*, 149 (5), 2403-10.

Chang, B, et al. (2002), 'Retinal degeneration mutants in the mouse', *Vision research*, 42 (4), 517-25.

Cockman, Matthew E, et al. (2000), 'Hypoxia inducible factor-α binding and ubiquitylation by the von Hippel-Lindau tumor suppressor protein', *Journal of Biological Chemistry*, 275 (33), 25733-41.

DiMattia, Gabriel E, Robin Varghese, and Graham F Wagner (1998), 'Molecular cloning and characterization of stanniocalcin-related protein', *Molecular and cellular endocrinology*, 146 (1), 137-40.

Ellard, Joseph P, et al. (2007), 'The respiratory effects of stanniocalcin-1 (STC-1) on intact mitochondria and cells: STC-1 uncouples oxidative phosphorylation and its actions are modulated by nucleotide triphosphates', *Molecular and cellular endocrinology*, 264 (1), 90-101.

Filvaroff, Ellen H, et al. (2002), 'Stanniocalcin 1 alters muscle and bone structure and function in transgenic mice', *Endocrinology*, 143 (9), 3681-90.

Gagliardi, Anthony D, et al. (2005), 'Human stanniocalcin-2 exhibits potent growth-suppressive properties in transgenic mice independently of growth hormone and IGFs', *American Journal of Physiology-Endocrinology and Metabolism*, 288 (1), E92-E105.

Grimm, Christian, et al. (2002), 'HIF-1-induced erythropoietin in the hypoxic retina protects against light-induced retinal degeneration', *Nature medicine*, 8 (7), 718-24.

Grimm, Christian and Gabriel Willmann (2012), 'Hypoxia in the eye: a two-sided coin', *High altitude medicine & biology*, 13 (3), 169-75.

Hulova, Irena and Hiroshi Kawauchi (1999), 'Assignment of disulfide linkages in chum salmon stanniocalcin', *Biochemical and biophysical research communications*, 257 (2), 295-99.

Ishibashi, Kenichi, et al. (1998), 'Molecular cloning of a second human stanniocalcin homologue (STC2)', *Biochemical and biophysical research communications*, 250 (2), 252-58.

Jaakkola, Panu, et al. (2001), 'Targeting of HIF-α to the von Hippel-Lindau ubiquitylation complex by O2-regulated prolyl hydroxylation', *Science*, 292 (5516), 468-72.

Kim, Sang Jin, et al. (2013), 'Stanniocalcin-1 protects retinal ganglion cells by inhibiting apoptosis and oxidative damage', *PloS one*, 8 (5), e63749.

Lafeber, FP, et al. (1988), 'Hypocalcin from Stannius corpuscles inhibits gill calcium uptake in trout', *American Journal of Physiology-Regulatory, Integrative and Comparative Physiology*, 254 (6), R891-R896.

Lal, Anita, et al. (2001), 'Transcriptional response to hypoxia in human tumors', *Journal of the National Cancer Institute*, 93 (17), 1337-43.

Lange, CA and JW Bainbridge (2011), 'Oxygen sensing in retinal health and disease.', *Ophthalmologica. Journal international d'ophtalmologie. International journal of ophthalmology. Zeitschrift fur Augenheilkunde*, 227 (3), 115-31.

Lange, Christina, et al. (2011), 'Normoxic activation of hypoxia-inducible factors in photoreceptors provides transient protection against light-induced retinal degeneration', *Investigative ophthalmology & visual science*, 52 (8), 5872-80.

Law, Alice YS and Chris KC Wong (2010a), 'Stanniocalcin-2 promotes epithelial–mesenchymal transition and invasiveness in hypoxic human ovarian cancer cells', *Experimental cell research*, 316 (20), 3425-34.

Law, Alice YS, et al. (2010b), 'Stanniocalcin-2 is a HIF-1 target gene that promotes cell proliferation in hypoxia', *Experimental cell research*, 316 (3), 466-76.

Law, AYS, et al. (2010), 'Identification and characterization of the hypoxia-responsive element in human stanniocalcin-1 gene', *Molecular and cellular endocrinology*, 314 (1), 118-27.

Leonard, Martin O, et al. (2003), 'The role of HIF-1α in transcriptional regulation of the proximal tubular epithelial cell response to hypoxia', *Journal of Biological Chemistry*, 278 (41), 40296-304.

Maxwell, Patrick H, et al. (1999), 'The tumour suppressor protein VHL targets hypoxia-inducible factors for oxygen-dependent proteolysis', *Nature*, 399 (6733), 271-75.

McCudden, Christopher R, et al. (2002), 'Characterization of mammalian stanniocalcin receptors mitochondrial targeting of ligand and receptor for regulation of cellular metabolism', *Journal of Biological Chemistry*, 277 (47), 45249-58.

Moore, EE, et al. (1999), 'Stanniocalcin 2: characterization of the protein and its localization to human pancreatic alpha cells.', *Hormone and metabolic research= Hormon-und Stoffwechselforschung= Hormones et metabolisme*, 31 (7), 406-14.

Ohh, Michael, et al. (2000), 'Ubiquitination of hypoxia-inducible factor requires direct binding to the &bgr;-domain of the von Hippel–Lindau protein', *Nature cell biology*, 2 (7), 423-27.

Roddy, Gavin W, et al. (2012), 'Stanniocalcin-1 rescued photoreceptor degeneration in two rat models of inherited retinal degeneration', *Molecular Therapy*, 20 (4), 788-97.

Samardzija, Marijana, et al. (2012), 'Activation of survival pathways in the degenerating retina of rd10 mice', *Experimental eye research*, 99 17-26.

Semenza, Gregg L (2012), 'Hypoxia-inducible factors in physiology and medicine', *Cell*, 148 (3), 399-408.

Stannius, H (1939), 'Uber nebenniere bei knochenfischen', *Arch Anat Physiol*, 6 97-101.

Varghese, Robin, et al. (1998), 'Comparative Analysis of Mammalian Stanniocalcin Genes 1', *Endocrinology*, 139 (11), 4714-25.

Varghese, Robin, et al. (2002), 'Overexpression of human stanniocalcin affects growth and reproduction in transgenic mice', *Endocrinology*, 143 (3), 868-76.

Vaupel, Peter, Friedrich Kallinowski, and Paul Okunieff (1989), 'Blood flow, oxygen and nutrient supply, and metabolic microenvironment of human tumors: a review', *Cancer research*, 49 (23), 6449-65.

Wagner, Graham F and Gabriel E Dimattia (2006), 'The stanniocalcin family of proteins', *Journal of Experimental Zoology Part A: Comparative Experimental Biology*, 305 (9), 769-80.

Wang, Guang L, et al. (1995), 'Hypoxia-inducible factor 1 is a basic-helix-loop-helix-PAS heterodimer regulated by cellular O2 tension', *Proceedings of the national academy of sciences*, 92 (12), 5510-14.

Westberg, Johan A, et al. (2007a), 'Hypoxic preconditioning induces elevated expression of stanniocalcin-1 in the heart', *American Journal of Physiology-Heart and Circulatory Physiology*, 293 (3), H1766-H1771.

Westberg, Johan A, et al. (2007b), 'Hypoxic preconditioning induces neuroprotective stanniocalcin-1 in brain via IL-6 signaling', *Stroke*, 38 (3), 1025-30.

Yeung, BHY, AYS Law, and Chris KC Wong (2012), 'Evolution and roles of stanniocalcin', *Molecular and cellular endocrinology*, 349 (2), 272-80.

Yeung, Ho Y, et al. (2005), 'Hypoxia-inducible factor-1-mediated activation of stanniocalcin-1 in human cancer cells', *Endocrinology*, 146 (11), 4951-60.

Yokobori, Takehiko, et al. (2010), 'Clinical significance of stanniocalcin 2 as a prognostic marker in gastric cancer', *Annals of surgical oncology*, 17 (10), 2601-07.

Yu, Dao-Yi and Stephen J Cringle (2001a), 'Oxygen distribution and consumption within the retina in vascularised and avascular retinas and in animal models of retinal disease', *Progress in retinal and eye research*, 20 (2), 175-208.

Yu, Dao-Yi, et al. (2001b), 'Oxygen distribution and consumption within the retina in vascularised and avascular retinas and in animal models of retinal disease', *Progress in retinal and eye research*, 20 (2), 175-208.

Zeiger, William, et al. (2011), 'Stanniocalcin 2 is a negative modulator of store-operated calcium entry', *Molecular and cellular biology*, 31 (18), 3710-22.

FIGURE LEGENDS

Figure 1. Gene expressions of *Stc1* and *Stc2* in the developing and degenerating retina. **(A)** Relative expression levels of *Stc1* (blue bars) and *Stc2* (red bars) in different tissues (X-axis) from 11 week old WT (C57BL/6) mice. **(B-C)** Relative expressions of *Stc1* **(B)** and *Stc2* **(C)** in the developing retina of wild-type (C57BL/6) mice (black line) and *rd10* mice (red line) from PND10 to PND 180. Expression was determined by semi-quantitative real-time PCR and normalized to *Actb*. Shown are mean values ± SD of N = 3. Significance was tested using Student's t-test (* P < 0.05, ** P < 0.01).

Figure 2. Retinal expression of *Stc2* in response to hypoxia. **(A)** Relative expressions of *Stc1* (blue line) and *Stc2* (red line) in retinas of 6-week old WT (Balb/c) mice exposed to hypoxia (6 h at 6% O_2). Tissue was collected immediately after hypoxia (Imm) or after 2h, 4h and 16h of reoxygenation following hypoxia. **(B)** Relative expressions of *Stc1*, *Stc2*, *Adm* and *Epo* at normoxia (black bars) and hypoxia (6 h at 7% O_2) (red bars) in wild-type (129S6) mice aged 7 weeks and 7 months. Expression levels were determined by semi-quantitative real-time PCR, normalized to *Actb* and shown relative to the levels in untreated controls (set to 1) **(A)** or to normoxic controls at 7 weeks of age (set to 1) **(B)**. Shown are mean values ± SD of N = 3. Significance was tested using Student's t-test (* P < 0.05, ** P < 0.01, *** P < 0.001).

Figure 3. Upregulation of *Stc2* on stabilization of HIF1A in the rod photoreceptors under normoxia. Relative expression of *Stc2* in Vhl^{flox} (black bars), Opsin-Cre;Vhl^{flox} (red bars), Vhl^{flox};$Hif1a^{flox}$ (black bars) and Opsin-Cre;Vhl^{flox}; $Hif1a^{flox}$ (blue bars) mice at the age of 11 weeks, 4 months, 6 months and 1 year (X axis). Expression was determined by semi-quantitative real-time PCR, normalized to *Actb* and shown relative to the levels in Vhl^{flox} (set to 1 for each age). Shown are mean values ± SD of N = 3. Significance was tested using Student's t-test (* P < 0.05, ** P < 0.01, *** P < 0.001).

Figure 4. Localization of STC2 protein at the retinal neurofilaments. Immunostainings of STC2 (red channel) in **(A)** Retinal flatmount of 7 week old WT (129S6) mice and, **(B-H)** retinal sections of 11 week old WT (129S6) mice. Nuclei are stained with DAPI (blue channel) and the green channel is used for GFAP **(C)**, GS **(D)**, Isolectin **(E)**, Synaptophysin **(F)** and BRN3A **(G and H)**. Scale bar: 50 µM.

Figure 5. Expression of *Stc2* in INL and GCL of wild-type mice. RNA was extracted from different retinal layers of wild-type mice (129S6) at 8 weeks of age, separated by LCM. **(A)** Relative expression of *Stc2* in the different retinal layers (X axis) – RPE (retinal pigment epithelium), ONL (outer nuclear layer), INL (inner nuclear layer) and GCL (ganglion cell layer), **(B)** The amplified PCR product of *Stc2* from the RPE, ONL, INL and GCL of N = 3

mice on an agarose gel, **(C)** Relative expression of layer-specific control genes – *Mct3* for RPE, *Gnat1* for ONL, *Vsx2* for INL and *Opn4* for GCL. Expression was determined by semi-quantitative real-time PCR and normalized to *Actb*. Shown are mean values ± SD of N = 3.

Figure 6. Upregulation of *Stc2* in the ONL on stabilization of HIF1A in rods. (A) Relative expression of *Stc2* in the ONL, INL and GCL of Opsin-Cre;*Vhl*^{flox} at 11 weeks of age. Expression was determined by semi-quantitative real-time PCR and normalized to *Actb* (N = 1), (B-E) Immunostaining of STC2 (red channel) and DAPI for nucleus (blue channel) in retinal sections of wild-type (129S6) (B), *Vhl*^{flox}*;Hif1a*^{flox} (C), Opsin-Cre;*Vhl*^{flox} (D) and Opsin-Cre;*Vhl*^{flox}*;Hif1a*^{flox} (E) mice at 11 weeks of age. Scale bar: 50 µM.

Figure 7. Normal retinal morphology in the absence of STC1 and STC2. (A-C) Retinal morphology of WT (C57BL/6) mice at 6 months (A), *Stc1-/-* (B) and *Stc2-/-* (C) at 9 months of age. (D-F) Immunostainings for STC2 in WT (C57BL/6), *Stc1-/-* and *Stc2-/-* retinal sections. (G-I) Immunostainings of BRN3A, SYN and GFAP in *Stc2-/-* mice. Images were acquired at 200 µm from the optic nerve head. Shown are representative images of N = 3 retinas per genotype. Scale bar: 50 µm.

Figure 1

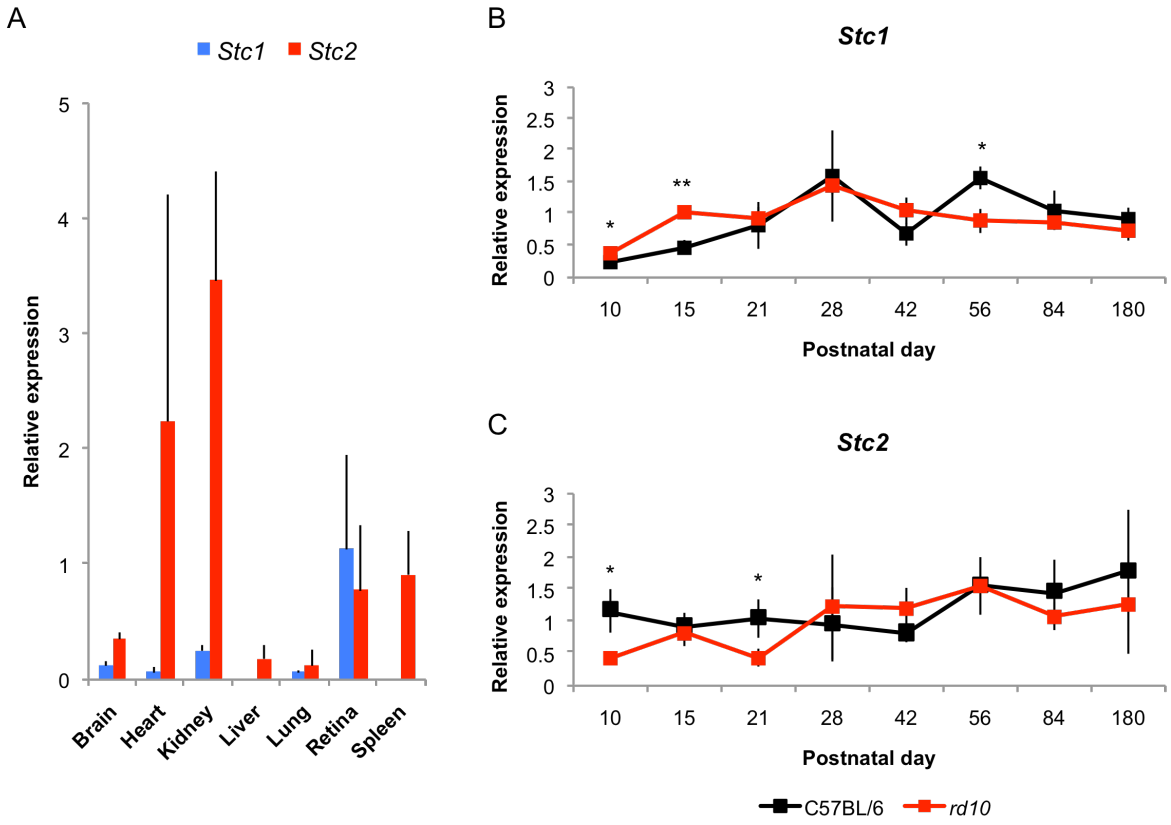

Figure 2

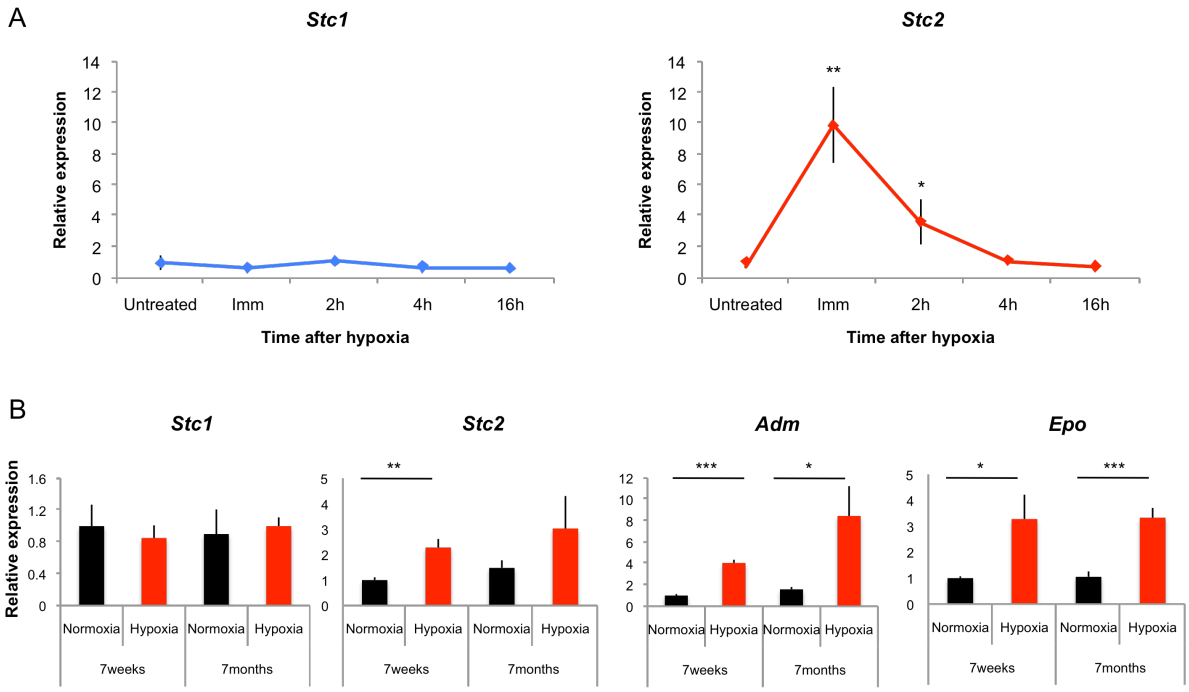

Figure 3

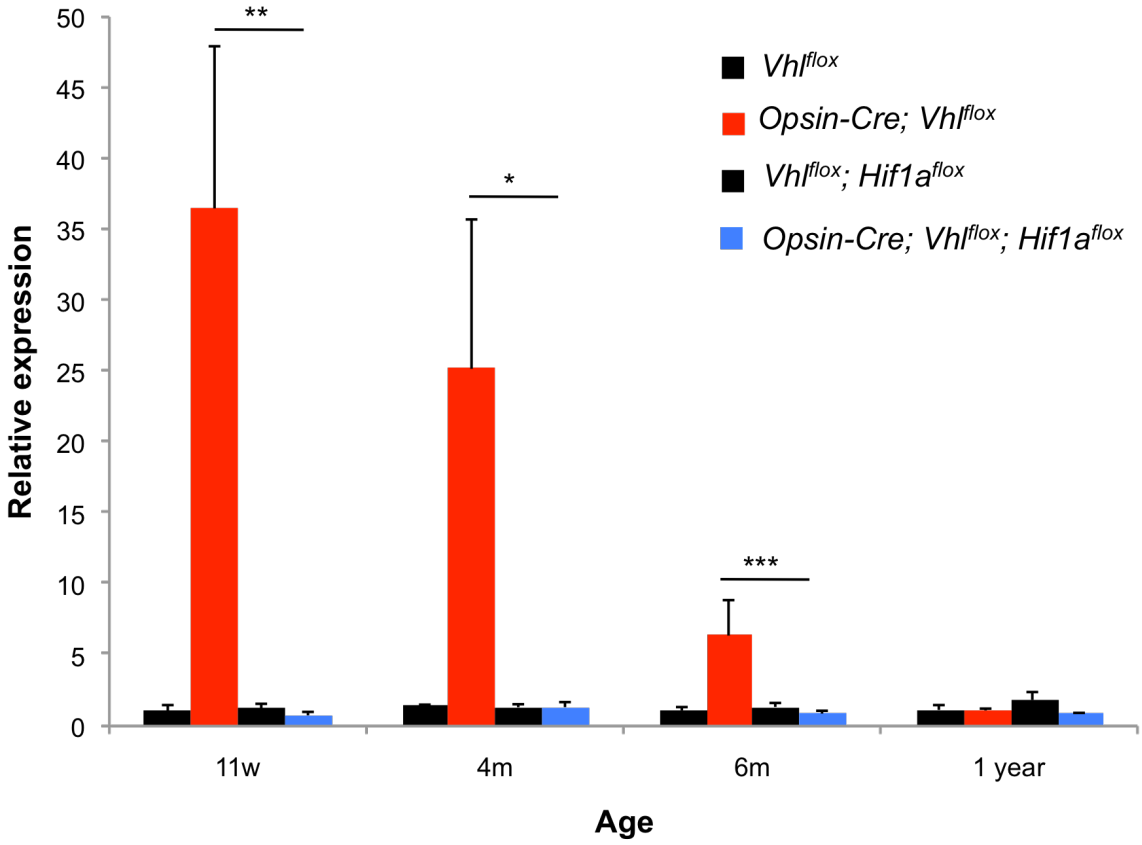

Figure 4

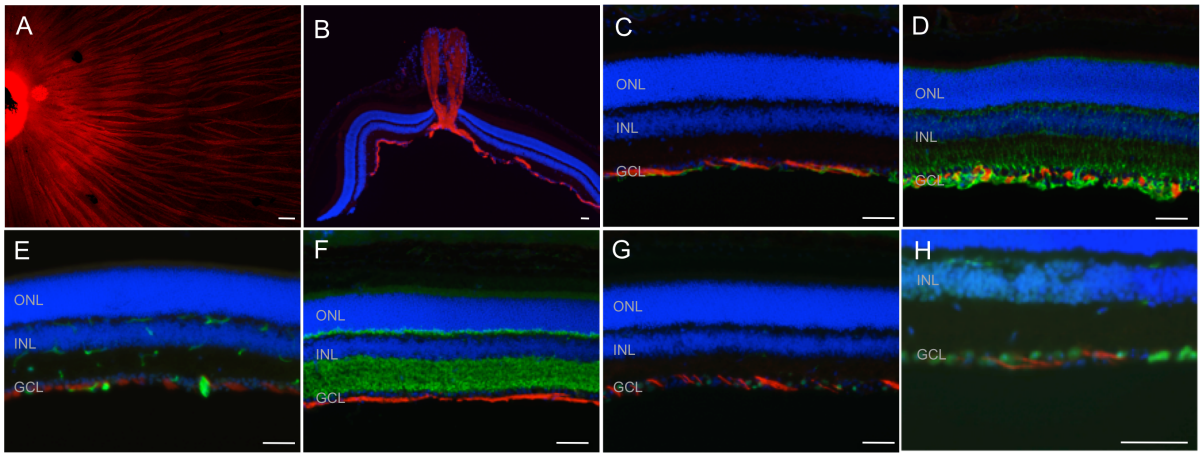

Figure 5

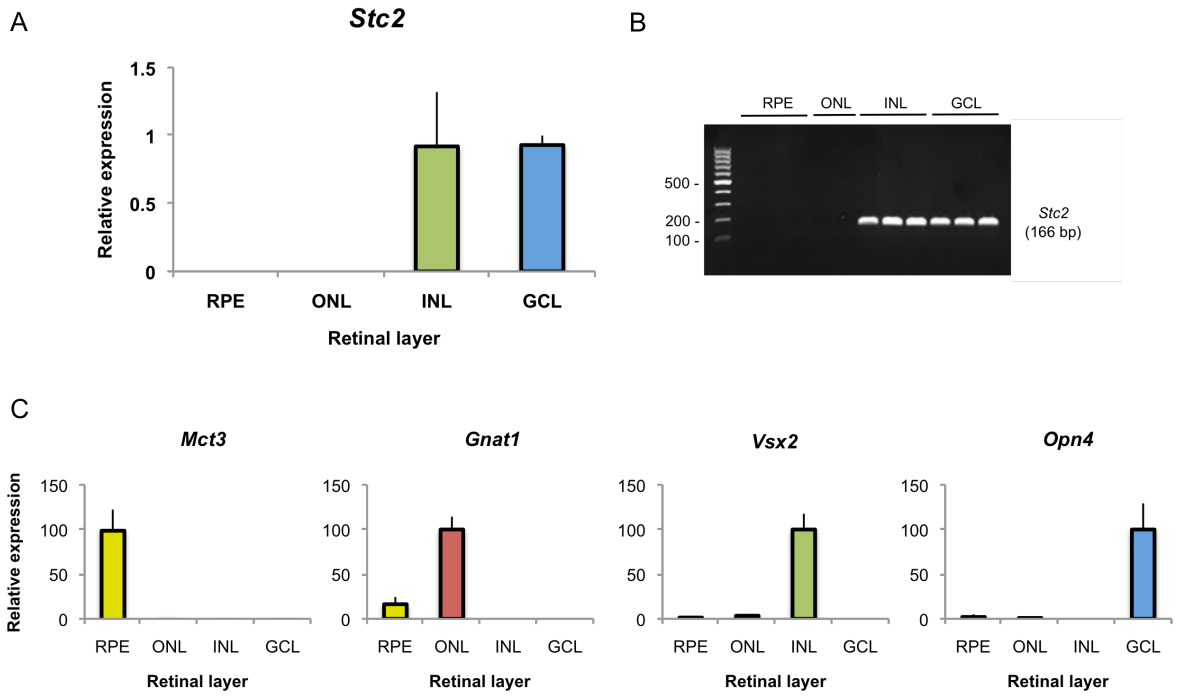

Figure 6

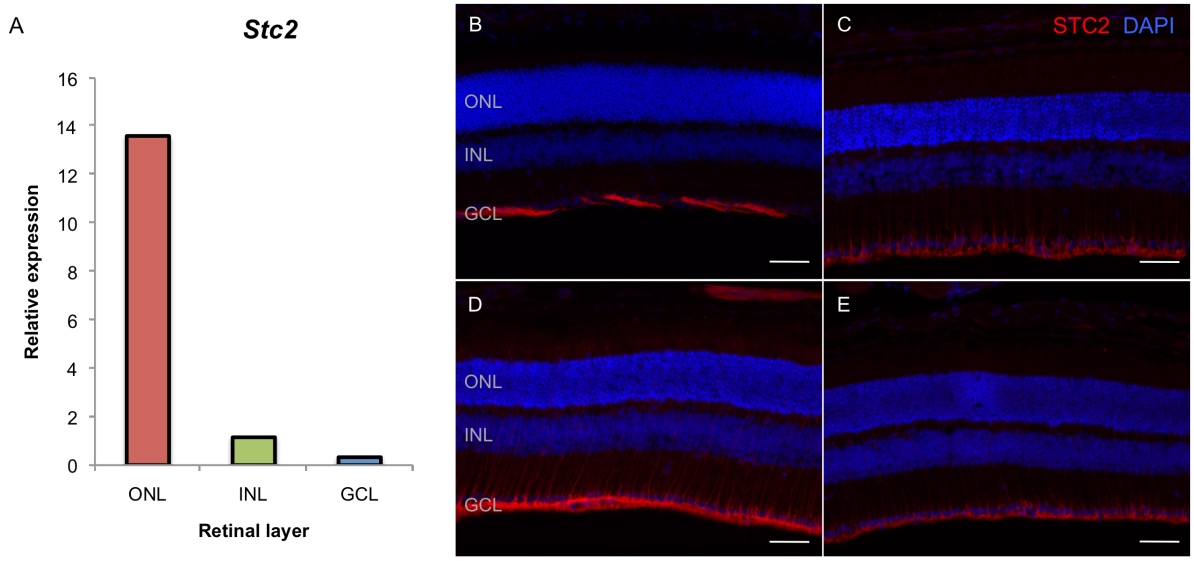

Figure 7

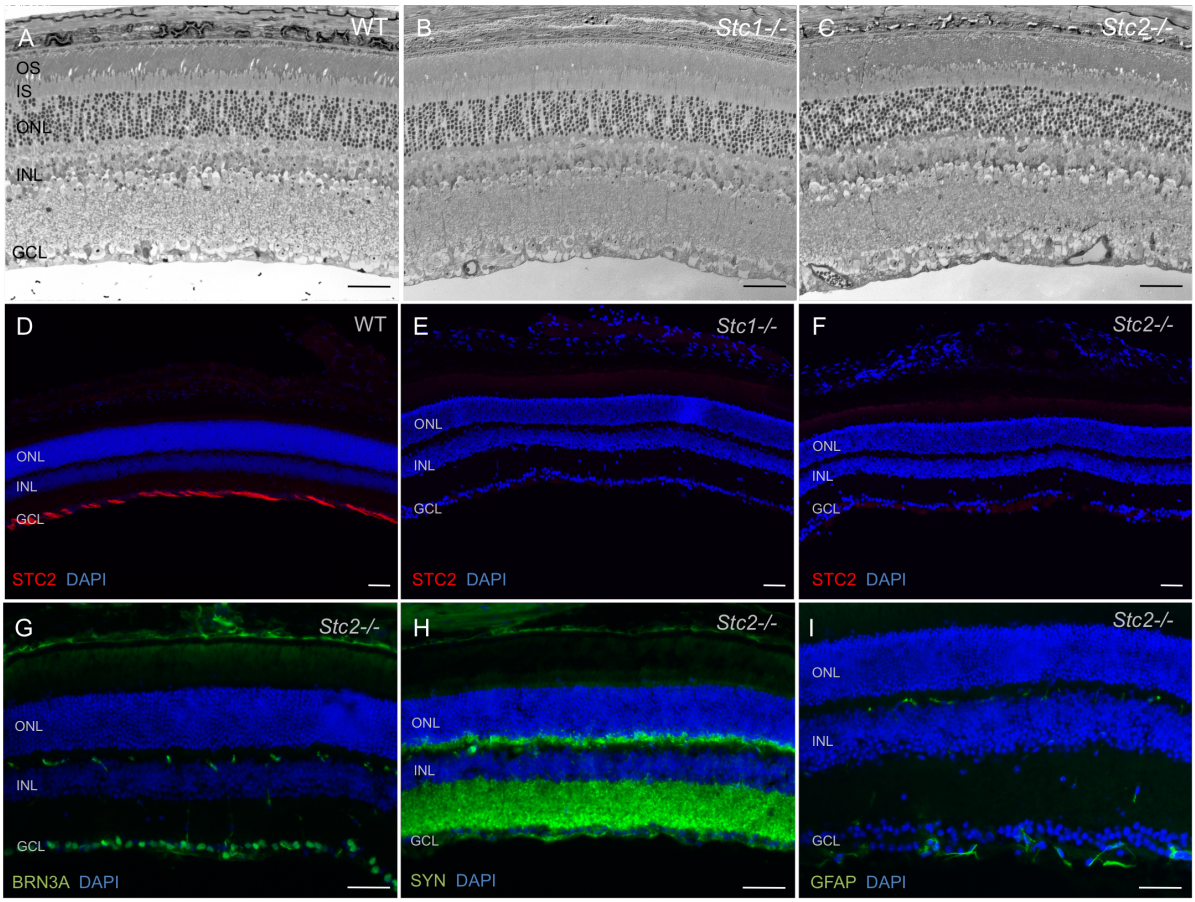
A
WT
OS
IS
ONL
INL
GCL
B
Stc1-/-
C
Stc2-/-
D
WT
ONL
INL
GCL
STC2 DAPI
E
Stc1-/-
ONL
INL
GCL
STC2 DAPI
F
Stc2-/-
ONL
INL
GCL
STC2 DAPI
G
Stc2-/-
ONL
INL
GCL
BRN3A DAPI
H
Stc2-/-
ONL
INL
GCL
SYN DAPI
I
Stc2-/-
ONL
INL
GCL
GFAP DAPI

Table 1. Primers used for semiquantitative real-time PCR

Gene	Forward primer	Reverse primer	Annealing temp (°C)	Amplicon (bp)
Actb	CAACGGCTCCGGCATGTGC	CTCTTGCTCTGGGCCTCG	62	153
Adm	TTCGCAGTTCCGAAAGAAGT	GGTAGCTGCTGGATGCTTGTA	62	77
Epo	GCCCTGCTAGCCAATTCC	GGCGACATCAATTCCTTCTG	60	128
Gnat1	GAGGATGCTGAGAAGGATGC	TGAATGTTGAGCGTGGTCAT	58	209
Mct3	GGCTCAACCCTAAATCCAGA	CTTCGGAGTTTCCTCACCAG	62	75
Opn4	CCAGCTTCACAACCAGTCCT	CAGCCTGATGTGCAGATGTC	62	111
Stc1	CCGGAAGCCATCACTGAA	GGCTTCGGACAAGTCGTTG	62	76
Stc2	AGCAGGAAGTGTCCAGCAAT	GGTTCACAAGGTCCACATAGG	62	166
Vsx2	CCAGGAGACAGGATACAGGTG	GGCTCCATAGAGACCATACT	62	111

Table 2. Antibodies used for immunofluorescence on retinal sections

Protein	Host	Supplier	Catalogue number	Dilution
BRN3A	mouse	Chemicon (Millipore); USA	MAB1585	1:300
ISOLECTIN	mouse	Life Technologies, USA	121413	1:300
GS	mouse	Millipore, USA	MAB302	1:500
STC2	rabbit	Acris antibodies, Herford, Germany	10314-1-AP	1:300
SYN	mouse	Novocastra, Mutenz, Switzerland	NCL-L-SYNAP-299	1:500

3.3. pH stress in the retina

Increased expression of the proton-sensing G protein-coupled receptor *Gpr65* during retinal degeneration

Divya Ail (DA), Véronique Rüfenacht (VR), Christian Caprara (CC), Marijana Samardzija (MS), and Christian Grimm (CG)

Author contributions:

Design: CG

Experiment: DA (RT-PCR, Imaging, Maintenance of mice), VR, CC

Interpretation: DA, VR, MS, CG

Manuscript: DA, CG

Manuscript correction: DA, VR, CC, MS, CG

Summary: The retina is sensitive to pH changes and hence in this paper we aimed to study the role of proton-sensing G-protein coupled receptors (GPCR) in the healthy and degenerating retina. We studied 3 GPCRs – *Gpr4, Gpr65* and *Gpr68* and showed their normal expression in WT retinas during development and ageing. Additionally we observed that only *Gpr65* is upregulated in both the induced and inherited models of retinal degeneration, while *Gpr4* and *Gpr68* were not responsive hinting towards their distinct functions in the retinas. The *Gpr65* KO mice had normal retinal morphology and function. However, the *Gpr65*-/-;*rd10* mice degenerated slightly faster, suggesting that the additional lack of *Gpr65* during degeneration tends to accelerate the process. Previous studies have shown the expression of *Gpr65* in several immune cells including macrophages; hence we looked at the activation of the microglia (the resident immune cells of the retina), in the presence or absence of *Gpr65*. We observed a slight increase in microglia activation although the expression of cytokines was not differentially regulated.

Increased expression of the proton-sensing G protein-coupled receptor *Gpr65* during retinal degeneration

Divya Ail[1,2,3], Véronique Rüfenacht[1,2,4], Christian Caprara[2,5], Marijana Samardzija[2], and Christian Grimm[2,3,6]

[1] Equal contributions, shared authorship.

[2] Lab for Retinal Cell Biology, Department of Ophthalmology, University of Zürich, Zürich, Switzerland.

[3] Neuroscience Center (ZNZ), University of Zürich, Zürich 8057, Switzerland.

[4] Present address: Division of Metabolism, University Children's Hospital Zürich, Zürich, Switzerland

[5] Present address: Swiss Stem Cell Foundation, Gentilino, Switzerland.

[6] Center for integrative human physiology (ZIHP), University of Zürich, Zürich, Switzerland.

Corresponding author:

Christian Grimm
Lab for Retinal Cell Biology
Department Ophthalmology
University of Zürich
Wagistrasse 14
CH 8952 Schlieren, Switzerland
Email: cgrimm@opht.uzh.ch
Tel: 0041 44 556 30 01

ABSTRACT

The retina is a metabolically highly active tissue that is sensitive to pH changes. Blinding diseases of the retina are often characterized by degeneration of photoreceptor cells altering the acid-base homeostasis of the tissue microenvironment and by an accompanying inflammatory response. GPR4, GPR65 and GPR68 are G protein-coupled receptors that aid cells to sense and survive conditions of acidic pH and inflammatory cells express *Gpr65* enhancing their viability. Hence, we investigated expression and function of these proton-sensing GPRs in the normal and degenerating retina. We observed increased retinal expression of *Gpr65*, but not of *Gpr4* and *Gpr68*, in mouse models of both inherited (*rd10*) and induced (light damage) retinal degeneration. Lack of GPR65 slightly accelerated photoreceptor degeneration in *rd10* mice and resulted in a strong activation of microglia after light-injury. Since GPR65 was dispensable for normal retinal development, function and ageing as evidenced by the evaluation of *Gpr65*$^{-/-}$ mice, our results indicate that the proton-sensing G protein coupled receptor GPR65 may be involved in a mechanism that supports survival of photoreceptors in the degenerating retina.

Keywords: *Gpr65*, TDAG8, retinal degeneration, light damage, *rd10*, microglia

INTRODUCTION

G protein-coupled receptor 65 (GPR65; also known as T-cell death-associated gene 8, TDAG8) belongs to a sub-family of proton-sensing receptors. Other members of this family include GPR4, GPR68 (OGR1; ovarian-cancer G-protein-coupled receptor) and GPR132 (G2A; G2 accumulation) (Justus et al., 2013; Okajima, 2013). Proteins of this family were originally characterized as receptors for lipid messengers such as sphingosylphosphorylcholine (SPC) (Mogi et al., 2005), lysophosphatidylcholine (LPC) (Kabarowski et al., 2002) and psychosine (Im et al., 2001; Wang et al., 2004). However, increasing evidence in recent years established their function as proton-sensors (Ludwig et al., 2003). Analysis of the extracellular domains of the membrane-bound GPR68 revealed that histidine residues at positions 17, 20, 84 and 269 mediate its pH sensitivity. At slightly alkaline pH, GPR68 is stabilized in an inactive state by direct hydrogen-bonding between these histidines. Loss of the bonding by protonation at lower pH causes a conformational change and renders the receptor active (Ludwig et al., 2003). Similarly, the histidine residues necessary for the activity of GPR4 (79, 165 and 269) (Liu et al., 2010) and GPR65 (10 and 14) (Radu et al., 2005) have been identified. The pH sensitivity of the more distantly related GPR132 has not been established, and hence, we excluded the gene from this study.

Whereas metabolic acidosis is a hallmark of various diseases such as diabetes (English and Williams, 2004) and chronic kidney disease (Bailey, 2005), local acidosis is found in the microenvironment of many tumors. This may be caused by insufficient blood perfusion, hypoxia, inflammation, and/or glycolytic cell metabolism, and might affect the malignancy and development of the tumor (Vaupel et al., 1989; Gatenby and Gillies, 2004). GPR65 might be involved in the regulation of tumor growth by supporting cell survival in such acidic conditions. It has been shown for example that overexpression of *Gpr65* in Lewis lung carcinoma cells increases tumor growth in mice possibly through evasion of acidosis induced cell death (Ihara et al., 2010). Similarly, overexpression of *Gpr65* might malignantly transform mammary epithelial cells (Sin et al., 2004) and acidic activation of GPR65 protein may render lymphoma cell lines resistant to apoptosis under stress conditions (Ryder et al., 2012). Furthermore, shRNA-mediated knockdown of *GPR65* in NCI-H460 human lung cancer cells decreased cell survival under acidic conditions (Ihara et al., 2010). Thus, GPR65 may act as a prosurvival factor in an acidic environment. However, it has also been reported, that *GPR65* expression is reduced by 50% in human lymphoma samples and that activation of GPR65 stimulates glucocorticoid-induced apoptosis and inhibits *c-Myc* oncogene expression (Li et al., 2013).

Acidosis and GPR65 may also influence the immune and inflammatory response associated with tumor growth as several studies indicate diverse effects of acidosis on inflammatory cells such as neutrophils, eosinophils, monocytes and macrophages (Lardner, 2001; Martinez et al., 2006; Jancic et al., 2012), as well as on the activation of the complement system (Hecke et al., 2001). *Gpr65* expression inhibits cytokine production in peritoneal macrophages under acidic conditions (Mogi et al., 2009) and supports viability of eosinophils by acting as the main proton-sensor and by reducing apoptosis (Kottyan et al., 2009). *Gpr65* expression has also been shown in natural killer cells (Maghazachi et al., 2004) and neutrophils (Murata et al., 2009).

The retina is a highly specialized tissue with an extraordinarily high energy demand. Due to the increased metabolism of photoreceptors in darkness, retinal pH follows a circadian rhythm with lower values at night (Dmitriev and Mangel, 2001). Furthermore, retinal function is sensitive to pH changes (Yang et al., 2005) and protons that are released with glutamate at the photoreceptor ribbon synapses act as feedback inhibitors for neurotransmitter release (Barnes et al., 1993; DeVries, 2001). Many blinding diseases of the retina are characterized by a degeneration of photoreceptor cells. Since photoreceptor cell death results in increased extracellular acidifcation (Perron et al., 2013) retinal degeneration may disturb pH homeostasis of the retinal microenvironment. In addition, such diseases often have an inflammatory component (Detrick and Hooks, 2010; Perez et al., 2013). Hence, we investigated the potential involvement of proton-sensing G protein-coupled receptors in retinal pathophysiology.

EXPERIMENTAL PROCEDURES

Animals and Genotyping - Animals were treated in accordance with the regulations of the veterinary authority of Zurich and the statement of the Association for Research in Vision and Ophthalmology (ARVO) for the use of animals in vision research. All mice were kept at the animal facility of the University Hospital Zurich in a 12h:12h light-dark cycle with food and water *ad libitum*. Light was maintained at 60 lux at cage level during the light period. Mice were euthanized by CO_2 inhalation followed by cervical dislocation. BALB/c mice were purchased from Harlan (Horst, The Netherlands), C57BL/6 mice from Charles River (Chatillon-sur-Chalaronne, France), 129S6 mice from Taconics (Ejby, Denmark) and *rd10* (C57BL/6 background) mice from Jackson laboratories (Bar Harbor, ME, USA). *Gpr65* knockout mice were generated by Deltagen (San Mateo, CA, USA) by replacing 74 bp in exon 2 by a *LacZ-Neo* insertion. *Gpr65*$^{-/-}$ mice were backcrossed for more than 6 generations on the C57BL/6 background (Kumar et al., in press). Genotyping for *Gpr65* was

done by conventional PCR using the following primers: forward primer 5'-TAA CTG CCA CTG TGA AGA CCA TGG C-3', reverse primer 5'-CAG GTC TGA CAG GGA CAG ACT GAA G-3', neo primer 5'-CCA TTC GAC CAC CAA GCG AAA CATC-3'. The neo-primer is knockout specific and binds to the neomycin cassette that replaces part of the *Gpr65* gene in *Gpr65*$^{-/-}$ mice. Amplification fragments were 208 bp for the wild type and ≈1 kb for the *Gpr65*$^{-/-}$ allele. Genotyping for *rd10* was done by PCR using the following primers: forward primer 5'-CTT TCT ATT CTC TGT CAG CAA AGC-3'; reverse primer 5'-CAT GAG TAG GGT AAA CAT GGT CTG-3'. Digestion of the amplification product with *HhaI* resulted in a 97 bp fragment for *rd10* or two fragments of 43 bp and 54 bp for wild type mice.

Light Exposure - Mice aged 6-8 weeks were dark-adapted overnight (16 h). Pupils were dilated with 1% cyclogyl (Alcon, Risch, Switzerland) and 5% neosynephrine (UrsaPharm, Saarbrücken, Germany) 30 minutes before exposure to 15'000 lux of white light for 2 hours (pigmented mice) or to 5'000 lux for 1 h (BALB/c) as described (Grimm and Reme, 2013). After exposure mice were kept in darkness overnight before being returned to the normal light-dark cycle until analysis. Age-matched mice that were dark-adapted but not exposed to light served as controls.

Electroretinogram (ERG) - ERGs were performed following a previously described protocol (Tanimoto et al., 2009). The ERG equipment consisted of a Ganzfeld bowl, a direct current amplifier, a PC-based control and recording unit (LKC UTAS-E 3000, LKC Technologies, Gaithersburg, MD, USA). Mice were dark-adapted overnight and anesthetized using 85 mg/kg ketamine (Parke-Davis, Berlin, Germany) and 4 mg/kg xylazine (Bayer AG, Leverkusen, Germany). The pupils were dilated with 1% cyclogyl (Alcon) and 5% neosynephrine (UrsaPharm), 30 minutes prior to performing single flash ERG recordings under dark-adapted (scotopic) and light-adapted (photopic) conditions. Light adaptation was accomplished with low background illumination starting 5 minutes before photopic recordings. Single white flash stimulus intensities ranged from -3.7 to 1.9 log cd*s/m^2 under scotopic and from -0.6 to 2.9 log cod*s/m^2 under photopic conditions, divided into ten and eight steps respectively. Ten responses per light intensity were averaged with an interstimulus interval of either 4.95 s (for -3.7, -3, -2.6, -2, -1.6, -1, -0.6, -0.02, 0.4 and 0.9 log cd*s/m^2) or 16.95 s (for 1.4, 1.9, 2.4 and 2.9 log cd*s/m^2).

Morphology and light microscopy - To analyze retinal morphology by light microscopy, eyes were enucleated and fixed in 2.5% glutaraldehyde in 0.1 M cacodylate buffer (pH 7.3) at 4°C overnight. After fixation, cornea and lens were removed, and the eyecup was separated into a superior and an inferior half by cutting through the optic nerve head (ONH). The trimmed tissue was washed in cacodylate buffer, contrasted with osmium tetroxide (1%,

1 h, room temperature), dehydrated by incubations in increasing ethanol concentrations, and embedded in Epon 812. Semi-thin sections (0.5 µm) were prepared and counterstained with toluidine blue. An Axioplan digitalized microscope (Zeiss Meditec, Jena, Germany) was used to examine the slides. Retinal thickness from the nerve fiber layer to the retinal pigment epithelium (RPE) was measured at fixed distances (200, 400, 600, 800, 1000, 1200, 1400, 1600 and 1800 µm) from the ONH using Photoshop software (Version CS5 extended, Adobe Systems, San Jose, CA, USA).

RNA isolation, cDNA synthesis and semiquantitative real-time PCR - Retinas were isolated through a corneal incision and immediately snap frozen in liquid nitrogen. Total RNA was isolated using RNeasy isolation kit (#74104, Qiagen, Hilden, Germany) or the High Pure RNA isolation kit (#11828665001, Roche Diagonistics, Basel, Switzerland). Residual genomic DNA was removed by a DNase I incubation step. RNA (650-1000 ng) was reverse transcribed using oligo(dT) and M-MLV reverse transcriptase (catalogue number: M1701, Promega, Madison, WI, USA). Ten ng of cDNA was used for gene expression analysis by semiquantitative real-time PCR using a LightCycler 480 instrument (Roche Diagnostics), the LightCycler 480 SYBR Green I Master mix (# 04887352001, Roche Diagnoistics), and specific primer pairs (Table 1). The primer pairs were designed to span large intronic sequences or to cover exon-exon boundaries. Gene expression was normalized to actin beta (*Actb*), and relative quantification was calculated using the comparative threshold method ($\Delta\Delta C_T$).

Immunofluorescence on retinal flatmounts - Eyes were enucleated and incubated for 3 to 5 minutes in 2% paraformaldehyde prepared in phosphate-buffered saline (PBS). After having removed cornea and lens, the eyeball was cut in a cloverleaf shape by making four incisions. The retina was dissected from the sclera and placed in PBS in a 48-well plate. Dissected retinas were post-fixed at room temperature for 1 h with 4% paraformaldehyde in PBS, washed with PBS, and incubated with blocking solution (3% normal goat serum, 0.3% Triton X-100 in PBS) for 1 h at room temperature. Anti-IBA1 antibodies (#019-19741; Wako Chemicals, Richmond, VA, US) were applied over night at 4°C. Tissue was washed 3 times with PBS and incubated with Cy3-conjugated secondary antibodies (Jackson ImmunoResearch, Soham, UK) for 1 h at room temperature. After three washing steps with PBS, the retinas were flat mounted onto slides, covered with anti-fade medium (10% Mowiol, Calbiochem, San Diego, CA, USA) and protected with cover slips. Labeled proteins were visualized using an Axioplan fluorescence microscope (Zeiss Meditec).

Statistical analysis - Statistical analysis was performed using Prism 4.0 software (GraphPad, San Diego, CA, USA). All data are presented as mean ± standard deviation

(SD). The number of samples (N) used for individual experiments is given in the figure legends. ANOVA or student's t-tests were used to check for significance between of means of groups. A *P*-value below 0.05 was considered significant.

RESULTS

Expression of proton-sensing GPCRs in the retina

It has been shown that *Gpr4*, *Gpr65* and *Gpr68* have diverse expression patterns in various tissues (Tomura et al., 2005), but their expression in the retina has not yet been studied. Hence we first analyzed the expression of these genes in the adult retina of pigmented (129S6, C57BL/6) and albinotic (BALB/c) wild type mouse strains. Since sequencing of all three genes in all three strains revealed several strain-specific single nucleotide polymorphisms (data not shown), we adapted the sequences of the PCR primers for perfect base pairing to the target sequences (Table 1). All primer pairs used for a particular gene amplified the product with similar efficiencies (data not shown). Whereas *Gpr4* and *Gpr65* had comparable expression levels in the three strains (Fig. 1A, B), expression of *Gpr68* was significantly lower in 129S6 mice (Fig. 1C). The reason for the reduced levels of *Gpr68* in retinas of 129S6 mice is not clear but indicates strain-specific differences in the expression of these receptors.

We also tested expression of the three *Gpr* genes during postnatal retinal development from post-natal day (PND) 1 to PND42. Expression of all three genes increased three to four-fold after PND1 and reached plateaus between PND15 and PND21. Whereas expression of *Gpr4* and *Gpr65* increased gradually, *Gpr68* levels showed a prominent increase between PND5 and PND15 (Fig. 1D-F).

Upregulation of *Gpr65* in models of inherited and induced retinal degeneration

Since degeneration of photoreceptors may influence extracellular pH (Perron et al., 2013) we tested whether expression of *Gpr4*, *Gpr65* and/or *Gpr68* might be affected in an inherited and an induced mouse model for retinal degeneration. *Rd10* mice carry a spontaneous mutation in the beta subunit of the rod phosphodiesterase (*Pde6b*) (Chang et al., 2002) leading to an autosomal recessive and progressing degeneration of photoreceptors starting around PND15, with loss of most photoreceptors by PND42 (Samardzija et al., 2012). Whereas expression of rod cell markers like rhodopsin (*Rho*) and rod transducin (*Gnat1*) is drastically reduced already during the degenerative process (Samardzija et al., 2012), expression of *Gpr65* was strongly increased between PND21 and PND180 (Fig. 2B).

In contrast, expression of *Gpr4* and *Gpr68* did not differ from control wild type mice, except for a slightly reduced expression of *Gpr4* at PND10 and PND15, and increased expression of *Gpr68* at PND180 (Fig. 2A, C). This pattern of expression suggests that only *Gpr65* is responsive to photoreceptor degeneration. Furthermore, it is likely that none of the three genes is strongly expressed in photoreceptors since no downregulation was observed despite loss of all photoreceptors after PND42. Similar to the expression in *rd10* mice, expression of *Gpr65* was strongly induced after exposure of wild type mice to high levels of white light, a treatment that induces rapid and severe loss of photoreceptors through apoptosis (Wenzel et al., 2005; Grimm and Reme, 2013). Expression increased already at 24 hours after exposure and peaked at 3 days, before levels sharply declined at day 5 and approached basal levels at around 30 days post exposure (Fig. 2E). Again, *Gpr4* and *Gpr68* did not respond to the degeneration and their expression remained at basal levels throughout the period of analysis (Fig. 2D, F). Interestingly, the peak of *Gpr65* expression coincided with the known time of strong microglia activity in the light damaged retina (Joly et al., 2009).

Normal retinal morphology and function in the absence of GPR65

Our data suggest that GPR65 may have a function in the degenerating retina. To evaluate whether GPR65 might be important for the normal, non-stressed retina, we examined retinal morphologies of *Gpr65*$^{-/-}$ mice at 12 weeks and 6 months of age. The retinal architecture including arrangement of cells and thickness of layers appeared normal in young and old mice lacking GPR65 (Fig. 3A). Absence of a phenotype was further supported by similar expression levels of marker genes for rods (*Gnat1*), cones (cone transducin, *Gnat2*), bipolar cells (visual system homeobox 2, *Vsx2*), horizontal cells (calbindin 1, *Calb1*), amacrine cells (calbindin 2, *Calb2*), ganglion cells (POU class 4 homeobox 1, *Pou4f1*) and Müller glia cells (glutamate-ammonia ligase, *Glul*) in retinas of *Gpr65*$^{-/-}$ and *Gpr65*$^{+/-}$ mice (Fig. 3B). The apparent differences in *Calb2* and *Glul* expression levels did not reach statistical significance (Student's t-test). Loss of *Gpr65* expression had no influence on the expression of *Gpr4* and *Gpr68* suggesting that these genes did not compensate for the absence of *Gpr65* (Fig 3B). In addition, expression of genes that are frequently found upregulated in the stressed retina (Samardzija et al., 2012) such as caspase1 (*Casp1*), glial fibrillary acidic protein (*Gfap*), fibroblast growth factor 2 (*Fgf2*), signal transducer and activator of transcription 3 (*Stat3*), endothelin 2 (*Edn2*) and leukemia inhibitory factor (*Lif*), and of the cytokines tumor necrosis factor (*Tnf)* and transforming growth factor beta 1 (*Tgfb1*) was not significantly different in mice of the two genotypes (Fig. 3B). Furthermore, ERG analyses revealed normal scotopic and photopic responses in *Gpr65*$^{-/-}$ mice with a- and b-wave amplitudes similar to controls (Fig. 3C). In summary, GPR65 may be dispensable for the development and maintenance of a normal retinal architecture and

function, and its absence from the adult retina may not cause tissue stress as evidenced by basal expression of stress-related genes.

Accelerated retinal degeneration in *rd10* mice in the absence of GPR65

Our analysis revealed that *Gpr65* was upregulated during retinal degeneration (Fig. 2) suggesting a potential role of GPR65 in the degenerative process. Thus, we tested whether lack of GPR65 would influence degeneration in *rd10* mice by analyzing *Gpr65*$^{-/-}$*;rd10* double mutant mice. Retinal morphology of *Gpr65*$^{-/-}$*;rd10* mice appeared comparable to wild type and *rd10* mice at PND15, before onset of degeneration (Fig 4A). This is consistent with our conclusion that GPR65 is not essential for normal retinal development (Fig. 3). At PND21, *rd10* mice showed the typical signs of photoreceptor degeneration such as appearance of pyknotic nuclei, thinning of the ONL and disorganization of the outer segments. These features were slightly further enhanced in the *Gpr65*$^{-/-}$*;rd10* mice suggesting that absence of GPR65 may accelerate photoreceptor loss under pathological conditions (*rd10*). At PND42, both *rd10* and *Gpr65*$^{-/-}$*;rd10* mice had lost most photoreceptor cells (Fig. 4A). These observations were corroborated by measurements of the thicknesses of the entire retina (Fig. 4B) and the ONL (Fig. 4C), which differed slightly between *Gpr65*$^{-/-}$*;rd10* and *rd10* mice at PND21 but not at PND15 and PND42.

Increased microglia activation in the degenerating retina in the absence of GPR65

Several studies have shown that acidosis and *Gpr65* are involved in inflammatory responses affecting diverse immune cells such as neutrophils (Martinez et al., 2006; Murata et al., 2009), eosinophils (Kottyan et al., 2009), macrophages (Mogi et al., 2009), monocytes (Jancic et al., 2012) and natural killer cells (Maghazachi et al., 2004). Microglia are the resident immune cells of the retina and express high levels of *Gpr65* (Siegert et al., 2012). They are responsible for immune surveillance and homeostasis to ensure normal retinal function (Karlstetter et al., 2010) and are activated when the retina experiences stress or injury. Activated microglia change from their resting ramified to an amoeboid shape and migrate towards the site of injury (Schwartz et al., 2006; Langmann, 2007). Hence, we tested the response of microglia in the retina of *Gpr65*$^{-/-}$ mice during degeneration. *Gpr65*$^{+/-}$ (controls) and *Gpr65*$^{-/-}$ mice were exposed to bright light to induce photoreceptor cell death, and microglia were observed five days after light exposure in damaged and non-damaged areas of the retina. Ramified resting microglia in non-damaged retinal areas as well as amoeboid activated microglia in damaged areas appeared slightly more numerous in mice lacking GPR65 (Fig. 5). Thus, microglia do not seem to depend on GPR65 to survive and function in the degenerating retina but the receptor may influence distribution and activation of microglia either directly or indirectly via enhanced cell death of photoreceptors (Fig. 4).

Expression of cytokines and chemokines in the degenerating retina

Cytokines and chemokines are expressed by various cell types in the retina and may be involved in neurodegenerative disease mechanisms by regulating tissue response to cell damage and/or attracting immune cells to the site of degeneration (Kreutzberg, 1995; Langmann, 2007). Since GPR65 may slightly affect photoreceptor death in disease models (Fig. 4), we tested whether individual genes involved in the above pathways might be differentially expressed in *Gpr65*$^{-/-}$ mice before and at 1 day after exposure to 2 hours of bright light, a treatment that induces photoreceptor degeneration. However, basal gene expression before and induced expresssion levels after light exposure (Fig. 6) were similar in control (*Gpr65*$^{+/-}$) and *Gpr65*$^{-/-}$ mice with either a strong and significant (*Edn2*, *Fgf2*, *Casp1*, chemokine (C-C motif) ligand 2 (*Ccl2*), *Ccl4*, *Ccl8*, *Ccl12*), a moderate (*Lif*, *Stat3*, *Gfap*, *Ccl5*) or no (*Tnf*, *Ccl9*, colony stimulating factor 1 receptor (*Csfr1*), chemokine (C-X3-C motif) ligand 1 (*Cx3cl1*)) upregulation. Note that at the time point analyzed (24 h after light exposure) some of the early responsive genes such as *Lif* may already approaching again basal expression levels after an initial strong upregulation (Samardzija et al., 2006a). The only exception may be *Tgfb1*, which was significantly upregulated in retinas of mice lacking GPR65 but not in controls. Upregulation of *Ccl2* and *Ccl4* did not reach significance in *Gpr65* knockouts because of highly variable expression levels.

DISCUSSION

Changes in extracellular and/or intracellular pH seem important for proper retinal function (Hirasawa et al., 2012; Wang et al., 2014), may play a role in degenerative processes (Reber et al., 2002; Takahashi et al., 2004; Perron et al., 2013), and follow the circadian rhythm (Dmitriev and Mangel, 2001) in the retina. Thus, it may not be surprising that the proton-sensing protein encoding genes *Gpr4*, *Gpr65* and *Gpr68* were expressed already in the early postnatal retina of the mouse, and that expression levels increased during development until adulthood. Although the expression pattern was similar for the three mouse strains tested, some strain specificity may nevertheless exist since *Gpr68* was found at significantly lower levels in retinas of adult 129S6 mice as compared to BALB/c and C57BL/6 mice. The reason behind this observation and the potentially ensuing physiological or functional consequences remain to be investigated.

Although all three genes showed a similar expression profile in the normal retina, only *Gpr65*, but not *Gpr4* or *Gpr68*, was affected by retinal degeneration. Exposure to damaging levels of white light induced a strong but transient increase of *Gpr65* expression that peaked

at 3 days post exposure. Expression of *Gpr65* declined sharply already at 5 days, but basal levels were reached only at about 30 days after light exposure. In the *rd10* mouse, timing of induction was similar with strongly increased levels shortly after onset of degeneration (which is around PND15 (Chang et al., 2007; Barhoum et al., 2008; Samardzija et al., 2012)). In contrast to the light damage model, however, *Gpr65* levels in the *rd10* mouse remained at elevated levels at least until 6 months of age. These different time courses may reflect the sharp and synchronous induction of cell death by acute light exposure and the slower and extended period of photoreceptor loss in *rd10* mice. Although most photoreceptors are lost already by PND42, some cells, especially cones, persist preferentially in the peripheral retina of the rd10 mouse. These cells degenerate slowly over an extended period of time since expression of cone cell markers is detectable for several months (Samardzija et al., 2012). High *Gpr65* expression correlated with the published increased levels of Caspase-1 and GFAP proteins in the two models (Samardzija et al., 2006b; Samardzija et al., 2012) and coincided with microglial activation (Joly et al., 2009; Peng et al., 2014). This may suggest a function of GPR65 in the regulation of an immune-like response in the retina. Indeed, a recent report suggested that GPR65 acts as a negative regulator of inflammation (Onozawa et al., 2011), a conclusion that may be supported by our observation that microglia activation may have been stronger in degenerating retinas that lack GPR65 (see below).

Although *Gpr65* was not required for normal retinal development and function, its absence slightly accelerated photoreceptor loss in the retina of *rd10* mice. It has been reported previously that GPR65-mediated signaling can support survival of cells under acidic conditions, such as cancer cells in tumors (Sin et al., 2004; Ihara et al., 2010; Ryder et al., 2012) and some immune cells (Kottyan et al., 2009). Since degenerative processes and cell death lead to changes in the tissue microenvironment including acidification, increased *Gpr65* expression may contribute to processes that adapt cells to the changing tissue environment during retinal degeneration. Especially responsive to retinal alterations are the resident macro- and microglial cells that fulfill a variety of functions in retinal physiology and pathophysiology. Müller glia cells, for example, are highly reactive to stress and retinal degeneration, and support survival of neurons through production of protective growth factors, cytokines and other signaling molecules (Joly et al., 2008; Rhee et al., 2013). However, their (over) activation can also lead to gliosis contributing to degeneration and loss of vision (Bringmann et al., 2006). Similarly, microglia, which are the resident immune cells of the retina (Karlstetter et al., 2010), respond quickly to retinal injury in various ways. In the normal retina they localize mainly to the ganglion cell layer and have a ramified structure with extended processes surveying the surroundings for stress signals. After detection of such stress signals microglia become activated, acquire an amoeboid shape and migrate to the

site of injury or stress where they transform into phagocytes and participate in the clearance of cellular debris (Schwartz et al., 2006; Langmann, 2007; Karlstetter et al., 2014b). Although it is difficult to label microglia as 'good' or 'bad', increasing evidence indicate that activated microglia may be neurotoxic and may contribute to processes of retinal inflammation accelerating neurodegeneration (Xu et al., 2009; Karlstetter et al., 2014a; Karlstetter et al., 2014b; Zeng et al., 2014). Recently it was shown that *Gpr65* is one of the major transcripts in mouse microglia (Siegert et al., 2012), that GPR65 is the major acid sensing receptor expressed in these cells (Jin et al., 2014) and that GPR65 mediated signaling may repress expression of inflammatory genes, effectively blunting the inflammatory response to cell damage (Jin et al., 2014). Here we observed that expression of *Gpr65* peaked at three days after light exposure (Fig. 2), at a time that correlates with strong microglial activity in the light-damaged retina (Joly et al., 2009). We showed that microglia were still activated at five days after light exposure and seemingly even more so in retinas of *Gpr65*$^{-/-}$ mice (Fig. 5). Whether this was a direct consequence of the absence of GPR65 signaling or was indirectly caused by increased retinal stress remains to be investigated. However, it may suggest that increased microglia activity in *Gpr65*$^{-/-}$ may have contributed to the slightly accelerated photoreceptor degeneration observed in *rd10* mice because activated retinal microglia elicit production and secretion of several cytokines and chemokines, a response that contributes to neurodegenerative disease mechanisms (Kreutzberg, 1995; Langmann, 2007). In this respect it is interesting to note that several cytokine or chemokine encoding genes such as *Tgfb1*, *Ccl2*, *Ccl4* and *Ccl5* showed a tendency towards a higher expression after light exposure in the *Gpr65*$^{-/-}$ mice. Although the effect was rather weak, cells in the retina of *Gpr65*$^{-/-}$ mice may thus produce more inflammatory cytokines, thereby increasing retinal stress and cell death. In conclusion, this study shows that *Gpr65* is not essential for normal retinal development and function, but may be part of the tissue response to retinal stress or degeneration.

ACKNOWLEDGEMENTS

The authors are grateful to Marie-Gabrielle Ludwig and Dr. Klaus Seuwen (Novartis Institute for BioMedical Research (NIBR), Basel, Switzerland) for discussions and for sharing the *Gpr65*$^{-/-}$ mice, and to Carsten Wagner (University of Zürich, Zürich, Switzerland) for providing breeding pairs of these mice. We thank Cornelia Imsand, Andrea Gubler and Christel Beck for their skillful assistance in experimental procedures. This work was supported by the Swiss National Science Foundation (31003A_133043 and 31003A_149311).

REFERENCES

Bailey, J. L. (2005) Metabolic acidosis: an unrecognized cause of morbidity in the patient with chronic kidney disease. *Kidney Int Suppl* S15-S23.

Barhoum, R., Martinez-Navarrete, G., Corrochano, S., Germain, F., Fernandez-Sanchez, L., de la Rosa, E. J., de la Villa, P. and Cuenca, N. (2008) Functional and structural modifications during retinal degeneration in the rd10 mouse. *Neuroscience* **155**, 698-713.

Barnes, S., Merchant, V. and Mahmud, F. (1993) Modulation of transmission gain by protons at the photoreceptor output synapse. *Proc Natl Acad Sci U S A* **90**, 10081-10085.

Bringmann, A., Pannicke, T., Grosche, J., Francke, M., Wiedemann, P., Skatchkov, S. N., Osborne, N. N. and Reichenbach, A. (2006) Muller cells in the healthy and diseased retina. *Prog Retin Eye Res* **25**, 397-424.

Chang, B., Hawes, N. L., Hurd, R. E., Davisson, M. T., Nusinowitz, S. and Heckenlively, J. R. (2002) Retinal degeneration mutants in the mouse. *Vision Res* **42**, 517-525.

Chang, B., Hawes, N. L., Pardue, M. T., German, A. M., Hurd, R. E., Davisson, M. T., Nusinowitz, S., Rengarajan, K., Boyd, A. P., Sidney, S. S., Phillips, M. J., Stewart, R. E., Chaudhury, R., Nickerson, J. M., Heckenlively, J. R. and Boatright, J. H. (2007) Two mouse retinal degenerations caused by missense mutations in the beta-subunit of rod cGMP phosphodiesterase gene. *Vision Res* **47**, 624-633.

Detrick, B. and Hooks, J. J. (2010) Immune regulation in the retina. *Immunol Res* **47**, 153-161.

DeVries, S. H. (2001) Exocytosed protons feedback to suppress the Ca2+ current in mammalian cone photoreceptors. *Neuron* **32**, 1107-1117.

Dmitriev, A. V. and Mangel, S. C. (2001) Circadian clock regulation of pH in the rabbit retina. *J Neurosci* **21**, 2897-2902.

English, P. and Williams, G. (2004) Hyperglycaemic crises and lactic acidosis in diabetes mellitus. *Postgrad Med J* **80**, 253-261.

Gatenby, R. A. and Gillies, R. J. (2004) Why do cancers have high aerobic glycolysis? *Nat Rev Cancer* **4**, 891-899.

Grimm, C. and Reme, C. E. (2013) Light damage as a model of retinal degeneration. *Methods Mol Biol* **935**, 87-97.

Hecke, F., Hoehn, T., Strauss, E., Obladen, M. and Sonntag, J. (2001) In-vitro activation of complement system by lactic acidosis in newborn and adults. *Mediators Inflamm* **10**, 27-31.

Hirasawa, H., Yamada, M. and Kaneko, A. (2012) Acidification of the synaptic cleft of cone photoreceptor terminal controls the amount of transmitter release, thereby forming the receptive field surround in the vertebrate retina. *J Physiol Sci* **62**, 359-375.

Ihara, Y., Kihara, Y., Hamano, F., Yanagida, K., Morishita, Y., Kunita, A., Yamori, T., Fukayama, M., Aburatani, H., Shimizu, T. and Ishii, S. (2010) The G protein-coupled receptor T-cell death-associated gene 8 (TDAG8) facilitates tumor development by serving as an extracellular pH sensor. *Proc Natl Acad Sci U S A* **107**, 17309-17314.

Im, D. S., Heise, C. E., Nguyen, T., O'Dowd, B. F. and Lynch, K. R. (2001) Identification of a molecular target of psychosine and its role in globoid cell formation. *J Cell Biol* **153**, 429-434.

Jancic, C. C., Cabrini, M., Gabelloni, M. L., Rodriguez Rodrigues, C., Salamone, G., Trevani, A. S. and Geffner, J. (2012) Low extracellular pH stimulates the production of IL-1beta by human monocytes. *Cytokine* **57**, 258-268.

Jin, Y., Sato, K., Tobo, A., Mogi, C., Tobo, M., Murata, N., Ishii, S., Im, D. S. and Okajima, F. (2014) Inhibition of interleukin-1beta production by extracellular acidification through the TDAG8/cAMP pathway in mouse microglia. *J Neurochem* **129**, 683-695.

Joly, S., Francke, M., Ulbricht, E., Beck, S., Seeliger, M., Hirrlinger, P., Hirrlinger, J., Lang, K. S., Zinkernagel, M., Odermatt, B., Samardzija, M., Reichenbach, A., Grimm, C. and Reme, C. E. (2009) Cooperative phagocytes: resident microglia and bone marrow immigrants remove dead photoreceptors in retinal lesions. *Am J Pathol* **174**, 2310-

2323.
Joly, S., Lange, C., Thiersch, M., Samardzija, M. and Grimm, C. (2008) Leukemia inhibitory factor extends the lifespan of injured photoreceptors in vivo. *J Neurosci* **28**, 13765-13774.
Justus, C. R., Dong, L. and Yang, L. V. (2013) Acidic tumor microenvironment and pH-sensing G protein-coupled receptors. *Front Physiol* **4**, 354.
Kabarowski, J. H., Xu, Y. and Witte, O. N. (2002) Lysophosphatidylcholine as a ligand for immunoregulation. *Biochem Pharmacol* **64**, 161-167.
Karlstetter, M., Ebert, S. and Langmann, T. (2010) Microglia in the healthy and degenerating retina: insights from novel mouse models. *Immunobiology* **215**, 685-691.
Karlstetter, M., Nothdurfter, C., Aslanidis, A., Moeller, K., Horn, F., Scholz, R., Neumann, H., Weber, B. H., Rupprecht, R. and Langmann, T. (2014a) Translocator protein (18 kDa) (TSPO) is expressed in reactive retinal microglia and modulates microglial inflammation and phagocytosis. *J Neuroinflammation* **11**, 3.
Karlstetter, M., Scholz, R., Rutar, M., Wong, W. T., Provis, J. M. and Langmann, T. (2014b) Retinal microglia: Just bystander or target for therapy? *Prog Retin Eye Res*
Kottyan, L. C., Collier, A. R., Cao, K. H., Niese, K. A., Hedgebeth, M., Radu, C. G., Witte, O. N., Khurana Hershey, G. K., Rothenberg, M. E. and Zimmermann, N. (2009) Eosinophil viability is increased by acidic pH in a cAMP- and GPR65-dependent manner. *Blood* **114**, 2774-2782.
Kreutzberg, G. W. (1995) Microglia, the first line of defence in brain pathologies. *Arzneimittelforschung* **45**, 357-360.
Kumar, N., Velic, A., Soliz, J., Shi, Y., Li, K., Wang, S., Weaver, J. L., Sen, J., Abbott, S. B. G., Lazarenko, R. M., Ludwig, M.-G., Peres-Reyes, E., Mohebbi, N., Bettoni, C., Gassmann, M., Suply, T., Seuwen, K., Guyenet, P. G., Wagner, C. A. and Bayliss, D. A. (in press) Regulation of breathing by CO2 requires the proton-activated receptor GPR4 in retrotrapezoid nucleus neurons. *Science*
Langmann, T. (2007) Microglia activation in retinal degeneration. *J Leukoc Biol* **81**, 1345-1351.
Lardner, A. (2001) The effects of extracellular pH on immune function. *J Leukoc Biol* **69**, 522-530.
Li, Z., Dong, L., Dean, E. and Yang, L. V. (2013) Acidosis decreases c-Myc oncogene expression in human lymphoma cells: a role for the proton-sensing G protein-coupled receptor TDAG8. *Int J Mol Sci* **14**, 20236-20255.
Liu, J. P., Nakakura, T., Tomura, H., Tobo, M., Mogi, C., Wang, J. Q., He, X. D., Takano, M., Damirin, A., Komachi, M., Sato, K. and Okajima, F. (2010) Each one of certain histidine residues in G-protein-coupled receptor GPR4 is critical for extracellular proton-induced stimulation of multiple G-protein-signaling pathways. *Pharmacol Res* **61**, 499-505.
Ludwig, M. G., Vanek, M., Guerini, D., Gasser, J. A., Jones, C. E., Junker, U., Hofstetter, H., Wolf, R. M. and Seuwen, K. (2003) Proton-sensing G-protein-coupled receptors. *Nature* **425**, 93-98.
Maghazachi, A. A., Knudsen, E., Jin, Y., Jenstad, M. and Chaudhry, F. A. (2004) D-galactosyl-beta1-1'-sphingosine and D-glucosyl-beta1-1'-sphingosine induce human natural killer cell apoptosis. *Biochem Biophys Res Commun* **320**, 810-815.
Martinez, D., Vermeulen, M., Trevani, A., Ceballos, A., Sabatte, J., Gamberale, R., Alvarez, M. E., Salamone, G., Tanos, T., Coso, O. A. and Geffner, J. (2006) Extracellular acidosis induces neutrophil activation by a mechanism dependent on activation of phosphatidylinositol 3-kinase/Akt and ERK pathways. *J Immunol* **176**, 1163-1171.
Mogi, C., Tobo, M., Tomura, H., Murata, N., He, X. D., Sato, K., Kimura, T., Ishizuka, T., Sasaki, T., Sato, T., Kihara, Y., Ishii, S., Harada, A. and Okajima, F. (2009) Involvement of proton-sensing TDAG8 in extracellular acidification-induced inhibition of proinflammatory cytokine production in peritoneal macrophages. *J Immunol* **182**, 3243-3251.
Mogi, C., Tomura, H., Tobo, M., Wang, J. Q., Damirin, A., Kon, J., Komachi, M., Hashimoto, K., Sato, K. and Okajima, F. (2005) Sphingosylphosphorylcholine antagonizes proton-

sensing ovarian cancer G-protein-coupled receptor 1 (OGR1)-mediated inositol phosphate production and cAMP accumulation. *J Pharmacol Sci* **99**, 160-167.
Murata, N., Mogi, C., Tobo, M., Nakakura, T., Sato, K., Tomura, H. and Okajima, F. (2009) Inhibition of superoxide anion production by extracellular acidification in neutrophils. *Cell Immunol* **259**, 21-26.
Okajima, F. (2013) Regulation of inflammation by extracellular acidification and proton-sensing GPCRs. *Cell Signal* **25**, 2263-2271.
Onozawa, Y., Komai, T. and Oda, T. (2011) Activation of T cell death-associated gene 8 attenuates inflammation by negatively regulating the function of inflammatory cells. *Eur J Pharmacol* **654**, 315-319.
Peng, B., Xiao, J., Wang, K., So, K. F., Tipoe, G. L. and Lin, B. (2014) Suppression of microglial activation is neuroprotective in a mouse model of human retinitis pigmentosa. *J Neurosci* **34**, 8139-8150.
Perez, V. L., Saeed, A. M., Tan, Y., Urbieta, M. and Cruz-Guilloty, F. (2013) The eye: A window to the soul of the immune system. *J Autoimmun* **45**, 7-14.
Perron, N. R., Beeson, C. and Rohrer, B. (2013) Early alterations in mitochondrial reserve capacity; a means to predict subsequent photoreceptor cell death. *J Bioenerg Biomembr* **45**, 101-109.
Radu, C. G., Nijagal, A., McLaughlin, J., Wang, L. and Witte, O. N. (2005) Differential proton sensitivity of related G protein-coupled receptors T cell death-associated gene 8 and G2A expressed in immune cells. *Proc Natl Acad Sci U S A* **102**, 1632-1637.
Reber, F., Kasper, M., Siegner, A., Kniep, E., Seigel, G. and Funk, R. H. (2002) Alteration of the intracellular pH and apoptosis induction in a retinal cell line by the AGE-inducing agent glyoxal. *Graefes Arch Clin Exp Ophthalmol* **240**, 1022-1032.
Rhee, K. D., Nusinowitz, S., Chao, K., Yu, F., Bok, D. and Yang, X. J. (2013) CNTF-mediated protection of photoreceptors requires initial activation of the cytokine receptor gp130 in Muller glial cells. *Proc Natl Acad Sci U S A* **110**, E4520-E4529.
Ryder, C., McColl, K., Zhong, F. and Distelhorst, C. W. (2012) Acidosis promotes Bcl-2 family-mediated evasion of apoptosis: involvement of acid-sensing G protein-coupled receptor Gpr65 signaling to Mek/Erk. *J Biol Chem* **287**, 27863-27875.
Samardzija, M., Wariwoda, H., Imsand, C., Huber, P., Heynen, S. R., Gubler, A. and Grimm, C. (2012) Activation of survival pathways in the degenerating retina of rd10 mice. *Exp Eye Res* **99**, 17-26.
Samardzija, M., Wenzel, A., Aufenberg, S., Thiersch, M., Reme, C. and Grimm, C. (2006a) Differential role of Jak-STAT signaling in retinal degenerations. *FASEB J* **20**, 2411-2413.
Samardzija, M., Wenzel, A., Thiersch, M., Frigg, R., Reme, C. and Grimm, C. (2006b) Caspase-1 ablation protects photoreceptors in a model of autosomal dominant retinitis pigmentosa. *Invest Ophthalmol Vis Sci* **47**, 5181-5190.
Schwartz, M., Butovsky, O., Bruck, W. and Hanisch, U. K. (2006) Microglial phenotype: is the commitment reversible? *Trends Neurosci* **29**, 68-74.
Siegert, S., Cabuy, E., Scherf, B. G., Kohler, H., Panda, S., Le, Y. Z., Fehling, H. J., Gaidatzis, D., Stadler, M. B. and Roska, B. (2012) Transcriptional code and disease map for adult retinal cell types. *Nat Neurosci* **15**, 487-95, S1.
Sin, W. C., Zhang, Y., Zhong, W., Adhikarakunnathu, S., Powers, S., Hoey, T., An, S. and Yang, J. (2004) G protein-coupled receptors GPR4 and TDAG8 are oncogenic and overexpressed in human cancers. *Oncogene* **23**, 6299-6303.
Takahashi, A., Masuda, A., Sun, M., Centonze, V. E. and Herman, B. (2004) Oxidative stress-induced apoptosis is associated with alterations in mitochondrial caspase activity and Bcl-2-dependent alterations in mitochondrial pH (pHm). *Brain Res Bull* **62**, 497-504.
Tanimoto, N., Muehlfriedel, R. L., Fischer, M. D., Fahl, E., Humphries, P., Biel, M. and Seeliger, M. W. (2009) Vision tests in the mouse: Functional phenotyping with electroretinography. *Front Biosci (Landmark Ed)* **14**, 2730-2737.
Tomura, H., Mogi, C., Sato, K. and Okajima, F. (2005) Proton-sensing and lysolipid-sensitive

G-protein-coupled receptors: a novel type of multi-functional receptors. *Cell Signal* **17**, 1466-1476.

Vaupel, P., Kallinowski, F. and Okunieff, P. (1989) Blood flow, oxygen and nutrient supply, and metabolic microenvironment of human tumors: a review. *Cancer Res* **49**, 6449-6465.

Wang, J. Q., Kon, J., Mogi, C., Tobo, M., Damirin, A., Sato, K., Komachi, M., Malchinkhuu, E., Murata, N., Kimura, T., Kuwabara, A., Wakamatsu, K., Koizumi, H., Uede, T., Tsujimoto, G., Kurose, H., Sato, T., Harada, A., Misawa, N., Tomura, H. and Okajima, F. (2004) TDAG8 is a proton-sensing and psychosine-sensitive G-protein-coupled receptor. *J Biol Chem* **279**, 45626-45633.

Wang, T. M., Holzhausen, L. C. and Kramer, R. H. (2014) Imaging an optogenetic pH sensor reveals that protons mediate lateral inhibition in the retina. *Nat Neurosci* **17**, 262-268.

Wenzel, A., Grimm, C., Samardzija, M. and Reme, C. E. (2005) Molecular mechanisms of light-induced photoreceptor apoptosis and neuroprotection for retinal degeneration. *Prog Retin Eye Res* **24**, 275-306.

Xu, H., Chen, M. and Forrester, J. V. (2009) Para-inflammation in the aging retina. *Prog Retin Eye Res* **28**, 348-368.

Yang, Z., Alvarez, B. V., Chakarova, C., Jiang, L., Karan, G., Frederick, J. M., Zhao, Y., Sauve, Y., Li, X., Zrenner, E., Wissinger, B., Hollander, A. I., Katz, B., Baehr, W., Cremers, F. P., Casey, J. R., Bhattacharya, S. S. and Zhang, K. (2005) Mutant carbonic anhydrase 4 impairs pH regulation and causes retinal photoreceptor degeneration. *Hum Mol Genet* **14**, 255-265.

Zeng, H., Ding, M., Chen, X. X. and Lu, Q. (2014) Microglial NADPH oxidase activation mediates rod cell death in the retinal degeneration in rd mice. *Neuroscience* **275**, 54-61.

FIGURE LEGENDS

Figure 1. Gene expression levels of proton-sensing GPCRs in the retina. **(A-C)** Relative expression levels of **(A)** *Gpr4*, **(B)** *Gpr65* and **(C)** *Gpr68* in retinas of 129S6, BALB/c and C57BL/6 mice at PND60 – PND74. **(D-F)** Relative expressions of **(D)** *Gpr4*, **(E)** *Gpr65* and **(F)** *Gpr68* during retinal development in BALB/c mice. Expression was determined by semi-quantitative real-time PCR, normalized to *Actb* and expressed relative to the levels in 129S6 **(A-C)** or to PND1 **(D-F)**. Shown are mean values ± SD of $N = 3$. Significance was tested using two-way ANOVA analysis (*** $P < 0.001$).

Figure 2. Upregulation of *Gpr65* expression during inherited and induced retinal degeneration. **(A-C)** Relative expression of **(A)** *Gpr4*, **(B)** *Gpr65* and **(C)** *Gpr68* in *rd10* (red) and control wild type C57BL/6 (black) mice at time points as indicated. **(D-F)** Relative expressions of **(D)** *Gpr4*, **(E)** *Gpr65* and **(F)** *Gpr68* before (dark ctrl), immediately (imm) or at various time points (as indicated) after exposure of wild type BALB/c mice to 5'000 lux of white light for 1 h. Expression levels were determined by semi-quantitative real-time PCR, normalized to *Actb* and expressed relative to the levels of controls at PND10 **(A-C)** or to controls not exposed to light **(D-F)**. Shown are mean values ± SD of $N = 3$. Significance at individual time points was tested using Student's t-test (* $P < 0.05$, ** $P < 0.01$, *** $P < 0.001$).

Figure 3. Normal retinal morphology and function in absence of GPR65 **(A)** Retinal morphology of $Gpr65^{+/-}$ and $Gpr65^{-/-}$ mice at 12 weeks and 6 months of age. Images were taken from the temporal retina at 200 µm from the optic nerve head. Shown are representative images of $N = 3$ retinas per genotype and time point. Scale bar, 50 µm. **(B)** Relative expression levels of selected genes in retinas of 12-week-old $Gpr65^{+/-}$ (black columns) and $Gpr65^{-/-}$ (red columns) mice. Expression levels were determined by semi-quantitative real-time PCR, normalized to *Actb* and expressed relative to the levels of $Gpr65^{+/-}$ control mice. Shown are mean values ± SD of $N = 3$. Significance was tested using Student's t-test. * $P < 0.05$. **(C)** Scotopic and photopic electroretinograms of $Gpr65^{+/-}$ and $Gpr65^{-/-}$ mice at 12 weeks of age. Top panels: representative traces of individual mice, Bottom panels: Scotopic a- and b- wave amplitudes and photopic b-wave amplitudes as a function of light intensity for $N = 3$ mice (6 retinas) per genotype.

Figure 4. Slight acceleration of retinal degeneration in *rd10* mice in the absence of GPR65. **(A)** Retinal morphology of C57BL/6, *rd10* and $Gpr65^{-/-}$*;rd10* mice at PND15, PND21 and PND42. Shown are representative sections of $N = 3$ animals for all genotypes and ages, except for C57BL/6 at PND21 and $Gpr65^{-/-}$*;rd10* at PND42 ($N = 2$). Scale bar: 50 µm. **(B)**

Retinal thickness and **(C)** ONL thickness of C57BL/6 (black), *rd10* (red) and *Gpr65*$^{-/-}$*;rd10* (blue) mice, measured at 200, 400, 600, 800, 1000, 1200, 1400, 1600 and 1800 µm from the optic nerve head (0). Shown are mean values ± SD of *N* = 3 animals for all genotypes and ages, except for C57BL/6 at PND21 and *Gpr65*$^{-/-}$*;rd10* at PND42 (*N* = 2). Significance was tested using Student's t-test.

Figure 5. Strong activation of microglia in light damaged retinas lacking GPR65. *Gpr65*$^{+/-}$ and *Gpr65*$^{-/-}$ mice were exposed to 15'000 lux of white light for 2 h, and tested for microglia after 5 days of recovery by immunostaining of retinal flat mounts with an antibody against IBA1. Shown are representative images of non-damaged and damaged retinal areas as indicated. Focal plane was at the outer plexiform layer. Scale bar: 50 µM. *N* = 2.

Figure 6. Gene expression in light damaged retinas of 6-8 week old *Gpr65*$^{+/-}$ and *Gpr65*$^{-/-}$ mice. Expression of selected genes was determined before (dark control, DC, black columns) and at 1 day after exposure to 15'000 lux of white light for 2 h (LE, red columns) by real-time PCR. Levels were normalized to *Actb* and expressed relative to the dark control of *Gpr65*$^{+/-}$ mice (set to 1). As expression of *Ccl8* was below detection limit in retinas of dark controls, *Ccl8* levels in light exposed mice were expressed relative to *Actb*. Shown are mean values ± SD of *N* = 3. n.d. - not detectable. Significance was tested using Student's t-test (* $P < 0.05$, ** $P < 0.01$, *** $P < 0.001$).

Figure 1

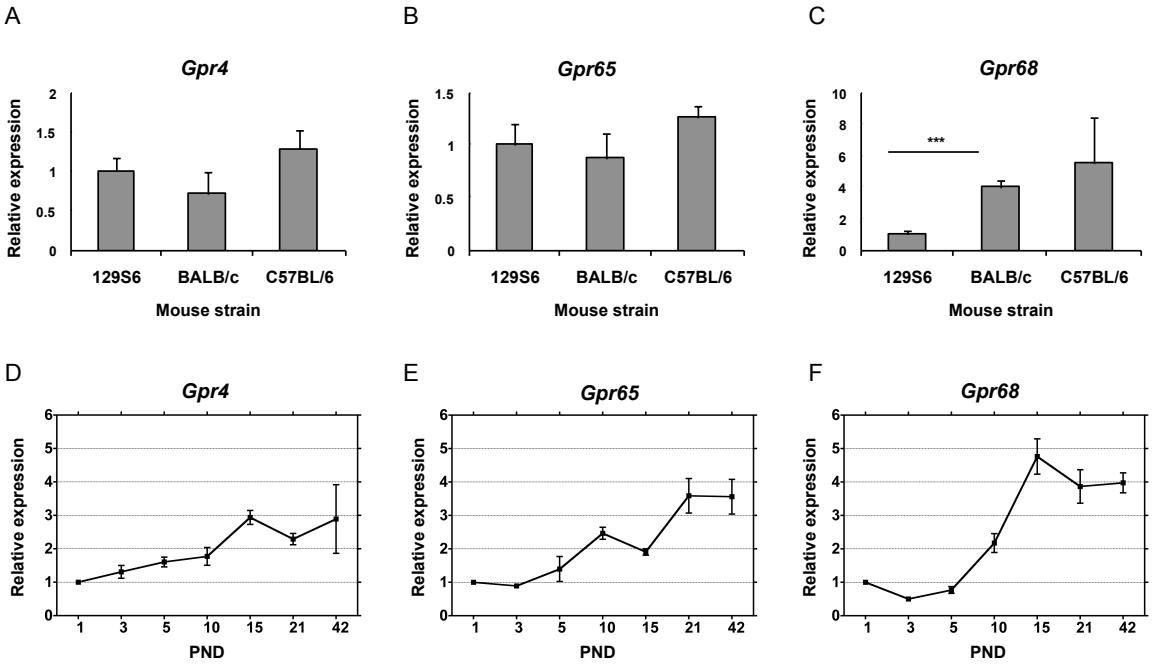
A
Gpr4
Relative expression
2
1.5
1
0.5
0
129S6
BALB/c
C57BL/6
Mouse strain
B
Gpr65
Relative expression
1.5
1
0.5
0
129S6
BALB/c
C57BL/6
Mouse strain
C
Gpr68
Relative expression
***
10
8
6
4
2
0
129S6
BALB/c
C57BL/6
Mouse strain
D
Gpr4
Relative expression
6
5
4
3
2
1
0
1
3
5
10
15
21
42
PND
E
Gpr65
Relative expression
6
5
4
3
2
1
0
1
3
5
10
15
21
42
PND
F
Gpr68
Relative expression
6
5
4
3
2
1
0
1
3
5
10
15
21
42
PND

Figure 2

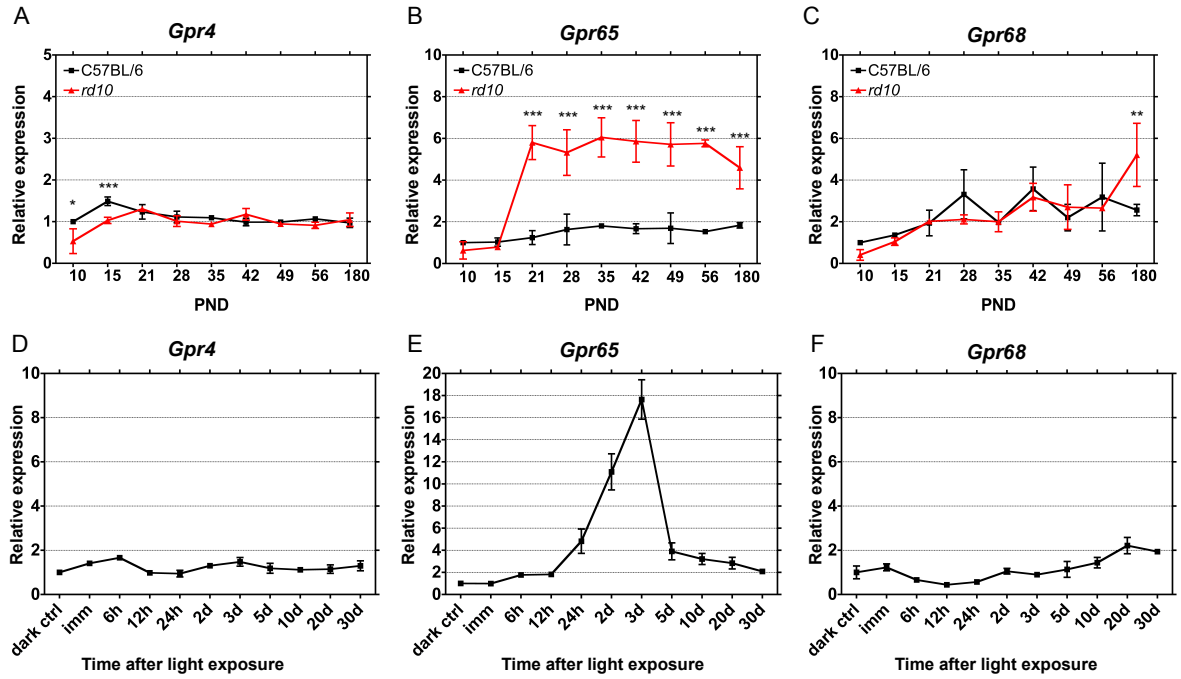
A
Gpr4
C57BL/6
rd10
Relative expression
PND
B
Gpr65
C
Gpr68
D
Gpr4
E
Gpr65
F
Gpr68
dark ctrl
imm
6h
12h
24h
2d
3d
5d
10d
20d
30d
Time after light exposure

Figure 3

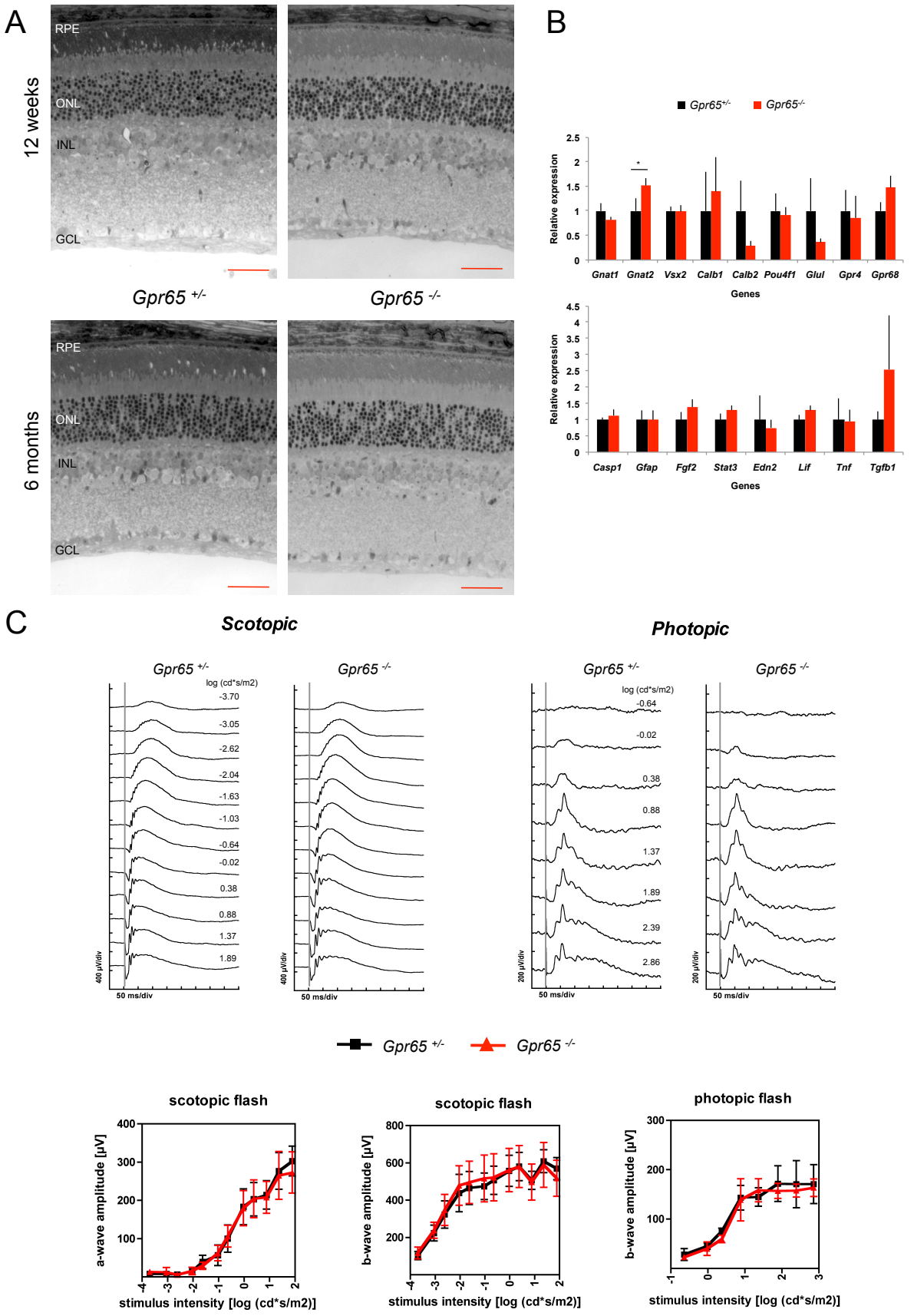
A
12 weeks
6 months
RPE
ONL
INL
GCL
Gpr65 +/-
Gpr65 -/-
B
Gpr65+/-
Gpr65-/-
Relative expression
Gnat1
Gnat2
Vsx2
Calb1
Calb2
Pou4f1
Glul
Gpr4
Gpr68
Genes
Casp1
Gfap
Fgf2
Stat3
Edn2
Lif
Tnf
Tgfb1
C
Scotopic
Photopic
log (cd*s/m2)
50 ms/div
400 µV/div
200 µV/div
scotopic flash
photopic flash
a-wave amplitude [µV]
b-wave amplitude [µV]
stimulus intensity [log (cd*s/m2)]

Figure 4

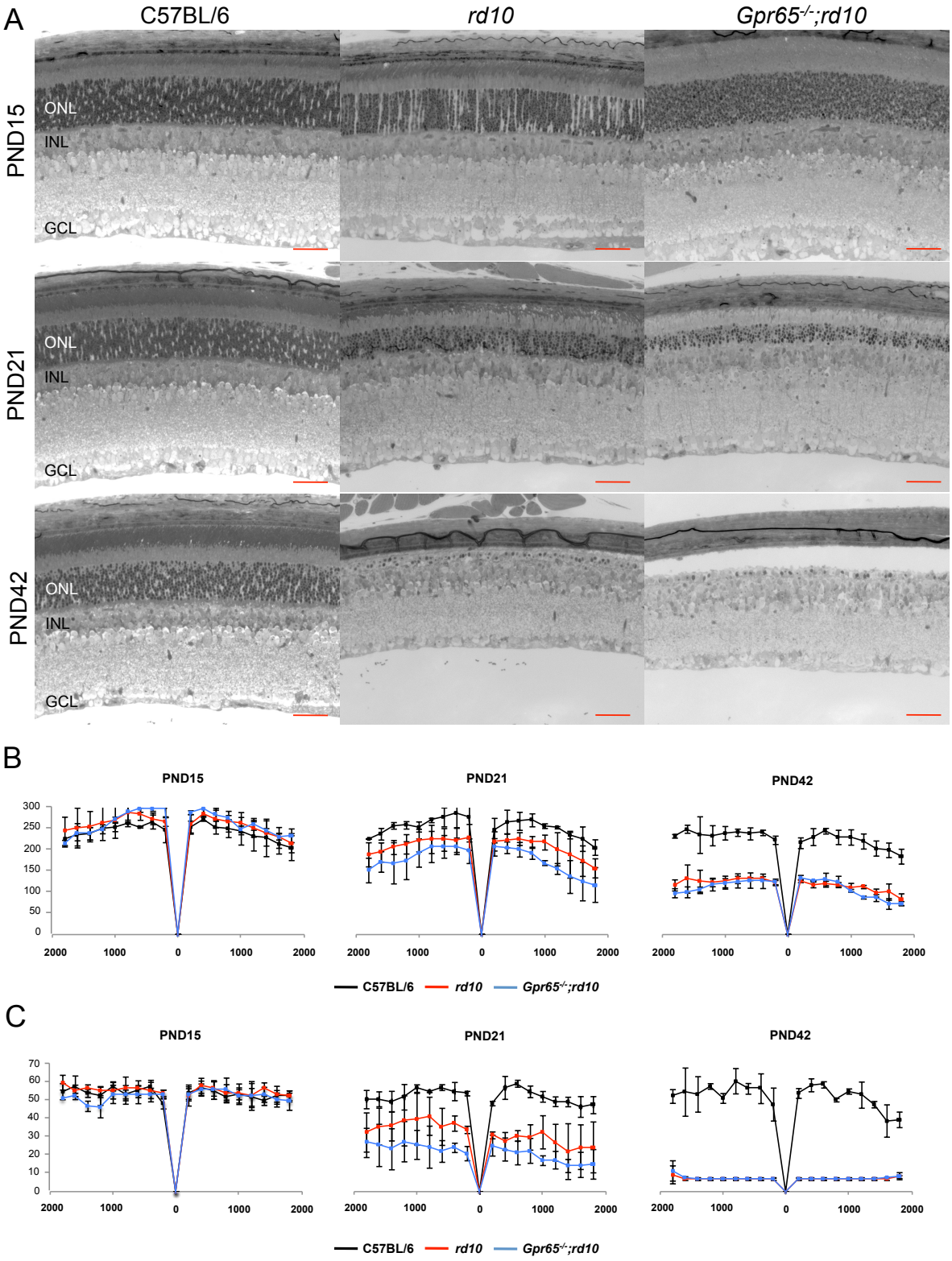
A
C57BL/6
rd10
Gpr65-/-;rd10
PND15
PND21
PND42
ONL
INL
GCL
B
PND15
PND21
PND42
300
250
200
150
100
50
0
2000
1000
0
1000
2000
C57BL/6
rd10
Gpr65-/-;rd10
C
PND15
PND21
PND42
70
60
50
40
30
20
10
0
2000
1000
0
1000
2000
C57BL/6
rd10
Gpr65-/-;rd10

Figure 5

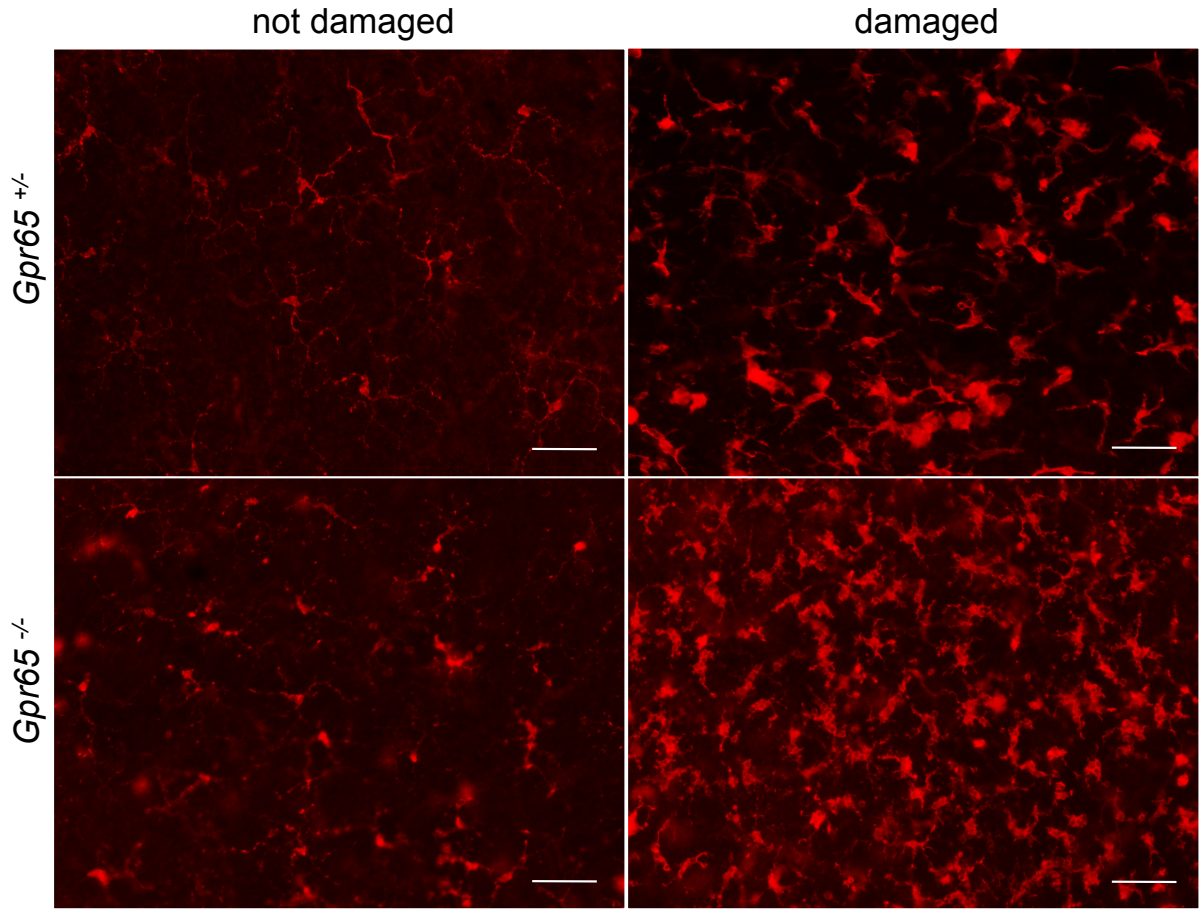

Figure 6

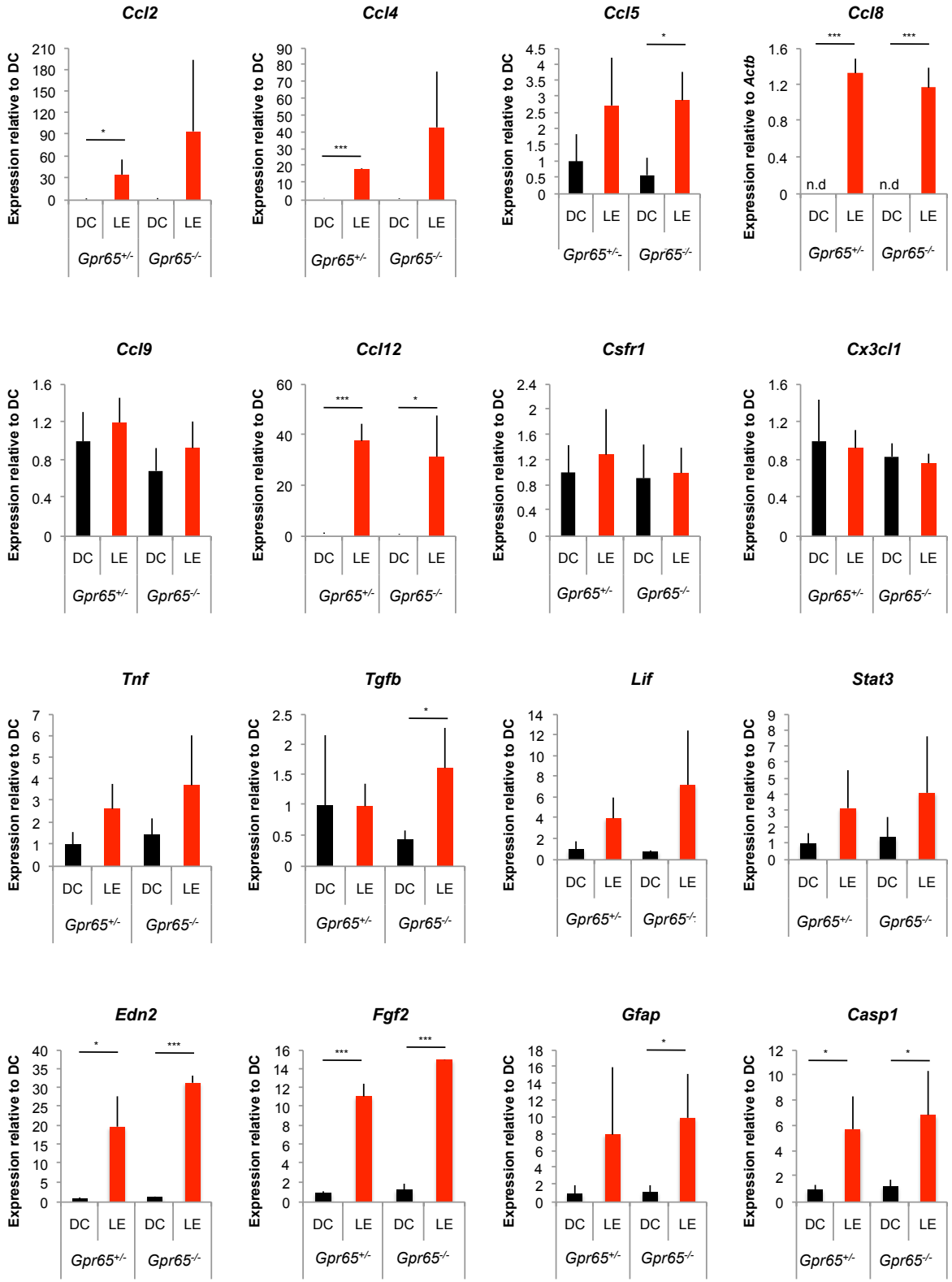
Ccl2
Ccl4
Ccl5
Ccl8
Ccl9
Ccl12
Csfr1
Cx3cl1
Tnf
Tgfb
Lif
Stat3
Edn2
Fgf2
Gfap
Casp1
Expression relative to DC
Expression relative to Actb
n.d
DC
LE
Gpr65+/-
Gpr65-/-

Table 1. Primers used for semiquantitative real-time PCR

Gene	Forward primer	Reverse primer	Annealing temp(°C)	Amplicon size (bp)
Actb	CAACGGCTCCGGCATGTGC	CTCTTGCTCTGGGCCTCG	62	153
Gpr4 (BALB/c)	CGGAGCAGGCCTAGCAATCT	TGAGTAAGTGGCAGAGCACAGG	60	158
Gpr4 (C57BL/6)	CGGAGCAGGCCTAGCAATCT	TGAGTAAGTGGTGGAGCACAGG	60	158
Gpr4 (129S6)	CGGAGCAGCCTAGCAGTCG	TGAGTAAGTGGCAGAGCACAGG	60	157
Gpr65 (BALB/c)	GCCAGCCTCCTCAGTCAAGA	GATTGGAGATTGGTCGATGC	60	125
Gpr65 (C57BL/6)	GCCAGCCTCCTCAGTCAAGA	GATTGGAGATTGGTCGGTGC	60	125
Gpr65 (129S6)	GCCAGCCTCCTCAGTCAAGA	GATAGGAGATTGGTCGGTGC	60	125
Gpr68	GACCTACCTGTGGGACAGAA	GCCAATCCCTCTCTTGCCAT	58	178
Gnat1	GAGGATGCTGAGAAGGATGC	TGAATGTTGAGCGTGGTCAT	58	209
Gnat2	GCATCAGTGCTGAGGACAAA	CTAGGCACTCTTCGGGTGAG	58	192
Vsx2	CCAGAAGACAGGATACAGGTG	GGCTCCATAGAGACCATACT	60	111
Calb1	GGATTGGAGCTATCACCGGA	GACTTCAGTTGCTGGCATCG	60	146
Calb2	TTCCTGTCTGACCTCCTGA	ACATCCGTAGTATGGTCTGG	62	85
Pou4f1	CGCCGCTGCAGAGCAACCTCTT	TGGTACGTGGCGTCCGGCTT	62	130
Glul	TCCGCAAAGACCCCAACAAG	CCATTATCCGTTTACAGATGTGC	62	99
Casp1	GGCAGGAATTCTGGAGCTTCAA	GTCAGTCCTGGAAATGTGCC	60	138
Gfap	CCACCAAACTGGCTGATGTCTA	TTCTCTCCAAATCCACACGAGC	62	240
Fgf2	TGTGTCTATCAAGGGAGTGTGT	ACCAACTGGAGTATTTCCGTGA	62	158
Stat3	CAAAACCCTCAAGAGCCAAGG	TCACTCACAATGCTTCTCCGC	62	133
Edn2	AGACCTCCTCCGAAAGCTG	CTGGCTGTAGCTGGCAAAG	60	64
Lif	AATGCCACCTGTGCCATACG	CAACTTGGTCTTCTCTGTCCCG	60	216
Tnf	CCACGCTCTTCTGTCTACTGA	GGCCATAGAACTGATGAGAGG	62	92
Tgfb1	GCAACATGTGGAACTCTACCAG	CAGCCACTCAGGCGTATCA	62	94
Ccl2	GGCTCAGCCAGATGCAGTTA	CTGCTGCTGGTGATCCTCTT	60	108
Ccl4	CAAGCCAGCTGTGGTATTC	AGCTGCTCAGTTCAACTCC	62	109
Ccl5	GCTCCAATCTTGCAGTCGT	CTAGAGCAAGCGATGACAGG	62	165
Ccl8	CCAGATAAGGCTCCAGTCA	ACAGAGAGACATACCCTGCT	62	147
Ccl9	CAACTGCTCTTGGAATCTGG	AGGCAGCAATCTGAAGAGTC	62	136
Ccl12	CCTCAGGTATTGGCTGGAC	GACACTGGCTGCTTGTGATT	62	124
Csf1r	CCCTGGAGGCTATGGAGTTG	CCACTAGGCTCGATGACAGG	62	91

4. CONCLUDING DISCUSSION

A mouse model to study hypoxic aspects of retinal degeneration

AMD is a multifactorial disease and a major cause of visual impairment resulting in a huge social and economic burden. Age-related retinal changes – such as reduced density of choriocapillaries, thickening of the bruch's membrane, accumulation of lipofuscin and by-products of oxidative processes in the RPE, drusen accumulation, reduced ability of the RPE to clear the remnants of oxidative stress (Seddon and Chen, 2004), can affect the oxygen and nutrient supply to the photoreceptors causing a mild but chronic hypoxic situation, as the photoreceptors rely on the choroid for O_2 and nutrient supply. In addition to these age-related changes, lifestyle choices contribute to the chances of developing the disease. Smoking and obesity are two lifestyle factors that are highly correlated to the disease. Finally the most important factor is genetic propensity to acquire the disease as mutations in many genes involved in complement pathways (*Cfb, CFh, C3, Cfi* and *C2*), cholesterol metabolism (*Cetp, Lipc, Abca1* and *ApoE*), extracellular matrix remodelling (*Htra1*, *Timp3, Col8a1*) and oxidative stress (*Arms2*) are linked to the disease (macularisk.com). The disease is characterized by drusen accumulation, loss of photoreceptors, RPE atrophy and in certain cases aberrant vessel formation and leakage (CNV). Hence, apart from several factors that contribute to the chances of acquiring the disease, there are also several features of the disease that manifest to varying degrees in different patients, making the development of a standard animal model for study quite challenging.

As mentioned earlier, attempts have been made to develop models to study specific causes or features of the disease, but the hypoxic aspect has not been considered before. The age-related changes that affect oxygen supply and consumption may have a major impact on disease development and progression. And since HIFs are major transcription factors that regulate cellular responses to hypoxia, we aimed at developing mouse models that accumulate HIF1A (Opsin-Cre;*Vhl*^{flox}) or lack HIF1A (Opsin-Cre;*Vhl*^{flox};*Hif1a*^{flox}) specifically in the rod photoreceptors. Earlier models using a Pax6 promoter to delete *Vhl* in the developing retina resulted in degeneration in peripheral retina (Lange et al., 2011b), but the vascular phenotype was most obvious in these mice, as the vessels were severely malformed (Kurihara et al., 2010). Also the deletion of *Hif1a* using a *Pax6* promoter resulted in failure of development of the intermediate plexus of the retinal vessels (Caprara et al., 2011). We used an Opsin promoter to drive Cre expression in the rods to delete the floxed *Vhl* gene, which led to loss of photoreceptors on HIF1A accumulation (Lange et al., 2011a) and this degeneration phenotype was completely rescued in the Opsin-Cre;*Vhl*^{flox};*Hif1a*^{flox} mice. In the developing retina HIF1A is required mainly for the

correct formation of vessels, but in the adult retina when the blood vessels are completely developed HIF1A is not important.

Another reason these mice are a good 'hypoxia model for degeneration' is that the degeneration is age-related. We observed that at 11 weeks of age the retinas of the HIF1A stabilized mice appear stressed, with upregulation of stress-pathway related genes, indications of gliosis and minor morphological changes especially in the outer segments of the photoreceptors. These features are further worsened at 4 months, 6 months and 1 year of age. This slow and progressive manner of degeneration is a distinctive feature of AMD. Hence, these mice not only mimic the slow progression of the disease as it might occur in humans, but also provide a large window of opportunity to test therapies, which can be administered between 10-16 weeks of age and monitored at 6-12 months. This would be a major advantage over some other mouse models wherein the degeneration is often faster and more dramatic.

Photoreceptors are the major and the most abundant cells in the retina, and rely on choroidal blood supply the most, whereas the other cells of the INL and GCL rely on the retinal vasculature. Since age-related changes affect the choroidal supply to the retina the outer retina (photoreceptors and RPE) is most likely to experience hypoxia. Thus, our mice (Opsin-Cre;*Vhl*^{flox} and Opsin-Cre;*Vhl*^{flox};*Hif1a*^{flox}) enable the study of a hypoxia-like situation specifically the role of HIF1A, in the rods (most abundant photoreceptors). In both the genotypes, the other cell types (even the RPE cells) as well as the retinal vessels are not majorly affected.

Apart from age-related degeneration, these mice do not display other features of AMD. Drusen accumulation is one of the most distinctive features of the disease, but drusen deposits (as in humans) have not been observed in mice, although drusen-like deposits have been reported (Imamura et al., 2006; Luhmann et al., 2009). RPE atrophy often occurs before or along with loss of photoreceptors in the disease, which could be due to the fact that the RPE depends on choroidal blood supply too and may experience hypoxia as much as the photoreceptors. In the Opsin-Cre;*Vhl*^{flox} mice, the RPE is not majorly affected, except at older age, which may be a secondary effect of photoreceptor degeneration. Mice were developed with the deletion of *Vhl* specifically in the RPE, but due to the usage of an early promoter the observed phenotype related to developmental defects such as aniridia, microphthalmia and persistence of embryonic vascular structures into adulthood in addition to loss of RPE cells (Lange et al., 2012) (A conditional knockdown of *Vhl* in the RPE of adult mice may be a plausible solution). Thus, the Opsin-Cre;*Vhl*^{flox} mice may not emulate all features of the disease but yet would prove useful for studying hypoxic aspects of degeneration and testing therapies over a larger time frame.

Several cellular mechanisms are affected by hypoxia in the retina

We established that the stabilization (Opsin-Cre;*Vhl*^{flox} mice) or deletion of HIF1A (Opsin-Cre;*Vhl*^{flox};*Hif1a*^{flox} mice) respectively caused or prevented degeneration. But the exact mechanisms are not clearly understood yet. This led us to perform a transcriptome analysis comparing the two genotypes, resulting in a list of many differentially regulated genes, which were part of diverse pathways. One such group of genes found to be upregulated were the complement factors. This was an exciting turn of events as complement factors are genetically linked to AMD and the biochemical analyses of drusen deposits revealed fragments of complement factors. But a connection to hypoxia was never established, hence we hypothesized that maybe the aged hypoxic retina stabilizes HIF1A, which upregulates complement factors that accumulate and aggravate the effect, finally causing cell death. We confirmed an upregulation in the different complement factors – *C3, C4b, Cfh, Cfi, Cfb* and *Serping1* tested by real-time PCR, but there were huge variations within the same group. Further these factors were also upregulated in *rd10* mice, after the onset of degeneration suggesting that complement pathway activation may not be a direct but a secondary effect of HIF1A mediated mechanisms in the Opsin-Cre;*Vhl*^{flox} mice. The complement factors are not known to be direct targets of HIF1A, and we did not identify any HRE elements on analyzing a 2 kb region upstream of the coding sequence of *C3* gene, hence not providing evidence of HIF1A binding.

Metabolic adaptations occur in cells in response to nutrient availability, stress and environmental changes. Although these adaptations help the cells to cope with and survive the periods of stress, they may be detrimental to cellular function and survival in the long run. One such hypoxia-mediated adaptation is a shift from the efficient energy production by oxidative phosphorylation to the less efficient process of glycolysis. This low metabolic activity (essentially like a stand-by mode for cells) helps cells in the short-term, but extended periods of glycolysis affects pH homeostasis, accumulates metabolites which may not be cleared away and most importantly causes ATP depletion affecting essentially all ATP dependent cellular mechanisms. Some preliminary tests in our mice indicated that stabilized HIF1A might cause such a metabolic shift in the retina, hinting towards one possible mechanism responsible for degeneration, but detailed analyses of the metabolites and proteins involved will be required to establish a connection.

Mechanisms that degrade the extracellular matrix are a common feature of degenerative processes (Nita et al., 2014). Our transcriptome data contained several matrix metalloproteinases (MMPs) that are involved in the degradation of ECM. Cytokines and chemokines that are part of stress-related signalling pathways and inflammatory responses

were also found to be upregulated. Further analyses of these pathways will result in a better understanding of the degeneration mechnisms.

A systematic approach for better understanding of the impact of hypoxia

As several pathways directly or indirectly related to HIF1A converge to finally cause degeneration, a systematic approach would be required to understand each aspect individually and collectively with respect to hypoxia and retinal degeneration. As a first step towards this goal we compared the transcriptomes of the mice with HIF1A stabilized (Opsin-Cre;*Vhl*^{flox}) to the ones lacking HIF1A (Opsin-Cre;*Vhl*^{flox};*Hif1a*^{flox}) in the rods. Analysis of some pathways/ mechanisms was done as described earlier and in addition we also verified individual candidates by real-time PCR (Section 3.2.1).

One such candidate – *Stc2* was highly upregulated in response to hypoxia, and its role in the retina has not been previously described. Unlike *Stc2, Stc1* was not identified in the transcriptome data. We were able to show that *Stc2* has normal and comparable expression during development and retinal degeneration. However, under hypoxic conditions it was upregulated in the retina while its paralog *Stc1* was not. Further, using our mouse models with HIF1A stabilized and deleted in the rods we were able to show that only *Stc2* and not *Stc1* was HIF1A regulated as the presence of HIF1a in the rods even under normoxia was sufficient to increase gene expression of *Stc2*. The retinas of *Stc1-/-* and *Stc2-/-* mice seem to develop normally, indicating their non-essential role during development, which may become essential if these mice undergo hypoxic stress. The normal expression of the gene is in the INL and GCL and the protein localized to the neurofilaments (STC2 is a secreted protein). Hence it is worthwhile to further investigate the exact retinal processes that *Stc2* may be involved in, as this will shed light on how hypoxia in the photoreceptors affects other cell types.

Anti-Hif1a as a therapy to prevent degeneration

Anti-VEGF is used as a therapy for the wet form of AMD that is characterized by neovascularization. But, the effectiveness of the therapy is not consistent, as there are variations in patient response to therapy. Nonetheless it is still the treatment provided for wet AMD patients mostly because of the lack of an alternative. *Vegf* is a target of HIF1A, and hence, blocking/ knocking down *Hif1a*, might be a better alternative. Like *Vegf,* many other genes are targets of HIF1A and blocking the main regulator, will prevent the effects of the targets. HIF1A is required during early stages for the correct vascular development, but in adult mice loss of HIF1A does not have a major effect. On the contrary the accumulation of HIF1A, as could be the case in the aged hypoxic retinas, causes degeneration. Hence, targeting and knocking down *Hif1a* in diseased retinas might be an effective therapy.

Therapy for dry-AMD is an unmet medical need. The Opsin-Cre;*Vhl*^{flox} mice serve as a model for dry form of the disease, wherein knocking down *Hif1a* would prevent degeneration (as is the case of Opsin-Cre;*Vhl*^{flox};*Hif1a*^{flox} mice).

I tested several siRNA sequences against *Hif1a*, and selected the most effective one. siRNAs are unstable, easily degraded by cellular mechanisms and cannot be packaged into Adeno-associated viruses (AAVs) for injections, hence usage of shRNAs is preferred. Thus, the selected shRNA against *Hif1a* was sent for packaging into AAVs. These AAVs containing the shRNA against *Hif1a* would be injected sub-retinally into the Opsin-Cre;*Vhl*^{flox} mice at 11 weeks of age, and the rescue of degeneration would be analyzed at 6 months of age. If these studies prove successful, this could be translated to the clinics, as already subretinal injections of AAVs containing CNGB1 is proposed as a therapy for a form of autosomal recessive retinitis pigmentosa (Koch et al., 2012) and gene therapy by injections of AAVs containing RPE65 for a form Leber's congenital amaurosis is in clinical trials (Hauswirth et al., 2008).

Stress beyond hypoxia and HIF1A

Apart from hypoxia, the retina is sensitive to other stresses that can alter the cellular function and tissue homeostasis - one such stress being acidosis/ pH stress. G-protein coupled receptors (GPRs) might aid the retinal cells in coping with pH changes. We analyzed three *Gprs* - *Gpr4, Gpr65* and *Gpr68* and were able to show the normal expression of in the retinas of WT mice. When the expression was tested in inherited and induced models of retinal degeneration, only *Gpr65* was upregulated during degeneration, hinting towards specific and distinct roles of the GPRs in the retina. The *Gpr65-/-* mice had normal retinal structure and function, suggesting that the protein is not required during development or for normal function, but might have an essential role in stress response. Furthermore, the additional loss of *Gpr65* in degenerating mice (*rd10;Gpr65-/-*) caused accelerated degeneration and more activated microglia were observed in the *Gpr65-/-* following light exposure. This study provided evidence for the differential response (in healthy and degenerating conditions) of *Gprs* in the retina.

Taken together, the results of my work contribute to a better understanding of hypoxic stress specifically the role of HIF1A in the retina, as well as open up interesting dimensions for further investigation.

5. APPENDIX

5.1 References

Aimee, Y Yu, et al. (1998), 'Temporal, spatial, and oxygen-regulated expression of hypoxia-inducible factor-1 in the lung', *American Journal of Physiology-Lung Cellular and Molecular Physiology*, 275 (4), L818-L826.

Ambati, Jayakrishna, et al. (2003), 'An animal model of age-related macular degeneration in senescent Ccl-2-or Ccr-2-deficient mice', *Nature medicine*, 9 (11), 1390-97.

Consortium, AMD Gene (2013), 'Seven new loci associated with age-related macular degeneration', *Nature Genetics*, 45 (4), 433-39.

Anderson, DH, et al. (2010), 'The pivotal role of the complement system in aging and age-related macular degeneration: hypothesis re-visited.', *Prog Retin Eye Res*, 29 (2), 95-112.

Ara, J, et al. (2011), 'Hypoxic-preconditioning induces neuroprotection against hypoxia-ischemia in newborn piglet brain.', *Neurobiol Dis*, 43 (2), 473-85.

Arjamaa, O, et al. (2009a), 'Regulatory role of HIF-1alpha in the pathogenesis of age-related macular degeneration (AMD).', *Ageing Res Rev*, 8 (4), 349-58.

Arjamaa, Olli, et al. (2009b), 'Regulatory role of HIF-1α in the pathogenesis of age-related macular degeneration (AMD)', *Ageing research reviews*, 8 (4), 349-58.

Arshavsky, Vadim Y, Trevor D Lamb, and Edward N Pugh Jr (2002), 'G proteins and phototransduction', *Annual review of Physiology*, 64 (1), 153-87.

Baillat, David, et al. (2005), 'Integrator, a multiprotein mediator of small nuclear RNA processing, associates with the C-terminal repeat of RNA polymerase II', *Cell*, 123 (2), 265-76.

Balamurugan, Kuppusamy and Esta Sterneck (2013), 'The Many Faces of C/EBPδ and their Relevance for Inflammation and Cancer', *International journal of biological sciences*, 9 (9), 917.

Baraldi, Eugenio and Marco Filippone (2007), 'Chronic lung disease after premature birth', *New England Journal of Medicine*, 357 (19), 1946-55.

Beall, Cynthia M (2006), 'Andean, Tibetan, and Ethiopian patterns of adaptation to high-altitude hypoxia', *Integrative and Comparative Biology*, 46 (1), 18-24.

Blacker, Deborah, et al. (1998), 'Alpha-2 macroglobulin is genetically associated with Alzheimer disease', *Nature genetics*, 19 (4), 357-60.

Blaurock, AE and MHF Wilkins (1969), 'Structure of frog photoreceptor membranes',

Blaurock, AE (1972), 'Structure of the retinal membrane containing the visual pigments', *The Visual System* (Springer), 53-63.

Boulton, Mike (1991), 'Ageing of the retinal pigment epithelium', *Progress in retinal research*, 11 125-51.

Bressler, NM (2001), 'Photodynamic therapy of subfoveal choroidal neovascularization in age-related macular degeneration with verteporfin: two-year results of 2 randomized clinical trials-tap report 2.', *Archives of ophthalmology*, 119 (2), 198-207.

Bringmann, Andreas, et al. (2006), 'Müller cells in the healthy and diseased retina', *Progress in retinal and eye research*, 25 (4), 397-424.

Bruick, Richard K (2000), 'Expression of the gene encoding the proapoptotic Nip3 protein is induced by hypoxia', *Proceedings of the National Academy of Sciences*, 97 (16), 9082-87.

Bruick, Richard K and Steven L McKnight (2001), 'A conserved family of prolyl-4-hydroxylases that modify HIF', *Science*, 294 (5545), 1337-40.

Caprara, Christian, et al. (2011), 'HIF1A is essential for the development of the intermediate plexus of the retinal vasculature', *Investigative ophthalmology & visual science*, 52 (5), 2109-17.

Caprara, Christian and Christian Grimm (2012), 'From oxygen to erythropoietin: relevance of hypoxia for retinal development, health and disease', *Progress in retinal and eye research*, 31 (1), 89-119.

Carmeliet, Peter and Rakesh K Jain (2000), 'Angiogenesis in cancer and other diseases', *nature*, 407 (6801), 249-57.

Carter-Dawson, Louvenia D and Matthew M Lavail (1979), 'Rods and cones in the mouse retina. I. Structural analysis using light and electron microscopy', *Journal of Comparative Neurology*, 188 (2), 245-62.

Chen, Jing and Lois EH Smith (2007), 'Retinopathy of prematurity', *Angiogenesis*, 10 (2), 133-40.

Chen, Ling, Peizeng Yang, and Aize Kijlstra (2002), 'Distribution, markers, and functions of retinal microglia', *Ocular immunology and inflammation*, 10 (1), 27-39.

Cheng, Wei-Cheng, et al. (2007), 'Mice lacking the Obox6 homeobox gene undergo normal early embryonic development and are fertile', *Developmental Dynamics*, 236 (9), 2636-42.

Chouker, A, et al. (2012), 'In vivo hypoxic preconditioning protects from warm liver ischemia-reperfusion injury through the adenosine A2B receptor.', *Transplantation*, 94 (9), 894-902.

Cockman, Matthew E, et al. (2000), 'Hypoxia inducible factor-α binding and ubiquitylation by the von Hippel-Lindau tumor suppressor protein', *Journal of Biological Chemistry*, 275 (33), 25733-41.

Coffey, Peter J, et al. (2007), 'Complement factor H deficiency in aged mice causes retinal abnormalities and visual dysfunction', *Proceedings of the National Academy of Sciences*, 104 (42), 16651-56.

Combadière, Christophe, et al. (2007), 'CX3CR1-dependent subretinal microglia cell accumulation is associated with cardinal features of age-related macular degeneration', *The Journal of clinical investigation*, 117 (117 (10), 2920-28.

Dayan, Frédéric, et al. (2006), 'The oxygen sensor factor-inhibiting hypoxia-inducible factor-1 controls expression of distinct genes through the bifunctional transcriptional character of hypoxia-inducible factor-1α', *Cancer research*, 66 (7), 3688-98.

Despriet, Dominiek DG, et al. (2009), 'Complement component C3 and risk of age-related macular degeneration', *Ophthalmology*, 116 (3), 474-80. e2.

Deville, Jean-Laurent, et al. (2010), 'Adrenomedullin as a therapeutic target in angiogenesis', *Expert opinion on therapeutic targets*, 14 (10), 1059-72.

Dirnagl, Ulrich, Costantino Iadecola, and Michael A Moskowitz (1999), 'Pathobiology of ischaemic stroke: an integrated view', *Trends in neurosciences*, 22 (9), 391-97.

Dithmar, Stefan, et al. (2000), 'Ultrastructural changes in Bruch's membrane of apolipoprotein E–deficient mice', *Investigative ophthalmology & visual science*, 41 (8), 2035-42.

Dixon, James A, et al. (2009), 'VEGF Trap-Eye for the treatment of neovascular age-related macular degeneration',

Edwards, AO, et al. (2005), 'Complement factor H polymorphism and age-related macular degeneration.', *Science*, 308 (5720), 421-24.

Ema, Masatsugu, et al. (1997), 'A novel bHLH-PAS factor with close sequence similarity to hypoxia-inducible factor 1α regulates the VEGF expression and is potentially involved in lung and vascular development', *Proceedings of the National Academy of Sciences*, 94 (9), 4273-78.

Erickson, Page A, et al. (1987), 'Glial fibrillary acidic protein increases in Müller cells after retinal detachment', *Experimental eye research*, 44 (1), 37-48.

Erler, Janine T, et al. (2006), 'Lysyl oxidase is essential for hypoxia-induced metastasis', *Nature*, 440 (7088), 1222-26.

Esteban, Miguel A, et al. (2006), 'Regulation of E-cadherin expression by VHL and hypoxia-inducible factor', *Cancer research*, 66 (7), 3567-75.

Evans, JR (2001), 'Risk factors for age-related macular degeneration.', *Prog Retin Eye Res*, 20 (2), 227-53.

Group, Age-Related Eye Disease Study Research (2001), 'A randomized, placebo-controlled, clinical trial of high-dose supplementation with vitamins C and E, beta carotene, and zinc for age-related macular degeneration and vision loss: AREDS report no. 8', *Archives of ophthalmology*, 119 (10), 1417.

Group, Eye Diseases Prevalence Research (2004), 'Prevalence of age-related macular degeneration in the United States', *Archives of ophthalmology*, 122 (4), 564.

Falls, Douglas L (2003), 'Neuregulins: functions, forms, and signaling strategies', *Experimental cell research*, 284 (1), 14-30.

Fein, Alan and Ete Zoltan Szuts (1982), *Photoreceptors, their role in vision*, (5; CUP Archive).

Ferrara, Napoleone, Hans-Peter Gerber, and Jennifer LeCouter (2003), 'The biology of VEGF and its receptors', *Nature medicine*, 9 (6), 669-76.

Ferris III, Frederick L, et al. (2013), 'Clinical classification of age-related macular degeneration', *Ophthalmology*, 120 (4), 844-51.

Fruttiger, Marcus (2007), 'Development of the retinal vasculature', *Angiogenesis*, 10 (2), 77-88.

Fujita, Teizo (2002), 'Evolution of the lectin–complement pathway and its role in innate immunity', *Nature Reviews Immunology*, 2 (5), 346-53.

Gilbert, Clare (2008), 'Retinopathy of prematurity: a global perspective of the epidemics, population of babies at risk and implications for control', *Early human development*, 84 (2), 77-82.

Gold, Bert, et al. (2006), 'Variation in factor B (BF) and complement component 2 (C2) genes is associated with age-related macular degeneration', *Nature genetics*, 38 (4), 458-62.

Gordon, EA, et al. (2013), 'Combining docking site and phosphosite predictions to find new substrates: identification of smoothelin-like-2 (SMTNL2) as a c-Jun N-terminal kinase (JNK) substrate.', *Cell Signal*, 25 (12), 2518-29.

Graham, Charles H, et al. (1999), 'Hypoxia-mediated stimulation of carcinoma cell invasiveness via upregulation of urokinase receptor expression', *International journal of cancer*, 80 (4), 617-23.

Grimm, C, et al. (2005), 'Neuroprotection by hypoxic preconditioning: HIF-1 and erythropoietin protect from retinal degeneration.', *Semin Cell Dev Biol*, 16 (4-5), 531-38.

Grimm, Christian, et al. (2002), 'HIF-1-induced erythropoietin in the hypoxic retina protects against light-induced retinal degeneration', *Nature medicine*, 8 (7), 718-24.

Grimm, Christian, et al. (2007), 'Hypoxic preconditioning and erythropoietin protect retinal neurons from degeneration', *Hypoxia and Exercise* (Springer), 119-31.

Grimm, Christian and Gabriel Willmann (2012), 'Hypoxia in the eye: a two-sided coin', *High altitude medicine & biology*, 13 (3), 169-75.

Grimm, Christian and Charlotte E Remé (2013), 'Light damage as a model of retinal degeneration', *Retinal Degeneration* (Springer), 87-97.

Grosche, Jens, Wolfgang Härtig, and Andreas Reichenbach (1995), 'Expression of glial fibrillary acidic protein (GFAP), glutamine synthetase (GS), and Bcl-2 protooncogene protein by Müller (glial) cells in retinal light damage of rats', *Neuroscience letters*, 185 (2), 119-22.

Grossniklaus, Hans E, Shin J Kang, and Lennart Berglin (2010), 'Animal models of choroidal and retinal neovascularization', *Progress in retinal and eye research*, 29 (6), 500-19.

Gu, Jie, Justine Milligan, and L Eric Huang (2001), 'Molecular mechanism of hypoxia-inducible factor 1α-p300 interaction A leucine-rich interface regulated by a single cysteine', *Journal of Biological Chemistry*, 276 (5), 3550-54.

Gu, Yi-Zhong, et al. (1997), 'Molecular characterization and chromosomal localization of a third alpha-class hypoxia inducible factor subunit, HIF3alpha.', *Gene expression*, 7 (3), 205-13.

Hageman, Gregory S, et al. (2006), 'Extended haplotypes in the complement factor H (CFH) and CFH-related (CFHR) family of genes protect against age-related macular degeneration: characterization, ethnic distribution and evolutionary implications', *Annals of medicine*, 38 (8), 592-604.

Hageman, GS and DH Anderson… (2005), 'A common haplotype in the complement regulatory gene factor H (HF1/CFH) predisposes individuals to age-related macular degeneration', *Proceedings of the …*,

Haines, JL, et al. (2005), 'Complement factor H variant increases the risk of age-related macular degeneration.', *Science*, 308 (5720), 419-21.

Hauswirth, William W, et al. (2008), 'Treatment of leber congenital amaurosis due to RPE65 mutations by ocular subretinal injection of adeno-associated virus gene vector: short-term results of a phase I trial', *Human gene therapy*, 19 (10), 979-90.

Hollyfield, Joe G, et al. (2008), 'Oxidative damage–induced inflammation initiates age-related macular degeneration', *Nature medicine*, 14 (2), 194-98.

Holz, Frank G, et al. (2014), 'Geographic Atrophy: Clinical Features and Potential Therapeutic Approaches', *Ophthalmology*, 121 (5), 1079-91.

Imamura, Yutaka, et al. (2006), 'Drusen, choroidal neovascularization, and retinal pigment epithelium dysfunction in SOD1-deficient mice: a model of age-related macular degeneration', *Proceedings of the National Academy of Sciences*, 103 (30), 11282-87.

Iwata, Nobuhisa, et al. (2001), 'Metabolic regulation of brain Aβ by neprilysin', *Science*, 292 (5521), 1550-52.

Jaakkola, P, et al. (2001), 'Targeting of HIF-alpha to the von Hippel-Lindau ubiquitylation complex by O2-regulated prolyl hydroxylation.', *Science*, 292 (5516), 468-72.

Jakobsdottir, Johanna, et al. (2008), 'C2 and CFB genes in age-related maculopathy and joint action with CFH and LOC387715 genes', *PloS one*, 3 (5), e2199.

Jelkmann, Wolfgang (2004), 'Molecular biology of erythropoietin', *Internal medicine*, 43 (8), 649-59.

Jiang, Bing-Hua, et al. (1997), 'Transactivation and inhibitory domains of hypoxia-inducible factor 1α modulation of transcriptional activity by oxygen tension', *Journal of Biological Chemistry*, 272 (31), 19253-60.

Jiang, Ke, et al. (2014), 'STAT3 promotes survival of mutant photoreceptors in inherited photoreceptor degeneration models', *Proceedings of the National Academy of Sciences*, 111 (52), E5716-E5723.

Joly, Sandrine, et al. (2008), 'Leukemia inhibitory factor extends the lifespan of injured photoreceptors in vivo', *The Journal of neuroscience*, 28 (51), 13765-74.

Jones, SE, et al. (1999), 'Retinal expression of gamma-crystallins in the mouse.', *… ophthalmology & visual …*,

Justilien, Verline, et al. (2007), 'SOD2 knockdown mouse model of early AMD', *Investigative ophthalmology & visual science*, 48 (10), 4407-20.

Karlstetter, M and T Langmann (2012), '[Immune mechanisms in retinal degeneration].', *Klin Monbl Augenheilkd*, 229 (3), 221-26.

Kim, Nam-Gon, et al. (2003), 'Hypoxic induction of caspase-11/caspase-1/interleukin-1β in brain microglia', *Molecular brain research*, 114 (2), 107-14.

Kimura, Hideo, et al. (2001), 'Identification of hypoxia-inducible factor 1 ancillary sequence and its function in vascular endothelial growth factor gene induction by hypoxia and nitric oxide', *Journal of Biological Chemistry*, 276 (3), 2292-98.

Klein, RJ, et al. (2005), 'Complement factor H polymorphism in age-related macular degeneration.', *Science*, 308 (5720), 385-89.

Klein, Ronald, et al. (2004), 'The epidemiology of age-related macular degeneration', *American journal of ophthalmology*, 137 (3), 486-95.

Kliewer, SA, et al. (1994), 'Differential expression and activation of a family of murine peroxisome proliferator-activated receptors', *Proceedings of the National Academy of Sciences*, 91 (15), 7355-59.

Koch, S, et al. (2012), 'Gene therapy restores vision and delays degeneration in the CNGB1(-/-) mouse model of retinitis pigmentosa.', *Hum Mol Genet*, 21 (20), 4486-96.

Koivunen, Peppi, et al. (2004), 'Catalytic properties of the asparaginyl hydroxylase (FIH) in the oxygen sensing pathway are distinct from those of its prolyl 4-hydroxylases', *Journal of Biological Chemistry*, 279 (11), 9899-904.

Kunisada, Keita, et al. (1996), 'Activation of JAK-STAT and MAP kinases by leukemia inhibitory factor through gp130 in cardiac myocytes', *Circulation*, 94 (10), 2626-32.

Kurihara, Toshihide, et al. (2010), 'von Hippel-Lindau protein regulates transition from the fetal to the adult circulatory system in retina', *Development*, 137 (9), 1563-71.

Lange, C, et al. (2011a), 'Normoxic activation of hypoxia-inducible factors in photoreceptors provides transient protection against light-induced retinal degeneration.', *Invest Ophthalmol Vis Sci*, 52 (8), 5872-80.

Lange, Christina, et al. (2011b), 'Retina-specific activation of a sustained hypoxia-like response leads to severe retinal degeneration and loss of vision', *Neurobiology of disease*, 41 (1), 119-30.

Lange, Clemens AK, et al. (2012), 'Von Hippel-Lindau protein in the RPE is essential for normal ocular growth and vascular development', *Development*, 139 (13), 2340-50.

Lau, Dana, et al. (2000), 'Retinal degeneration is slowed in transgenic rats by AAV-mediated delivery of FGF-2', *Investigative ophthalmology & visual science*, 41 (11), 3622-33.

Lin, M, et al. (2011), 'Ischaemia-induced retinal neovascularisation and diabetic retinopathy in mice with conditional knockout of hypoxia-inducible factor-1 in retinal Müller cells', *Diabetologia*, 54 (6), 1554-66.

Ling, Lowell, Janet J Maguire, and Anthony P Davenport (2013), 'Endothelin-2, the forgotten isoform: emerging role in the cardiovascular system, ovarian development, immunology and cancer', *British journal of pharmacology*, 168 (2), 283-95.

Lisy, K and DJ Peet (2008), 'Turn me on: regulating HIF transcriptional activity', *Cell Death & Differentiation*, 15 (4), 642-49.

Liu, Yong-Lei, et al. (2006), 'Regulation of the chemokine receptor CXCR4 and metastasis by hypoxia-inducible factor in non small cell lung cancer cell lines', *Cancer biology & therapy*, 5 (10), 1320-26.

Loboda, Agnieszka, Alicja Jozkowicz, and Jozef Dulak (2010), 'HIF-1 and HIF-2 transcription factors—similar but not identical', *Molecules and cells*, 29 (5), 435-42.

Luhmann, Ulrich FO, et al. (2009), 'The drusen-like phenotype in aging Ccl2 knockout mice is caused by an accelerated accumulation of swollen autofluorescent subretinal macrophages', *Investigative ophthalmology & visual science*, 50 (12), 5934.

Group, Macular Photocoagulation Study (1986), 'Argon laser photocoagulation for neovascular maculopathy: three-year results from randomized clinical trials', *Archives of Ophthalmology*, 104 (5), 694.

Magabo, KS, J Horwitz, and J Piatigorsky… (2000), 'Expression of βB2-crystallin mRNA and protein in retina, brain, and testis', *… ophthalmology & visual …*,

Mahon, PC, K Hirota, and GL Semenza (2001), 'FIH-1: a novel protein that interacts with HIF-1alpha and VHL to mediate repression of HIF-1 transcriptional activity.', *Genes Dev*, 15 (20), 2675-86.

Majmundar, Amar J, Waihay J Wong, and M Celeste Simon (2010), 'Hypoxia-inducible factors and the response to hypoxic stress', *Molecular cell*, 40 (2), 294-309.

Makino, Yuichi, et al. (2001), 'Inhibitory PAS domain protein is a negative regulator of hypoxia-inducible gene expression', *Nature*, 414 (6863), 550-54.

Malek, G, et al. (2005), 'Apolipoprotein E allele-dependent pathogenesis: a model for age-related retinal degeneration', *Proceedings of the National Academy of Sciences of the United States of America*, 102 (33), 11900-05.

Maller, Julian B, et al. (2007), 'Variation in complement factor 3 is associated with risk of age-related macular degeneration.', *Nature genetics*, 39 (10), 1200-01.

Marc, Robert E and Harry G Sperling (1977), 'Chromatic organization of primate cones', *Science*, 196 (4288), 454-56.

Masland, Richard H (2001), 'The fundamental plan of the retina', *Nature neuroscience*, 4 (9), 877-86.

Mata, Nathan L, et al. (2001), 'Delayed dark-adaptation and lipofuscin accumulation in abcr+/− mice: implications for involvement of ABCR in age-related macular degeneration', *Investigative ophthalmology & visual science*, 42 (8), 1685-90.

Maxwell, Patrick H, et al. (1999), 'The tumour suppressor protein VHL targets hypoxia-inducible factors for oxygen-dependent proteolysis', *Nature*, 399 (6733), 271-75.

Maynard, MA and M Ohh (2007), 'The role of hypoxia-inducible factors in cancer', *Cellular and Molecular Life Sciences*, 64 (16), 2170-80.

Mishima, H and K Kondo (1981), 'Extrusion of lysosomal bodies from apical mouse retinal pigment epithelium', *Albrecht von Graefes Archiv für klinische und experimentelle Ophthalmologie*, 216 (3), 209-17.

Mishima, Hiromu and Haruyuki Hasebe (1978), 'Some observations in the fine structure of age changes of the mouse retinal pigment epithelium', *Albrecht von Graefes Archiv für klinische und experimentelle Ophthalmologie*, 209 (1), 1-9.

Mitchell, Paul, Wayne Smith, and Jie Jin Wang (1998), 'Iris color, skin sun sensitivity, and age-related maculopathy: the Blue Mountains Eye Study', *Ophthalmology*, 105 (8), 1359-63.

Mitchell, Paul (2011), 'A systematic review of the efficacy and safety outcomes of anti-VEGF agents used for treating neovascular age-related macular degeneration: comparison of ranibizumab and bevacizumab', *Current Medical Research & Opinion*, 27 (7), 1465-75.

Mojsilovic-Petrovic, Jelena, et al. (2007), 'Hypoxia-inducible factor-1 (HIF-1) is involved in the regulation of hypoxia-stimulated expression of monocyte chemoattractant protein-1 (MCP-1/CCL2) and MCP-5 (Ccl12) in astrocytes', *J Neuroinflammation*, 4 (12), 10.1186.

Molnar, J, et al. (2003), 'Structural and functional diversity of lysyl oxidase and the LOX-like proteins', *Biochimica et Biophysica Acta (BBA)-Proteins and Proteomics*, 1647 (1), 220-24.

Motoki, Kiyohisa, et al. (1997), 'Cloning and chromosomal mapping of mouse ladinin, a novel basement membrane zone component', *Genomics*, 39 (3), 323-30.

Nakamura, Hiroyuki, et al. (2000), 'Brevican is degraded by matrix metalloproteinases and aggrecanase-1 (ADAMTS4) at different sites', *Journal of Biological Chemistry*, 275 (49), 38885-90.

Nita, M, et al. (2014), 'Age-related macular degeneration and changes in the extracellular matrix.', *Med Sci Monit*, 20 1003-16.

Ohh, M, et al. (2000), 'Ubiquitination of hypoxia-inducible factor requires direct binding to the beta-domain of the von Hippel-Lindau protein.', *Nat Cell Biol*, 2 (7), 423-27.

Park, Kyu Hyung, et al. (2009), 'Complement component 3 (C3) haplotypes and risk of advanced age-related macular degeneration', *Investigative ophthalmology & visual science*, 50 (7), 3386-93.

Perez, VL and RR Caspi (2015), 'Immune mechanisms in inflammatory and degenerative eye disease.', *Trends Immunol*, 36(6) (6), 354-63.

Provis, Jan M, Claudia M Diaz, and Bogdan Dreher (1998), 'Ontogeny of the primate fovea: a central issue in retinal development', *Progress in neurobiology*, 54 (5), 549-81.

Purves, Dale, et al. 'Neuroscience, 2008', *De Boeck, Sinauer, Sunderland, Mass*,

Ramkumar, Hema L, Jun Zhang, and Chi-Chao Chan (2010), 'Retinal ultrastructure of murine models of dry age-related macular degeneration (AMD)', *Progress in retinal and eye research*, 29 (3), 169-90.

Rattner, Amir, et al. (2013), 'Endothelin-2 signaling in the neural retina promotes the endothelial tip cell state and inhibits angiogenesis', *Proceedings of the National Academy of Sciences*, 110 (40), E3830-E3839.

Raychaudhuri, Soumya, et al. (2011), 'A rare penetrant mutation in CFH confers high risk of age-related macular degeneration', *Nature genetics*, 43 (12), 1232-36.

Reynolds, Robyn, et al. (2009), 'Plasma complement components and activation fragments: associations with age-related macular degeneration genotypes and phenotypes', *Investigative ophthalmology & visual science*, 50 (12), 5818-27.

Rickman, Catherine Bowes, et al. (2013), 'Dry Age-Related Macular Degeneration: Mechanisms, Therapeutic Targets, and Imaging', *Investigative ophthalmology & visual science*, 54 (14), ORSF68-ORSF80.

Rudrasingham, Varuni, et al. (1999), 'α-2 Macroglobulin gene and Alzheimer disease', *Nature genetics*, 22 (1), 17-19.

Samardzija, Marijana, et al. (2012), 'Activation of survival pathways in the degenerating retina of rd10 mice', *Experimental eye research*, 99 17-26.

Sandbach, Jennifer M, et al. (2001), 'Ocular pathology in mitochondrial superoxide dismutase (Sod2)–deficient mice', *Investigative ophthalmology & visual science*, 42 (10), 2173-78.

SanGiovanni, John Paul, et al. (2008), 'The relationship of dietary ω-3 long-chain polyunsaturated fatty acid intake with incident age-related macular degeneration: AREDS report No. 23', *Archives of ophthalmology*, 126 (9), 1274-79.

Schnitzer, Jutta (1988), 'Astrocytes in mammalian retina', *Progress in retinal research*, 7 209-31.

Seddon, Johanna M, et al. (1994), 'Dietary carotenoids, vitamins A, C, and E, and advanced age-related macular degeneration', *Jama*, 272 (18), 1413-20.

Seddon, Johanna M, et al. (1996), 'A prospective study of cigarette smoking and age-related macular degeneration in women', *Jama*, 276 (14), 1141-46.

Seddon, Johanna M, et al. (2003), 'Progression of age-related macular degeneration: association with body mass index, waist circumference, and waist-hip ratio', *Archives of Ophthalmology*, 121 (6), 785-92.

Seddon, Johanna M and Clara A Chen (2004), 'The epidemiology of age-related macular degeneration', *International ophthalmology clinics*, 44 (4), 17-39.

Seddon, Johanna M, et al. (2006), 'C-reactive protein and homocysteine are associated with dietary and behavioral risk factors for age-related macular degeneration', *Nutrition*, 22 (4), 441-43.

Seddon, Johanna M, et al. (2013), 'Rare variants in CFI, C3 and C9 are associated with high risk of advanced age-related macular degeneration', *Nature genetics*,

Semenza, Gregg L (2007), 'HIF-1 mediates the Warburg effect in clear cell renal carcinoma', *Journal of bioenergetics and biomembranes*, 39 (3), 231-34.

Semenza, Gregg L et al. (2012), 'Hypoxia-inducible factors in physiology and medicine', *Cell*, 148 (3), 399-408.

Shoshani, Tzipora, et al. (2002), 'Identification of a novel hypoxia-inducible factor 1-responsive gene, RTP801, involved in apoptosis', *Molecular and cellular biology*, 22 (7), 2283-93.

Sickel, W (1972), 'Electrical and metabolic manifestations of receptor and higher-order neuron activity in vertebrate retina', *The Visual System* (Springer), 101-18.

Simonson, Tatum S, et al. (2010), 'Genetic evidence for high-altitude adaptation in Tibet', *Science*, 329 (5987), 72-75.

Song, Ruo-Hua, et al. (2007), 'Aggrecan degradation in human articular cartilage explants is mediated by both ADAMTS-4 and ADAMTS-5', *Arthritis & Rheumatism*, 56 (2), 575-85.

Sowter, Heidi M, et al. (2001), 'HIF-1-dependent regulation of hypoxic induction of the cell death factors BNIP3 and NIX in human tumors', *Cancer research*, 61 (18), 6669-73.

Stone, J, et al. (1995), 'Development of retinal vasculature is mediated by hypoxia-induced vascular endothelial growth factor (VEGF) expression by neuroglia', *The Journal of neuroscience*, 15 (7), 4738-47.

Strauss, Olaf (2005), 'The retinal pigment epithelium in visual function', *Physiological reviews*, 85 (3), 845-81.

Stubbs, Marion and John R Griffiths (2010), 'The altered metabolism of tumors: HIF-1 and its role in the Warburg effect', *Advances in enzyme regulation*, 50 (1), 44-55.

Suguri, T, et al. (1996), 'Increased plasma GlyCAM-1, a mouse L-selectin ligand, in response to an inflammatory stimulus.', *Journal of leukocyte biology*, 60 (5), 593-97.

Sung, Ching-Hwa and Jen-Zen Chuang (2010), 'The cell biology of vision', *The Journal of cell biology*, 190 (6), 953-63.

Suter, Marianne, et al. (2000), 'Age-related macular degeneration: The lipofuscin component A2E detaches pro-apoptotic proteins from mitochondria and induces apoptosis in mammalian retinal pigment epithelial cells', *Journal of Biological Chemistry*,

Szel, A, et al. (1992), 'Unique topographic separation of two spectral classes of cones in the mouse retina', *Journal of Comparative Neurology*, 325 (3), 327-42.

Taylor, TB, et al. (2015), 'Transglutaminase 3 present in the IgA aggregates in dermatitis herpetiformis skin is enzymatically active and binds soluble fibrinogen.', *J Invest Dermatol*, 135(2) (2), 623-25.

Tezel, Gülgün and Martin B Wax (2004), 'Hypoxia-Inducible Factor 1α in the Glaucomatous Retina and OpticNerve Head', *Archives of ophthalmology*, 122 (9), 1348-56.

Thiersch, Markus, et al. (2009), 'Retinal neuroprotection by hypoxic preconditioning is independent of hypoxia-inducible factor-1α expression in photoreceptors', *European Journal of Neuroscience*, 29 (12), 2291-302.

Tuo, Jingsheng, et al. (2007), 'Murine ccl2/cx3cr1 deficiency results in retinal lesions mimicking human age-related macular degeneration', *Investigative ophthalmology & visual science*, 48 (8), 3827-36.

Vander Heiden, Matthew G, Lewis C Cantley, and Craig B Thompson (2009), 'Understanding the Warburg effect: the metabolic requirements of cell proliferation', *science*, 324 (5930), 1029-33.

Vasireddy, Vidyullatha, et al. (2006), 'Elovl4 5-bp–deletion knock-in mice develop progressive photoreceptor degeneration', *Investigative ophthalmology & visual science*, 47 (10), 4558-68.

Vasireddy, Vidyullatha, et al. (2009), 'Elovl4 5-bp deletion knock-in mouse model for Stargardt-like macular degeneration demonstrates accumulation of ELOVL4 and lipofuscin', *Experimental eye research*, 89 (6), 905-12.

Vaupel, Peter and Arnulf Mayer (2007), 'Hypoxia in cancer: significance and impact on clinical outcome', *Cancer and Metastasis Reviews*, 26 (2), 225-39.

Wang, Guang L, et al. (1995), 'Hypoxia-inducible factor 1 is a basic-helix-loop-helix-PAS heterodimer regulated by cellular O2 tension', *Proceedings of the national academy of sciences*, 92 (12), 5510-14.

Williams, David S and Vanda Lopes (2011), 'The many different cellular functions of MYO7A in the retina', *Biochemical Society transactions*, 39 (5), 1207.

Yancopoulos, George D, et al. (2000), 'Vascular-specific growth factors and blood vessel formation', *Nature*, 407 (6801), 242-48.

Yates, JR, et al. (2007), 'Complement C3 variant and the risk of age-related macular degeneration.', *N Engl J Med*, 357 (6), 553-61.

Yetemian, Rosanne M and Cheryl M Craft (2011), 'Characterization of the pituitary tumor transforming gene 1 knockout mouse retina', *Neurochemical research*, 36 (4), 636-44.

Yoshida, Takeshi, et al. (2005), 'The potential role of amyloid β in the pathogenesis of age-related macular degeneration', *Journal of Clinical Investigation*, 115 (10), 2793.

Zeiger, William, et al. (2011), 'Stanniocalcin 2 is a negative modulator of store-operated calcium entry', *Molecular and cellular biology*, 31 (18), 3710-22.

Zhan, L, et al. (2011), 'Hypoxic preconditioning induces neuroprotection against transient global ischemia in adult rats via preserving the activity of Na(+)/K(+)-ATPase.', *Neurochem Int*, 59 (1), 65-72.

5.2. Additional methods

Fundus imaging and fluorescein angiography - Pupils were dilated with 1% cyclogyl and 5% phenylephrine. 30 min post-dilation, mice were anesthetized with ketamine (66.7 mg/kg) and xylazine (11.7 mg/kg) and corneas were moistened with 2% methocel (OmniVision, Puchheim, Germany). Fundi were monitored and photographed using a mouse imaging system (Micron III, Phoenix Research Laboratories, Pleasanton, CA, USA). Fluorescein solution (2% in PBS; AK-FLUOR; Lake Forest, IL, USA) was injected intraperitoneally and eyes were analyzed immediately.

Retinal flatmounts and immunofluorescence – Enucleated eyes were fixed for 3-5 min in 2% (w/v) paraformaldehyde (PFA) in PBS. The sclera was dissected from the eyes and the lens, iris and vitreous were removed. The retina was flattened and stored in methanol at -20°C. before use, the retina was post-fixed in 4% PFA in PBS for 10 min. For immunofluorescence, the flatmounted retina was washed in PBS and incubated in blocking solution (1% fetal bovine serum, 0.1% tritonX-100 in PBS) for 1 h. Flatmounts were then incubated with Alexa594-conjugated isolectin-A4 (Invitrogen, Basel, Switzerland, Catalogue number – 121413) at 4°C overnight, washed and mounted in MOWIOL anti-fade medium (Calbiochem, San Diego, CA, USA). The flatmounts were then imaged and analyzed using a digitalized Axiovision microscope (Carl Zeiss AG, Feldbach, Switzerland).

siRNA knockdown of *Hif1a* in vitro – Mouse fibroblast cells – NIH3t3 (LGC standards, Wesel Germany, #ATCC-CRL-1658) were seeded in a 6 well plate at a density of 25000 cells/well and left at 37°C, 21% O_2 overnight. Cells were transfected with *Hif1a* siRNAs (Dharmacon, Fischer scientific, Wohlen, Switzerland), using the lipofectamine RNAiMAX reagent (Life Technologies, Zug, Switzerland, Catalogue no. 13778) and incubated overnight at 37°C, 21% O_2. Then the control plate was left at normoxia and the other plate was kept at hypoxia (37°C, 0.2% O_2 for 6 hr) in a hypoxic chamber (Baker Ruskinn Invivo$_2$ 400, South Wales, UK). After 6 h, the cells were lysed, centrifuged and the supernatant collected for proteins that were analyzed for HIF1A by western blotting.

Other experimental procedures are listed in the corresponding sections, as follows –

Section 3.1.1 – Transcriptome analysis, Morphology and light microscopy, Hypoxic treatment of animals, Western blotting, RNA isolation, cDNA preparation, Semi-quantitative real-time PCR, Immunofluorescence on retinal cryosections, RPE flatmounts preparation and analysis, Lactate assay and Statistical analysis.

Section 3.2.3 - Morphology and light microscopy, Western blotting, RNA isolation, cDNA preparation, Semi-quantitative real-time PCR, Immunofluorescence on retinal cryosections, Laser capture microdissection and Statistical analysis.

Section 3.3 – Light exposure, Electroretinogram, Morphology and light microscopy, Western blotting, RNA isolation, cDNA preparation, Semi-quantitative real-time PCR, Immunofluorescence on retinal flatmounts, Statistical analysis.

5.3.1 DIFFERENTIALLY REGULATED GENES (TRANSCRIPTOME ANALYSIS)				
Opsin-Cre;*Vhl*^{flox} (Single) vs Opsin-Cre;*Vhl*^{flox};*Hif1a*^{flox} (Double)				
UPREGULATED GENES				
Entrez ID	**Gene Symbol**	**Description**	**fold change**	**pValue**
71957	Cpsf3l	cleavage and polyadenylation specific factor 3-like	228.5	5.20E-09
619297	C430049E01Rik	RIKEN cDNA C430049E01 gene	143.5	5.39E-09
223780	Adm2	adrenomedullin 2	70.8	1.19E-06
13615	Edn2	endothelin 2	65.8	3.12E-08
76487	Ppp1r3g	protein phosphatase 1, regulatory (inhibitor) subunit 3G	59.1	5.15E-06
213742	Xist	inactive X specific transcripts	35.3	3.01E-02
240913	Adamts4	a disintegrin-like and metallopeptidase with thrombospondin type 1 motif, 4	24.7	2.89E-04
236220	LOC236220	hypothetical protein LOC236220	24.3	1.34E-05
11535	Adm	adrenomedullin	23.6	6.34E-08
16763	Lad1	ladinin	23.3	3.38E-05
67573	Loxl4	lysyl oxidase-like 4	22.4	2.51E-04
381359	Prdm12	PR domain containing 12	19.6	1.37E-05
12051	Bcl3	B-cell leukemia/lymphoma 3	18.7	4.52E-06
233187	Lim2	lens intrinsic membrane protein 2	17	2.37E-02
17339	Mip	major intrinsic protein of eye lens fiber	16.3	2.49E-02
21818	Tgm3	transglutaminase 3, E polypeptide	15.6	4.76E-04
75290	4930557B15Rik	RIKEN cDNA 4930557B15 gene	14.4	1.07E-02
20856	Stc2	stanniocalcin 2	13.8	5.69E-07
319506	7530428D23Rik	RIKEN cDNA 7530428D23 gene	13.6	5.51E-02
276829	Smtnl2	smoothelin-like 2	13.3	2.79E-07
14663	Glycam1	glycosylation dependent cell adhesion molecule 1	13	1.27E-03
67573	Loxl4	lysyl oxidase-like 4	12.6	1.99E-05
15006	H2-Q1	histocompatibility 2, Q region locus 1	12.3	9.49E-06
68380	0610042G04Rik	RIKEN cDNA 0610042G04 gene	11.9	3.10E-08
14173	Fgf2	fibroblast growth factor 2	11.7	7.27E-06
192199	Rspo1	R-spondin homolog (Xenopus laevis)	11.4	2.04E-02
213742	Xist	inactive X specific transcripts	11.3	2.45E-02
12954	Cryaa	crystallin, alpha A	11	1.64E-02
100039660	Ect2l	epithelial cell transforming sequence 2 oncogene-like	10.9	3.46E-05
77998	Grifin	galectin-related inter-fiber protein	10.7	1.75E-02
15019	H2-Q8	histocompatibility 2, Q region locus 8	10.6	2.15E-09
238692	Zfp874a	zinc finger protein 874a	10.4	4.21E-06
54382	Tcstv1	2-cell-stage, variable group, member 1	10.4	2.32E-04
214301	Crygn	crystallin, gamma N	10.3	1.19E-02
12268	C4b	complement component 4B (Childo blood group)	10.2	1.60E-05

18073	Nid1	nidogen 1	10.2	1.54E-02
12962	Crybb3	crystallin, beta B3	10.2	1.19E-02
19013	Ppara	peroxisome proliferator activated receptor alpha	9.9	4.40E-06
12609	Cebpd	CCAAT/enhancer binding protein (C/EBP), delta	9.5	2.12E-06
100043899	R3hdml	R3H domain containing-like	9.4	1.68E-03
434280	Gm5607	predicted gene 5607	9.4	3.64E-02
94224	Srd5a2	steroid 5 alpha-reductase 2	9.2	1.74E-02
79554	Gltpd1	glycolipid transfer protein domain containing 1	9.2	1.19E-04
30923	Foxe3	forkhead box E3	9.1	4.89E-03
68662	Scgb3a1	secretoglobin, family 3A, member 1	9.1	8.28E-05
19153	Prx	periaxin	8.7	4.70E-03
14611	Gja3	gap junction protein, alpha 3	8.6	1.76E-02
74492	Kbtbd13	kelch repeat and BTB (POZ) domain containing 13	8.6	2.12E-03
13646	Klk1b22	kallikrein 1-related peptidase b22	8.6	5.57E-05
DOWNREGULATED GENES				
Entrez ID	**Gene Symbol**	**Description**	**fold change**	**pValue**
329478	C130078N14	hypothetical protein C130078N14	137.6	1.52E-12
76681	Trim12a	tripartite motif-containing 12A	70.8	8.54E-09
80509	Med8	mediator of RNA polymerase II transcription, subunit 8 homolog (yeast)	40.7	1.54E-06
69301	1700008P20Rik	RIKEN cDNA 1700008P20 gene	40.5	2.20E-07
30939	Pttg1	pituitary tumor-transforming gene 1	38.1	1.81E-10
258198	Olfr224	olfactory receptor 224	37	2.80E-05
433100	AA388235	expressed sequence AA388235	36.6	3.36E-11
54631	Nphs1	nephrosis 1 homolog, nephrin (human)	36.4	4.80E-07
69301	1700008P20Rik	RIKEN cDNA 1700008P20 gene	34	1.95E-06
17996	Neb	nebulin	31.8	0.09391
75764	Slx1b	SLX1 structure-specific endonuclease subunit homolog B (S. cerevisiae)	29.5	4.22E-09
14537	Gcnt1	glucosaminyl (N-acetyl) transferase 1, core 2	28.7	3.59E-11
26908	Eif2s3y	eukaryotic translation initiation factor 2, subunit 3, structural gene Y-linked	25.7	0.06617
26900	Ddx3y	DEAD (Asp-Glu-Ala-Asp) box polypeptide 3, Y-linked	20.4	0.06557
30939	Pttg1	pituitary tumor-transforming gene 1	19.6	3.72E-06
109685	Hyal3	hyaluronoglucosaminidase 3	19.3	3.57E-06
73061	3110007F17Rik	RIKEN cDNA 3110007F17 gene	19.2	3.63E-10
72154	Zfp157	zinc finger protein 157	18.9	2.11E-07
67705	1810058I24Rik	RIKEN cDNA 1810058I24 gene	17.4	9.13E-06
74602	4833428L15Rik	RIKEN cDNA 4833428L15 gene	14.5	2.38E-07
17921	Myo7a	myosin VIIA	14.1	3.64E-08
26450	Rbbp9	retinoblastoma binding protein 9	13.7	0.06114
214523	Tmprss4	transmembrane protease, serine 4	12	2.07E-08

72461	Prcp	prolylcarboxypeptidase (angiotensinase C)	10	9.91E-09
100040410	Gm14957	predicted gene 14957	9.8	1.31E-07
269209	Stk36	serine/threonine kinase 36 (fused homolog, Drosophila)	9.7	4.68E-06
94216	Col4a6	collagen, type IV, alpha 6	9	0.0003704
140709	Emid2	EMI domain containing 2	8.9	9.73E-07
70979	4931417G12Rik	RIKEN cDNA 4931417G12 gene	8.2	2.47E-08
73061	3110007F17Rik	RIKEN cDNA 3110007F17 gene	8.1	0.005393
76681	Trim12a	tripartite motif-containing 12A	7.9	0.0001357
209760	Tmc7	transmembrane channel-like gene family 7	7.8	1.24E-05
68668	Klk5	kallikrein related-peptidase 5	7.5	0.0122
229613	6330549D23Rik	RIKEN cDNA 6330549D23 gene	7.1	4.86E-07
71687	Tmem25	transmembrane protein 25	6.5	7.66E-08
100040412	LOC100040412	lysine-specific demethylase 5D-like	6.4	0.09181
234138	BC019943	cDNA sequence BC019943	6.1	4.28E-08
19223	Ptgis	prostaglandin I2 (prostacyclin) synthase	6	2.71E-06
16181	Il1rn	interleukin 1 receptor antagonist	6	0.09192
74528	8430406I07Rik	RIKEN cDNA 8430406I07 gene	5.9	0.00656
18261	Ocm	oncomodulin	5.8	1.41E-05
75080	4930518C09Rik	RIKEN cDNA 4930518C09 gene	5.7	0.01449
234199	Fgl1	fibrinogen-like protein 1	5.7	0.0005564
66442	Spc25	SPC25, NDC80 kinetochore complex component, homolog (S. cerevisiae)	5.5	0.0001349
107047	Psmg2	proteasome (prosome, macropain) assembly chaperone 2	5.4	0.03946
234138	BC019943	cDNA sequence BC019943	5.3	1.72E-07
231507	Plac8	placenta-specific 8	5.2	0.0001051
72902	Spock3	sparc/osteonectin, cwcv and kazal-like domains proteoglycan 3	5.1	0.01586
12319	Car8	carbonic anhydrase 8	5.1	5.94E-06
***Opsin-Cre;Vhl^{flox}* (Single) *vs Vhl^{flox};Hif1a^{flox}* (Control)**				
UPREGULATED GENES				
Entrez ID	**Gene Symbol**	**Description**	**fold change**	**pValue**
213742	Xist	inactive X specific transcripts	472.78	6.51E-09
71957	Cpsf3l	cleavage and polyadenylation specific factor 3-like	162.92	4.09E-07
619297	C430049E01Rik	RIKEN cDNA C430049E01 gene	151.07	4.52E-09
76487	Ppp1r3g	protein phosphatase 1, regulatory (inhibitor) subunit 3G	79.68	8.93E-10
213742	Xist	inactive X specific transcripts	79.02	2.37E-07
223780	Adm2	adrenomedullin 2	71.96	9.09E-08
13615	Edn2	endothelin 2	62.64	4.30E-08
67573	Loxl4	lysyl oxidase-like 4	33.95	1.83E-05
240913	Adamts4	a disintegrin-like and metallopeptidase with thrombospondin type 1 motif, 4	31.92	0.0001611
70045	2610528A11Rik	RIKEN cDNA 2610528A11 gene	30.83	2.05E-08

16763	Lad1	ladinin	30.3	6.58E-07
236220	LOC236220	hypothetical protein LOC236220	26.36	9.73E-06
14663	Glycam1	glycosylation dependent cell adhesion molecule 1	25.18	3.39E-05
11535	Adm	adrenomedullin	23.71	1.12E-07
17339	Mip	major intrinsic protein of eye lens fiber	22.92	0.008083
214301	Crygn	crystallin, gamma N	22.34	0.006261
192199	Rspo1	R-spondin homolog (Xenopus laevis)	21.68	0.007823
233187	Lim2	lens intrinsic membrane protein 2	21.61	0.004186
12954	Cryaa	crystallin, alpha A	20.93	0.007343
20856	Stc2	stanniocalcin 2	20.74	1.13E-06
77998	Grifin	galectin-related inter-fiber protein	19.81	0.003584
12051	Bcl3	B-cell leukemia/lymphoma 3	19.46	1.62E-06
276829	Smtnl2	smoothelin-like 2	17.03	9.83E-08
381359	Prdm12	PR domain containing 12	16.16	1.72E-05
75290	4930557B15Rik	RIKEN cDNA 4930557B15 gene	16.03	0.008547
100039660	Ect2l	epithelial cell transforming sequence 2 oncogene-like	15.46	1.72E-05
67573	Loxl4	lysyl oxidase-like 4	15.31	9.15E-06
12962	Crybb3	crystallin, beta B3	14.55	0.003442
21818	Tgm3	transglutaminase 3, E polypeptide	14.54	2.99E-05
667977	Gm8909	predicted gene 8909	14.18	0.007455
74492	Kbtbd13	kelch repeat and BTB (POZ) domain containing 13	13.33	1.03E-05
22300	Vmn2r123	vomeronasal 2, receptor 123	12.97	4.27E-09
68662	Scgb3a1	secretoglobin, family 3A, member 1	11.88	4.83E-05
20296	Ccl2	chemokine (C-C motif) ligand 2	11.87	0.0003137
210321	BC048679	cDNA sequence BC048679	11.86	0.01211
12268	C4b	complement component 4B (Childo blood group)	11.8	3.69E-06
15019	H2-Q8	histocompatibility 2, Q region locus 8	11.48	6.27E-08
68380	0610042G04Rik	RIKEN cDNA 0610042G04 gene	11.43	1.66E-07
18073	Nid1	nidogen 1	11.19	0.007656
12310	Calca	calcitonin/calcitonin-related polypeptide, alpha	11.06	1.77E-07
18542	Pcolce	procollagen C-endopeptidase enhancer protein	10.99	0.0001002
12957	Cryba1	crystallin, beta A1	10.96	0.009598
12958	Cryba2	crystallin, beta A2	10.93	0.009546
14611	Gja3	gap junction protein, alpha 3	10.84	0.003981
238692	Zfp874a	zinc finger protein 874a	10.84	5.79E-06
12960	Crybb1	crystallin, beta B1	10.83	0.01173
12609	Cebpd	CCAAT/enhancer binding protein (C/EBP), delta	10.74	1.59E-06
100043899	R3hdml	R3H domain containing-like	10.71	0.001889
12960	Crybb1	crystallin, beta B1	10.68	0.01213

DOWNREGULATED GENES				
Entrez ID	**Gene Symbol**	**Description**	**fold change**	**pValue**
329478	C130078N14	hypothetical protein C130078N14	170	3.04E-11
258198	Olfr224	olfactory receptor 224	68.41	2.21E-06
80509	Med8	mediator of RNA polymerase II transcription, subunit 8 homolog (yeast)	68.14	3.21E-07
76681	Trim12a	tripartite motif-containing 12A	42.19	2.23E-08
30939	Pttg1	pituitary tumor-transforming gene 1	38.46	1.03E-09
26908	Eif2s3y	eukary translation initiation factor 2, subunit 3, structural gene Y-linked	32.27	0.05194
77936	BC065403	cDNA sequence BC065403	32.14	1.52E-07
54631	Nphs1	nephrosis 1 homolog, nephrin (human)	31.05	1.02E-07
69301	1700008P20Rik	RIKEN cDNA 1700008P20 gene	27.89	1.07E-06
14537	Gcnt1	glucosaminyl (N-acetyl) transferase 1, core 2	25.32	1.14E-09
30939	Pttg1	pituitary tumor-transforming gene 1	23.56	1.84E-06
69301	1700008P20Rik	RIKEN cDNA 1700008P20 gene	22.76	1.02E-05
26900	Ddx3y	DEAD (Asp-Glu-Ala-Asp) box polypeptide 3, Y-linked	22.54	0.05882
75764	Slx1b	SLX1 structure-specific endonuclease subunit homolog B (S. cerevisiae)	19.69	2.71E-09
72154	Zfp157	zinc finger protein 157	17.27	4.90E-07
73061	3110007F17Rik	RIKEN cDNA 3110007F17 gene	16.56	2.97E-08
74602	4833428L15Rik	RIKEN cDNA 4833428L15 gene	15.67	5.37E-08
26450	Rbbp9	retinoblastoma binding protein 9	13.03	0.06533
433100	AA388235	expressed sequence AA388235	12.37	0.0134
67705	1810058I24Rik	RIKEN cDNA 1810058I24 gene	12.13	4.14E-05
269209	Stk36	serine/threonine kinase 36 (fused homolog, Drosophila)	10.94	4.27E-06
214523	Tmprss4	transmembrane protease, serine 4	10.51	2.39E-08
17427	Mns1	meiosis-specific nuclear structural protein 1	9.951	1.01E-06
100040410	Gm14957	predicted gene 14957	9.301	7.81E-08
100040412	LOC100040412	lysine-specific demethylase 5D-like	8.768	0.05389
72461	Prcp	prolylcarboxypeptidase (angiotensinase C)	8.663	1.35E-08
16061	Igh-VJ558	immunoglobulin heavy chain (J558 family)	8.56	0.0004181
73162	Otud3	OTU domain containing 3	8.453	0.06001
140709	Emid2	EMI domain containing 2	8.323	1.01E-06
17921	Myo7a	myosin VIIA	8.034	1.77E-07
94216	Col4a6	collagen, type IV, alpha 6	7.748	0.0003292
78609	8030411F24Rik	RIKEN cDNA 8030411F24 gene	6.854	1.46E-05
69611	Lce1d	late cornified envelope 1D	6.772	0.01599
20592	Kdm5d	lysine (K)-specific demethylase 5D	6.665	0.05474
71687	Tmem25	transmembrane protein 25	6.476	6.43E-08
229613	6330549D23Rik	RIKEN cDNA 6330549D23 gene	6.44	8.57E-07

12769	Ccr9	chemokine (C-C motif) receptor 9	6.149	0.00552
66442	Spc25	SPC25, NDC80 kinetochore complex component, homolog (S. cerevisiae)	5.952	7.49E-05
67133	Gp2	glycoprotein 2 (zymogen granule membrane)	5.727	0.02909
67828	Lce1f	late cornified envelope 1F	5.707	0.00443
68694	Lce1e	late cornified envelope 1E	5.555	0.0036
76681	Trim12a	tripartite motif-containing 12A	5.55	0.0004647
74528	8430406I07Rik	RIKEN cDNA 8430406I07 gene	5.487	0.008492
73061	3110007F17Rik	RIKEN cDNA 3110007F17 gene	5.415	0.01026
271221	5031414D18Rik	RIKEN cDNA 5031414D18 gene	5.399	0.09344
209760	Tmc7	transmembrane channel-like gene family 7	5.343	4.51E-05
319742	Mpzl3	myelin protein zero-like 3	5.332	0.006575
22290	Uty	ubiquitously transcribed tetratricopeptide repeat gene, Y chromosome	5.085	0.04838
16061	Igh-VJ558	immunoglobulin heavy chain (J558 family)	5.068	3.86E-05
Opsin-Cre;*Vhl*^{flox};*Hif1a*^{flox} (Double) vs *Vhl*^{flox};*Hif1a*^{flox} (Control)				
UPREGULATED GENES				
Entrez ID	**Gene Symbol**	**Description**	**fold change**	**pValue**
70045	2610528A11Rik	RIKEN cDNA 2610528A11 gene	24.04	2.38E-09
213742	Xist	inactive X specific transcripts	13.42	8.96E-02
17996	Neb	nebulin	13.39	1.97E-01
213742	Xist	inactive X specific transcripts	7.028	5.04E-02
109685	Hyal3	hyaluronoglucosaminidase 3	6.959	1.26E-02
70979	4931417G12Rik	RIKEN cDNA 4931417G12 gene	6.84	1.02E-06
19076	Prim2	DNA primase, p58 subunit	5.255	7.60E-09
232801	Lilra5	leukocyte immunoglobulin-like receptor, subfamily A (with TM domain), member	4.874	9.85E-02
272643	Prss43	protease, serine, 43	4.814	5.00E-02
77044	Arid2	AT rich interactive domain 2 (ARID, RFX-like)	4.807	3.88E-02
382109	Fbxw26	F-box and WD-40 domain protein 26	4.708	9.60E-02
434794	Xlr4a	X-linked lymphocyte-regulated 4A	4.484	8.59E-03
331529	Gm5128	predicted gene 5128	4.13	2.66E-02
106610	AI504002	expressed sequence AI504002	4.01	2.89E-01
223332	Ranbp3l	RAN binding protein 3-like	3.692	1.05E-01
16816	Lcat	lecithin cholesterol acyltransferase	3.592	2.17E-01
434540	Psg20	pregnancy-specific glycoprotein 20	3.536	1.57E-01
12040	Bckdhb	branched chain ketoacid dehydrogenase E1, beta polypeptide	3.503	2.70E-01
18216	Ntsr1	neurotensin receptor 1	3.475	1.09E-01
50500	Ttpa	tocopherol (alpha) transfer protein	3.417	1.32E-01
628171	Olfr936	olfactory receptor 936	3.39	5.31E-03
67722	4921517D21Rik	RIKEN cDNA 4921517D21 gene	3.386	2.20E-02
73748	Gadl1	glutamate decarboxylase-like 1	3.326	1.48E-02

71078	Adam30	a disintegrin and metallopeptidase domain 30	3.298	8.24E-02
100042761	Gm10697	predicted gene 10697	3.258	1.69E-01
246229	Bivm	basic, immunoglobulin-like variable motif containing	3.25	2.97E-01
329972	Spata21	spermatogenesis associated 21	3.172	8.72E-02
258757	Olfr1013	olfactory receptor 1013	3.152	6.98E-02
100046359	LOC100046359	ig heavy chain V region VH558 A1/A4-like	3.119	5.72E-02
234311	Ddx60	DEAD (Asp-Glu-Ala-Asp) box polypeptide 60	3.105	1.12E-01
70896	Speer1-ps1	spermatogenesis associated glutamate (E)-rich protein 1, pseudogene 1	2.97	5.28E-02
114662	Prss29	protease, serine, 29	2.968	1.56E-01
433100	AA388235	expressed sequence AA388235	2.956	2.10E-01
545548	Lce3a	late cornified envelope 3A	2.933	3.65E-03
258408	Olfr463	olfactory receptor 463	2.934	1.85E-01
258927	Olfr481	olfactory receptor 481	2.927	6.82E-02
277345	Wfdc16	WAP four-disulfide core domain 16	2.924	9.92E-02
12534	Cdk1	cyclin-dependent kinase 1	2.903	8.44E-03
244071	Agbl1	ATP/GTP binding protein-like 1	2.899	8.76E-02
98763	AA407782	expressed sequence AA407782	2.895	4.34E-01
171186	Vmn1r38	vomeronasal 1 receptor 38	2.881	2.25E-01
12770	Ccr1l1	chemokine (C-C motif) receptor 1-like 1	2.864	1.06E-01
213402	Armc2	armadillo repeat containing 2	2.86	1.24E-01
258354	Olfr168	olfactory receptor 168	2.86	2.08E-01
27083	Xlr4b	X-linked lymphocyte-regulated 4B	2.853	3.77E-02
56773	Chst5	carbohydrate (N-acetylglucosamine 6-O) sulfotransferase 5	2.844	5.65E-02
268482	Krt12	keratin 12	2.833	6.68E-02
268482	Krt12	keratin 12	2.812	6.74E-02
57277	Slurp1	secreted Ly6/Plaur domain containing 1	2.808	2.82E-02
DOWNREGULATED GENES				
Entrez ID	**Gene Symbol**	**Description**	**fold change**	**pValue**
77936	BC065403	cDNA sequence BC065403	14.45	0.001686
435845	Tmprss11c	transmembrane protease, serine 11c	11.06	0.2154
277773	BC049635	cDNA sequence BC049635	6.02	0.4197
12836	Col7a1	collagen, type VII, alpha 1	5.74	0.2868
353371	Oxct2b	3-oxoacid CoA transferase 2B	5.46	0.01235
271221	5031414D18Rik	RIKEN cDNA 5031414D18 gene	5.32	0.09902
11808	Apoa4	apolipoprotein A-IV	5.27	0.0973
668501	Zfp507	zinc finger protein 507	4.24	0.2897
84095	Pi4k2a	phosphatidylinositol 4-kinase type 2 alpha	4.23	0.3137
17427	Mns1	meiosis-specific nuclear structural protein 1	3.94	0.01575
51925	D2Ertd640e	DNA segment, Chr 2, ERATO Doi 640, expressed	3.85	0.0002779

77394	9530025H10Rik	RIKEN cDNA 9530025H10 gene	3.83	0.09673
54486	Hpgds	hematopoietic prostaglandin D synthase	3.81	0.06928
100043706	Gm4598	predicted gene 4598	3.76	0.02922
224552	Vmn2r98	vomeronasal 2, receptor 98	3.75	0.1685
26876	Adh4	alcohol dehydrogenase 4 (class II), pi polypeptide	3.73	0.3138
436003	Gm5736	predicted gene 5736	3.58	0.09749
68789	Trmt61b	tRNA methyltransferase 61 homolog B (S. cerevisiae)	3.45	0.1156
22696	Zfp37	zinc finger protein 37	3.32	0.3113
98736	1700034H15Rik	RIKEN cDNA 1700034H15 gene	3.32	0.1861
102144	AI746383	expressed sequence AI746383	3.26	0.1173
224079	Atp13a4	ATPase type 13A4	3.25	0.1649
207854	Fmr1nb	fragile X mental retardation 1 neighbor	3.2	0.06387
69319	1700001K23Rik	RIKEN cDNA 1700001K23 gene	3.2	0.0002839
258310	Olfr145	olfactory receptor 145	3.13	0.09426
73252	1600022D10Rik	RIKEN cDNA 1600022D10 gene	3.11	0.06589
93689	Lmod1	leiomodin 1 (smooth muscle)	3.09	0.03443
666021	2300003K06Rik	RIKEN cDNA 2300003K06 gene	3.07	0.1078
76585	Lce1i	late cornified envelope 1I	2.99	0.00587
69611	Lce1d	late cornified envelope 1D	2.96	0.02876
100038617	Gm10466	predicted gene 10466	2.95	0.1431
237890	Slfn14-ps	schlafen family member 14, pseudogene	2.95	0.1693
546903	Vmn1r39	vomeronasal 1 receptor 39	2.95	0.0906
16867	Lhcgr	luteinizing hormone/choriogonadotropin receptor	2.94	0.1029
277667	Gm13089	predicted gene 13089	2.91	0.06277
80287	Apobec3	apolipoprotein B mRNA editing enzyme, catalytic polypeptide 3	2.91	0.1317
258744	Olfr875	olfactory receptor 875	2.9	0.09924
319229	Sctr	secretin receptor	2.89	0.1336
69566	2310016D03Rik	RIKEN cDNA 2310016D03 gene	2.82	0.02048
56057	Btg4	B-cell translocation gene 4	2.81	0.0473
384244	Gm5294	predicted gene 5294	2.81	0.1151
93671	Cd163	CD163 antigen	2.81	0.1767
16061	Igh-VJ558	immunoglobulin heavy chain (J558 family)	2.8	0.007337
71206	Katnal2	katanin p60 subunit A-like 2	2.79	0.3081
56092	Cts7	cathepsin 7	2.78	0.05438
387513	Tas2r138	taste receptor, type 2, member 138	2.77	0.3596
258097	Olfr1500	olfactory receptor 1500	2.75	0.09798
100504089	LOC100504089	calcium-binding protein p22-like	2.74	0.2235
106763	Ttbk1	tau tubulin kinase 1	2.73	0.08259

5.3.2 FUNCTIONAL GROUPS				
Opsin-Cre;*Vhl*^{flox} (Single) vs Opsin-Cre;*Vhl*^{flox};*Hif1a*^{flox} (Double) - Upregulated genes				
GROUP 1 (Enrichment score = 17.02)				
Entrez ID	**Gene Symbol**	**Description**	**fold change**	**pValue**
214301	Crygn	crystallin, gamma N	10.3	1.19E-02
12966	Crygc	crystallin, gamma C	5.2	2.33E-02
12969	Crygf	crystallin, gamma F	4.3	1.93E-05
12957	Cryba1	crystallin, beta A1	6.5	2.68E-02
12965	Crygb	crystallin, gamma B	6.3	6.89E-03
12960	Crybb1	crystallin, beta B1	6.8	3.44E-02
12970	Crygs	crystallin, gamma S	3.7	4.01E-02
12959	Cryba4	crystallin, beta A4	4.6	5.95E-02
12968	Cryge	crystallin, gamma E	6.2	4.65E-07
12962	Crybb3	crystallin, beta B3	10.2	1.19E-02
12961	Crybb2	crystallin, beta B2	6.9	3.60E-02
12958	Cryba2	crystallin, beta A2	7	3.48E-02
12967	Crygd	crystallin, gamma D	5.1	6.78E-03
12964	Cryga	crystallin, gamma A	7.8	4.88E-03
GROUP 2 (Enrichment score = 7.36)				
Entrez ID	**Gene Symbol**	**Description**	**fold change**	**pValue**
654812	Angptl7	angiopoietin-like 7	4.6	2.84E-02
192199	Rspo1	R-spondin homolog (Xenopus laevis)	11.4	2.04E-02
280635	Emilin3	elastin microfibril interfacer 3	3.4	1.57E-02
228796	Bpil3	bactericidal/permeability-increasing protein-like 3	5.7	8.06E-05
68662	Scgb3a1	secretoglobin, family 3A, member 1	9.1	8.28E-05
20284	Scrg1	scrapie responsive gene 1	3	3.17E-02
240913	Adamts4	a disintegrin-like and metallopeptidase (reprolysin type) with thrombospondin type 1 motif, 4	24.7	2.89E-04
20856	Stc2	stanniocalcin 2	13.8	5.69E-07
77673	Defb41	defensin beta 41	3	8.34E-02
100043899	R3hdml	R3H domain containing-like	9.4	1.68E-03
99543	Olfml3	olfactomedin-like 3	3.1	3.25E-03
100689	Spon2	spondin 2, extracellular matrix protein	3.8	9.11E-04
GROUP 3 (Enrichment score = 5.16)				
Entrez ID	**Gene Symbol**	**Description**	**fold change**	**pValue**
232345	A2m	alpha-2-macroglobulin	4.8	7.72E-03
20730	Spink3	serine peptidase inhibitor, Kazal type 3	3.9	2.25E-04
100043899	R3hdml	R3H domain containing-like	9.4	1.68E-03
75526	Spinlw1	serine protease inhibitor-like, with Kunitz and WAP domains 1 (eppin)	3	1.51E-04

GROUP 4 (Enrichment score = 3.38)				
Entrez ID	**Gene Symbol**	**Description**	**fold change**	**pValue**
12266	C3	complement component 3	3.1	9.52E-05
14962	Cfb	complement factor B	3.2	2.89E-02
12268	C4b	complement component 4B (Childo blood group)	10.2	1.60E-05
18050	Klk1b3	kallikrein 1-related peptidase b3	6.9	7.95E-05
12630	Cfi	complement component factor i	6	2.02E-05
13646	Klk1b22	kallikrein 1-related peptidase b22	8.6	5.57E-05
12258	Serping1	serine (or cysteine) peptidase inhibitor, clade G, member 1	3.3	1.13E-04
GROUP 5 (Enrichment score = 3.32)				
Entrez ID	**Gene Symbol**	**Description**	**fold change**	**pValue**
15945	Cxcl10	chemokine (C-X-C motif) ligand 10	7.4	2.25E-04
20296	Ccl2	chemokine (C-C motif) ligand 2	6.8	8.04E-04
20293	Ccl12	chemokine (C-C motif) ligand 12	2.9	9.22E-03
20311	Cxcl5	chemokine (C-X-C motif) ligand 5	4.7	8.04E-04
GROUP 6 (Enrichment score = 2.19)				
Entrez ID	**Gene Symbol**	**Description**	**fold change**	**pValue**
15019	H2-Q8	histocompatibility 2, Q region locus 8	10.6	2.15E-09
15007	H2-Q10	histocompatibility 2, Q region locus 10	3.2	1.64E-04
15002	H2-Ob	histocompatibility 2, O region beta locus	2.4	3.43E-02
667977	Gm8909	predicted gene 8909	5.4	4.67E-07
GROUP 7 (Enrichment score = 0.98)				
Entrez ID	**Gene Symbol**	**Description**	**fold change**	**pValue**
231832	Tmem184a	transmembrane protein 184a	3.7	1.54E-04
71862	Gpr160	G protein-coupled receptor 160	2.9	5.52E-02
76718	Catsperg2	cation channel, sperm-associated, gamma 2	3.8	4.56E-05
327766	Tmem26	transmembrane protein 26	3.2	1.05E-03
83961	Nrg4	neuregulin 4	5.7	6.03E-04
14611	Gja3	gap junction protein, alpha 3	8.6	1.76E-02
69354	Slc38a4	solute carrier family 38, member 4	5.4	1.19E-02
17339	Mip	major intrinsic protein of eye lens fiber	16.3	2.49E-02
18414	Osmr	oncostatin M receptor	3.2	7.73E-05
14616	Gja8	gap junction protein, alpha 8	7	2.41E-02
235435	Lctl	lactase-like	6.3	4.55E-02
94346	Tmem40	transmembrane protein 40	5.7	3.88E-02
233187	Lim2	lens intrinsic membrane protein 2	17	2.37E-02
80879	Slc16a3	solute carrier family 16 (monocarboxylic acid transporters), member 3	4	7.99E-05
63959	Slc29a1	solute carrier family 29 (nucleoside transporters), member 1	2.9	8.74E-06

GROUP 8 (Enrichment score = 0.59)				
Entrez ID	**Gene Symbol**	**Description**	**fold change**	**pValue**
19013	Ppara	peroxisome proliferator activated receptor alpha	9.9	4.40E-06
14283	Fosl1	fos-like antigen 1	5.3	8.74E-06
12609	Cebpd	CCAAT/enhancer binding protein (C/EBP), delta	9.5	2.12E-06
26424	Nr5a2	nuclear receptor subfamily 5, group A, member 2	3.4	4.01E-02
14462	Gata3	GATA binding protein 3	4.7	1.16E-02
GROUP 9 (Enrichment score = 0.07)				
Entrez ID	**Gene Symbol**	**Description**	**fold change**	**pValue**
238692	Zfp874a	zinc finger protein 874a	10.4	4.21E-06
69368	Wdfy1	WD repeat and FYVE domain containing 1	5.4	7.77E-08
329581	Birc7	baculoviral IAP repeat-containing 7 (livin)	4.4	0.0007944
232966	Zfp114	zinc finger protein 114	5.8	2.22E-07

5.3.3 Abbreviations

A2M	Alpha 2 macroglobulin
AAV	Adeno-associated virus
Actb	Actin beta subunit
Adamts4	A disintegrin-like and metallopeptidase with thrombospondin type 1 motif, 4
Adm	Adrenomedullin
AMD	Age related macular degeneration
BM	Bruch's membrane
Brn3a	Brain-specific homeobox/ POU domain protein 3A
C3	Complement fcator 3
C4b	Complement factor 4b
Casp	Caspase
Ccl2	Chemokine (C-C motif) ligand 2
cDNA	Complementary DNA
Cepbd	CCAAT/enhancer binding protein (C/EBP), delta
Cfb	Complement factor b
Cfh	Complement fcator h
Cfi	Complement factor i
Calb2	Calbindin 2
CNV	Choroidal neovascularization
Cpsf3l	Cleavage and polyadenylation specific factor 3-like
Csfr	Colony stimulating factor receptor
Cx3cl	chemokine (C-X3-C motif) ligand
ECM	Extra cellular matrix
Edn2	Endothelin 2
Fgf2	Fibroblast growth factor 2
Fih	Factor inhibiting HIF
GCL	Ganglion cel layer
Gfap	Glial fibrillary acidic protein

Glul	Glutamate-ammonia ligase (glutamine synthetase)
Glycam1	Glycosylation dependent cell adhesion molecule 1
Gnat1	Guanine nucleotide binding protein, alpha transducing 1 (rods)
Gnat2	guanine nucleotide binding protein, alpha transducing 2 (cones)
GPR	G-protein coupled receptor
Hif1a	Hypoxia inducible factor- alpha subunit
Hif1b	Hypoxia inducible factor - beta subunit
HRP	Horse raddish peroxidase
INL	Inner nuclear layer
IPL	Inner plexiform layer
IS	Inner segments
Lad1	Ladinin
LCM	Laser capture microdissection
Ldha	Lactate dehydrogenase, isoform a
Lif	Leukemia inhibitory factor
Loxl4	Lysyl oxidase-like 4
Mct	Monocarboxylate transporter
Myo7a	Myosin VIIA
Nrg4	Neuregulin4
Obox6	Oocyte specific homeobox 6
ONL	Outer nuclear layer
OPL	Outer plexiform layer
Opn4	Opsin 4 (melanopsin)
OS	Outer segments
PCR	Polymerase chain reaction
Pdc	Pyruvate dehydrogenase complex
Pdk	Pyruvate dehydrogenase kinase
Pdp	Pyruvate dehydrogenase phosphatase
Phd	Prolyl hydroxylase
PND	Postnatal day

Ppara	Peroxisome proliferator activated receptor alpha
Pttg1	Pituitary tumor-transforming gene 1
qPCR	Quantitative PCR
rd10	Retinal degeneration 10
Rpe	Retinal pigment epithelium
shRNA	Short hairpin RNA
siRNA	small interfering RNA
Smtnl2	Smoothelin-like 2
Stat3	Signal transducer and activator of transcription 3
Stc1	Stanniocalcin 1
Stc2	Stanniocalcin 2
Tgf	Tissue growth factor
Tgm3	Transglutaminase 3, E polypeptide
Tnf	Tissue necrosis factor
Vegf	Vascular endothelial growth factor
Vhl	Von-Hippel Lindau
Vsx2	Visual system homeobox 2

5.3.4. PRIMERS USED FOR SEMIQUANTITATIVE REAL-TIME PCR

Gene	Forward primer	Reverse primer	Annealing temperature (°C)	Amplicon size (bp)
A2M	ACTCGATGAGGAGGCGGTA	GGTAAGATAAGCCAGGAGCA	62	148
Adamts4	CGGGCACTGGGCTACTACT	TCACAGCCAGCATGGATACA	62	113
Cpsf3l	CAGACAGTTCAGGTGGATGAT	CAGACTCCGAGCCCACTTTA	62	100
Glycam1	GCTCTCCTGCCTGGGTCCAAAG	GATTCTATCACCACATTATCTT	62	185
Lad1	CACCCAGAATGGAGCTCAG	CACCTGCCGCCTCTGTCTCCG	62	154
Loxl4	GTTGCACAACTGCCACACA	GGAGTGCAGTAATGGCTTC	62	108
Myo7a	CACGATGACTGGCAGATTGGCA	TCTGTCTGTATGGCCTTGT	62	96
Nrg4	GTAATCTGTCGGCAGCTT	TGTTCTCTGTGGCTGTGACG	62	169
Obox6	TCACTAGAGGACTCTGGCACA	GCAACCCTCTGATTTCAGGTTCT	62	190
Ppara	GCCAAGTTGAAGTTCAAGGC	TCCACCATGTTGGATGGATGT	62	133
Pttg1	GGACAGTCAACAGAGTTGCCGA	GCATCATCAGGAGCAGGAACA	62	136
Smtln2	GCATCTTGGAGAACGGACA	CAGAGAATTTCTCGGACTCG	62	168
Tgm3	TGTACTACGATGCCATGGGA	GACCTGCCATCCATTGTATG	62	125
C3	TACCTGGACCAGACCGAA	GAGCTGGGCTGTTTGAAG	62	113
C4b	TGGACATGGCTCTGTATGCT	AGCATCCTGGAACACCTGAA	62	140
Cfb	GTGAACATCAATGCCTTAGCTTCC	CCATGCCACAGAGACTCAGAGA	62	133
Cfh	GGCAAGTGGAAGTGATGTGT	CATTGTCAATAGGTGGAGGAG	62	99
Cfi	GACTGCTGCGCACTGTGTCA	GAAGGTGGCTCCATTATATT	62	148
SerpinG1	CCATTCAGCATTGCCAGCCT	TTAGTGCTTGGTGGACACAG	62	121

Other primers are listed in the corresponding sections, as follows

Section 3.1.1 – *Actb, Adm, Casp1, Cepbd, Edn2, Fgf2, Gnat1, Hif1a, Hif2a, Ldha, Mct4, Pdk1, Stat3, Vhl*

Section 3.2.3 – *Actb, Adm, Epo, Gnat1, Mct3, Opn4, Stc1, Stc2, Vsx2*

Section 3.3 – *Actb, Gpr4, Gpr65, Gpr68, Gnat1, Gnat2, Vsx2, Calb1, Calb2, Pou4f1, Glul, Casp1, Gfap, Fgf2, Stat3, Edn2, Lif, Tnf, Tgfb, Ccl2, Ccl4, Ccl5, Ccl8, Ccl9, Ccl12, Csfr1, Cx3cl*

6. CURRICULUM VITAE

Personal information

First name(s) / Surname(s)	**Divya Ail**
Address(es)	Present: Hürststrasse 94, 8046 Zürich, Switzerland. Permanent: F3, Chamundi Apts, 966/1, 1st cross, Laxmipuram, Mysore, Karnataka, India- 570004
Telephone(s)	0041 786 44 99 91
E-mail	divyail3@gmail.com
Nationality	Indian
Date of birth	30.08.1984
Gender	female

Education and training

Dates	Sept 2011 – 2015 (tentative – Sept)
Title of qualification to be awarded	PhD
Institute	Lab of Retinal Cell Biology, USZ/UZH (Group: Prof. Christian Grimm)
University	University of Zurich, Switzerland
PhD Program	Neuroscience (Part of Life Science Zürich Graduate school)
Project Title	Elucidating the molecular mechanisms of HIF1A mediated age-related retinal degeneration

Dates	Oct 2007 – Sept 2009
Title of qualification awarded	Master of Science (MSc)
subject	Molecular Bioengineering
University	TU Dresden, Germany
Grade	1.8 (Gut/Good) Thesis grade – 1.1 (Sehr Gut/ very good)

Dates	2002 – 2006
Title of qualification awarded	Bachelor of Engineering (BE)
subject	Biotechnology
University	MVJCE, VTU, Karnataka, India
Grade	76.7% (First class with distinction)

Work experience

Dates	Dec 2009 – July 2011 – Research assistant
Institute	IMSB, ETHZ, Switzerland (Group: Prof. Ernst Hafen)
Project Title	Functional analysis of novel candidates of the IIS/TOR signalling pathway.

Dates	Sept 2008 – Mar 2009 - Student Lab assistant
Institute	Max Planck Institute-CBG, Dresden, Germany (Group: Dr. C P Heisenberg)
Project Title	GFP screen of zebrafish morphogenesis mutants

Dates	May 2007 – Oct 2007 - Project assistant
Institute	CFTRI, Mysore, Karnataka, India (Lab: Dr. Anup Krishna/ Dr. Raghav Rao)
Project Titles	Process development for making chitosan based films for food packaging applications.

Research Papers

Increased expression of the proton-sensing G protein-coupled receptor *Gpr65* during retinal degeneration. **Ail D**, Rüfenacht V, Caprara C, Samardzija M, Grimm C, (submitted to Neuroscience)

P38 MAPK signaling acts upstream of LIF-dependent neuroprotection during photorecptor degeneration. Agca C, Gubler A, Traber G, Beck C, Imsand C, **Ail D**, Caprara C, Grimm C, **Cell Death and Disease, 2013**

Phosphoryplation of Smo tail is controlled by membrane localization and is dispensible for clustering. Kupinski AP, Raabe I, Michel M, **Ail D**, Brusch L, Weidemann T, Bökel C, **Journal of Cell Science, 2013**

Co-curricular Activities

Academic

Scientific Symposiums

Oral presentations:

* ZHIP symposium 2014 (UZH-Physiology dept.) at **Zurich, Switzerland**
* Swiss Eye Research Week (SERM 2013) in **Biel, Switzerland**.

Poster presentations:

* FENS 2014 (European Neuroscience symposium) at **Milan, Italy**
* Young Reseacher Vision Camp 2013 at Castle **Wildenstein, Germany**
* ARVO 2013 (Association for research in vision and ophthalmology) at **Seattle, USA.** (I was awarded a travel grant by the ZNZ PhD program, LSGSZ for this conference)
* 8th symposium of Zurich center for Integrative Human Physiology 2012 in **Zurich, Switzerland**.
* ZNZ PhD retreat 2012 in **Valens, Switzerland**.
* iGEM 2009, MIT**, Boston, USA**.

Others

Teaching (2012 – 2015) — Involved in the teaching of lab-course in Neurobiology (University of Zurich - master students)

Institute seminars (2014) — Involved in the initiation and organization of Wagi seminars at the institute.

Famelab (2013) — Famelab is a science communication competition (part of the Cheltenham Science Festival,UK) Organized by British Council and Cheltenham Science Festival, UK

Won the first place at the Swiss famelab heat 2013 held at CERN, Geneva.
Was also awarded a special TEDx-CERN prize at the event.
Won the second place in the Swiss finals of Famelab 2013.

iGEM, MIT, USA (2009) — iGEM is a international synthetic biology competition for university students

Summer School at ETHZ (2008) — Summer school for learning advanced microscopy techniques conducted by CIMST and ETHZ. I was funded by 'Gesellschaft von Freunden und Foerderern der TU Dresden e.V.'

Best outgoing student award (2006) — I received this award in 2006 for representing my college at several cultural and technical competitions from 2002-2006.

Extra-curricular Activities

Non Academic

University of Basel (2015) — I was invited to give a talk to students of the social anthropology department on "Involvement of skilled Indian immigrants in home-country development."

Round-table-ILO, United Nations (2013) — I was invited to United Nations (Geneva) to give a presentation at the round-table on project – "Migration, Scientific diasporas and Development: Impact of skilled return migration on development in India." The round-table was part of a joint project by EPF-Lausanne, IDSK and JNU-India and ILO,UN.

Asha for Education (Since 2010) — I am part of the charity organization 'Asha for education-Zürich chapter', which is involved with supporting primary education of children in Indian villages. Positions held at Asha – General Secretary (2011, 2012), Editor of the Asha Annual report (2009). I have helped in the organizing of several fund-raising events in Zurich.

7. ACKNOWLEDGEMENTS

First and foremost, I would like to thank Prof. Christian Grimm for accepting me into the Lab of retinal cell biology, and providing the chance to work on an interesting project that was both intellectually challenging and fulfilling. I would like to thank him not only for sharing his scientific perspectives, constant guidance through the experimental work, but also for his patience with the writing and reviewing of manuscripts. Thanks are also due to him for broadening my research prospects with opportunities to attend conferences and establishing meaningful collaborations. Being part of his team has helped me learn and grow and has been an immensely fulfilling experience.

Thanks to my PhD committee members – Dr. Corinne Kostic and Prof. Ian Frew for their valuable inputs during my committee meetings and reviewing my thesis.

I would like to thank several members of the lab who have provided their support to varying extents. Dr. Marijana Samardzija for guidance with experimental techniques, discussion, helpful advice and for being such a valuable source of information in the lab. Dr. Christian Caprara for discussions on the hypoxia projects, performing some crucial experiments and helping with the mouse work. Dr. Jadwiga Oczos for help with experiments and for providing samples. Dr. Cavit Agca for the spontaneous meetings to 'talk science' in Zurich, Bern and Basel! Andrea Gubler, Cornelia Imsand and Christel Beck for their excellent technical assistance that enabled and eased my work considerably; and all the other lab members for their support, questions and discussions during lab meetings and presentations.

I would like to thank all my friends in and around Zurich who have helped keep my spirits high through the entire duration of my PhD – Sujit, Indrani, Rahul, Lia, Ginu, Bindu, Priyanka and Agnes – for the conversations, food and travel. Your company made my stay in Zurich all the more pleasurable. Thanks to Dipanjan for the moral support!

A special thanks to my friends Akhil and Shakeela, who have been part of the 'growing years' and still chosen to stick around, and Dileep for thinking so highly of me (helps me set higher expectations of myself).

At last, most importantly I would like to thank my family – Deepti and Rohan for the fun times, and especially my parents Balakrishna and Shailaja Ail who have always been there for me. Thanks for having faith in me, for your unconditional moral and emotional support, and for wishing the best for me. This wouldn't have been possible without you!